Finite-Element Software Package
for the analysis of 2D & 3D structures
based on smart materials
Version 6.0.0

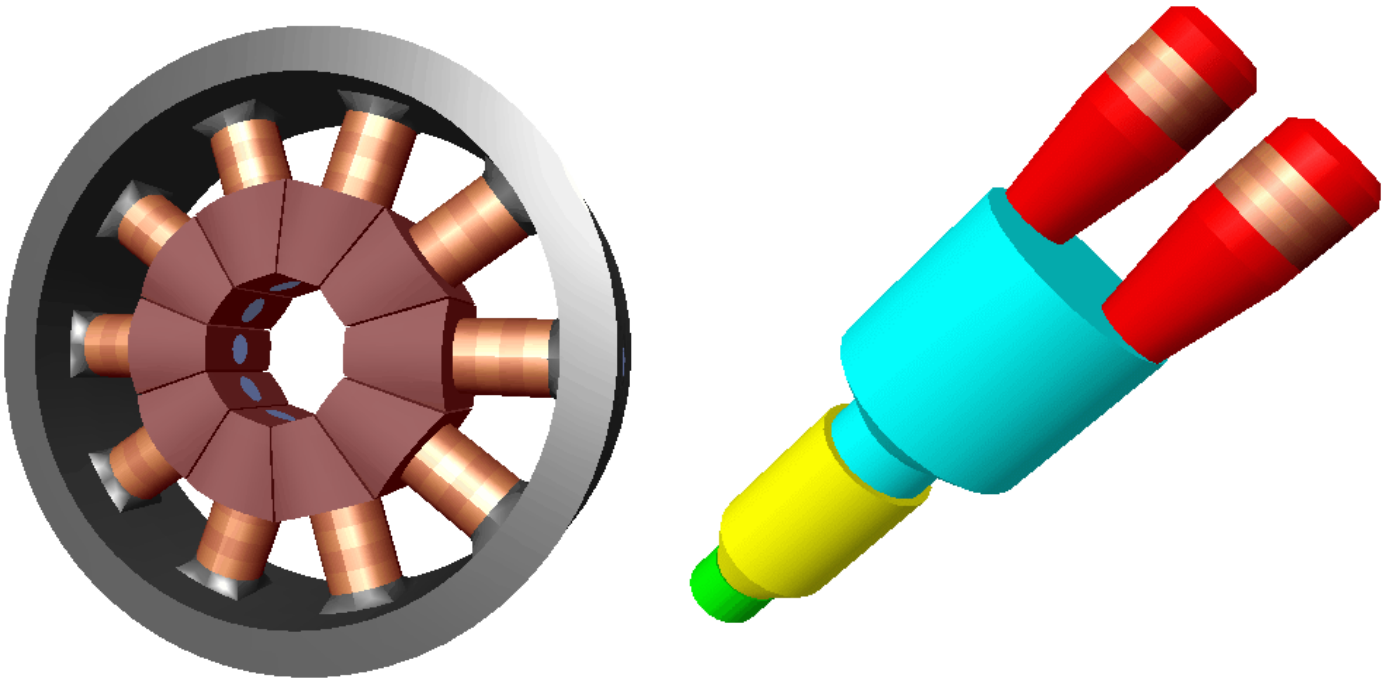

USER's MANUAL

July 2005

Institut Supérieur d'Electronique et du Numérique,

Acoustics Laboratory

(Associated with the CNRS, IEMN-UMR 8520)

The finite element code **ATILA** has been developed for the « Centre d'Etude et de Recherche de Détection Sous-marine (C.E.R.D.S.M.), » « Direction des Constructions Navales (D.C.N.-Toulon), » at the Acoustics Laboratory of the Institut Supérieur d'Electronique du Numérique (I.S.E.N., 41 Boulevard Vauban, 59046 Lille CEDEX, France).

Table of Contents

1 GENERAL PRESENTATION

1.1 Introduction

ATILA is a finite element code that has been specifically developed to aid in the design of sonar transducers, but can also be used for all types of transducers (industrial machining, cleaning, welding, nondestructive testing, acoustic imaging, actuators) or for passive structures. Its working domain is one of small and linear strains. It allows the static, modal, harmonic and transient analysis of unloaded elastic, piezoelectric, electrostricitve or magnetostrictive structures, as well as the harmonic and transient analysis of radiating elastic or piezoelectric structures (in any fluid, water or air, for example) and modal or harmonic analysis of periodic structures with 1D, 2D or 3D periodicity, and thermal analysis. It is able to perform analyses of axisymmetrical, bi- or three-dimensional structures. Depending upon the problem, it provides: the displacement field, the nodal plane positions, the stress field, near-field and far-field pressures, transmitting voltage response, directivity patterns, electrical impedance. Its ability to describe the behavior of different transducers (Tonpilz transducers, double headmass, axisymmetrical length expanders, free-flooded rings, flextensional transducers, bender-bars, cylindrical and trilaminar hydrophones) and the accuracy of the results have been valided by modeling many different structures and comparing numerical and experimental results. Most results have been described in numerous reports, papers and articles; some of them are listed in the bibliography in the next section.

For a steady-state solution, thermal behavior is weakly coupled to the electromechanical response. The method thus may take advantage of the order of magnitude greater time constant for thermal effects compared to mechanical behavior. A two-step analysis is performed whereby the electro-mechanical behavior is first computed, and the resulting dissipated power is then applied as a heat generator to determine the resulting temperature of the system.

ATILA is the result of many years of research done mainly by K. Anifrani, J. Assaad, R. Bossut, J.-L. Carton, J.-C. Debus, J.-N. Decarpigny, B. Dubus, R. Edde, A. Ghaddar, B. Hamonic, A.-C. Hladky-Hennion, P. Langlet, D. Morel and P. Tierce at I.S.E.N., B. Tocquet, and D. Boucher at D.C.N (Toulon) , F. Claeyssen R. Le Letty, N. Lhermet and F.-X. Zgainsky at Cedrat-Recherche, and testing is still being done at I.S.E.N.

ATILA is mainly written in standard FORTRAN 77, except for some system interfacings written in C. It totals more than 220,000 lines of code (including 6000 lines of C code). It has been carefully designed to be easily portable on almost all platforms. First developed on an IBM 370 series mainframe (VM/CMS), it is maintained at I.S.E.N. on IBM-PC compatible computers (32-bit applications under Windows 98, Windows NT, Windows2000, WindowsXP and Linux) and MACOSX operating systems. Other test platforms were: a HP715/75 (HP-UX 9.03), two Sparc2 workstations (one with Solaris 2.3, one with SunOS 4.1.3), a DECstation 5000/125 (Ultrix RISC 4.2a), an IBM RS6000 workstation (AIX 3.2.5), and. Ports have been successfully tested on DEC Alpha workstations (OSF 1.2 and 2.0), and on an SGI workstation (IRIX 4.0. Previous ports were done on DEC VAX stations and mainframes and on DEC Alpha stations with OPEN VMS, but these are no longer supported.

ATILA code chairmen are:

Pr. Jean-Claude DEBUS Tel: (+33) 320 30 40 50
Dr. Pascal MOSBAH Tel: (+33) 320 30 40 50
Laboratoire d'Acoustique Fax: (+33) 320 30 40 51
Institut Supérieur d'Électronique du Nord
41. boulevard Vauban,
59046 LILLE CEDEX, FRANCE

A description of the different steps of an **ATILA** job and where to find them in the User's Manual follows the list of selected references. A detailed description of these steps appears in the following chapters.

1.2 References

1.2.1 PhD Thesis

1) J.-N. DECARPIGNY, « Application de la méthode des éléments finis à l'étude de transducteurs piézoélectriques », *(Application of the Finite Element Method to the Modeling of Piezoelectric Transducers)*, Thèse de Doctorat d'État, Université des Sciences et Techniques de Lille, (1984).

2) R. BOSSUT, « Modélisation de transducteurs piézoélectriques annulaires immergés par la méthode des éléments finis », *(Finite Element Modeling of Free-Flooded Ring Transducers)*, Thèse de Doctorat-Ingénieur, Université de Valenciennes et du Hainaut-Cambrésis, (1985).

3) P. TIERCE, « Modélisation du transducteur Isabelle par la méthode des éléments finis », *(Finite Element Modeling of the Isabelle Transducers)*, Thèse de Doctorat-Ingénieur, Université de Valenciennes et du Hainaut-Cambrésis, (1985).

4) B. HAMONIC, « Contribution à l'étude du rayonnement de transducteurs utilisant des vibrations de coques minces », *(Contribution to the Analysis of Radiating Transducers Using Thin Shell Vibrations)*, Thèse de Doctorat en Mécanique, Université des Sciences et Techniques de Lille, (1987).

5) K. ANIFRANI, « Contribution à l'étude de structures piézoélectriques à l'aide de la méthode des éléments finis », *(Contribution to the Analysis of Piezoelectric Structure Using the Finite Element Method)*, Thèse de Doctorat en Sciences des Matériaux, Université des Sciences et Techniques de Lille, (1988).

6) F. CLAEYSSEN, « Conception et réalisation de transducteurs sonar basse fréquence à base d'alliages magnétostrictifs terres rares-fer », *(Design and Assembling of Low Frequency Sonar Transducers Using Magnetostrictive Rare Earth Alloys)*, Thèse de Doctorat en Électronique, I.N.S.A. de Lyon, (1989).

7) B. DUBUS, « Analyse des limitations de puissance des transducteurs piézoélectriques », *(Analysis of the Power Limitations of Piezoelectric Transducers)*, Thèse de Doctorat en Sciences des Matériaux, Université des Sciences et Techniques de Lille, (1989).

8) A.-C. HLADKY-HENNION, « Application de la méthode des éléments finis à la modélisation de structures périodiques utilisées en acoustique, » *(Application of the Finite Element Method to the Modeling of Periodic Structures Used in Acoustics)*, Thèse de Doctorat en Sciences des Matériaux, Université des Sciences et Techniques de Lille, (1990).

9) A. GHADDAR, « Étude de la dégradation des coques en matériaux composites utilisées dans les transducteurs flextensionnels à l'aide de la méthode des éléments finis, » *(Finite Element Analysis of the Damage of Composite Shells used for Flextensional Transducers)*, Thèse de Doctorat en Mécanique, Université des Sciences et Techniques de Lille, (1992).

10) J. ASSAAD, « Modélisation des transducteurs piézoélectriques haute fréquence à l'aide de la méthode des éléments finis, » *(Finite Element Modeling of High Frequency Piezoelectric Transducers)*, Thèse de Doctorat en Électronique, Université de Valenciennes et du Hainaut-Cambrésis, (1992).

11) P. LANGLET, « Analyse de la propagation des ondes acoustiques dans les matériaux périodiques à l'aide de la méthode des éléments finis », (*Analysis of the acoustic wave propagation in periodic materials using the finite element method*), Thèse de Doctorat en Electronique, Université des Sciences et Technologies de Valenciennes et du Hainaut-Cambrésis, (1993)

12) R. LE LETTY, « Conception de moteurs piézoactifs à l'aide de la modélisation, » (*Modeling of piezoactive motors*), Thèse de Doctorat en Acoustique, Institut National des Sciences Appliquées de Lyon, (1994).

13) D. EKEOM, « Modélisation par éléments finis du rayonnement de transducteur piézoélectrique dans un puits de forage », (*Finite element modeling of the radiation of piezoelectric transducers in wells*), Thèse de Doctorat en Mécanique, Université des Sciences et Techniques de Lille (1997)

14) H. OUAZZANI TOUHAMI, « Modélisation par la méthode des éléments finis du phénomène de contact dans les moteurs piezoactifs », (*Finite element modeling of the contact phenomenon in piezoactive motors*), Thèse de Doctorat en Mécanique, Université des Sciences et Techniques de Lille (1998)

15) J. COUTTE, « Modélisation de céramiques électrostrictives pour transducteurs électroacoustiques », (*Modeling of electrostrictive ceramics for electroacoustic transducers*), Thèse de Doctorat en Mécanique, Université des Sciences et Techniques de Lille (1998)

16) S.RAFANOMEZANTSOA, « Modélisation par éléments finis de matériaux à mémoire de forme ». *(Finite element modelling of shape memory alloy materials)* Thèse de Doctorat en mécanique, Université des Sciences et Techniques de Lille (2001),

17) B.CUGNIET, « Etude d'une antenne de type mosaïque », *(Mosaic type array modelling)* Thèse de Doctorat, Université de Valenciennes et du Hainaut-Cambrésis, co-encadré par J.Assaad (IEMN-DOAE), (2002)

18) E.LENGLET, « Etude de réseaux de fibres piézoélectriques », *(Active fiber piezoelectric composite)* Thèse de Doctorat (2003)

19) M.BERRAKI, «Etude théorique et modélisation d'une source piézoélectrique enterrée unidirectionnelle pour applications sismiques » *(Piezoelectric directional buried source modelling for seismic application)* Thèse de Doctorat (2004).

1.2.2 Articles

1) J.-N. DECARPIGNY, J.-C. DEBUS, B. TOCQUET, D. BOUCHER, "In-air analysis of piezoelectric Tonpilz transducers in a wide frequency band using a mixed finite element-plane wave method", J. Acoust. Soc. Am. 78, 1499-1507 (1985).

2) B. HAMONIC, J.-C. DEBUS, J.-N. DECARPIGNY, D. BOUCHER, B. TOCQUET, "Application of axisymmetrical thin shell finite elements to the analysis of a radiating flexural shell sonar transducer", in "Shell and Spatial Structures: Computational Aspects", Ed. Springer-Verlag, 43-53 (1986).

3) D. BOUCHER, B. TOCQUET, "Finite element analysis of low frequency sonar transducers", Proc. Inst. of Acoust. 9, Pt 2, 42-50 (1987).

4) B.DUBUS, J.C.DEBUS, J.N.DECARPIGNY, D.MOREL, D.BOUCHER,"Determination of the mechanical limits of piezoelectric transducers using the finite element method", Communication MM2, 113th ASA meeting, Indianapolis, J. Acoust. Soc. Am.,Suppl. 1, 81, (1987).

5) B. STUPFEL, C. GRANGER, J.-N. DECARPIGNY, "Finite element modeling of a pressure-gradient hydrophone", Proc. Inst. of Acoust. 9, Pt 2, 134-142 (1987).

6) D. BOUCHER, "Design and modeling of low frequency sonar projectors", UDT Conference Proceedings, Microwave Exhibition and Publishers Ltd, (1988).

7) B. HAMONIC, "Application of the finite element method to the design of power piezoelectric sonar transducers", Proceedings of the International Workshop on Power Sonic and Ultrasonic Transducer Design, Lille, Ed. Springer-Verlag, 143-159 (1988).

8) J.N.DECARPIGNY, J.C.DEBUS, R.BOSSUT, B.HAMONIC, B.DUBUS, P.TIERCE, D.MOREL, K.ANIFRANI, D.BOUCHER, "Analyse de transducteurs piézoélectriques par éléments finis : le code ATILA", Actes du congrès international Strucome 88, Ed. Hermès, pp 341-354, (1988).

9) P. TIERCE, J.-N. DECARPIGNY, "Power sonic and ultrasonic transducer design for macrosonics applications", Proceedings of the International Workshop on Power Sonic and Ultrasonic Transducer Design, Lille, Ed. Springer-Verlag, 185-207 (1988).

10) R. BOSSUT, J.-N. DECARPIGNY, "Finite element modeling of radiating structures using dipolar damping elements", J. Acoust. Soc. Am. 86, 1234-1244 (1989).

11) B. HAMONIC, J.-C. DEBUS, J.-N. DECARPIGNY, D. BOUCHER, B. TOCQUET, “Analysis of a radiating thin shell sonar transducer using the finite element method”, J. Acoust. Soc. Am. 86, 1245-1253 (1989).

12) B. DUBUS, B. HAMONIC, J.-C. DEBUS, J.-N. DECARPIGNY, D. BOUCHER, “Analysis of the power limitations of sonic and ultrasonic transducers using the finite element method”, Proceedings of Ultrasonics International 89, 340-345 (1989).

13) B.DUBUS, J.C.DEBUS, J.N.DECARPIGNY, D.BOUCHER, “Finite element modeling of piezoelectric transducers including internal losses”, Communication LL6, 117th ASA meeting, Syracuse, J. Acoust. Soc. Am., Suppl. 1, 85, (1989).

14) A.C.HENNION, R.BOSSUT, J.N.DECARPIGNY, C.AUDOLY, “Application of the finite element method to the modeling of plane wave scattering by a compliant tube grating at oblique incidence”, Communication EEE5, J.Acoust. Soc. Am., Suppl 1, 85, 117th ASA meeting, Syracuse, (1989)

15) A.C. HENNION, R. BOSSUT, J.-N. DECARPIGNY, C. AUDOLY, “Analysis of the scattering of a plane acoustic wave by a periodic structure using the finite element method : application to compliant tube gratings”, J. Acoust. Soc. Am. 87, 1861-1870 (1990).

16) B. HAMONIC, J.-C. DEBUS, J.-N. DECARPIGNY, Proceedings of the International Workshop on ATILA, Ed. COMES, Lille, (1990).

17) A.C.HENNION, R.BOSSUT, J.N.DECARPIGNY, C.AUDOLY, « Application de la méthode des éléments finis à la modélisation de structures périodiques utilisées en acoustique » J. Phys., 51 C2, pp.399-402 (1990).

18) B.DUBUS, R.E.MONTGOMERY, “Hydrophone noise induced by turbulent boundary layer pressure fluctuations”, Communication 2EA1, 120th ASA meeting, San Diego, J. Acoust. Soc. Am., Suppl. 1, 88, (1990).

19) A.C.HLADKY-HENNION, J.N.DECARPIGNY, “Analysis of the scattering of a plane acoustic wave by a doubly periodic structure using the finite element method”, Communication 6EA8, 120th ASA meeting, San Diego, J.Acoust. Soc. Am., Suppl 1, 88, (1990)

20) A.C.HENNION, R.BOSSUT, J.N.DECARPIGNY, C.AUDOLY, “Application of the finite element method to analyze the scattering of a plane acoustic wave from doubly periodic structures”, Proceedings of the international workshop on ATILA, Ed. COMES, pp.49-55 (1990).

21) A.C.HENNION, B.HAMONIC, J.N.DECARPIGNY, « Modélisation bidimensionnelle de structures élastiques périodiques », Journée thématique sur les revêtements anéchoïques de sous-marins, Acte des Conférences, 6-12, Ed. DRET/SDR, Groupe 2 (1990).

22) F. CLAEYSSEN, R. BOSSUT, D. BOUCHER, “Modeling and Characterization of the magnetostrictive coupling”, Proceedings of the international workshop on power transducers for sonics and ultrasonics, Toulon, Ed. Springer-Verlag, 136-155 (1990).

23) B. HAMONIC, J.-C. DEBUS, A. LAVIE, “Analysis of the interaction between transducers in a low frequency, high power array: physics and numerical modeling”, Proceedings of UDT 91, 197-203 (1991).

24) A.C. HLADKY-HENNION, “Finite element analysis of periodic structures used in underwater acoustics”, Proceedings of UDT 91, 930-935 (1991).

25) B. DUBUS, J.-C. DEBUS, J.-N. DECARPIGNY, D. BOUCHER, “Analysis of the mechanical limitations of high power piezoelectric transducers using the finite element modeling”, Ultrasonics 29, 201-207 (1991).

26) A.C.HLADKY, J.N.DECARPIGNY, B.HAMONIC, “Modeling of active periodic structures using the finite element method”, J. Acoust. Soc. Am., Suppl. 1, 6EA6, 91, (1991).

27) B.Dubus, “A coupled finite element/boundary element approach for the analysis of electromechanical transducers”, 1st Modeling Users’Group Meeting, Orlando, (1991).

28) J.C. DEBUS, B. HAMONIC, J.N. DECARPIGNY, “Finite element modeling of composite shells used in low frequency transducers”, Journal de la S.F.A., Vol.4 n°4, 435-457 (1991).

29) A.C. HENNION, J.N. DECARPIGNY, “Application of the finite element method to the analysis of the scattering of a plane acoustic wave by doubly periodic structures”, Proc. 1st. Physical Acoustics Symposium, Courtrai, Belgique, 359-364 (1991).

30) A.C. HLADKY-HENNION, J.N. DECARPIGNY, “Analysis of the scattering of a plane acoustic wave by a doubly periodic structure using the finite element method: application to Alberich anechoïc coatings”, J. Acoust. Soc. Am., 90, 3356-3367 (1991).

31) A.C. HLADKY-HENNION, J.N. DECARPIGNY, “Application of the finite element method to the modeling of 2D and 3D passive or active periodic structures”, Conference Proceedings, Ultrasonics International 91, Le Touquet, 415-418 (1991).

32) J. ASSAAD, B. DUBUS, B. HAMONIC, J.N. DECARPIGNY, J.C. DEBUS, R. BOSSUT, D. BOUCHER, “Finite element modeling of ultrasonic transducers using the ATILA code”, Conference Proceedings, Ultrasonics International 91, Le Touquet, 371-374 (1991).

33) R. LE LETTY, F. CLAEYSSEN, B. HAMONIC, R. BOSSUT, “Numerical modeling of ultrasonic motors taking into account piezoelectric excitation”, Proceedings of Actuator ‘92, Third International Conference on new actuators, (1992).

34) A.LAVIE, B.DUBUS, “Coupling finite element and boundary element methods for the analysis of the acoustic scattering by elastic structures”, La Nouvelle Orléans, Communication 5pPA5, 124th ASA meeting, J. Acoust. Soc. Am. 92, n°4 pt 2, (1992)

35) B.DUBUS, A.LAVIE, D.DECULTOT, G.MAZE, “Elastic scattering by a thin cylindrical shell bounded by hemispherical endcaps at various incidences”, La Nouvelle Orléans, Communication 5pPA6, 124th ASA meeting, J. Acoust. Soc. Am. 92, n°4 pt 2 , (1992).

36) A.LAVIE, B.DUBUS, « Modélisation de la diffusion acoustique par un couplage éléments finis-équations intégrales », GESPA, Le Havre (1992).

37) F. CLAEYSSEN, R. LE LETTY, B. HAMONIC, R. BOSSUT, « Analyse d’un moteur ultrasonore piézoélectrique à l’aide de la modélisation », J. Phys., Suppl.III. n°4 C1, 381-385 (1992).

38) A.C. HLADKY-HENNION, J.N. DECARPIGNY, « Application de la méthode des éléments finis à la modélisation de structures périodiques actives », J. Phys., Suppl.III. n°4 C1, 387-390 (1992).

39) A. LAVIE, B. DUBUS, « Analyse de la diffraction acoustique d’une onde incidente plane par une structure élastique à l’aide d’une méthode mixte éléments finis - équations intégrales », J. Phys., Suppl.III. n°4 C1, 957-960 (1992).

40) P. LANGLET, A.C. HLADKY-HENNION, J.N. DECARPIGNY, « Analyse de la propagation d’ondes acoustiques dans les structures périodiques à l’aide de la méthode des éléments finis », J. Phys., Suppl.III. n°4 C1, 1065-1068 (1992).

41) A.C. HLADKY-HENNION, J.N. DECARPIGNY, “Note on the validity of using plane-wave type relations to characterize Alberich anechoïc coatings”, J. Acoust. Soc. Am., 92, 2878-2882 (1992).

42) A.C.HLADKY-HENNION, J.N.DECARPIGNY, “Finite element modeling of active periodic structures: application to 1-3 piezocomposites”, J. Acoust. Soc. Am. 94, pp.621-635 (1993)

43) D.CERTON, A.C.HLADKY-HENNION, M.LETHIECQ, R.DUFAIT, F.PATAT, “1-3 piezo-composite material: 3D modeling and experimental results”, Ultrasonics International 93, Conference Proceedings, Ed. Butterworth Vienne, pp.121-124 (1993).

44) A.C.HLADKY-HENNION, “Modeling of Active and Passive Periodic Structures” Proceedings of the International Workshop on Transducers for Sonics and Ultrasonics, Ed. Technomic Publishing, pp.77-94, Lancaster, (1993).

45) J.ASSAAD, C.BRUNEEL, J.N.DECARPIGNY, B.DUBUS, “Far-field directivity patterns for YZw/36° lithium-niobate bars”, Ultrasonics International 93 Conference Proceedings, Ed. Butterworth, pp 415-418, (1993).

46) B.DUBUS, “Finite Element modeling of piezoelectric transducters”, Office of Naval Research workshop in Perspective on Piezoelectric Material Research, London, (1993).

47) A.C.HLADKY, P.LANGLET, « Modélisation par éléments finis du comportement acoustique de matériaux actifs et passifs », Premières Journées d’Etude sur les Matériaux utilisés en acoustique, Lesquin, (1993).

48) A.C.HLADKY, « Etude de la propagation des ondes acoustiques dans des dièdres à l’aide des éléments finis », Séminaire GESPA sur la Diffusion Acoustique, Marseille, (1993).

49) A.LAVIE, B.DUBUS, R.BOSSUT, « Modélisation numérique de la diffusion acoustique par une structure LINE », Séminaire GESPA sur la Diffusion Acoustique, Marseille, (1993).

50) B.DUBUS, “Coupling finite element and boundary element methods on a mixed solid-fluid/fluid-fluid boundary for radiation or scattering problems”, J. Acoust. Soc. Am. 96-6, pp 3792-3799, (1994).

51) A.LAVIE, B.DUBUS, « Modélisation de la Diffusion acoustique par des cibles LINE : étude théorique des régimes libre et forcé », GESPA, Corte, (1994)

52) D.EKEOM, B.DUBUS, “Coupling finite element and impedance element to model the radiation of piezoelectric transducers in boreholes”, Communication 4pEA12, 128th ASA meeting, Austin, J. Acoust. Soc. Am. 96 n°5 pt 2, (1994)

53) A.C.HLADKY, « Modélisation par éléments finis de matériaux piézo-composites », Journées Transducteurs piézo-électriques innovants : des matériaux aux applications, Tours, (1994).

54) A.C.HLADKY-HENNION, R.BOSSUT, “Finite element modeling of single periodic curved gratings”, J. Acoust. Soc. Am., 95, N°5 Pt 2, 4aEA7, (1994).

55) A.LAVIE, B.DUBUS, « Méthodes numériques en diffusion acoustique », présentation invitée à la journée Science et Défense, Acoustique Diffusion et Détection, Le Havre, (1994).

56) A.C.HLADKY-HENNION, R.BOSSUT, « Etude de la propagation des ondes acoustiques dans les dièdres avec l’aide de la méthode des éléments finis », J. Phys. Vol. 4, Colloque N°5, Suppl. JP III, n°5, Vol. II, C5, pp.689-692, (1994).

57) A.C.HLADKY-HENNION, J.C.DEBUS, B.HAMONIC, “Recent development in numerical modeling of transduction materials for future sonar transducers”, Proceedings of OCEANS 94, pp.358-363, (1994).

58) P. LANGLET, A.C. HLADKY-HENNION, J.N. DECARPIGNY, « Homogénéisation de matériaux périodiques à l’aide de la méthode des éléments finis », J. Phys., Suppl. III, 4, C5, 921-924 (1994).

59) B. DUBUS, D. BOUCHER,‘An analytical evaluation of the heating of low-frequency sonar projectors’, J. Acoust. Soc. Am. 95, 1983-1990. (April 1994).

60) P. LANGLET, A.C. HLADKY-HENNION, J.N. DECARPIGNY, “Analysis of the propagation of plane acoustic waves in passive periodic materials using the finite element method”, J. Acoust. Soc. Am., 98, 2792-2800 (1995).

61) A.C. HLADKY-HENNION, P. LANGLET, J.N. DECARPIGNY, “Finite element modeling of periodic structures and materials”, Advances in Science and Technology, ed. P. Vincenzini, Techna, Faenza, 315-322 (1995).

62) A.C. HLADKY-HENNION, “Finite element analysis of the propagation of acoustic waves in waveguides”, J. Sound and Vib., 194, pp 119-136 (1995).

63) A.C.HLADKY-HENNION, R.BOSSUT, J.C.DEBUS, “Recent developments in numerical modeling of transduction materials”, Proceedings of the 1995 Design Engineering Technical Conference, Boston, Ed. ASME, Vol 3.B, pp.481-488, (1995)

64) B.DUBUS, A.LAVIE, D.DÉCULTOT, G.MAZE, “Coupled finite element/boundary element method for the analysis of the acoustic scattering from elastic targets”, ASME 15th biennal conference on vibration and noise, Acoustics of submerged structures and transduction for systems, Boston, Vol. 3 part B, pp 25-32, (1995).

65) A.C.HLADKY, P.LANGLET, « Etude de la propagation des ondes acoustiques dans les diédres à l'aide de la méthode des éléments finis », Séminaire GESPA sur la Diffusion Acoustique, Lille, (1995)

66) B.DUBUS, A.LAVIE, « Diffusion acoustique par des structures LINE : régimes libre et forcé, effets d'arêtes et ellipses de polarisation », GESPA, Villeneuve d'Ascq, (1995).

67) A.C.HLADKY-HENNION, P.LANGLET, M.DE BILLY, "Finite element analysis of the propagation of acoustic waves along tips of elastic immersed wedges", Proceeding of the 3rd European Conference on Underwater Acoustics, Heraklion, (1996).

68) S.ALKOY, A.DOGAN, A.C.HLADKY, P.LANGLET, J.COCHRAN, R.E.NEWNHAM, "Miniature piezoelectric hollow sphere transducers" Proceedings of the 1996 IEEE International Frequency Control Symposium, pp.586-594, Honolulu (1996).

69) S.ALKOY, A.DOGAN, A.C.HLADKY, J.K.COCHRAN, R.E.NEWNHAM, "Vibration Modes of PZT hollow spheres transducers", Proceedings of the IEEE International Symposium on the Applications of Ferroelectrics, East Brunswick, p 519-522, (1996).

70) J.C.DEBUS, B.DUBUS, M.MCCOLLUM, S.BLACK, "Finite element modeling of PMN electrostrictive materials", Proceedings of the 3rd International Conference on Intelligent Materials, édité par P.F. Gobin et J. Tatibouët, SPIE, pp 913-918, (1996).

71) J.C.DEBUS, B.DUBUS, J.DUBOIS, M.MCCOLLUM, S.BLACK, "2D modeling of PMN electrostrictive materials using the finite element code ATILA", Proceedings of the 3rd European Conference on Underwater Acoustics, édité par J.S. Papadakis, Crete University Press, vol. II, pp 1001-1006, (1996).

72) C.CAMPOS-POZUELO, B.DUBUS, "Estudio de la propagacion nonlineal de ondas acusticas en medios fluidos mediante el metodo de elementos finitos", Proceedings of tecniacustica, pp 287-290, (1996).

73) A.LAVIE, B.DUBUS, A.ELGHAOUTY, « Diffusion acoustique en régime transitoire à l'aide d'un couplage éléments finis-équations intégrales », GESPA, DRET-PARIS, Université de Bordeaux 1, Talence, (1996).

74) J.C.DEBUS, B.DUBUS, J.DUBOIS, M.MCCOLLUM, S.BLACK, "2D modeling and characterization of PMN electrostrictive materials using the finite element code ATILA", Communication 1pEA8, 132th ASA meeting, J. Acoust. Soc. Am. 99, n°4pt2, Honolulu, (1996).

75) C.CAMPOS-POZUELO, A.LAVIE, B.DUBUS, G.RODRIGUEZ-CORRAL, J.A.GALLEGO-JUAREZ, "Numerical and experimental study of radiated field of high-power ultrasonic transducers for industrial application in gases", Communication 4pEA11, 132th ASA meeting, J. Acoust. Soc. Am. 99, n°4pt2, Honolulu, (1996).

76) A.LAVIE, B.DUBUS, "Scattering from an axisymmetric structure insonified at any incidence using a coupled finite element/boundary element method", Communication 4pUW11, 132th ASA meeting, J. Acoust. Soc. Am. 99, n°4pt2, Honolulu, (1996).

77) S.ALKOY, A.DOGAN, R.E.NEWNHAM, A.C.HLADKY AND J.K.COCHRAN, "Vibration modes of tangentially poled PZT hollow spheres", 1996 ONR Transducer Materials and Transducers Workshop, 25-27 March 1996, University Park - USA

78) S.ALKOY, A.DOGAN, R.E.NEWNHAM, A.C.HLADKY AND J.K.COCHRAN, "Piezoelectric hollow sphere transducers", 98th American Ceramic Society 1996 Annual Meeting, 14-17 April 1996, Indianapolis - USA

79) A.C.HLADKY, « Modélisation par éléments finis de dièdres », Séminaire GESPA sur la diffusion Acoustique, Bordeaux, (1996).

80) S.ALKOY, A.DOGAN, A.C.HLADKY, R.E.NEWNHAM, "Piezoelectric Hollow spheres", Proceedings of the III Ceramics Congress organized by Turkish Ceramic Society held on 22-25 October 1996 in Istanbul, Turkey, pp.363-371.

81) S.ALKOY, P.D.LOPATH, R.E.NEWNHAM, A.C.HLADKY, J, K.COCHRAN, "Focused spherical transducers for ultrasonic imaging" Proceedings of the IEEE International Ultrasonic Symposium, p 991-994, Toronto-Canada, (1997).

82) M.DE BILLY, P.LANGLET, A.C.HLADKY-HENNION, “On the velocity of the “pseudo-edge waves” and on the conversion of the antisymmetric edge modes”, Actes du 4ème Congrès Français d’Acoustique, Vol 2, pp.817-820, Marseille, Avril 1997.

83) .DOGAN, J.BRAIDIC, G.LENKNER, J.F.TESSLER, A.C.HLADKY, R.E.NEWNHAM, “Comparison of composite transducers utilizing different piezoelectric coefficients”, IMF-9 Ferroelectric Meeting, Corée, august 1997

84) J.COUTTE-DUBOIS, J.C.DEBUS, B.DUBUS, « Modélisation de céramiques électrostrictives PMN et application aux transducteurs électroacoustiques » Actes du 4ème Congrès Français d’Acoustique, Technea, vol.1, pp.27-30, (1997).

85) D.EKEOM, B.DUBUS, C.GRANGER, « Modélisation du rayonnement de transducteurs piézoélectriques dans un puit de forage à l’aide d’une méthode couplée éléments finis-décomposition en k », Actes du 4ème Congrès Français d’Acoustique, Technea, vol.1, pp.31-34, (1997).

86) A.LAVIE, B.DUBUS, « Coupled finite element boundary element method for scattering problems by axisymmetric bodies at oblique incidence », Actes du 4ème Congrès Français d’Acoustique, Tecnea, vol.2, pp 801-804, (1997).

87) J.COUTTE, J.C.DEBUS, B.DUBUS, R.BOSSUT, “Non-linear time domain analysis of electrostrictive materials by the finite element method”, Communication 4pEA3, 133th ASA meeting, State College, (1997).

88) A.C.HLADKY, “Recent developments in the finite element modelling of transduction materials”, 1997 ONR Transducer Materials and Transducers Workshop, 29 April - 1 May 1997, University Park - USA.

89) S.ALKOY, R.E.NEWNHAM, A.C.HLADKY, “Size dependent properties of tangentially poled sphere transducers”, 1997 ONR Transducer Materials and Transducers Workshop, 29 April - 1 May 1997, University Park - USA

90) S.ALKOY, A.DOGAN, A.C.HLADKY-HENNION, J.K.COCHRAN, R.E.NEWNHAM, “Piezoelectric Hollow Sphere Transducers”, 21st International Center for Actuators and Transducers Symposium (ICAT), 23-24 April 1997, University Park, Pennsylvania.

91) DOGAN, J.BRAIDIC, G.LENKNER, J.F.TESSLER, A.C.HLADKY, R.E.NEWNHAM, “Comparison of ceramic-metal composite transducers driven by different piezoelectric modes”, 1997 ONR Transducer Materials and Transducers Workshop, 29 April - 1 May 1997, University Park - USA.

92) J.C.DEBUS, B.DUBUS, J.COUTTE, R.BOSSUT, “2D modeling of PMN electrostrictive materials using the finite element code ATILA”, Miniworkshop on transducer modeling, Monterey, (1997).

93) N.D.VEKSLER, A.LAVIE, B.DUBUS, “Scattering of a plane acoustic wave by a cylindrical shell with hemispherical endcaps: analysis of peripheral waves”, Euromech 369 on fluid-structure interaction in acoustics, Delft, (1997).

94) S.ALKOY, R.E.NEWNHAM, A.C.HLADKY, “Effect of dimensions and materials on the characteristics of hollow sphere transducers”, 99th American Ceramic Society 1997 Annual Meeting, 5-8 May 1997, Cincinatti-USA

95) A.C. HLADKY-HENNION, P.LANGLET, M. DE BILLY, “Finite element analysis of the propagation of acoustic waves along waveguides immersed in water”, J.Sound and Vib., 200(4), pp 519-530 (1997).

96) S.ALKOY, A.DOGAN, A.C.HLADKY, P.LANGLET, J.COCHRAN, R.E.NEWNHAM, “Miniature piezoelectric hollow sphere transducers” IEEE Transactions on Ultrasonics, Ferroelectrics and Frequency Control, Vol.44, n°5, 1067-1076, (1997)

97) A.C. HLADKY-HENNION, R. BOSSUT, M. DE BILLY, “Time analysis of immersed waveguides using the finite element method”, J.Acoust. Soc. Am., 104(1), 64-71, (1998)

98) A.C. HLADKY-HENNION, P. LANGLET, R. BOSSUT, M. DE BILLY, “Finite element modelling of radiating waves in immersed wedges” J. Sound and Vib., 212(2), 265-274 (1998)

99) S.ALKOY, A.C.HLADKY-HENNION, J.K.COCHRAN, R.E.NEWNHAM, “Size Dependent Properties of Hollow Sphere Transducers” 4th Ceramic congress organized by the Turkish Ceramic Society, September 22-25, 1998, Eskisehir, Turkey

100)A.C.HLADKY-HENNION, S.ALKOY, P.LOPATH, R.E.NEWNHAM, “Finite element modeling of transduction materials with application to piezoelectric hollow sphere transducers”, Proceeding of the 1998 IEEE International Frequency Control Symposium, pp. 709-714, Pasadena, California (1998)

101)A.C.HLADKY-HENNION, A.DOGAN, R.E.NEWNHAM, “Finite element modeling of transduction materials with application to cymbal actuators and sensors”, Proceeding of Actuators 98, 6th International Conference on New Actuators, pp. 292-295, Bremen, Germany (1998)

102)A.DOGAN, A.C.HLADKY-HENNION, R.E.NEWNHAM, “Finite element analysis of the composite transducers utilizing different piezoelectric coefficients” 1998 IEEE International Symposium on Applications of Ferroelectrics (ISAF), Août 98, Montreux, Switzerland

103)J.ZHANG, W.J.HUGHES, A.C.HLADKY-HENNION, R.E.NEWNHAM, “Concave Cymbal Transducer”, 1998 IEEE International Symposium on Applications of Ferroelectrics (ISAF), Montreux, Switzerland, 225-258, (1998)

104)C.CAMPOS-POZUELO, B.DUBUS, J.A.GALLEGO-JUAREZ, “Numerical analysis of high intensity ultrasonic processing systems”, Proceedings of the 16th ICA/135th ASA meeting, Seattle, (1998).

105)J.COUTTE, J.C.DEBUS, B.DUBUS, R.BOSSUT, C.GRANGER, G.HAW, “Finite element modeling of PMN electrostrictive materials and application to the design of transducers”, Proceedings of the 1998 IEEE International Frequency Control Symposium, pp 703-708, (1998).

106)S.ALKOY, P.D.LOPATH, A.C.HLADKY, J.K.COCHRAN, R.E.NEWNHAM, “Piezoelectric Hollow Sphere Transducers” the 24th International Center for Actuators and Transducers Symposium, (ICAT), April 20-21, 1998, University Park, Pennsylvania.

107)A.GOZLAN, A.C.HLADKY-HENNION, “Simple Model of passive damping using piezoelectric materials”, 1998 ONR Transducer Materials and Transducers Workshop, 12-14 May 1998, University Park, USA

108)A.ELGHAOUTY, A.LAVIE, B.DUBUS, « Méthode des équations intégrales appliquée à la diffraction acoustique en régime temporel », journées GAPSUS, Lyon, (1998).

109)S.ALKOY, A.C.HLADKY-HENNION, J.K.COCHRAN, R.E.NEWNHAM, “PZT-polymer Composite hydrophones prepared from hollow ceramic spheres”, 100th American Ceramic Society 1998, Annual Meeting, Mai 1998, Cincinatti, USA

110)J.COUTTE, J.C.DEBUS, B.DUBUS, R.BOSSUT, C.GRANGER, G.HAW, “Design and testing of an ultrasonic electrostrictive transducer”, ONR transducer materials and transducers workshop, State College, (1998).

111)S.ALKOY, A.C.HLADKY-HENNION, J.K.COCHRAN, R.E.NEWNHAM, “Hollow Sphere Microprobe Hydrophones” 1998 ONR Transducer Materials and Transducers Workshop, 12-14 May 1998, University Park, USA

112)J.C. DEBUS, B. DUBUS, J. COUTTE, “Finite element modeling of lead magnesium niobate electrostrictive materials: static analysis”, J.Acoust. Soc. Am. 103-6, 3336-3343, (1998).

113)C. CAMPOS-POZUELO, A. LAVIE, B. DUBUS, G. RODRIGUEZ-CORRAL, J.A. GALLEGO-JUAREZ, “Numerical and experimental study of airborne acoustic field of stepped plate high-power ultrasonic transducers”, Acustica-Acta Acustica 84-6, 1042-1046, (1998).

114)D. EKEOM, B. DUBUS, C. GRANGER, “Coupled finite-element wave number decomposition method for the modeling of piezoelectric transducers in fluid-filled boreholes”, J.Acoust. Soc. Am. 104-5, 2779-2789, (1998).

115)C. CAMPOS-POZUELO, B. DUBUS, J.A. GALLEGO-JUAREZ, “Finite element analysis of the non linear propagation of high intensity acoustic waves”, J.Acoust. Soc. Am., 106-1, 91-101, (1999).

116)A.C.HLADKY-HENNION, P.LANGLET, R.BOSSUT, M.DE BILLY, “Finite element methods applied to the propagation of acoustic waves along immersed wedges”, 137 th ASA meeting, n°4pPAa, Berlin, (1999)

117)A.ELGHAOUTY, B.DUBUS, A.LAVIE, “A time-domain numerical model for the acoustic scattering from rigid or elastic targets”, communication 4aPAa8, 137th ASA meeting/Forum Acusticum 99, Berlin, (1999).

118)S.ALKOY, R.MEYER, A.C.HLADKY-HENNION, J.K.COCHRAN, R.E.NEWNHAM, “Miniature Omnidirectional Hydrophones and Directional Arrays from Piezoelectric Hollow Spheres”, 1999 ONR Transducer Materials and Transducers Workshop, 13-15 April 1999, University Park, USA

119)S.ALKOY, R.MEYER, A.C.HLADKY-HENNION, J.K.COCHRAN, W.J. HUGHES, R.E.NEWNHAM, “Omnidirectional Miniature Transducers and Directional Arrays from Piezoelectric Hollow Spheres”, 101st Annual Meeting of the American Ceramic Society, April 25-28, 1999, Indianapolis, Indiana.

120)B.DUBUS, J.C.DEBUS, R.BOSSUT, A.C.HLADKY, J.COUTTE, L.BUCHAILLOT, « Modélisation par éléments finis de la transduction électromécanique (piézoélectricité, piézomagnétisme, électrostriction) : formulation théorique et exemples d’applications », 2e réunion de travail MECAMAT couplages Multiphysiques, Versailles, (1999)

121)N.D. VEKSLER, A. LAVIE, B. DUBUS, “Peripheral waves generated in a cylindrical shell with hemispherical endcaps by a plane acoustic wave at axial incidence”, Wave Motion 31, 349-369, (2000).

122)M. DE BILLY, A.C. HLADKY-HENNION, R. BOSSUT, “On the localization of the antisymmetric flexural edge waves for obtuse angles”, Ultrasonics, 36, 995-1001, (1998).

123)M.DE BILLY, A.C.HLADKY-HENNION, “The effect of imperfections on acoustic wave propagation along a wedge waveguide”, Ultrasonics, 37, 413-416, (1999)

124)J. ZHANG, W.J. HUGHES, A.C. HLADKY-HENNION, R.E. NEWNHAM, “Concave Cymbal Transducers”, MRL, Material Research Innovation, 2, 252-255, (1999).

125)S.ALKOY, R.J.MEYER, A.C.HLADKY-HENNION, W.J.HUGHES, J.K.COCHRAN, R.E.NEWNHAM, “Hydrophone Arrays from piezoelectric Hollow Spheres” 1999 IEEE International Ultrasonics Symposium, Lake Tahoe, 18-21 October 1999.

126)S. ALKOY, A.C. HLADKY, A. DOGAN, J.K. COCHRAN, R.E. NEWNHAM, “Piezoelectric hollow spheres for microprobe hydrophones” Ferroelectrics, Vol. 226, n° 1-4, 11-25, (1999).

127)B. DUBUS, J.-C. DEBUS, J. COUTTE, « Modélisation de matériaux piézoélectriques et électrostrictifs par la méthode des éléments finis », Revue Européenne des Eléments Finis 8-(5-6), 580-606, (1999).

128)N.D.VEKSLER, B.DUBUS, A.LAVIE, “Acoustic wave scattering by an ellipsoïdal shell”, AC. Phys. 45-1, 53-58, (1999).

129)A.C. HLADKY-HENNION, P. LANGLET, M. DE BILLY, “Conical radiating waves in immersed wedges” J. Acoust. Soc. of America, 108(6), 3079-3083 (2000).

130)L.BUCHAILLOT, S.RAFANOMEZANTSOA, A.C.HLADKY-HENNION, I.ROCH, “Numerical modelling of shape memory alloy nonlinear behavior laws : application to an adaptative structure”, Proceedings of Shape Memory and Superelastic Technologies (SMST), Pacific Grove, Monterey, (2000).

131)S.ALKOY, R.J.MEYER, A.C.HLADKY-HENNION, W.J.HUGHES, J.K.COCHRAN, R.E.NEWNHAM, “Transducer arrays from piezoelectric Hollow Spheres”, 2000 IEEE International Symposium on Applications of Ferroelectrics, (ISAF), Août 2000, Honolulu, (2000).

132)B.DUBUS, C.CAMPOS-POZUELO, “Numerical modeling of high power ultrasonic systems: current status and future trends”, communication invitée, Ultrasonics 38-(1-8), 337-344, (2000).

133)J.COUTTE, E.LENGLET, B.DUBUS,”Numerical modeling of magnetostrictive materials using the finite element code ATILA”, 2000 US Navy workshop on Acoustic transduction materials and devices, State College, (2000).

134)R.E.NEWNHAM, J.ZHANG, A.C.HLADKY-HENNION, J.TESSLER, W.J.HUGUES, R.MEYER, “Cymbal transducers”, 2000 ONR Workshop on Acoustic Transduction Materials and Devices, 11-13 April 2000, University park, USA.

135)J.ZHANG, J.HUGUES, A.C.HLADKY-HENNION, R.E.NEWNHAM, “Underwater characteristics of cymbal transducers and arrays”, 2000 ONR Workshop on Acoustic Transduction Materials and Devices, 11-13 April 2000, University park, USA

136)S.ALKOY, R.MEYER, A.C.HLADKY-HENNION, W.J.HUGUES, J.K.COCHRAN, R.E.NEWNHAM, “Arrays and piezocomposite transducers from hollow spheres”, 2000 ONR Workshop on Acoustic Transduction Materials and Devices, 11-13 April 2000, University park, USA

137)A.C.HLADKY-HENNION, S.RAFANOMEZANTSOA, L.BUCHAILLOT, “Numerical modelling of shape memory alloy nonlinear behavior laws : application to an adaptative structure”, 2000 ONR Workshop on Acoustic Transduction Materials and Devices, 11-13 April 2000, University park, USA

138)J.ZHANG, A.C.HLADKY-HENNION, P.BOUCHILLOUX, R.E.NEWNHAM, “Modeling of cymbal Transducers and arrays”, ATILA workshop, 14 April 2000, University Park, USA.

139)A.C.HLADKY-HENNION, S.RAFANOMEZANTSOA, L.BUCHAILLOT, “Numerical modelling of shape memory alloy nonlinear behavior laws : application to an adaptative structure”, ATILA Workshop, 14 April 2000, University park, USA

140)N.D.VEKSLER, B.DUBUS, A.LAVIE, “Acoustic wave scattering from a composed shell reinforced by a single rib: characteristics of peripheral waves”, Ultrasonics 38-(1-8), 838-841, (2000).

141)A.LAVIE, B.DUBUS, A.ELGHAOUTY, “Acoustic scattering in time domain using the boundary element method”, Actes du 5ème Congrès Français d’Acoustique, Presses Polytechniques et Universitaires Romandes, 129-133, (2000)

142)J.COUTTE, E.LENGLET, B.DUBUS, « Modélisation non linéaire de matériaux magnétostrictifs pour l’analyse statique », Actes du 5ème Congrès Français d’Acoustique, Presses Polytechniques et Universitaires Romandes, 637-640, (2000)

143)J.-C.DEBUS, J.COUTTE, B.DUBUS, “Non-linear analysis of electrostrictive materials by the finite element method”, Proceedings of the acoustics week in Canada 2000, Acoustique Canadienne 28-3, 34-37, (2000)

144)A.C.HLADKY-HENNION, S.RAFANOMEZANTSOA, L.BUCHAILLOT, “Finite Element Modeling of smart materials: application to an adaptive structure using SMA”, Proceedings of 3rd CanSmart Workshop on Smart Materials and Structures, September 28-29 2000, St Hubert, Quebec, Canada, pp 133-142.

145)A.C.HLADKY-HENNION, C.GRANGER, “Finite element modeling of damping using piezoelectric materials”, Semaine de l’Acoustique Canadienne, Sherbrooke, 28-29 September 2000, Proceedings Vol 28, N°3, 64-65.

146)B.CUGNET, J.ASSAAD, A.C.HLADKY-HENNION, F.HAINE, “Influence of the quarter wave matching layers on the response of bar transducers”, 2000 IEEE International Ultrasonic Symposium, Porto-Rico, Volume 2, 1135-1138, (2000)

147)J. ZHANG, A.-C. HLADKY-HENNION, W.J. Hughes, R.E. Newnham, “Modeling and underwater characterization of cymbal transducers and arrays”, IEEE, Transactions on Ultrasonics, Ferroelectrics and Frequency Control, Vol. 48, n°2, 560-568, (2001).

148)J. ZHANG, A.-C. HLADKY-HENNION, W.J. Hughes, R.E. Newnham, “A miniature class V flextensional cymbal transducer with directional beam patterns: the double-driver”, Ultrasonics 39, 91-95, (2001).

149)J.COUTTE, J.-C.DEBUS, R.BOSSUT, B.DUBUS, “Finite element modeling of lead magnesium niobate electrostrictive materials: dynamic analysis”, J.Acoust., Soc. Am., 109-4, 1403-1411, (2001)

150)J.C. DEBUS, “Latest developments in ATILA Thermal Computations”, Proc. 2nd Annual ATILA Workshop in U.S., Baltimore, (May 2001)

151)B.DUBUS, C.CAMPOS-POZUELO, “A numerical model of the ultrasonic cavitation in liquids”, 17th International Congress on Acoustics, Rome, (2001)

152)J.-C. DEBUS, B. DUBUS, C. GRANGER, A.-C.HLADKY-HENNION, P. MOSBAH, P. BOUCHILLOUX, “Design and analysis of piezoelectric transducers using the finite element method”, Piezoelectric Materials for the End User Symposium, February 24-27, Interlaken, Switzerland

153)A.C.HLADKY-HENNION, S.RAFANOMEZANTSOA, L.BUCHAILLOT, P.BOUCHILLOUX, “Finite element modeling of smart materials: application to an adaptive structure using SMA”, to be published in “Modeling, Signal processing and Control in Smart Structures”, Proceedings of the conference, SPIE 2001, Newport Beach, March 2001

154)B.CUGNET, A.-C.HLADKY-HENNION, J.ASSAAD, “Numerical technique to reduce the cross coupling in acoustical arrays», Ultrasonics International 2001, Delft, Netherlands, 3-5 july 2001

155)E.LENGLET, A.-C.HLADKY-HENNION, E.DELETOMBE, “Numerical homogenization techniques applied to active fiber composites», 17th International Congress on Acoustics, Rome, 2-7 september 2001

156)A.-C.HLADKY-HENNION, M.DE BILLY, “Study of the propagation of compressional acoustic waves through curved bodies», au 17th International Congress on Acoustics, Rome, 2-7 september 2001

157)R.-E.NEWNHAM, J.ZHANG, S.ALKOY, R.MEYER, W.-J. HUGHES, A.-C.HLADKY-HENNION, J.COCHRAN, D.MARKLEY, “Cymbal and BB underwater transducers and arrays», proceeding of 10th US-Japan Seminar on Dielectric and Piezoelectric Ceramics, Providence, R.I., Sept 27-29 2001

158)R.-E.NEWNHAM, S.ALKOY, A.-C.HLADKY-HENNION, W.-J. HUGHES, D.MARKLEY, R.-J. MEYER, J.ZHANG, “Underwater flat-panel transducer array», Oceans 2001 MTS / IEEE, Honolulu, Hawaii, Novembre 5-8 2001

159)J.COUTTE, B.DUBUS, J.-C.DEBUS, C.GRANGER, “From finite element modeling of PMN electrostrictive materials to the realization and testing of Langevin type transducers”, Communication invitée, Ultrasonics International 2001, Delft, (2001)

160)C.CAMPOS-POZUELO, C.VANHILLE, B.DUBUS, “Numerical modelling of some problems in non linear acoustics”, Proceedings af the 17th International Congress on Acoustics, Vol. II (2001)

161)E. LENGLET, A.-C.HLADKY-HENNION, J.-C. DEBUS, Numerical homogenization techniques applied to piezo-composites”, soumis pour publication au J. Acoust. Soc. of America, (2002)

162)A.-C.HLADKY-HENNION, F.COHEN-TENOUDJI, A.DEVOS, M. DE BILLY, “On the existence of “sub-resonance» generated in a one-dimensional chain of identical spheres», accepté pour publication au J.Acoust. Soc. of America, (2002)

163)M. BERRAKI, B. DUBUS, A. BARONI, Radiation of directional seismic sources in an elastic half space, Proceedings of the EAGE 65th Conference and Exhibition, Z-99, (2003).

164)M. BERRAKI, B. DUBUS, A. BARONI, Rayonnement de sources directionnelles enfouies dans un demi-espace élastique, Actes des Journées du GDR Ultrasons, (2003).

165)JC.DEBUS, P.MOSBAH, Finite element modeling of transducers using ATILA code”; 6th CanSmart Meeting International Workshop Smart Materials & Structures, Montreal, October 2003, (Keynote presentation).

166)R.E. NEWNHAM, D.C. MARKLEY, R.J. MEYER, JR., W.J. HUGHES, A.-C. HLADKY-HENNION, J.K. COCHRAN, JR., “ Multimode Underwater Transducers,” American Ceramic Society Bulletin, vol. 83, n° 9, 25-28, (2004).

167)J. ASSAAD, A.-C.HLADKY, B. CUGNET, “Application of the FEM and the BEM to compute the field of a transducer mounted in a rigid baffle (3D case), Ultrasonics, vol 42, n°1-9, 443-446, (2004).

168)DOGAN, A.E. UZGUR, R.J. MEYER, A.C. HLADKY-HENNION, R.E. NEWNHAM, “ Materials for High Performance Cymbal Transducer, Journal of Electroceramics, 13, 403-408, (2004).

169)R.E. NEWNHAM, D.C. MARKLEY, R.J. MEYER, JR., W.J. HUGHES, A.-C. HLADKY-HENNION, J.K. COCHRAN, JR., “ Multimode Underwater Transducers,” Ceramic Transactions 150, 427-443, (2004).

170)A.-C.HLADKY-HENNION, R.E. NEWNHAM, D.C. MARKLEY, R.J. MEYER, J.K. COCHRAN, “The Wagon-Wheel transducer as a vector sensor and a directional projector, Proceedings of Actuators 2004, pp 747-750, Juin 2004, Bremen, Allemagne.

171)A.-C. HLADKY-HENNION , R.J. MEYER JR., D.C. MARKLEY, J.K. COCHRAN , R.E. NEWNHAM, “ The wagon-wheel transducer as a vector sensor and a directional projector,” Proceedings of the 106th Annual Meeting of the American Ceramic Society, vol CT169, p. 17-37 (2004).

172)A.C. HLADKY-HENNION, R.E. NEWNHAM, D.C. MARKLEY, R.J. MEYER, J.K. COCHRAN, “Design and fabrication of miniature and monolithic transducers”, International Conference on Material Technology and Design of Integrated Piezoelectric Devices, Courmayeur, Italie, 2-4 Février 2004.

173)D.C. MARKLEY, R.E. NEWNHAM, A.C. HLADKY-HENNION, J.K. COCHRAN, R.J. MEYER, A. SAFARI, M. ALLAHVERDI, “Monolithic Multimode Transducers prototyped using extrusion and fused deposition of ceramics (FDC) techniques”, 2004 US Navy Workshop on Acoustic Transduction Materials and Devices, 11-13 mai 2004, State College, PA, USA.

174)R.E. NEWNHAM, D.C. MARKLEY, , R.J. MEYER, A.C. HLADKY-HENNION, J.K. COCHRAN, “PZT vector sensor”, 2004 US Navy Workshop on Acoustic Transduction Materials and Devices, 11-13 mai 2004, State College, PA, USA.

175)R.E. NEWNHAM, D.C. MARKLEY, , R.J. MEYER, A.C. HLADKY-HENNION, J.K. COCHRAN, “Cymbal Transducers under pressure”, 2004 US Navy Workshop on Acoustic Transduction Materials and Devices, 11-13 mai 2004, State College, PA, USA.

176)D.C. MARKLEY, R.J. MEYER, R.E. NEWNHAM, A.-C.HLADKY-HENNION, “Miniature flextensional piezoelectric transducers with rectangular geometry for improved in-water acoustic bandwidth and power, 2004 IEEE International Ultrasonics, Ferroelectrics, and Frequency Control Joint 50th Anniversary Conference, P1U-M1-E1, Montreal, QC, Canada.

177)D.C. MARKLEY, R.E. NEWNHAM , A.-C.HLADKY-HENNION, J.K. COCHRAN, R.J. MEYER, A. SAFARI, M. ALLAHVERDI “Monolithic, multimode transducers prototyped using extrusion and fused deposition of ceramic (FDC) techniques, 2004 IEEE International Ultrasonics, Ferroelectrics, and Frequency Control Joint 50th Anniversary Conference, P1U-M1-E4, Montreal, QC, Canada.

1.3 General Organization of an ATILA job

A computation using **ATILA** is carried out in different steps, all accessible through the supervisor (see Chapter 1.4). This section briefly describes these steps and refers to the corresponding sections for additional information.

1.3.1 Model Definition

For a given physical problem, the user must define the kind of analysis needed, for example: computation of the static deformation of an elastic structure under a concentrated mechanical load, electrical short-circuited modal analysis of a piezoelectric ceramic stack, or computation of the transmitting voltage response of a transducer. This type of analysis is linked to solving subroutines described in Chapter 2. The user must also choose the type(s) of elements needed to describe the region under study: elastic, piezoelectric, magnetostrictive or fluid elements, bi-dimensional, three-dimensional or axisymmetrical elements, plane stress, plane strain, plate or shell elements, etc.
At this point, a first estimation of the computation size can generally be made by estimating the number of nodes, elements, and degrees-of-freedom. Also at this point, the user must gather all the physical parameters described in Chapter 3 and ensure their accuracy, which determines the accuracy of the final results. **This step is essential**.

1.3.2 Mesh Generation

Mesh generation involves the splitting of the aforementioned region under study into elements. This is accomplished by defining the nodes and by specifying their coordinates in a given order, called node-numbering order. Then, the elements are described by listing the nodes for each element in a given order, called topology. Chapter 3.3.26 describes the node coordinates and the topology. A detailed library of elements is presented in Chapter 4.2.
During the mesh generation, the user can use all the **ATILA** elements. These elements allow curved line modelling and lower density meshes. However, it is essential to ensure the validity of the geometrical aspect of the elements as well as the mesh size. In general the maximum permissible size of mesh spacing is related to the smallest acoustic wavelength used.
Mesh generation can be carried out completely by the user. However, in most cases, the structure's shape allows the use of an automatic mesh generator, which creates node coordinates and element topologies. If using **MOSAIQUE**, the user has only to define a gross splitting based on "super elements", and to select for each of them their automatic splitting into finite elements. This procedure is described in Chapter 5.2. **ATILA** may also be interfaced to other commercially available mesh generators (IDEAS, PREFLU, GID, etc.). Please contact the Chairman for more information.

1.3.3 Data File Preparation

The **ATILA** data file describes the type of analysis, the node coordinates, the element topology, the physical properties of the materials and the geometrical properties of the elements, the loading and excitation data and the boundary conditions. Chapter 3 describes the complete data file preparation and must be read carefully. Specific element information can be found in Chapter 4.2. Finally, when the automatic mesh generation code **MOSAIQUE** is used, the data entry file can largely be obtained automatically. An example of such a data file appears in Part II.
Checking the data file can be done by displaying the mesh using the program **WMDES**, accessible through the "Draw the mesh" button on the supervisor (see Page 19 for more details). The generated mesh can be seen on the screen or printed out on a graphics printer (with choice of total or partial mesh, and with or without node and element numbering).

1.3.4 Running a Job

The solver is launched using the supervisor (seeGeneral Organization of the ATILA supervisor Page 17 for more details). The solver is the interface to the program that sets the array sizes, calls up the subroutines for reading the data files, computes the elementary matrices, assembles these matrices into global matrices, solves the equations, and stores the results. It creates a results file and several data files for post-processing.

1.3.5 Using the Results and Post Processing

An example of a results file is given in Part III. After each run, a file containing the results (frequencies and eigenvectors, displacement and pressure fields, electrical impedance) is available. If desired, specific data are also stored for post-processing. A graphic display of the distorted structure, the voltage response, the directivity patterns or the parallel resistance and capacitance plot can be easily obtained by using the programs **WMDES**, **WPLOTSV**, **WPATTERN** and **WPLOTRPCP** now accessible through the supervisor. Animated views of the vibrating structure are also available with the program **ATILANIM**. Their use is described in Chapter 1.7.6.1

The user can also utilize **WISOVAL** to plot contours of constant value (isodisplacements, isopotentials, isopressures, isostresses, etc.) on the modeled structure**. WISOVAL** can be used only if the generation of the PST file was requested in the input data file.

1.3.6 Summary

In summary, the next page displays a simple flow chart of an **ATILA** finite-element job. Note that all these steps can be done using the supervisor; this will be detailed in the next section (see Page 19).

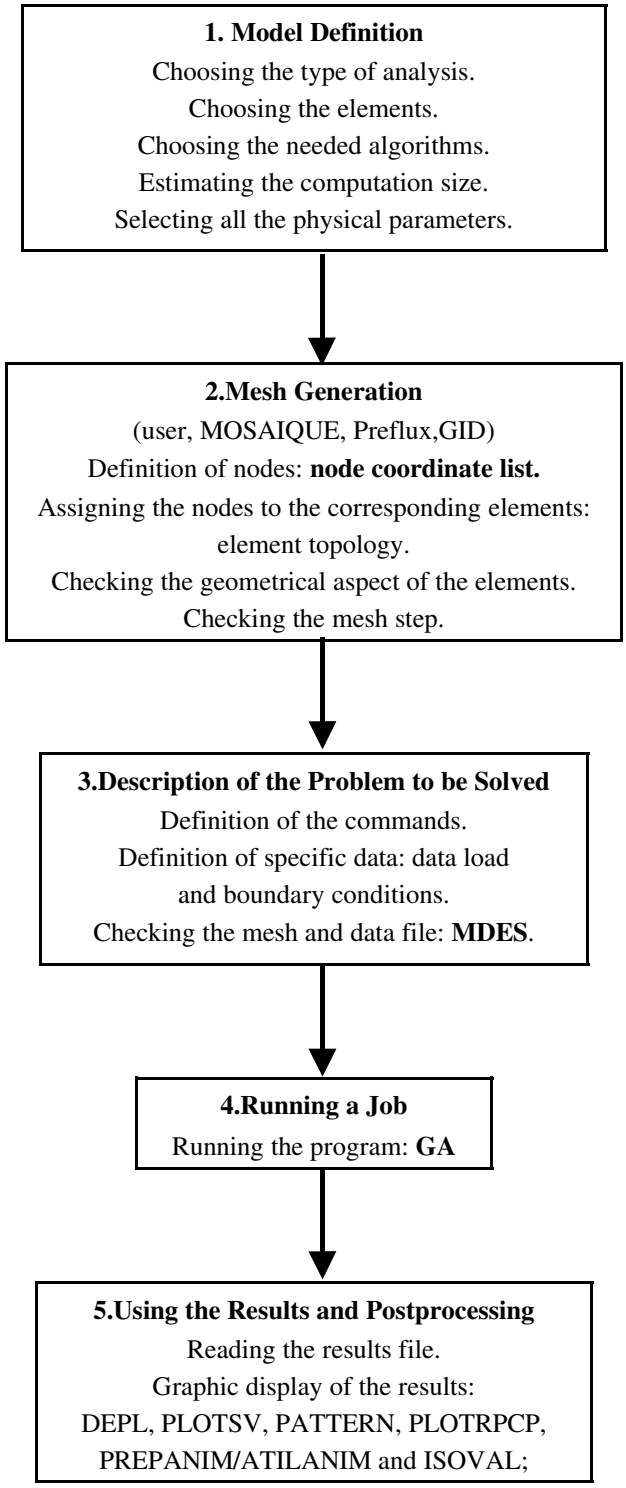

1.4 General Organization of the ATILA supervisor

This chapter describes how to run the **ATILA** program using the supervisor. The example selected is an in-water harmonic analysis of an axisymmetrical, radiating Tonpilz transducer (HAS04). This example was also used in Chapter 6.22 to describe the input data.
As discussed above, a computation using **ATILA** is carried out in 3 main steps. Each section briefly describes each step. The final section presents the many options available in the **ATILA** supervisor.

1.4.1 Preprocessor

After the definition of the model (type of analysis, choice of the elements, estimation of computation size, etc.), the mesh is generated either by the user or by **MOSAIQUE** and checked using a graphic display (Page 19).
Other currently available preprocessors consist of Preflu2D/3D and Preati as well as GID and its ATILA-GID interface. The corresponding Preflu2D/3D buttons on the ATILA supervisor are enabled when these modules are installed on your computer .

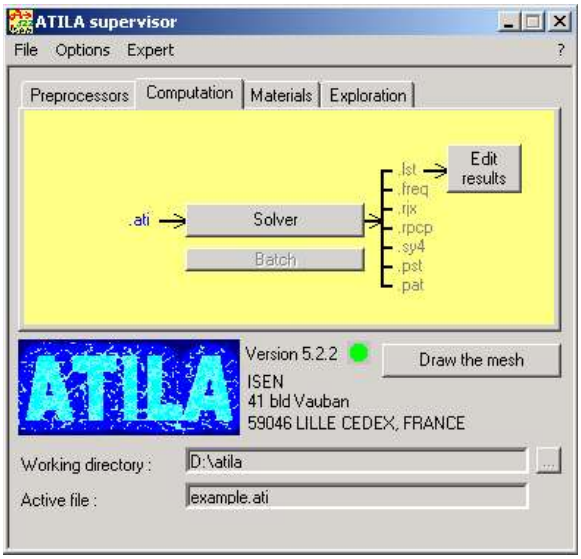

1.4.2 Computation

Using the **.ati** file, the problem is solved and provides a results file and files containing arrays for post-processing (chaper 1.7).

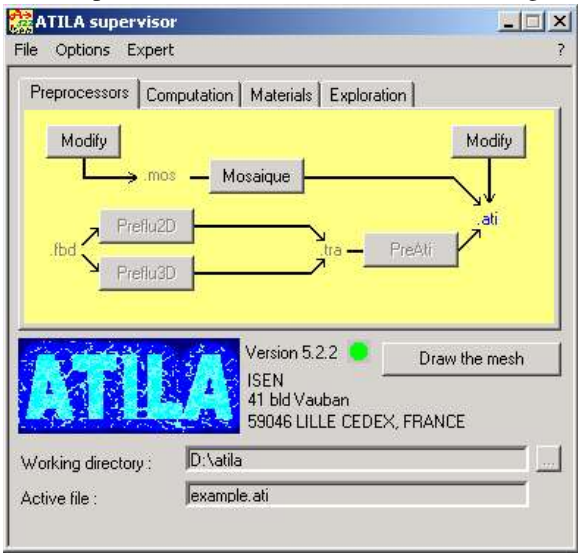

1.4.3 Exploration

The results file is analyzed in this section, through a file containing the results, graphic displays or animated views of the vibrating structure. The results analysis helps the designer to understand the physical behavior of the problem (Chapter 1.7).

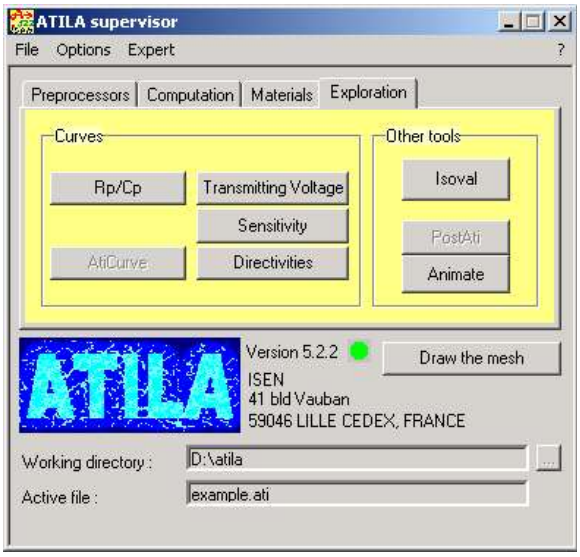

1.5 Preprocessors

First, for a given physical problem, the user must define the kind of analysis required (static, modal, harmonic, transient). The user must also choose the type(s) of elements needed to describe the region under study: elastic, piezoelectric, magnetostrictive or fluid elements, bi-dimensional, three-dimensional or axisymmetrical elements, plane stress, plane strain, plate or shell elements, etc.

1.5.1 Mesh Generation

Mesh generation can be carried out completely by the user. However, in most cases, the structure's form enables the use of an automatic mesh generator, which creates node coordinates and element topologies. Thus, the user has only to define a gross division based on "super elements", and to select for each of them their automatic division into finite elements. The corresponding file, named ***.mos** and described in Chapter 5.2, can easily be changed using the **Modify** button of the supervisor. The **MOSAIQUE** procedure automatically transforms the "super elements" into finite elements used by **ATILA**. The resulting file is an **.ati** file.

The **ATILA** data file describes the type of analysis, the node coordinates, the element topology, the physical properties of the materials and the geometrical properties of the elements, the loading and excitation data and the boundary conditions. Chapter 3 describes the complete preparation of the data file and should be read carefully. Finally, when the automatic mesh generation code **MOSAIQUE** is used, the data entry file can largely be obtained automatically. It is possible to change data in the **.ati** file using the **Modify** button.

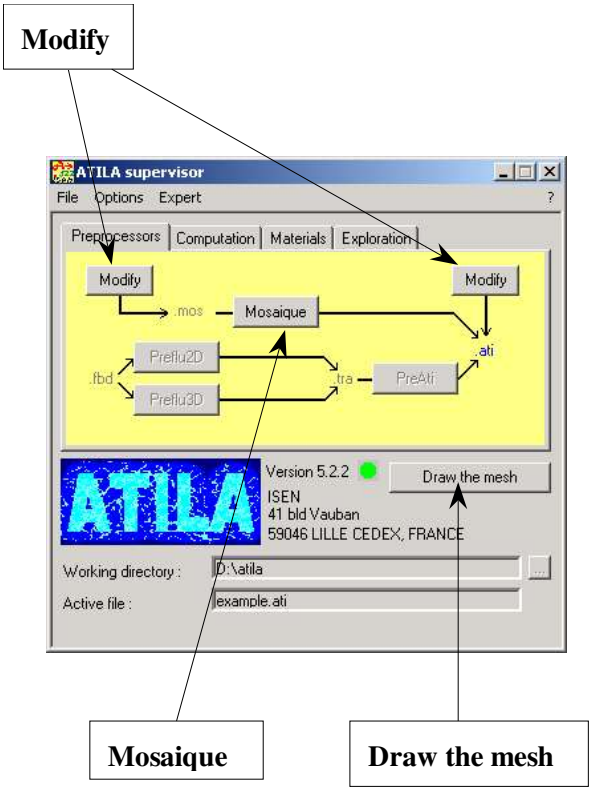

Checking the data file can be done with the **Draw the mesh** button. The generated mesh is shown directly on the screen. Many commands are available under these three menus: **File, Edit** and **Options.**

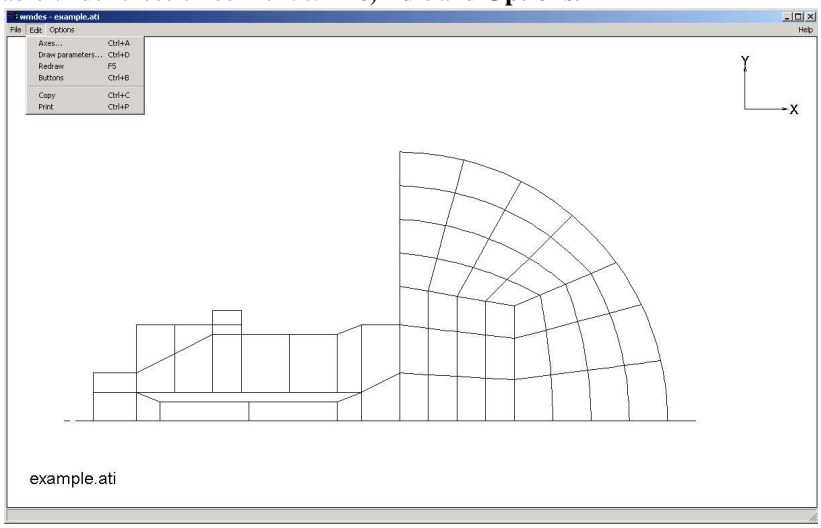

The File menu commands open another file, saves the drawing or quits the program.

The **Edit** menu contains several commands:

Axes sets the view angle respective to the mesh. The initial viewing direction shows the Oz axis pointing towards the viewer, so that the surface of the screen or paper is parallel to the x0y plane. For a tridimensional mesh, it is possible to change Theta and Phi angles. Theta is the angle from the 0z axis to the view point, while Phi is the angle from 0x axis to the projection of the view point on the x0y plane.

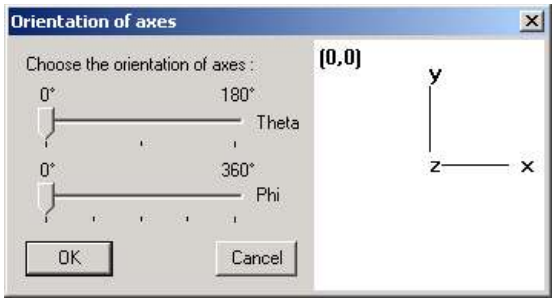

Initially, a **Simple mesh** is presented. With **Draw parameters** you can select the drawing or display method.

Simple mesh is used for an unexploded view of the mesh. The elements are shown with a full line. Nodes do not appear.

Exploded mesh is used for an exploded view of the mesh without node numbering. The elements are shrunk by a small factor and shown with a full line.

Exploded mesh with node numbers is used for an exploded view of the mesh with node numbering. The elements are shrunk by a small factor and shown with a full line. Nodes are shown as small circles, with numbering close to them.

Exploded mesh with element numbers is used for an exploded view of the mesh with element numbering. The elements are shrunk by a small factor and shown with a full line. Nodes are shown as small circles. Element numbering appears near the element's center.

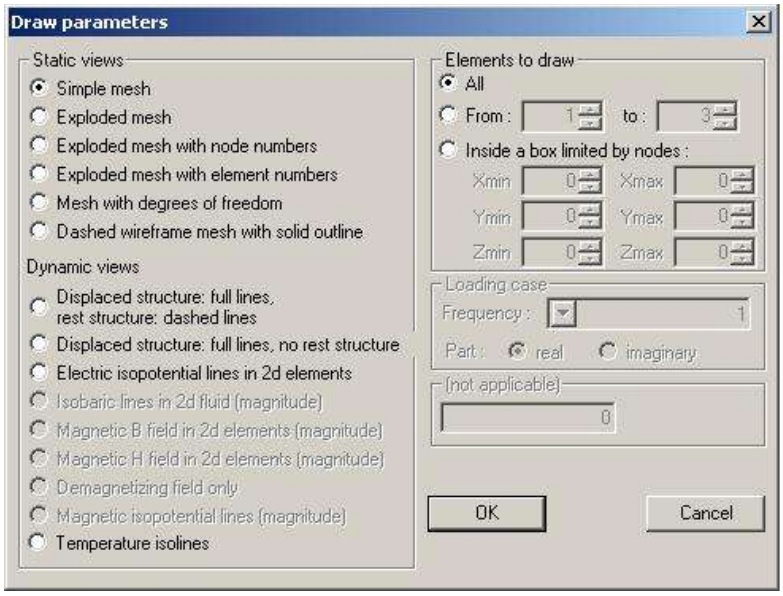

Mesh with degrees of freedom is used for an unexploded view of the mesh, with degrees of freedom shown as small vectors. The elements are shown with a dashed line. On each node is shown a series of vectors, corresponding to the direction of active degrees of freedom. Displacements U_x, U_y and U_z are shown with a simple arrow. Rotations θ_x, θ_y and θ_z are shown with a double arrow. Pressures are shown like U_x. Potentials are shown like θ_x. Excitation currents are not shown.

Dashed wireframe mesh with solid outline is used for an unexploded view of the mesh with dashed inside lines. The elements' vertices are shown with a full line if not connected to other elements; otherwise, they are shown with a dashed line. Nodes do not appear.

Together with the previous buttons, it is possible to select the **elements to draw**, by entering the numbers of the first and last shown element (**from** and **to** boxes). When the **all** button is used, the whole structure is shown. The user may also restrict the display to a parallelepiped box whose limits are given in the **Xmin, Xmax, Ymin, Ymax, Zmin** and **Zmax** boxes.

It is possible to use a zoom by pressing **shift Z** on the keyboard.

Redraw, copy and **print** are also commands available under the **Edit** menu. The drawing can be integrated in most Windows applications.

The **Options** command changes the language (**English** or **French**). It defines the language used for the entry input and output. In France, the default language is French; in other countries, it is English.

1.6 Computation

Clicking on the **Solver** button performs the **ATILA** computation, using the interface to the program that sets the array sizes, calls up the subroutines for reading the data files, computes the elementary matrices, assembles these matrices into global matrices, solves the equations, and stores the results. At the end, the computation will provide a results file and files containing arrays for post-processing.

After each run, the **.lst** file is available, containing the results (frequencies and eigenvectors, displacement and pressure fields, electrical impedance). It can be edited using the **Edit result** button. If desired, specific arrays are also stored for post-processing.

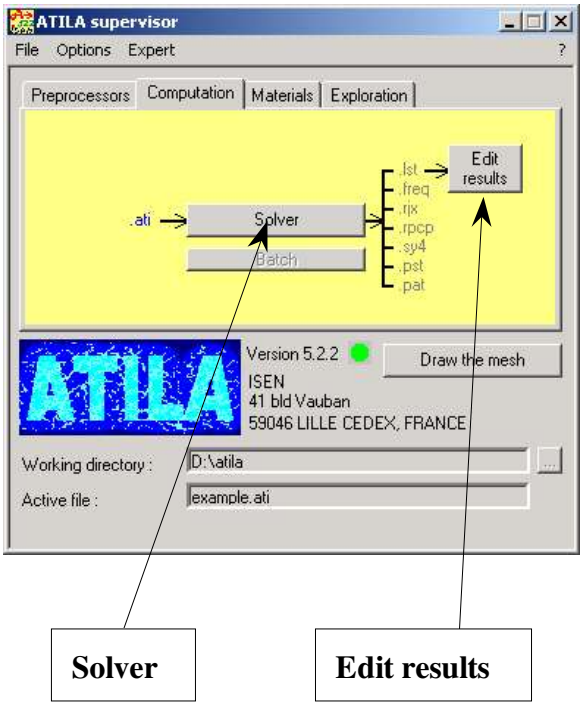

Solver **Edit results**

1.7 Exploration

Together with the results file, a graphic display of the distorted structure (**Draw the mesh**), the voltage response (**Transmitting Voltage**), the sensitivity (**Sensitivity**), the directivity patterns (**Directivities**), or the parallel resistance and capacitance plot (**Rp/Cp**) can easily be obtained using the **ATILA** exploration supervisor. Animated views of the vibrating structure (**Animate**) are also available.

The user can also use **ISOVAL** to plot contours of constant value (isodisplacements, isopotentials, isopressures, isostresses, etc.) on the modeled structure**. ISOVAL** can be used only if the generation of the PST file was requested in the job's data file (see Chapter 3.3.12). Each of these commands is described below.

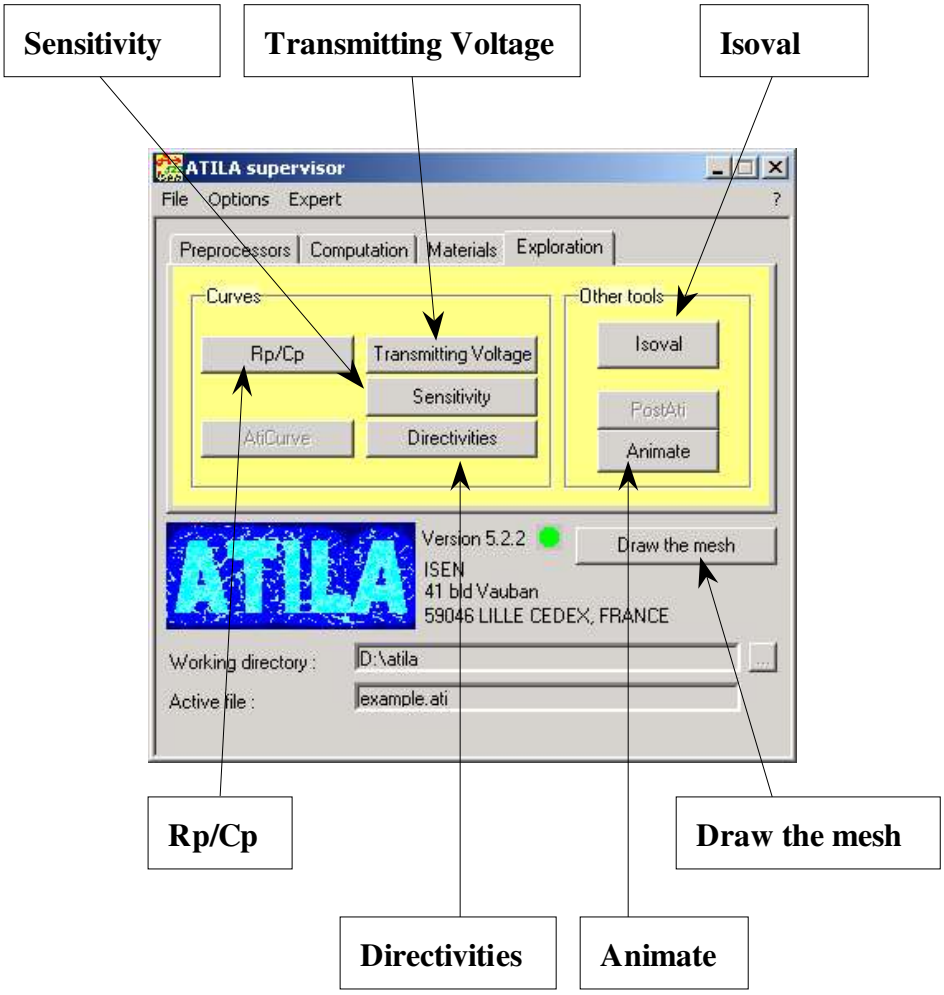

Note that the **AtiCurve** and **PostAti** buttons are enabled when the Preflu2D/3D and Preati modules are installed.

1.7.1 Rp/Cp

When dealing with underwater piezoelectric transducers, the designer needs to know the electrical impedance, generally given as an equivalent parallel circuit composed of a resistance and a capacitance. The **Rp/Cp** button provides plots of the values of these two components against the frequency. Using the **Copy** command, the data can be copied to an Excel file.

The frequencies provided in the data file are plotted by fitting a spline curve to the input data. The values of the parallel resistance and of the parallel capacitance as a function of the frequency are in the **.rpcp** file. Similarly, the **.rjx** file contains the real part and the imaginary part of impedance for each input frequency.

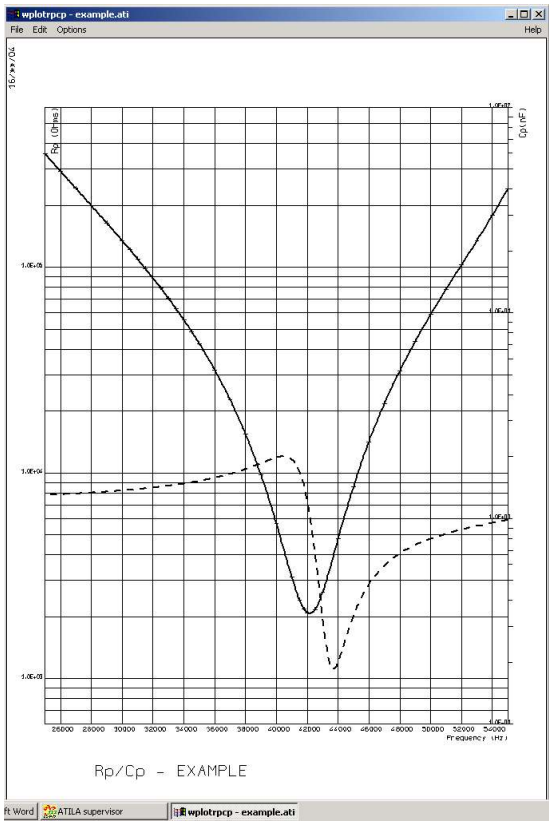

Using the **Draw parameter** button, one can choose a **linear** scale or a **logarithmic** scale for the frequency axis. Moreover, the frequency can be normalized (**Reference frequency**).

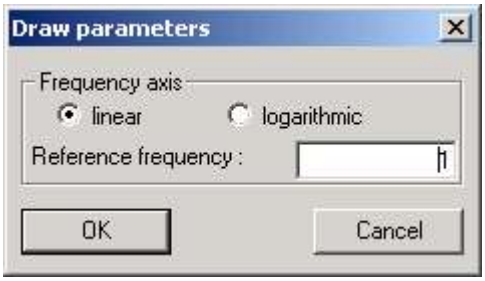

1.7.2 Remark

If the symmetries detected by the solver are incorrect, the user has to correct the values of Rp/Cp as well as the values of RjX.

1.7.3 Transmitting Voltage and Sensitivity

When dealing with underwater piezoelectric transducers, the designer needs to know the far field pressure in the fluid medium and its spatial distribution. He might also need to find out its sensitivity, which can be calculated from the transmitting voltage response and the electrical impedance via the reciprocity equation. The directivity index may also be valuable information. These parameters are available using the **Transmitting Voltage** button and the **Sensitivity** button.
The transmitting voltage response is the magnitude of the far field pressure, expressed in dB, ref. 1 µPa/Volt at 1m.

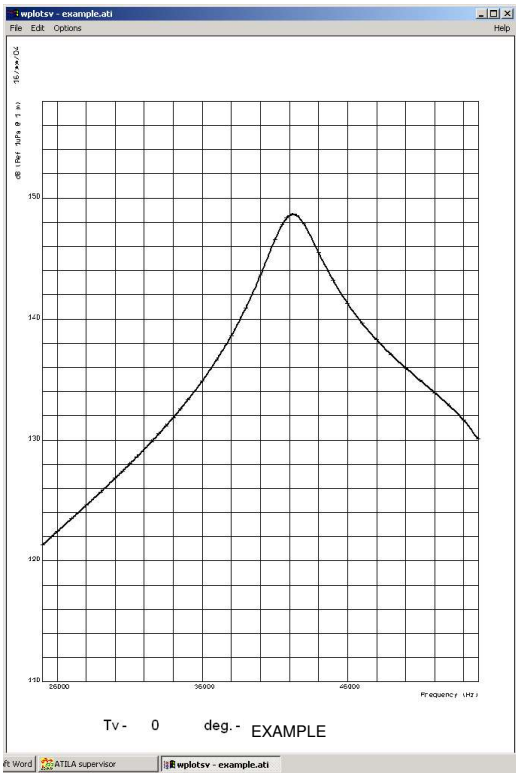

The sensitivity (voltage magnitude measured on the transducer for an incoming plane wave) is expressed in dB ref. 1 Volt/µPa:

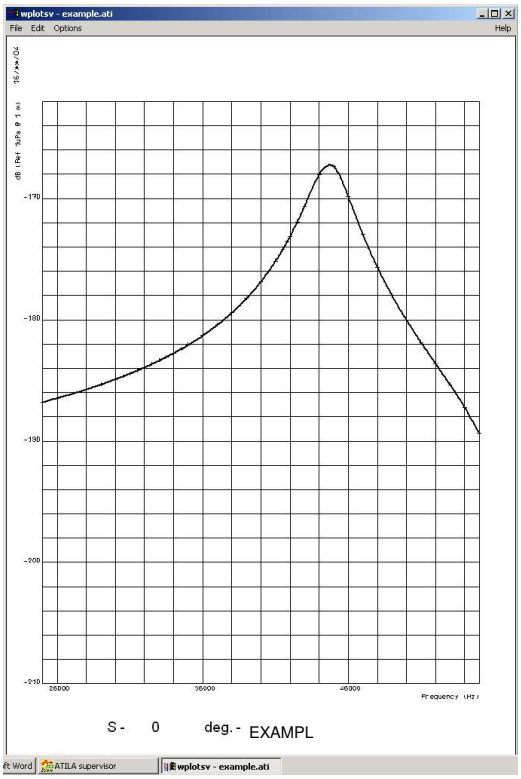

These plots are made for different directions, as a function of the frequency. The **Copy** command enables you to store the values in an Excel file.

Using the radio buttons appearing in the **Draw parameters** dialog, the **directivity index** (for a bidimensional structure) can be plotted. It describes the increase of source level compared to the omnidirectional case. The user can also change the **direction** in which **Sensitivity**, **Transmitting Voltage** and **Directivity index** are calculated. Moreover, it is possible to introduce the **Cable capacitance** that can affect the transducer impedance, to choose a **linear** or **logarithmic** scale, and to normalize the frequency (**Reference frequency**).

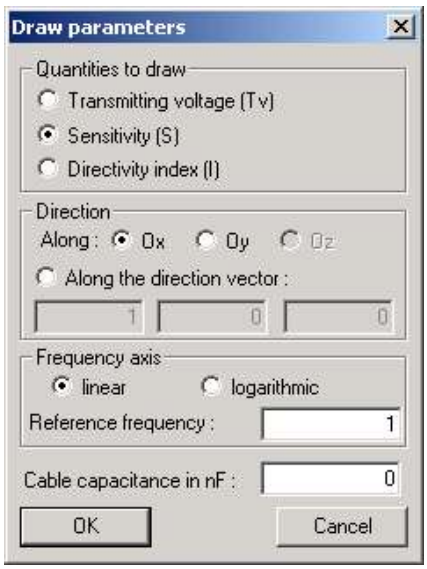

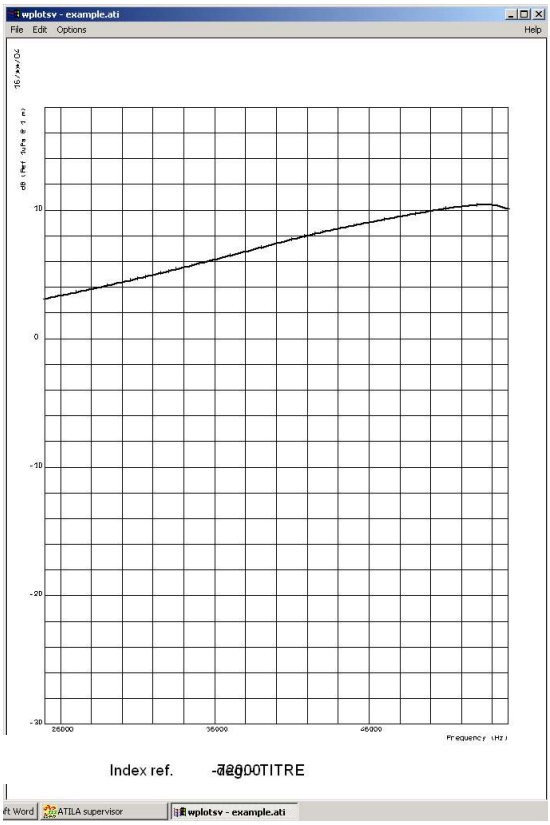

In the **.ATI** data file, the user must ensure that the excitation voltage magnitude is 1 Volt (which is the reference level). The frequencies provided in the data file are plotted by fitting a spline curve to the input data.

1.7.4 Directivities

When dealing with underwater piezoelectric transducers, the designer needs to know the far field pressure in the fluid medium and its spatial distribution. The aim of the **Directivities** button is to provide plots of the far field directivity patterns for several frequencies.
In the **.ati** data file, the user must ensure that the excitation voltage magnitude is 1 Volt (which is the reference level). Patterns are plotted by fitting a spline curve to the computed data.

Directivities uses a **.pat** file containing information about the far field pressure that the **ATILA** solver creates. This file can be recreated from the **.sy4** file (which is also created during the computation).

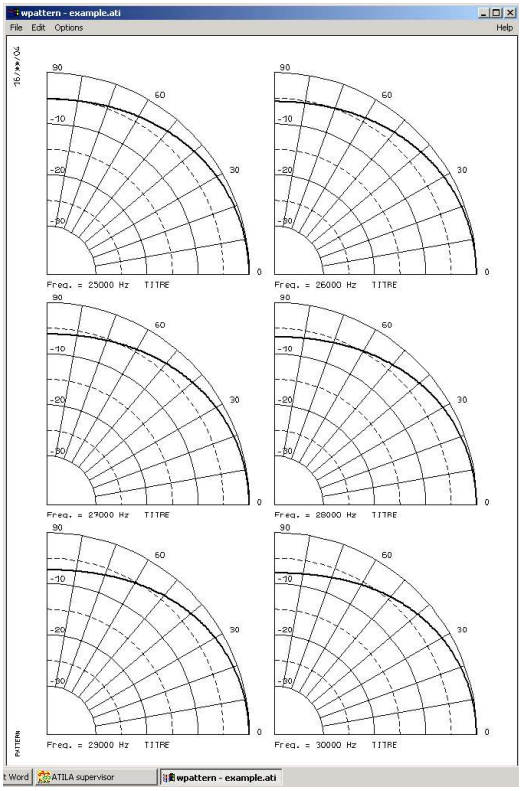

Initially, a quarter of the directivity pattern is drawn for the first six frequencies. Using the **Draw parameters** dialog, it is possible to plot 1, 2 or 4 quadrants. Using the **Copy** command, the diagrams can be inserted into any text file.

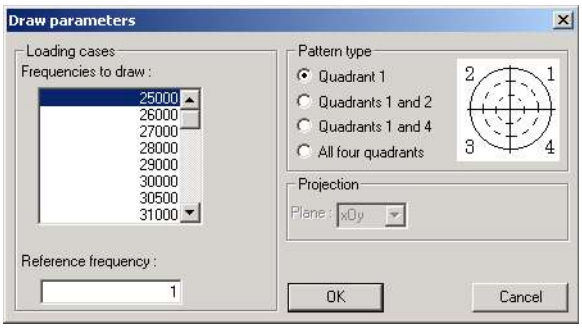

1.7.5 Draw the mesh

Initially, a **Simple mesh** is displayed. **Draw parameters** modifies the display. The buttons are similar to those from pre-processing, except that **Draw parameters** reads a **.sy4** file created after solving the problem with **ATILA**, instead of the data file. It also has buttons for dynamic views that are described below.

Displaced structure: full lines, rest structure: dashed lines. This option is used to plot the deformed shape of a structure. The solid elements of the structure at rest are shown with a dashed line, while those of the deformed shape are shown with a full line. Fluid elements and nodes do not appear.

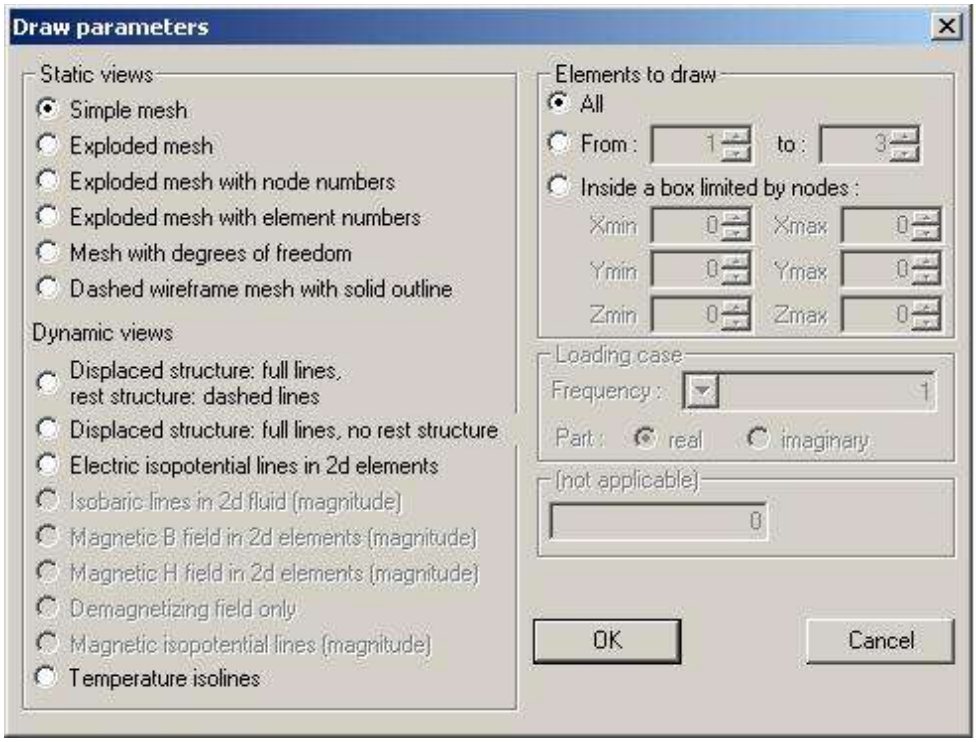

The user can modify the selected **frequency** (harmonic or modal analysis) or selected time (transient analysis), and the **displacement scale**. No frequency value is requested for a static analysis or when solving was performed for one frequency or time only. When a complex solver has been used, two graphics are provided. These correspond to the real and imaginary parts of the displacement (remember that the real displacement is the real part of the product of the complex displacement and the time dependency, which is $e^{j\omega t}$ in **ATILA**).

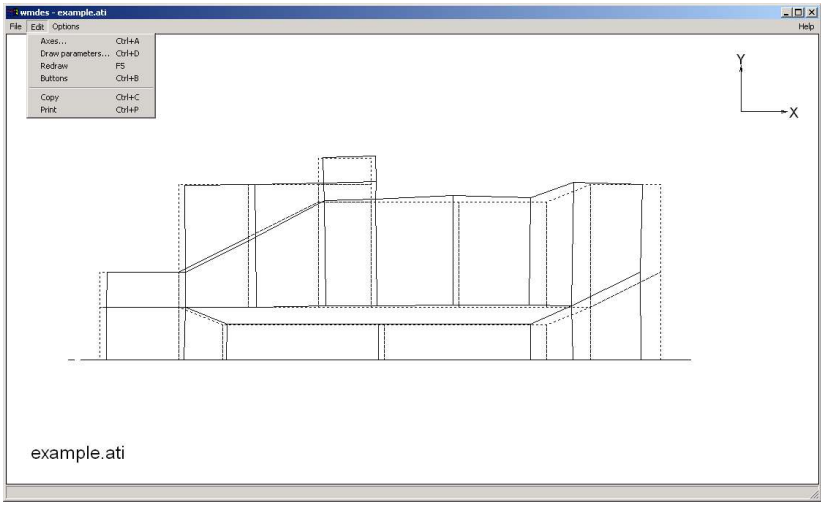

Electrical isopotential lines in 2D elements. This option is used to plot isovalues of the electric potential magnitude in piezoelectric domains of a bidimensional mesh. The solid elements of the structure are shown with a full line. Isovalues of the electric potential magnitude are shown with a full line, except the null isovalue, which is shown with a dashed line. Fluid elements and nodes do not appear.

The user can modify the selected frequency (harmonic or modal analysis) or selected time (transient analysis). No frequency value is requested for a static analysis or when solving was performed for one frequency or time only.

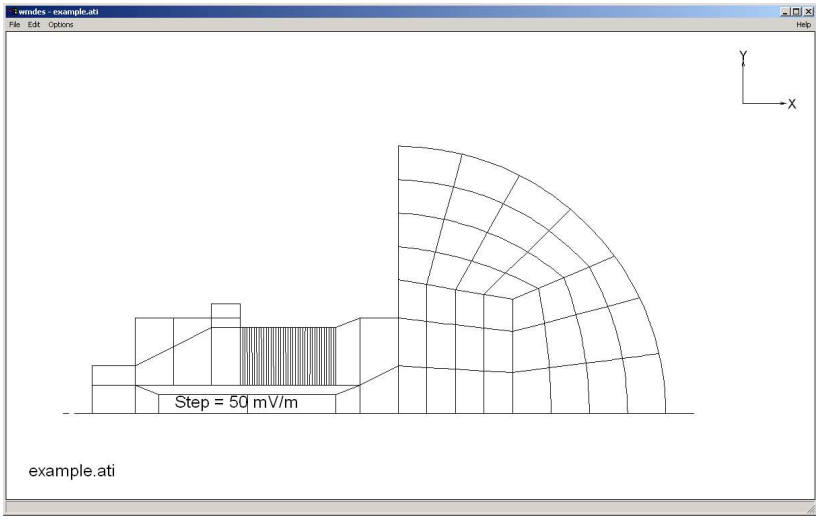

Isobaric lines in 2D fluid (magnitude). This option is used to plot isovalues of the pressure magnitude in fluid domains of a bidimensional mesh. The fluid elements of the structure are shown with a full line. Isovalues of the pressure magnitude are shown with a full line, except the null pressure isovalue, which is shown with a dashed line. Solid elements and nodes do not appear.

The user can modify the selected **frequency** (harmonic or modal analysis) or selected time (transient analysis). No frequency value is requested for a static analysis or when solving was performed for one frequency or time only.

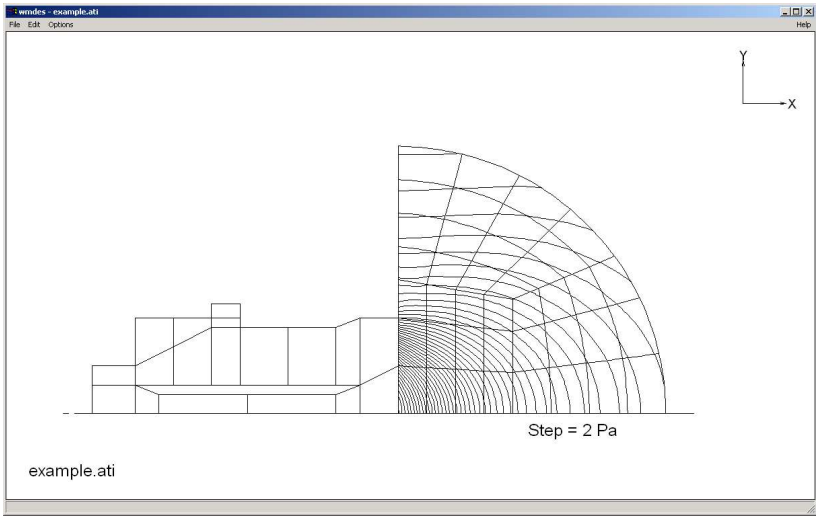

For magnetic and magnetostrictive domains, the following options are available.

Magnetic B field in 2D elements (magnitude). This option is used to display vectors of the magnetic field B in magnetic or magnetostrictive domains of a bidimensional mesh. The magnetic field includes the rotational part coming from the magnetic sources and the irrotational part deduced from the magnetic potential. The magnetic and magnetostrictive elements of the structure are shown with a full line. Magnetic field vectors are shown with a full line, starting from Gauss integration points, and of length proportional to the magnitude. Fluid elements and nodes do not appear.

The user can modify the selected frequency (harmonic or modal analysis) or selected time (transient analysis). No value is requested for a static analysis or when solving was performed for one frequency or time only. When a complex solver has been used, two graphics are provided. These correspond to the real and imaginary parts of the magnetic excitation field

(remember that the real value is the real part of the product of the complex value and the time dependency, which is $e^{j\omega t}$ in **ATILA**).

Magnetic H field in 2D elements (magnitude). This option is identical to the **Magnetic B field in 2D elements (magnitude)** option, except that the magnetic field H is shown instead of the magnetic induction B.

Demagnetizing field only. This option is identical to the **Magnetic B field in 2D elements (magnitude)** option, except that the rotational part of the magnetic field, coming from the magnetic sources, is not included. The irrotational part deduced from the magnetic potential is sometimes called the "demagnetizing field".

Magnetic isopotential lines (magnitude). This option is used to display isovalues of the reduced magnetic potential magnitude in magnetic or magnetostrictive domains of a bidimensional mesh. The magnetic and magnetostrictive elements of the structure are shown with a full line. Isovalues of the reduced magnetic potential magnitude are shown with a full line, except the null isovalue, which is shown with a dashed line. Fluid elements and nodes do not appear.

The user can modify the selected frequency (harmonic or modal analysis) or selected time (transient analysis). No value is requested for a static analysis or when solving was performed for one frequency or time only.

1.7.6 Wisoval

WISOVAL is an interactive post-processing graphical program for the creation and display of a shading or contour plot of results of an **ATILA** run (a shading plot is the default). **WISOVAL** displays in different colors the variation of a scalar value throughout the domain under study (isovalues of the displacement field components, of the stress field, isopotentials, isopressure, etc.). Isovalues are always represented in a plane. These can be plotted on the outer surface of a structure or in a cross-section.

WISOVAL requires the data stored in the post-processing file **.pst**. This file is generated by **ATILA** if a **GENERATION PST** entry has been provided in the **.ati** data file before using the solver (see Chapter 3.3.12). If this command does not appear in the **.ati** file, it is possible to rebuild the **.pst** file using the program **sy4topst** in Expert (see Chapter 1.8.6).

Initially, the X-displacement is displayed for the first frequency input in the .ati file.

Edit and **Option** commands may be used.

In the **Edit** menu, **Axes** (see Page 19) and **Draw parameters** are available. The plot type may be selected: **Displacement** in

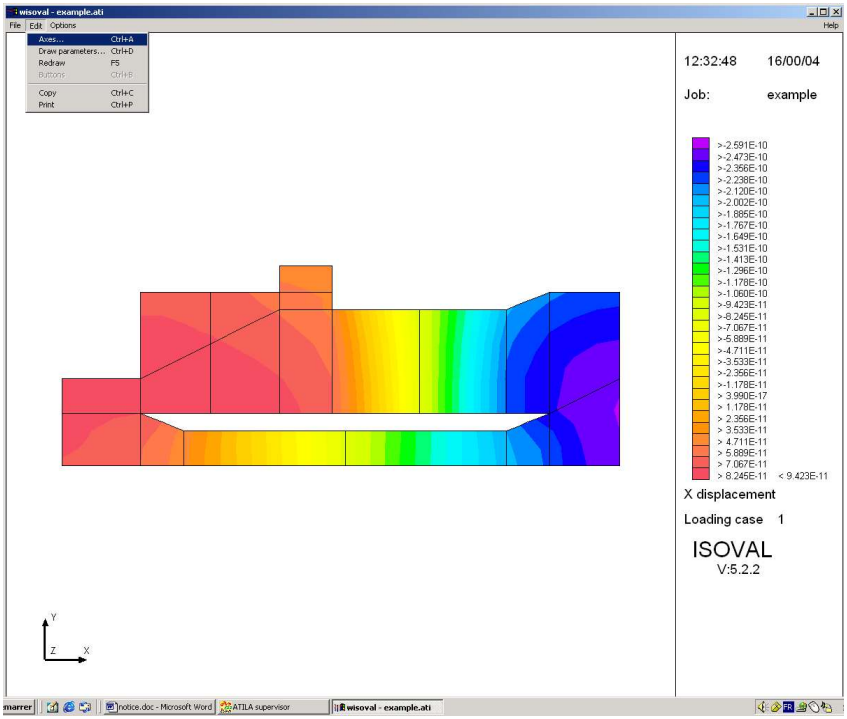

the x direction (**Ux**), in the y direction (**Uy**), in the z direction (**Uz**) and the **amplitude**, isovalues of the **Pressure** field, isovalues of the **Electric potential** and the isovalues of the **Temperature**. The user can also modify the selected frequency. For a tridimensional structure, cuts along planes are available.

In the **Option** menu, the main available commands are: **Legend**, to show or hide the legend on the right, **Mesh**, to show or to hide the full lines of the mesh, **Node numbering**, to show the nodes numbers and **Element numbering**, to show the elements numbers. Using **Color scale**, one shaded color can be selected, and **Composite** combines different options.

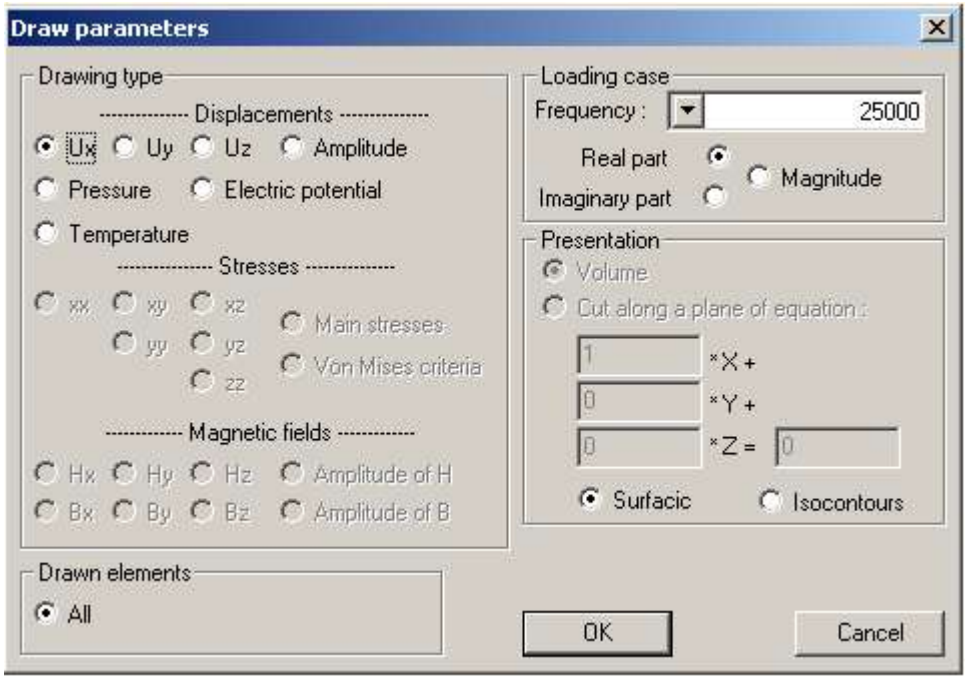

1.7.6.1 Animate

Animate performs animations. In fact, it can animate the displacement Snapshots that are equally spaced in one cycle of the harmonic response and are created from the **.sy4** file that the solver creates.
By moving the arrow on the screen, the view angle is changed.

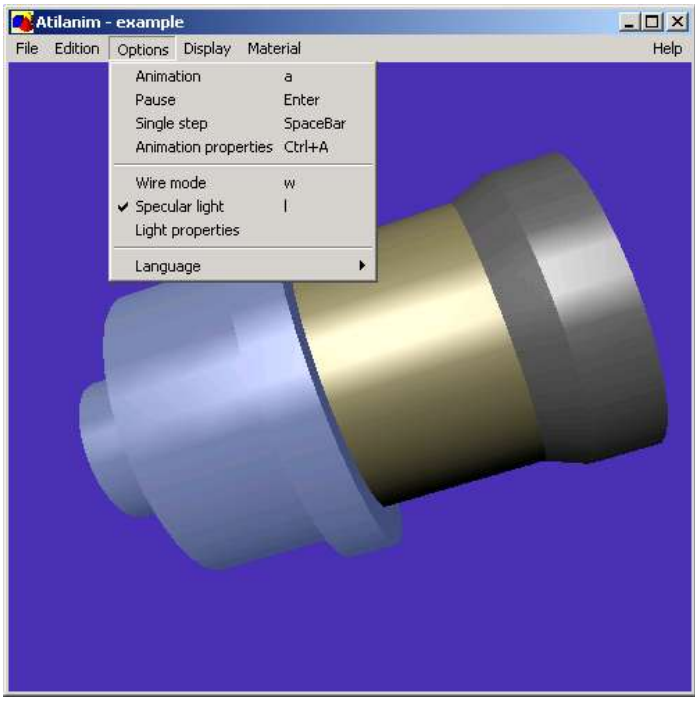

The main available options are: **Select frequency**, **Animation**, **Pause**. With **Animation properties, Frequency** and **magnitude** may be changed. **Wire mode** displays the structure in wireframe view. Colors and materials may be selected and changed using the **Select material** button.

The color white is assigned to any new material created. To modify this color, click on **Material**, then on **Add** the material.

1.8 Additional tools

1.8.1 Materials

With the help of the **Cpiezo** button, the user can display properties of the materials stored in the materials database. **Cpiezo** is not a complete tool, but it is helpful for simple cases. The values provided by the MATERIAL entry in the data file are the best place to check material properties. Depending on the number of properties, a given material is defined as elastic, fluid or piezoelectric/magnetostrictive. After clicking on the **Cpiezo** button, the user must enter the name of the material.
For an elastic material, the longitudinal and transverse speeds are displayed.
For a fluid material, the longitudinal speed is displayed.
For a piezoelectric (magnetostrictive) material, it is assumed that the material belongs to the crystalline class 6mm. The constants s^E, s^D, c^E, c^D, d, g, h, e, ε^S, ε^T; β^S and β^T (s^H, s^B, c^H, c^B, d, g, h, e, μ^S, μ^T; χ^S and χ^T) and the coupling factors k_{33}, k_{13}, k_{15}, and k^T are displayed.
You can create lossy piezoelectric or magnetostrictive materials from non-lossy ones, by specifying loss factors on the three main constants blocks (**Mpiezo**).
You can check that a piezoelectric or magnetostrictive material is effectively lossy (dissipating, not absorbing heat) (**Ppiezo**).

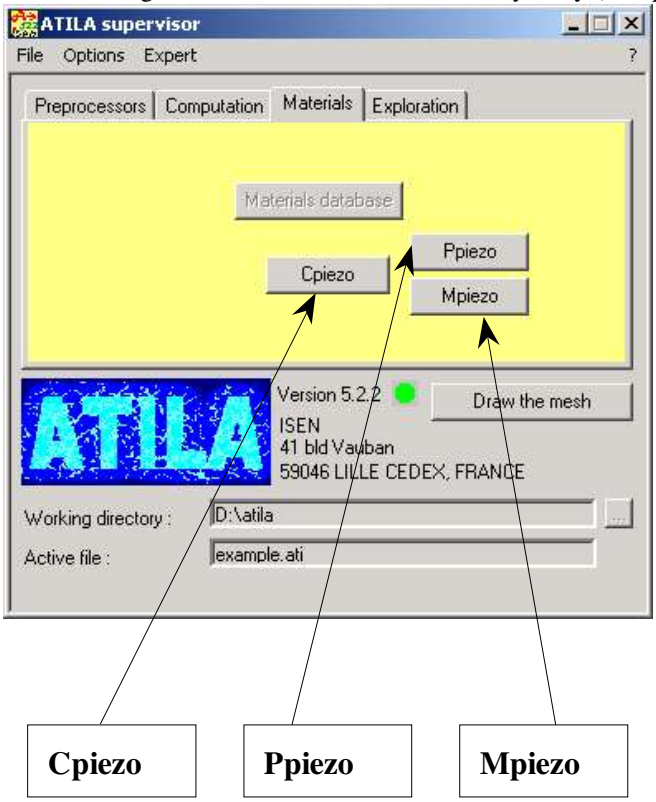

Materials Database button will soon be available.

1.8.2 Expert

The **Expert** menu points to different tools that are described below.

1.8.3 Atlist

After running a solver, the user can output the displacements for a selected frequency, time or loading case, exactly as the output of the solver when the **PRINTING** level is set to 1 or more. You can also output the displacement for several specific nodes and degrees of freedom for all frequencies, times or loading cases. These actions are driven by the program **ATLIST**.

1.8.4 Tmono, Tdip2

For active and/or radiating structures, in case the directivity patterns file (**.PAT** file) is accidentally deleted or corrupted, the user does not need to rerun the job. Because all valuable data is saved in the **.SY4** file, the directivity patterns file can be recreated with the programs **TDIP2** (2D structures, extrapolation method) or **TMONO** (when the fluid dampers stand in the far field).

1.8.5 Trpcp, Trpcp2

For active structures, in case the parallel impedance file (**.RPCP** file) is accidentally deleted or corrupted, the user does not need to rerun the job. Because all valuable data is saved in the **.SY4** file, the impedance file can be recreated with the program **TRPCP**. Alternatively, if the symmetries detected by the solver are incorrect, the user can force the symmetry factor with the help of the **TRPCP2** program.

1.8.6 Sy4topst

ISOVAL requires the data stored in the post-processing file **.pst**. This file is generated by **ATILA** if a **GENERATION PST** entry has been provided in the **.ati** data file before using the solver (see Section 3.3.12). If this command does not appear in the **.ati** file, it is possible to recreate the **.pst** file using the program **sy4topst**. Nevertheless, the stresses cannot be calculated using **sy4topst**. In that case, the user has to run the solver again.

1.8.7 Sy4tosup

This program gives the parameters that are used in modal superposition and represents the transducer with the help of an equivalent electrical circuit. Performing an **ANALYSIS MODAL** of an in-vacuum structure with **ATILA** gives the resonance frequencies, noted $f_R(m)$ and the corresponding displacement fields, noted $U_{mod}(n,m)$, where m is the mode number of the finite element analysis ($1 \le m \le NLOAD$) and n is the reference node number of the finite element mesh ($1 \le n \le N$) ; N is the total number of nodes in the structure. Then, the in-vacuum structure behavior can be represented by an equivalent electrical circuit, where the C0 blocked capacitance is in parallel with NLOAD branches. Each branch represents one mode and contains a capacitance $C(n,m)N^2(n,m)$ in series with an inductance $L(n,m)/N^2(n,m)$, whose values are independent of the node number n. Using the **sy4tosup** button, for a given node number, the program gives the values of N(n,m), C(n,m) and L (n,m). Then, the program uses the parameters of the equivalent electrical circuit to recalculate the resonance and the antiresonance frequencies of the structure. If these frequencies are not equal to the resonance and antiresonance frequencies given by an **ANALYSIS MODAL RESANTIRES**, it means that not enough NLOAD branches are taken into account in the equivalent electrical circuit. Thus, the user has to run the problem again an **ANALYSIS MODAL** with a higher number of NLOAD.

1.8.8 Sy4toHar

Using the modal superposition that has been performed with an **ANALYSIS MODAL**, **sy4tohar** calculates the displacement at a given node and at a given frequency from the data of the equivalent electrical circuit.

1.8.9 Celepo, Cdisp

When dealing with modal analysis of periodic materials, some useful information may be extracted from raw data: dispersion curves can be deduced from the different wave numbers and associated frequencies by careful ordering (program **CDISP**); the phase speed and mean polarization of each wave number and associated frequencies can be calculated (program **CELEPO**); from the low-frequency limit of longitudinal and transversal waves, a set of equivalent orthotropic material constants can be extracted.

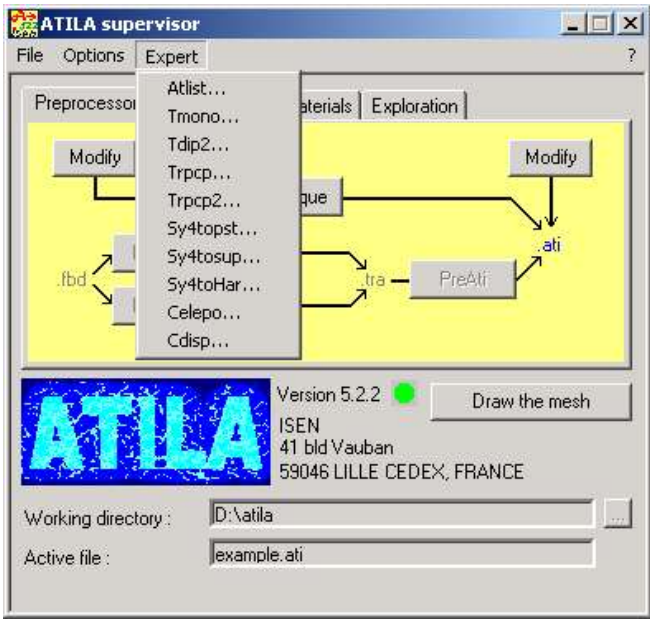

1.8.10 Options

The **Options** command changes the language (**English** or **French**). It defines the language used for the entry input and output. In France, the default language is French; in other countries, it is English.

2 DESCRIPTION OF THE FIELDS OF APPLICATION

2.1 General Formulation

This section describes the general formulation used in **ATILA** to model piezoelectric, electrostrictive* and magnetostrictive transducers radiating into a fluid, and provides a complete list of the possible types of analyses. Each type is then described in more detail in the following sections.

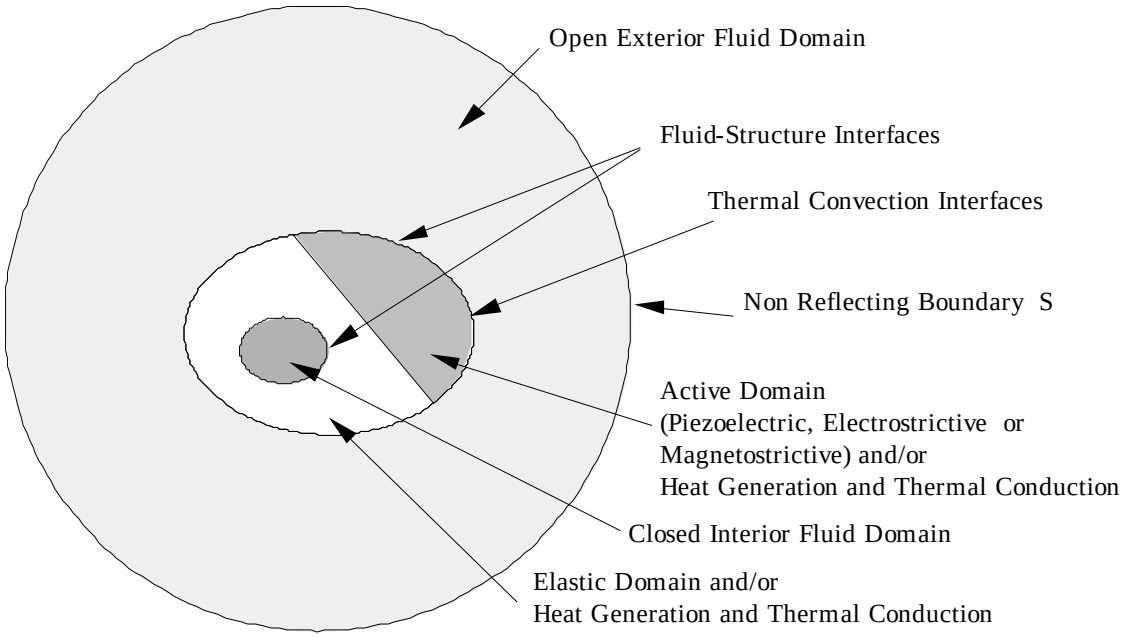

2.1.1 Modeling of Elastic, Piezoelectric or Magnetostrictive Structures

To model a radiating elastic, piezoelectric or magnetostrictive structure using **ATILA**, the finite-element mesh must contain the structure as well as part of the fluid domain, as shown in the figure above. The mesh of the structure under study and a part of the space surrounding it are necessary when modeling a magnetostrictive structure. This is not necessary for piezoelectric structures because common piezoelectric materials have a high relative permittivity. The piezoelectric materials are driven by electrodes (sets of electrically connected nodes) generating an electric field. The magnetostrictive materials are driven by a

magnetic field induced by sets of coils, each set being supplied by an electric current. The total magnetic field **H** can be broken up as:

$\mathbf{H} = \mathbf{H}_s + \mathbf{H}_r$

$\mathbf{H}_s$ is the magnetic field created by the source currents (the coils are not modeled) in vacuum:

$\mathbf{H}_s = \mathbf{H}_s^p I^p$

where I^p is the source current in the p^{th} set of coils. $\mathbf{H}_s^p$ is pre-determined for each coil using a classical Biot-Savart numerical integration. $\mathbf{H}_r$ is the irrotational component of the magnetic field and can be given as:

$\mathbf{H}_r = -\ \underline{\text{grad}}\ \phi$

where ϕ is the reduced magnetic potential.

The unknowns are the nodal values of the displacement field **U** in the whole structure, the electrical potential **Φ** in the piezoelectric material, the reduced magnetic potential **ϕ** in the magnetostrictive material and in a part of the surrounding space, the excitation currents **I** in the excitation coils and the pressure **P** in the fluid. The equations are those of elasticity in the structure, Poisson's equation in the piezoelectric or electrostrictive material, Maxwell's equations for the magnetostatic case (flux conservation) in the magnetic domain and Helmholtz's equation in the fluid. The electromechanical coupling is limited to the piezoelectric, electrostrictive or magnetostrictive domains. There is no electrical interaction between these two domains. Kinematic and dynamic continuity conditions are prescribed on the interfaces between the fluid and the structure. An appropriate radiation condition is applied to the surface boundary that surrounds the fluid domain. The natural condition prescribed on the external boundary of the magnetic mesh is a zero flux condition for the reduced magnetic field. The natural condition prescribed on the external boundary of a fluid mesh is a zero of the normal derivative of the pressure.

In matrix form, the complete set of equations of the problem can be written:

$$\begin{bmatrix} [K_{uu}]-\omega^2[M] & [K_{u\Phi}] & [K_{u\phi}] & [K_{uI}] & -[L] \\ [K_{u\Phi}]^T & [K_{\Phi\Phi}] & [0] & [0] & [0] \\ [K_{u\phi}]^T & [0] & [K_{\phi\phi}] & [K_{\phi I}] & [0] \\ [K_{uI}]^T & [0] & [K_{\phi I}]^T & [K_{II}] & [0] \\ -\rho^2 c^2 \omega^2 [L]^T & [0] & [0] & [0] & [H]-\omega^2[M_1] \end{bmatrix} \begin{bmatrix} \underline{U} \\ \underline{\Phi} \\ \underline{\phi} \\ \underline{I} \\ \underline{P} \end{bmatrix} = \begin{bmatrix} \underline{F} \\ -\underline{q} \\ -\underline{f} \\ -\underline{f_b} \\ \rho^2 c^2 \underline{\Psi} \end{bmatrix} \qquad (1)$$

where:

- **U**: vector of the nodal values of the components of the displacement field
- **Φ**: vector of the nodal values of the electrical potential
- **ϕ**: vector of the nodal values of the reduced magnetic potential
- **I**: vector of the prescribed values of the excitation currents (one component for each coil)
- **P**: vector of the nodal values of the pressure field
- **F**: vector of the nodal values of the applied forces
- **q**: vector of the nodal values of the electrical charges
- **f**: vector of the nodal values of the reduced magnetic field flux across the magnetic domain boundary
- $\mathbf{f_b}$: vector of the values of the reduced magnetic field flux seen by the coils (one component for each coil)
- **Ψ**: vector of the nodal values of the integrated normal derivative of the pressure on the surface boundary S
- $[K_{uu}]$: stiffness matrix
- $[K_{u\Phi}]$: piezoelectric matrix

$[K_{u\phi}]$: piezomagnetic coupling matrix

$[K_{uI}]$: source - structure coupling matrix

$[K_{\Phi\Phi}]$: dielectric matrix

$[K_{\phi I}]$: source - magnetization coupling matrix

$[K_{\phi\phi}]$: magnetic (pseudo-) stiffness matrix

$[K_{II}]$: inductance matrix in vacuum

[M]: consistent mass matrix

[H]: fluid (pseudo-) stiffness matrix

$[M_1]$: consistent (pseudo-) fluid mass matrix

[L]: coupling matrix at the fluid structure interface (connectivity matrix)

[0]: zero matrix

ω: angular frequency

ρ: fluid density

c: fluid sound speed

^{T} : means transposed

A large number of analyses can be done using this general equation. **ATILA** can solve the following problems (*quantities in parentheses are the results)*:

2.1.1.1 Static Analysis

STA1: computation of the static response of an elastic structure to a concentrated or distributed force (displacement field).

STA2: computation of the static response of a piezoelectric or magnetostrictive structure to a concentrated or distributed force (displacement field and electrical potential).

STA3: computation of the static response of an elastic structure to a forced displacement (displacement field).

STA4: computation of the static response of a piezoelectric or magnetostrictive structure to a forced displacement or a forced electrical potential (displacement field and electrical potential) or a forced magnetizing current (displacement field and reduced magnetic potential).

STA5: static analysis of a hydroelastic system, i.e., a structure including a fluid domain (displacement and pressure fields).

2.1.1.2 Modal Analysis

MOD1: modal analysis of an elastic structure (computation of the eigenfrequencies and the normal modes).

MOD2: modal analysis of a piezoelectric structure (computation of the resonance and anti-resonance frequencies and the normal modes for different electrical boundary conditions).

MOD3: modal analysis of a magnetostrictive structure (computation of the resonance and anti-resonance frequencies and the normal modes for different electrical boundary conditions).

MOD4: modal analysis of a closed fluid domain under zero pressure and/or zero flux boundary conditions (computation of eigenfrequencies and normal modes).

MOD5: modal analysis of a hydroelastic system, i.e., a structure including a fluid domain (computation of eigenfrequencies and normal modes).

MOD6: modal analyses of a one- or two- or three-dimensional periodic passive structure (for given wave vectors, computation of eigenfrequencies and normal modes)

MOD7: modal analyses of a one- or two- or three-dimensional periodic active structure (for given wave vectors, computation of eigenfrequencies and normal modes)

2.1.1.3 Harmonic Analysis

HAR1: harmonic analysis of an in-vacuum elastic structure (for a given frequency, computation of the displacement field in the structure).

HAR2: harmonic analysis of a non-radiating piezoelectric or magnetostrictive structure (for a given frequency, computation of the displacement field, the electrical potential, the reduced magnetic potential and the electrical impedance of the structure).

HAR3: computation of the pressure field radiated in an infinite fluid space by a vibrating surface where the displacement field is known at all points**.**

HAR4: harmonic analysis of an elastic structure driven by a force or a prescribed displacement, radiating in an infinite fluid space (for a given frequency, computation of the pressure and displacement fields).

HAR5: harmonic analysis of a piezoelectric or magnetostrictive structure electrically driven and radiating in an infinite fluid space (for a given frequency, computation of the pressure field, displacement field, electrical potential, reduced magnetic potential and the electrical impedance of the structure).

HAR6: harmonic analysis of an elastic or piezoelectric or magnetostrictive structure excited by an impinging wave (for a given frequency, computation of the pressure field, the displacement field, the electrical potential and the reduced magnetic potential).

HAR7: harmonic analysis of the diffraction of a plane-wave by a one- or two-dimensional periodic elastic structure (for a given frequency, computation of the pressure field, the displacement field and the reflection and transmission coefficients).

HAR8: harmonic analysis of a one- or two-dimensional periodic piezoelectric structure (for a given frequency, computation of the pressure field, the displacement field, the reflection and transmission coefficients, the free-field voltage sensitivity or the transmitting voltage response).

HAR9: harmonic analysis of a radiating piezoelectric or magnetostrictive structure using a coupled FEM-BEM method (for a given frequency, computation of the displacement field and the electrical impedance of the structure).

2.1.1.4 TRANSIENT ANALYSIS

TRA1: transient analysis of an in-vacuum elastic structure driven by external forces (for a given time, computation of the displacement field in the structure).

TRA2: transient analysis of an in-vacuum piezoelectric or magnetostrictive structure driven by external forces (for a given time, computation of the displacement field, the electric potential and the reduced magnetic potential).

TRA3: transient analysis of an in-vacuum piezoelectric or magnetostrictive structure electrically driven (for a given time, computation of the displacement field, the electric potential and the reduced magnetic potential).

TRA4: transient analysis of a piezoelectric or magnetostrictive structure electrically driven and radiating in an infinite fluid space (for a given time, computation of the pressure field, the displacement field, the electric potential and the reduced magnetic potential).

2.1.1.5 ELECTROSTRICTIVE MATERIALS

STES1: The first step is a static analysis of a electrostrictive structure, for which prescribed voltages, electric charges or stresses are given. The results provide the working point of the structure ; these are stored in a file of extension **.sst**.

TRAES1: The second step is a transient analysis of a electrostrictive structure, where voltage sinus or steps are used as excitations or chargesinus or steps are used as loads, representing values added to the initial static prescribed ones. The file of extension **.sst**, compatible with the first step analysis, must exist and be readable. The Central Difference Method is used in this case.

2.1.1.6 Thermal modelling of Elastic and Piezoelectric Material

Two kind of steady state thermal modelling can be performed using ATILA, the first classical consisting in calculating the temperature field according to prescribed temperatures and thermal convection interface, and the second in calculating the temperature field due to heat generated from material losses (see 2.1.4).
The system of equations is written as :

$$\left(\left[K_T\right]+\left[K_h\right]\right)\left[\underline{T}\right]=\left[Q\right]+\left[q\right]+\left[q_{T\infty}\right]$$

where:

$\left[K_T\right]$: conductivity matrix

$\left[K_h\right]$: convection matrix

$\underline{\mathbf{T}}$: vector of the nodal values of temperature,

$\underline{q}_{T\infty}$: vector of the nodal values of heat flux due to convection,

$\underline{\mathbf{q}}$: vector of the nodal values of heat flux,

$\underline{\mathbf{Q}}$: vector of the nodal values of heat flux due to dissipated power density,

Q is calculated from the dissipated power density due to material losses as defined by Holland [].
Example of thermal analysis:

THAR1: A two-step analysis is performed whereby the electro-mechanical behaviour is first computed for an harmonic analysis, and the resulting dissipated power is then applied as a heat generator to determine the resulting temperature of the system for a steady state solution (firstly displacement field and electric field, and then temperature field).

2.1.2 MODELING OF PERIODIC STRUCTURES WITH 1D OR 2D PERIODICITY

ATILA models structures having a one- or two-dimensional periodicity for radiation or scattering problems. In this case, the space is divided into 3 domains: domains I and III, which are semi-infinite and homogeneous fluid domains, and domain II, which includes the periodic structure and a portion of the near-field fluid (see figure below).

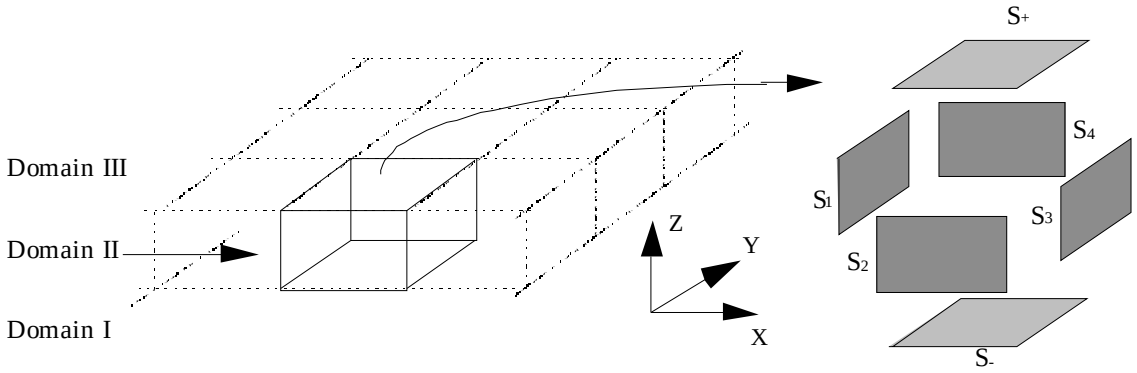

Region II is modeled using finite-elements and the user must supply the mesh for a unit cell. In Regions I and III, the pressure field is expanded on a plane-wave basis, homogeneous or evanescent, and is automatically generated. The matrix formulation of this problem includes the continuity conditions between different way of representing the pressure field at the I/II and II/III interfaces as well as Bloch-Flocquet conditions between successive unit cells. The computation of transmission and reflection coefficients assumes that only the specular components propagate to infinity.

2.1.3 MODELING OF PERIODIC STRUCTURES WITH 1D, 2D OR 3D PERIODICITY

ATILA models structures having a one-, two- or three-dimensional periodicity and no losses for eigenvalue problems. For a given wave vector, the code computes eigenfrequencies and normal modes. The angular frequency w is a periodical function of the wave vector; thus the problem can be reduced to the first Brillouin zone. Dispersion curves can be built varying the wave vector on the first Brillouin zone.

2.1.4 Modeling Internal Losses

In **ATILA**, losses in active or passive materials can be taken into account by using complex physical constants such as:
s = s' + js"
for a physical constant s. This is possible for nearly all the elements (see Chapter I.4) The user must ensure the coherence of the tensors (standard inequalities between real and imaginary parts. See for example: R. HOLLAND, "Representation of Dielectric, Elastic and Piezoelectric Losses by Complex Coefficients," IEEE, **SU14**, 18-20 (1967)). Furthermore, the user must take into account the changes in these parameters with frequency, if necessary, by updating the data file.

In the following sections, each type of analysis is described in detail. Part IV describes some test examples furnished with the **ATILA** code.

2.1.5 Transient analysis methods

In this analysis, the matrix equation (1) becomes:

$$\begin{bmatrix} [M] & [0] & [0] & [0] & [0] \\ [0] & [0] & [0] & [0] & [0] \\ [0] & [0] & [0] & [0] & [0] \\ [0] & [0] & [0] & [0] & [0] \\ [L]^T & [0] & [0] & [0] & \dfrac{[M_1]}{\rho^2 c^2} \end{bmatrix} \begin{bmatrix} \ddot{\underline{U}} \\ \ddot{\underline{\Phi}} \\ \ddot{\underline{\phi}} \\ \ddot{\underline{I}} \\ \ddot{\underline{P}} \end{bmatrix} + \frac{1}{\omega_0} \begin{bmatrix} [K''_{uu}] & [K''_{u\Phi}] & [K''_{u\phi}] & [K''_{uI}] & [0] \\ [K''_{u\Phi}]^T & [K''_{\Phi\Phi}] & [0] & [0] & [0] \\ [K''_{u\phi}]^T & [0] & [K''_{\phi\phi}] & [K''_{phiI}] & [0] \\ [K''_{uI}]^T & [0] & [K''_{phiI}]^T & [K''_{II}] & [0] \\ [0] & [0] & [0] & [0] & \left[\dfrac{H}{\rho^2 c^2}\right]^2 \end{bmatrix} \begin{bmatrix} \dot{\underline{U}} \\ \dot{\underline{\Phi}} \\ \dot{\underline{\phi}} \\ \dot{\underline{I}} \\ \dot{\underline{P}} \end{bmatrix}$$

$$+ \begin{bmatrix} [K'_{uu}] & [K'_{u\Phi}] & [K'_{u\phi}] & [K'_{uI}] & -[L] \\ [K'_{u\Phi}]^T & [K'_{\Phi\Phi}] & [0] & [0] & [0] \\ [K'_{u\phi}]^T & [0] & [K'_{\phi\phi}] & [K'_{phiI}] & [0] \\ [K'_{uI}]^T & [0] & [K'_{\phi I}]^T & [K'_{II}] & [0] \\ [0] & [0] & [0] & [0] & \left[\dfrac{H}{\rho^2 c^2}\right]^c \end{bmatrix} \begin{bmatrix} \underline{U} \\ \underline{\Phi} \\ \underline{\phi} \\ \underline{I} \\ \underline{P} \end{bmatrix} = \begin{bmatrix} \underline{F} \\ -\underline{q} \\ -\underline{f} \\ -\underline{f_b} \\ \dfrac{1}{\rho}\underline{\Psi} \end{bmatrix}$$

where $\dot{}$ and $\ddot{}$ denote the first and second time derivative, respectively. K′ and K″ denote the real and imaginary parts of K respectively. ω_0 is the pulsation at which the materials losses are provided. The preceding system of equations may be rewritten as follows:

$$[A]\ddot{\underline{X}} + [B]\dot{\underline{X}} + [C]\underline{X} = \underline{Y}$$

This differential equation is solved by an iterative method, taking a constant time step Δt ; the successive values of $\underline{X}$ and $\underline{Y}$ are noted $\underline{X}_n$ and $\underline{Y}_n$ and correspond to values calculated at the time $n\Delta t$. Three methods are implemented in **ATILA**: the Central Difference Method, the Newmark Method and the Wilson-θ Method.
Both methods are based on the same algorithm to calculate $\underline{Z}$:

$$\left([A] + a_1 h[B] + a_2 h^2[C]\right)\underline{Z} = \underline{Y}_{n+l} - [C]\left(\underline{X}_n + kh\dot{\underline{X}}_n + b_1\ddot{\underline{X}}_n\right) - [B]\left(k\dot{\underline{X}}_n + b_2\ddot{\underline{X}}_n + \frac{(k-1)}{2h}\underline{X}_n\right) + \frac{(k-1)}{h^2}[A]\left(2\underline{X}_n - \underline{X}_{n-1}\right)$$

$\underline{\mathbf{Z}}$ and the values of a_1, a_2, b_1, b_2, k, l and h depend on the chosen method and are explained below.

2.1.5.1 The Central Difference Method

This method consists in using a second order (parabolic) interpolation along the time axis and deriving the first and second order derivative from it:

$$\dot{\underline{X}}_n = \frac{1}{2\,Dt}\left(\underline{X}_{n+1} - \underline{X}_{n-1}\right)$$

$$\ddot{\underline{X}}_n = \frac{1}{Dt^2}\left(\underline{X}_{n+1} - 2\,\underline{X}_n + \underline{X}_{n-1}\right)$$

Replacing these values in the equation (2) above written at time step *n* leads to the following parameter values:

$\underline{\mathbf{Z}} = \underline{\mathbf{X}}_{n+1}/\Delta t^2$, $a_1 = ½$, $a_2 = b_1 = b_2 = k = l = 0$ and $h = \Delta t$.

Assuming that the initial first derivative of $\underline{\mathbf{X}}$ is zero, the algorithm is supplied with an initial value of $\underline{\mathbf{X}}_{-1}$:

$$\underline{X}_{-1} = \underline{X}_0 + \frac{Dt^2}{2}\left[A\right]^{-1}\left(\underline{Y}_0 - \left[C\right]\underline{X}_0\right)$$

This method is conditionally stable, i.e., knowing the highest eigenfrequency f_{max} of the lossless system of equations, the time step must satisfy:

$$pf_{\mathbf{max}}\,Dt < 1$$

2.1.5.2 The Newmark Method

This method consists in using a truncated Taylor series expansion of $\underline{\mathbf{X}}_{n+1}$ and its first derivative:

$$\begin{aligned}\underline{X}_{n+1} &= \underline{X}_n + Dt\,\dot{\underline{X}}_n + \frac{Dt^2}{2}\ddot{\underline{X}}_n + (6\mathrm{b})\frac{Dt^3}{6}\left(\frac{\ddot{\underline{X}}_{n+1} - \ddot{\underline{X}}_n}{Dt}\right)\\ \dot{\underline{X}}_{n+1} &= \dot{\underline{X}}_n + Dt\,\ddot{\underline{X}}_n + (2\,g)\frac{Dt^2}{2}\left(\frac{\ddot{\underline{X}}_{n+1} - \ddot{\underline{X}}_n}{Dt}\right)\end{aligned} \qquad (3)$$

The parameters β and ϒ may be arbitrarily chosen, but some are more appropriate than others. Introducing these equations in equation (2) above written at time step *n*+1 leads to the following parameter values:

$\underline{Z} = \ddot{\underline{X}}_{n+1}$, $a_1 = \gamma$, $a_2 = \beta$, $b_1 = (1-2\beta)\Delta t^2/2$, $b_2 = (1-\gamma)\Delta t$, $k = l = 1$ and $h = \Delta t$.

Assuming that the initial first derivative of $\underline{\mathbf{X}}$ is zero, the algorithm is supplied with an initial value of $\ddot{\underline{X}}_0$:

$$\ddot{\underline{X}}_0 = \left[A\right]^{-1}\left(\underline{Y}_0 - \left[C\right]\underline{X}_0\right)$$

This method will be unconditionally stable, provided that the following inequalities are satisfied:

$$g \geq \frac{1}{2},$$

$$\left(g + \frac{1}{2}\right)^2 - 4\,b < \left(\frac{1}{pf_{\max}\,Dt}\right)^2$$

where f_{max} is the highest eigenfrequency of the lossless system of equations. Note that a value of $\gamma > ½$ introduces a numerical damping, which is generally avoided. Names are given to usual couples of (γ,β): (1/2,0) stands for the Central Explicit Difference Method, (½,¼) for the Average Acceleration Method, (½,1⁄6) for the Linear Acceleration Method.

2.1.5.3 The Wilson-θ Method

This method is very similar to the Newmark Method, except that the equations (3) are first written for the time step $n+\theta$, $\theta \geq 1$, instead of $n+1$ (Δt is replaced with $\theta \Delta t$) and the parameters γ and β are respectively set to ½ and $^1/_6$. Once $\underline{\mathbf{X}}_{n+q}$ and its first and second time derivatives are calculated as above, a linear interpolation between $\underline{\mathbf{X}}_n$ and $\underline{\mathbf{X}}_{n+q}$ gives the solution $\underline{\mathbf{X}}_{n+1}$:

$$\underline{X}_{n+1} = \frac{\underline{X}_{n+q} + (q-1)\underline{X}_n}{q}$$

$$\dot{\underline{X}}_{n+1} = \frac{\dot{\underline{X}}_{n+q} + (q-1)\dot{\underline{X}}_n}{q}$$

$$\ddot{\underline{X}}_{n+1} = \frac{\ddot{\underline{X}}_{n+q} + (q-1)\ddot{\underline{X}}_n}{q}$$

This leads to the following parameter values:

$\underline{Z} = \ddot{\underline{X}}_{n+q}$, $a_1 = \theta/2$, $a_2 = \theta^2/6$, $b_1 = \theta^2 \Delta t^2/3$, $b_2 = \theta \Delta t/2$, $k = 1$, $l = \theta$ *and* $h = \theta \Delta t$.

The stability of this algorithm is more difficult to determine, but is proven for values of θ greater than 1.366.

Important note :

Extending these algorithms to piezoelectricity or magnetostriction may lead to inaccurate results, because of the quasi-static nature of electrical degrees of freedom: the matrix [A] of equation (2) becomes singular, f_{max} tends to infinity. In the case of the Central Difference Method, the implemented algorithm can deal with this, provided that the loss matrix [B] contains elastic losses only, i.e., $[K''_{uF}], [K''_{uf}], [K''_{uI}], [K''_{ff}], [K''_{fI}]$ and $[K''_{II}]$ are both null. In the case of the Newmark Method, a value of γ slightly greater than 0.5 will help in damping the spurious oscillations related to electric transients.

2.2 Types of Analysis

2.2.1 STATIC ANALYSIS OF AN ELASTIC STRUCTURE SUBJECTED TO A FORCE (STA1)

In this analysis, only the displacement field has to be computed and ω is equal to zero. Thus, the matrix equation (1) is reduced to:

$[K_{uu}]\ \underline{\mathbf{U}} = \underline{\mathbf{F}}$

The user provides the loading data **F**. The code computes **U**. **F** must be precisely defined for the finite-element model. This means that it must be divided by 2π if the model is axisymmetrical, and by 2 if a symmetrical plane limits the mesh. The user must define a mesh and boundary conditions eliminating the rigid body modes that induce singularities of the system of equations. Only one loading case can be solved at a time. Taking internal losses into account does not make physical sense in this analysis and thus is not possible.
The applied forces can be concentrated at the nodes (see **LOADS** entry) or distributed by using interface elements and by prescribing the pressure with the **EXCITATIONS** command. The matrix $[K_{uu}]$ is assembled and stored in a file by columns. Gaussian algorithms are used to solve the problem, in single or double precision. It is also possible to apply a force (**STA1**) and to prescribe displacements (**STA3**) at the same time.

2.2.2 STATIC ANALYSIS OF A PIEZOELECTRIC STRUCTURE SUBJECTED TO A FORCE (STA2)

In this analysis, the system of equations is reduced to:

$$\begin{bmatrix} [K_{uu}] & [K_{u\Phi}] \\ [K_{u\Phi}]^T & [K_{\Phi\Phi}] \end{bmatrix} \begin{bmatrix} \underline{U} \\ \underline{\Phi} \end{bmatrix} = \begin{bmatrix} \underline{F} \\ -\underline{q} \end{bmatrix}$$

The user supplies the loading data **F**. The code computes the displacement field **U** and the electrical potential **Φ**. **F** must be accurately defined for the finite-element model. This means that it must be divided by 2π if the model is axisymmetrical, and by 2 if a symmetry plane limits the mesh. It is essential that the boundary conditions eliminate the rigid body modes and ensure the uniqueness of the electrical potential (at least one electrical potential degree-of-freedom must be set to zero). Only one loading case can be solved at a time. Taking internal losses into account does not make physical sense in this analysis and thus is not possible. Magnetostrictive structures may also be treated by this analysis.
The applied forces can be concentrated at the nodes (see **LOADS** entry) or distributed by using interface elements and by prescribing the pressure with the **EXCITATIONS** command. The matrices are assembled and stored in a file by columns. Gaussian algorithms are used to solve the problem, in single or double precision. It is also possible to apply the forces (**STA2**) and prescribe displacements and/or electrical potentials (**STA4**) at the same time.

2.2.3 STATIC ANALYSIS OF AN ELASTIC STRUCTURE SUBJECTED TO A PRESCRIBED DISPLACEMENT (STA3)

In this analysis, the matrix equation to solve is identical to that of **STA1**:

$$[K_{uu}]\ \underline{\mathbf{U}} = \underline{\mathbf{F}}$$

The user provides the prescribed displacement on given nodes. The code computes the entire displacement field **U**. It is essential that the boundary conditions eliminate rigid body modes. Only one loading case can be solved at a time. Taking internal losses into account does not make physical sense in this analysis and thus is not possible.
Displacements are prescribed using the **EXCITATIONS** entry. The matrices are assembled and stored in a file by columns. Gaussian algorithms are used to solve the problem, in single or double precision. It is also possible to apply forces (**STA1**) and prescribe displacements at the same time (**STA3**).

2.2.4 ANALYSIS OF A PIEZOELECTRIC STRUCTURE SUBJECTED TO A PRESCRIBED DISPLACEMENT OR A PRESCRIBED ELECTRICAL POTENTIAL (STA4)

In this analysis, the matrix equation to solve is identical to that of **STA2**:

$$\begin{bmatrix} [K_{uu}] & [K_{u\Phi}] \\ [K_{u\Phi}]^T & [K_{\Phi\Phi}] \end{bmatrix} \begin{bmatrix} \underline{U} \\ \underline{\Phi} \end{bmatrix} = \begin{bmatrix} \underline{F} \\ -\underline{q} \end{bmatrix}$$

The user must provide the prescribed displacements and/or the prescribed electrical potentials on given nodes. The code computes the displacement field **U** and the electrical potential **Φ** over the entire structure. It is essential that the boundary conditions eliminate rigid body modes and ensure the uniqueness of the electrical potential (at least one potential degree-of-freedom must be set to zero). Only one loading case can be solved at a time. Taking internal losses into account does not make physical sense in this analysis and thus is not possible. Magnetostrictive structures may also be treated by this analysis.
Displacements are prescribed using the **EXCITATIONS** entry. The matrices are assembled and stored to file by columns. Gaussian algorithms are used to solve the problem, in single or double precision. It is also possible to apply forces (**STA2**) and prescribe displacements and/or prescribe electrical potentials (**STA4**) at the same time.

2.2.5 STATIC ANALYSIS OF A HYDROELASTIC SYSTEM (STA5)

In this analysis, the structure and fluid interact all along their interface. The pressure must be declared uniform in the fluid domain (or in each distinct fluid domain if several exist). The fluid surfaces that are not in contact with the structure must then support a zero pressure or zero flux pressure condition, as in the case of a tank. The system of equations (1) can be rewritten to be symmetric:

$$\begin{bmatrix} [K_{uu}] & [K_{u\Phi}] & [K_{u\phi}] & [K_{uI}] & -[L] \\ [K_{u\Phi}]^T & [K_{\Phi\Phi}] & [0] & [0] & [0] \\ [K_{u\phi}]^T & [0] & [K_{\phi\phi}] & [K_{\phi I}] & [0] \\ [K_{uI}]^T & [0] & [K_{\phi I}]^T & [K_{II}] & [0] \\ -[L]^T & [0] & [0] & [0] & [M_1]/\rho^2 c^2 \end{bmatrix} \begin{bmatrix} \underline{U} \\ \underline{\Phi} \\ \underline{\phi} \\ \underline{I} \\ \underline{P} \end{bmatrix} = \begin{bmatrix} \underline{F} \\ -\underline{q} \\ -\underline{f} \\ -\underline{f_b} \\ \underline{0} \end{bmatrix}$$

The user must provide the loading data **F**, -**q**, -$\mathbf{f}_b$ using the **LOADS** entry and/or the prescribed displacements **U**, electric potentials **Φ**, currents **I**, pressures **P** on given nodes using the **EXCITATIONS** entry. The code computes the displacement and pressure fields over the entire structure. **F**, -**q** and -$\mathbf{f}_b$ must be accurately defined for the finite-element model. This means that they must be divided by 2π if the model is axisymmetrical, by 2 if the mesh is limited by a symmetry plane, etc. The user must define a mesh and the boundary conditions, eliminating the rigid body modes associated with the singularity of the system of equations. Only one loading case can be solved at a time. Taking internal losses into account does not make physical sense in this analysis and thus is not possible.
The applied forces must be concentrated at the nodes (see **LOADS** entry). Displacements are prescribed using the **EXCITATIONS** entry. The matrices are assembled and stored to file by columns. Gaussian algorithms are used to solve the problem, in single or double precision.

2.2.6 MODAL ANALYSIS OF AN ELASTIC STRUCTURE (MOD1)

In this analysis, only the displacement field is relevant and the loading vector is set to zero. The system of equations is reduced to:

$$([K_{uu}] - \omega^2 [M])\ \underline{\mathbf{U}} = \underline{\mathbf{0}}$$

The code computes the eigenvalues and eigenvectors of the linear system that are the characteristic frequencies and modes of the structure. The computation is done using real values with no internal losses. Eigenvectors are normalized such that $\underline{\mathbf{U}}^T$ [M] $\underline{\mathbf{U}}$ = 1, [M] acting for the meshed structure, that is including the axisymmetry factor 2π for axisymmetric structures but not including symmetry factors induced by explicit boundary conditions.
The matrices $[K_{uu}]$ and [M] are assembled and stored to file by columns. Lanczos' algorithm is used to solve the problem. It can be solved only in double precision. It has to be noted that:

- ✔ the retained algorithm provides the rigid body modes when they exist
- ✔ this algorithm computes the eigenvalues very accurately even when the resonance modes are very close or when there is an ill-conditioned matrix.

2.2.7 MODAL ANALYSIS OF A PIEZOELECTRIC STRUCTURE (MOD2)

In this analysis, the system of equations is reduced to:

$$\begin{bmatrix} [K_{uu}] - \omega^2 [M] & [K_{u\Phi}] \\ [K_{u\Phi}]^T & [K_{\Phi\Phi}] \end{bmatrix} \begin{bmatrix} \underline{U} \\ \underline{\Phi} \end{bmatrix} = \begin{bmatrix} \underline{0} \\ -\underline{q} \end{bmatrix}$$

For different electrical boundary conditions, the code computes the eigenvalues and eigenvectors of the linear system that are the structure's eigenvalues and eigenvectors. The computation is done using real values with no internal losses. Eigenvectors are normalized such that $\underline{\mathbf{U}}^T$ [M] $\underline{\mathbf{U}}$ = 1, [M] acting for the meshed structure, that is including the axisymmetry factor 2π for axisymmetric structures but not including symmetry factors induced by explicit boundary conditions.
The first equation system in this section can be rewritten, isolating the electrical potentials linked to the electrodes in the vector $\underline{\mathbf{\Phi}}_e$ and the internal electrical potentials in the vector $\underline{\mathbf{\Phi}}_i$:

$$\begin{bmatrix} [K_{\Phi_e\Phi_e}] & [K_{\Phi_e\Phi_e}]^T & [K_{u\Phi_e}]^T \\ [K_{\Phi_i\Phi_e}] & [K_{\Phi_i\Phi_i}] & [K_{u\Phi_i}]^T \\ [K_{u\Phi_e}] & [K_{u\Phi_i}] & [K_{uu}] - \omega^2 [M] \end{bmatrix} \begin{bmatrix} \underline{\Phi}_e \\ \underline{\Phi}_i \\ \underline{U} \end{bmatrix} = \begin{bmatrix} -\underline{q} \\ \underline{0} \\ \underline{0} \end{bmatrix}$$

The short-circuit modal analysis, obtained by taking $\underline{\mathbf{\Phi}}_e = \underline{\mathbf{0}}$ for the potential of the electrodes, leads to computation of the resonance modes. The open-circuit modal analysis, obtained by taking $\underline{\mathbf{q}} = \underline{\mathbf{0}}$, leads to the computation of the antiresonance modes. Calculating the resonance and antiresonance modes can be carried out in one step (see Section I.3.D, **ANALYSIS** entry). In this case the excitation electrodes are referenced in the **EXCITATIONS** entry.
The matrices are assembled and stored to file by columns. Lanczos' algorithm is used to solve the problem. It can be done only in double precision. It has to be noted that:

- ✔ the retained algorithm provides the rigid body modes when they exist
- ✔ this algorithm computes the eigenvalues very accurately even when the resonance modes are very close or when there is an ill-conditioned matrix.

Remark: The electrical degrees-of-freedom are placed at the beginning of the assembled matrix. The numerical system can differ in size from a harmonic analysis. Also, any provided *mechanical* excitation will be treated as blocked.

2.2.8 MODAL ANALYSIS OF A MAGNETOSTRICTIVE STRUCTURE (MOD3)

In this analysis, the system of equations is reduced to:

$$\begin{bmatrix} [K_{uu}]-\omega^2[M] & [K_{u\Phi}] & [K_{uI}] \\ [K_{u\Phi}]^T & [K_{\Phi\Phi}] & [K_{\Phi I}] \\ [K_{uI}]^T & [K_{\Phi I}]^T & [K_{II}] \end{bmatrix} \begin{bmatrix} \underline{U} \\ \underline{\Phi} \\ \underline{I} \end{bmatrix} = \begin{bmatrix} \underline{0} \\ \underline{0} \\ -\underline{f_b} \end{bmatrix}$$

For different electrical boundary conditions, the code computes the eigenvalues and eigenvectors of the linear system that are the structure's eigenvalues and eigenvectors. The computation is done using real values with no internal losses. Eigenvectors are normalized such that $\underline{\mathbf{U}}^T$ [M] $\underline{\mathbf{U}}$ = 1, [M] acting for the meshed structure, that is including the axisymmetry factor 2π for axisymmetric structures but not including symmetry factors induced by explicit boundary conditions.

The open-circuit modal analysis, obtained by taking $\underline{\mathbf{I}} = \underline{\mathbf{0}}$, leads to the computation of the antiresonance modes. The short-circuit modal analysis, obtained by taking $\underline{\mathbf{f}}_b = \underline{\mathbf{0}}$, leads to the computation of the resonance modes. Calculating the resonance and antiresonance modes can be carried out in one step (see Section I.3.D, **ANALYSIS** entry). In this case the excitation currents are referenced in the **EXCITATIONS** entry.

The matrices are assembled and stored to file by columns. Lanczos' algorithm is used to solve the problem. It can be done only in double-precision. It has to be noted that:

- ✔ the retained algorithm provides the rigid body modes when they exist
- ✔ this algorithm computes the eigenvalues very accurately even when the resonance modes are very close or when there is an ill-conditioned matrix.

Remark: The electrical degrees-of-freedom are placed at the beginning of the assembled matrix. The numerical system can differ in size from a harmonic analysis. Also, any provided mechanical excitation will be treated as blocked.

2.2.9 MODAL ANALYSIS OF A CLOSED FLUID DOMAIN (MOD 4)

In this analysis, only the pressure field is concerned. Moreover, as zero pressure and/or zero flux conditions are applied on every boundary, the components of $\underline{\Psi}$ appearing in the equation are all zeros. Thus:

$$([H] - \omega^2[M_1]) \quad \underline{\mathbf{P}} \quad = \quad \underline{\mathbf{0}}$$

The code computes the eigenvalues and eigenvectors of the linear system that are the eigenfrequencies and modes of the fluid domain. The user must remember that the zero flux condition is the natural condition of the finite-element formulation and that it applies automatically to all boundaries, if no other condition is prescribed. This modal analysis can for example be used to determine the frequencies associated with singularities occurring in the use of an external Helmholtz integral formulation (irregular frequencies). The computation is done using real values with no internal losses. This type of analysis can be done only in double precision.

2.2.10 MODAL ANALYSIS OF A CLOSED HYDROELASTIC SYSTEM (MOD5)

In this analysis, the structure and the fluid interact all along their interface. The fluid domain must be closed, no radiating element being included in this model. The fluid surfaces not in contact with the structure must then support zero pressure or zero flux conditions. By restricting the system of equations to the displacement and pressure fields, the following is obtained:

$$\begin{bmatrix} [K_{uu}]-\omega^2[M] & -[L] \\ -\rho^2 c^2 \omega^2 [L]^T & [H]-\omega^2[M_1] \end{bmatrix} \begin{bmatrix} \underline{U} \\ \underline{P} \end{bmatrix} = \begin{bmatrix} \underline{0} \\ \underline{0} \end{bmatrix}$$

The code computes the eigenvalues and eigenvectors of the linear system that are the eigenfrequencies and modes of the structure including the fluid domain. The computation is done using real values with no internal losses.
The solid part can contain a piezoelectric or magnetostrictive material only if valid boundary conditions are imposed. The matrix equation is then more complicated than the equation above. The nonsymmetric Lanczos' algorithm is used to solve the problem. The problem can be solved only in double precision.

2.2.11 MODAL ANALYSIS OF A PERIODIC ELASTIC STRUCTURE (MOD6)

In this analysis, only the displacement field is relevant and the loading vector is set to zero. Only a bidimensional or tridimensional cell of the elastic structure is meshed. The user specifies the wave vector, i.e., the wave number and the direction of propagation of the acoustic wave, as well as the faces of the elementary cell on which the Bloch-Floquet condition are applied (see Section I.3.D, **PERIODIC**, **ANGLES**, **WAVENUMBER** entries). The system of equations is reduced to:

$$([K_{uu}] - \omega^2 [M])\ \underline{\mathbf{U}} = \underline{\mathbf{0}}$$

where the stiffness and mass matrices have been modified after the assembly phase to take the specific implicit boundary conditions into account. The code computes the real eigenvalues and complex eigenvectors of the linear hermitic system that are the characteristic frequencies and modes of the structure for the given wave number.
The matrices are assembled and stored to file by columns. Lanczos' algorithm for hermitic matrices is used to solve the problem. The problem can be solved only in double precision.

2.2.12 MODAL ANALYSIS OF A PERIODIC PIEZOELECTRIC STRUCTURE (MOD7)

In this analysis, only a bidimensional or tridimensional cell of the active structure is meshed. The user specifies the wave vector, i.e., the wave number and the direction of propagation of the acoustic wave, as well as the faces of the elementary cell on which the Bloch-Floquet condition are applied (see Section I.3.D, **PERIODIC**, **ANGLES**, **WAVENUMBER** entries). For piezoelectric structures, the system of equations is reduced to:

$$\begin{bmatrix} [K_{uu}]-\omega^2[M] & [K_{u\Phi}] \\ [K_{u\Phi}]^T & [K_{\Phi\Phi}] \end{bmatrix} \begin{bmatrix} \underline{U} \\ \underline{\Phi} \end{bmatrix} = \begin{bmatrix} \underline{0} \\ -\underline{q} \end{bmatrix}$$

where the stiffness and mass matrices have been modified after the assembly phase to take the specific implicit boundary conditions into account. The first equation system in this section can be rewritten, isolating the electrical potentials linked to the electrodes in the vector $\underline{\mathbf{\Phi}}_e$ and the internal electrical potentials in the vector $\underline{\mathbf{\Phi}}_i$:

$$\begin{bmatrix} [K_{\Phi_e\Phi_e}] & [K_{\Phi_e\Phi_e}]^T & [K_{u\Phi_e}]^T \\ [K_{\Phi_i\Phi_e}] & [K_{\Phi_i\Phi_i}] & [K_{u\Phi_i}]^T \\ [K_{u\Phi_e}] & [K_{u\Phi_i}] & [K_{uu}]-\omega^2[M] \end{bmatrix} \begin{bmatrix} \underline{\Phi}_e \\ \underline{\Phi}_i \\ \underline{U} \end{bmatrix} = \begin{bmatrix} -\underline{q} \\ \underline{0} \\ \underline{0} \end{bmatrix}$$

The short-circuit modal analysis, obtained by taking $\underline{\mathbf{\Phi}}_e = \underline{\mathbf{0}}$ for the potential of the electrodes, leads to computation of the resonance modes. The open-circuit modal analysis, obtained by taking $\underline{\mathbf{q}} = \underline{\mathbf{0}}$, leads to the computation of the antiresonance modes. The code computes the real eigenvalues and complex eigenvectors of the linear hermitic system that are the characteristic frequencies and modes of the structure for the given wave number. The computation is done using real values with no internal losses. Note that this analysis is valid for magnetostrictive structures if the magnetic sources are also periodic (i.e., a constant magnetic field).
The matrices are assembled and stored to file by columns. Lanczos' algorithm for hermitic matrices is used to solve the problem. The problem can be solved only in double precision.
Calculating the resonance and antiresonance modes cannot be carried out in one step.

Remark: The electrical degrees-of-freedom are placed at the beginning of the assembled matrix. The numerical system can differ in size from a harmonic analysis.

2.2.13 HARMONIC ANALYSIS OF AN IN-VACUO ELASTIC STRUCTURE (HAR1)

In this analysis, known harmonic displacements and/or forces are imposed on the elastic structure. The system of equations becomes:

$$([K_{uu}] - \omega^2[M]) \quad \underline{\mathbf{U}} \quad = \quad \underline{\mathbf{F}}$$

The user provides the prescribed displacements and/or forces on given nodes and the code computes the entire displacement field. The user controls the frequency scan. The displacements and/or forces are prescribed using the **EXCITATIONS** and/or **LOADS** commands.

The matrices are assembled and stored to file by columns. Gaussian algorithms are used to solve the problem, in single or in double precision. The internal losses of the materials can be taken into account.

2.2.14 HARMONIC ANALYSIS OF AN IN-VACUO PIEZOELECTRIC OR MAGNETOSTRICTIVE STRUCTURE (HAR2)

In this analysis, known harmonic loads and/or excitations are applied on the piezoelectric and/or magnetostrictive structure. The system of equations becomes:

$$\begin{bmatrix} [K_{uu}]-\omega^2[M] & [K_{u\Phi}] & [K_{u\phi}] & [K_{uI}] \\ [K_{u\Phi}]^T & [K_{\Phi\Phi}] & [0] & [0] \\ [K_{u\Phi}]^T & [0] & [K_{\phi\phi}] & [K_{\Phi I}] \\ [K_{uI}]^T & [0] & [K_{\phi I}]^T & [K_{II}] \end{bmatrix} \begin{bmatrix} \underline{U} \\ \underline{\Phi} \\ \underline{\phi} \\ \underline{I} \end{bmatrix} = \begin{bmatrix} \underline{F} \\ -\underline{q} \\ -\underline{f} \\ -\underline{f_b} \end{bmatrix}$$

The code computes the displacement field $\underline{\mathbf{U}}$, the electrical potential $\underline{\mathbf{\Phi}}$, the reduced magnetic potential $\underline{\boldsymbol{\phi}}$, the magnetic source currents $\underline{\mathbf{I}}$, the electrical impedance of the structure from the electric charge $\underline{\mathbf{q}}$, and the magnetic flux $\underline{\mathbf{f}}_b$ seen from the coils. The value provided for the impedance actually corresponds to the modelled structure. If the model is reduced by half or by a quarter by symmetry, the impedance value provided by the program must be divided by 2 or 4. If the model is axisymmetrical, the impedance value must be divided by 2π. The user controls the frequency scan.

The matrices are assembled and stored in a file by columns. Gaussian algorithms are used to solve the problem, in single or double precision. The internal losses in the materials can be taken into account.

2.2.15 COMPUTATION OF THE PRESSURE FIELD RADIATED BY A VIBRATING SURFACE WITH A KNOWN DISPLACEMENT FIELD (HAR3)

In this analysis, the structure radiates an acoustic wave in an infinite medium and it is assumed that the displacement field is known for each frequency. The system of equations is thus expressed in the form:

$$\left([H] - \omega^2 \left[M_1 \right] \right) \underline{P} = \rho c^2 \underline{\Psi} + \rho^2 c^2 \omega^2 [L]^T \underline{U}$$

The $\underline{\mathbf{\Psi}}$ vector defines the radiation condition applied on the external surface S limiting the fluid domain:

$$\underline{\Psi} = -\frac{1}{\rho c}\left(\frac{1}{nR} + \mathrm{j}\frac{\omega}{c}\right)[D]\ \underline{P} + \frac{1}{n\rho c}\left(\frac{\frac{1}{R} - \mathrm{j}\frac{\omega}{c}}{1 + \frac{\omega^2 R^2}{c^2}}\right)[D']\underline{P}$$

where R is the radius of the boundary surface S. [D] and [D'] are obtained by assembling the damping elements on that surface. *n* equals 1 for axisymmetric or 3D meshes, 2 for plain-strain meshes. The first term is the monopolar contribution associated with a spherical (*n*=1) or cylindrical (*n*=2) wave impedance condition, and the second term is the dipolar contribution. The damping term can be written:

$$\rho c^2 \underline{\Psi} = [G]\underline{P}$$

where [G] represents a complex linear operator that is frequency dependent. Consequently:

$$\left([H] - \omega^2 [M_1] - [G] \right) \underline{P} = \rho^2 c^2 \omega^2 [L]^T \underline{U}$$

The user must provide **U** and the excitation frequency. The code computes **P**. The radiating surface on which [G] is computed is a spherical (*n*=1) or cylindrical (*n*=2) surface, the center of which corresponds to the acoustical center of the radiation field. Its radius is determined by the user to ensure the convergence of the computation. If the damping elements are monopolar, the boundary surface must be in the far field. If the elements are dipolar, the boundary surface can be in the near field. In this case, the information on the far field is not available until an appropriate post-processing is done by the **TDIP2** program (see Section I.6.C).

To define **U**, the **EXCITATIONS** entry must be used (see Section I.3.D) to specify the values of the displacement for each interface degree-of-freedom on the solid. The matrices are assembled and stored to file by columns. Gaussian algorithms are used to solve the problem, in single or in double precision. Internal losses can be taken into account.

2.2.16 HARMONIC ANALYSIS OF A RADIATING ELASTIC STRUCTURE (HAR4)

Using the operator [G] described in the preceding paragraph, the system of equations can be written:

$$\begin{bmatrix} [K_{uu}] - \omega^2 [M] & -[L] \\ -\rho^2 c^2 \omega^2 [L]^T & [H] - \omega^2 [M_1] \end{bmatrix} \begin{bmatrix} \underline{U} \\ \underline{P} \end{bmatrix} = \begin{bmatrix} \underline{F} \\ [G]\underline{P} \end{bmatrix}$$

The user must specify the excitation frequency and define the prescribed excitations and/or loads located on the nodes (see section I.3.D., **EXCITATIONS** and **LOADS** entries). The code computes the real and imaginary parts of the displacement and pressure fields. It is possible to restart with new excitation frequencies without the need for a new assembly phase. In this case, the number of cases of loading must remain unchanged, but the number of computation frequencies can be smaller than the initial number of frequencies (see Section I.3.D., **FREQUENCY** and **NLOAD** entries).

After symmetrization, the system can be written:

$$\begin{bmatrix} [K_{uu}] - \omega^2 [M] & -[L] \\ -[L]^T & \dfrac{[H]}{\rho^2 c^2 \omega^2} - \dfrac{[M_1]}{\rho^2 c^2} \end{bmatrix} \begin{bmatrix} \underline{U} \\ \underline{P} \end{bmatrix} = \begin{bmatrix} \underline{F} \\ \dfrac{[G]}{\rho^2 c^2 \omega^2} \underline{P} \end{bmatrix}$$

The matrices are assembled and stored in a file by columns. Gaussian algorithms are used to solve the problem, in single or double precision. The internal losses of materials can be taken into account. The information about the damping elements, the conditions on the boundary, the near field and the far field, presented in **HAR3**, still apply.

2.2.17 HARMONIC ANALYSIS OF A RADIATING PIEZOELECTRIC OR MAGNETOSTRICTIVE STRUCTURE (HAR5)

Using the operator [G] described in **HAR3**, the system of equations is written:

$$\begin{bmatrix} [K_{uu}]-\omega^2[M] & [K_{u\Phi}] & [K_{u\phi}] & [K_{uI}] & -[L] \\ [K_{u}]^T & [K_{\Phi\Phi}] & [0] & [0] & [0] \\ [K_{uf}]^T & [0] & [K_{\phi\phi}] & [K_{\phi I}] & [0] \\ [K_{uI}]^T & [0] & [K_{\phi I}]^T & [K_{II}] & [0] \\ -\rho^2 c^2 \omega^2 [L]^T & [0] & [0] & [0] & [H]-\omega^2[M_1] \end{bmatrix} \begin{bmatrix} \underline{U} \\ \underline{\Phi} \\ \underline{\phi} \\ \underline{I} \\ \underline{P} \end{bmatrix} = \begin{bmatrix} \underline{F} \\ -\underline{q} \\ -\underline{f} \\ -\underline{f_b} \\ [G]\underline{P} \end{bmatrix}$$

The system of equations is symmetrized in the form:

$$\begin{bmatrix} [K_{uu}]-\omega^2[M] & [K_{u\Phi}] & [K_{u\phi}] & [K_{uI}] & -[L] \\ [K_{u\Phi}]^T & [K_{\Phi\Phi}] & [0] & [0] & [0] \\ [K_{u\phi}]^T & [0] & [K_{\Phi\Phi}] & [K_{\phi I}] & [0] \\ [K_{uI}]^T & [0] & [K_{\Phi I}]^T & [K_{II}] & [0] \\ -[L]^T & [0] & [0] & [0] & \dfrac{[H]}{\rho^2 c^2 \omega^2} - \dfrac{[M_1]}{\rho^2 c^2} \end{bmatrix} \begin{bmatrix} \underline{U} \\ \underline{\Phi} \\ \underline{\phi} \\ \underline{I} \\ \underline{P} \end{bmatrix} = \begin{bmatrix} \underline{F} \\ -\underline{q} \\ -\underline{f} \\ -\underline{f_b} \\ \dfrac{[G]}{\rho^2 c^2 \omega^2}\underline{P} \end{bmatrix}$$

The user provides the excitation frequency and usually defines the currents in the coils. The code computes the real and imaginary parts of the entire pressure and displacement fields, the reduced magnetic potential and the electrical impedance.

The user must provide the excitation frequency and define the prescribed excitations and/or loads (see section I.3.D., **EXCITATIONS** and **LOADS** entries). The code computes the real and imaginary parts of the entire pressure and displacement fields, the electrical potential $\underline{\mathbf{\Phi}}$, the reduced magnetic potential $\underline{\boldsymbol{\phi}}$, the currents in magnetic sources $\underline{\mathbf{I}}$ and the electrical impedance of the structure from the electric charge $\underline{\mathbf{q}}$ and the magnetic flux $\underline{\mathbf{f}}_b$ seen from the coils. The value provided for the impedance corresponds to the structure actually modelled. If the model is reduced to a half or a quarter by symmetry, the impedance value provided by the program must be divided by 2 or 4. If the model is axisymmetrical, the impedance value must be divided by 2π.

The matrices are assembled and stored in a file by columns. Gaussian algorithms are used to solve the problem, in single or double precision. The internal losses of materials can be taken into account. The information given in **HAR3** on damping elements, conditions of near field and far field on the boundary surface is still valid.

2.2.18 HARMONIC ANALYSIS OF AN ELASTIC OR PIEZOELECTRIC OR MAGNETOSTRICTIVE STRUCTURE EXCITED BY AN IMPINGING WAVE (HAR6)

The pressure $\underline{\mathbf{P}}$ and the flux $\rho c^2 \underline{\mathbf{\Psi}}$ are split in two parts: the incident pressure $\underline{\mathbf{P}}_i$ and flux $\rho c^2 \underline{\mathbf{\Psi}}_i$ and the elastic scattered pressure $\underline{\mathbf{P}}_{es}$ and flux $\rho c^2 \underline{\mathbf{\Psi}}_{es}$. Since $\underline{\mathbf{P}}_i$ is known, the corresponding terms can be moved to the right hand side of the set of equations. Also, $\underline{\mathbf{\Psi}}_i$ can be expressed in terms of the nodal values of the pressure normal derivative:

$$\underline{\Psi}_i = [D] \frac{\partial P_i}{\partial n}$$

where [D] is a matrix already provided by the damping elements (see **HAR3**). Using the operator [G] described in **HAR3**, the system of equations is written, in symmetric form:

$$\begin{bmatrix} [K_{uu}]-\omega^2[M] & [K_{u\Phi}] & [K_{u\phi}] & [K_{uI}] & -[L] \\ [K_{u\Phi}]^T & [K_{\Phi\Phi}] & [0] & [0] & [0] \\ [K_{uf}]^T & [0] & [K_{\phi\phi}] & [K_{fI}] & [0] \\ [K_{uI}]^T & [0] & [K_{\phi I}]^T & [K_{II}] & [0] \\ -[L]^T & [0] & [0] & [0] & \dfrac{[H]}{\rho^2 c^2 \omega^2}-\dfrac{[M_1]}{\rho^2 c^2} \end{bmatrix} \begin{bmatrix} \underline{U} \\ \underline{\Phi} \\ \underline{\phi} \\ \underline{I} \\ \underline{P}_{es} \end{bmatrix} = \begin{bmatrix} \underline{F}+[L]\underline{P}_i \\ -\underline{q} \\ -\underline{f} \\ -\underline{f}_b \\ \dfrac{[G]}{\rho^2 c^2 \omega^2}\underline{P}_{es}+\dfrac{[D]}{\rho\omega^2}\dfrac{\partial \underline{P}_i}{\partial n}-\left(\dfrac{[H]}{\rho^2 c^2 \omega^2}-\dfrac{[M_1]}{\rho^2 c^2}\right)\underline{P}_i \end{bmatrix}$$ It

is possible to apply simultaneously several prescribed excitations (electrical potentials, displacements, pressures, currents in the magnetic sources) and/or loads (force, electrical charge). The user must provide the excitation frequency and define the prescribed excitations and/or loads (see section I.3.D., **EXCITATIONS** and **LOADS** entries) and the incident pressure field via a C or Fortran function **INCPRE** (see I.3 command **PRESSURE**). The code computes the real and imaginary parts of the entire pressure and displacement fields, the electrical potential, the reduced magnetic potential, the excitation currents, and the electric impedances. The information given in **HAR3** on damping elements, conditions of near field and far field on the boundary surface is still valid.

2.2.19 HARMONIC ANALYSIS OF THE SCATTERING OF A PLANE-WAVE BY A PERIODIC ELASTIC STRUCTURE (HAR7)

In this analysis, only a bidimensional or tridimensional elementary cell of the elastic structure and a part of the fluid domain that surrounds it are meshed. The matrix equation is reduced to:

$$\begin{bmatrix} [K_{uu}]-\omega^2[M] & -[L] \\ -\rho^2 c^2 \omega^2 [L]^T & [H]-\omega^2[M_1] \end{bmatrix} \begin{bmatrix} \underline{U} \\ \underline{P} \end{bmatrix} = \begin{bmatrix} \underline{0} \\ \rho c^2 \underline{\Psi}_i \end{bmatrix}$$

where the various stiffness, mass, and connectivity matrices have been modified after the assembly phase to take into account the specific boundary conditions and where $\underline{\Psi}_i$ is the normal derivative of the pressure field incident on the mesh boundary. The single or double periodicity of the mesh is taken into account by a specific Bloch type phase relation between nodes separated by one mesh step. On the fluid mesh boundaries, the pressure field is matched to a homogeneous or evanescent plane-wave series expansion. It is possible to model structures with fluid on both sides or only on the front side. Different fluids can be used on the front and the back sides.

The user specifies the frequency and the incidence angle of the incident wave as well as the symmetry planes of the elementary cell that correspond to the Bloch condition (see Paragraph I.3.E.2). The code computes the real and imaginary parts of the pressure and displacement fields as well as the transmission and reflection coefficients.

The matrices are assembled and stored to file by columns. The phase relation between nodes separated by one mesh step as well as the coupling with homogeneous and evanescent plane-waves on the mesh boundaries are incorporated into the matrices, which then become non-symmetrical. Gaussian algorithms are used to solve the problem, in single or double precision. The internal losses of the materials can be taken into account.

2.2.20 HARMONIC ANALYSIS OF A PERIODIC PIEZOELECTRIC OR MAGNETOSTRICTIVE STRUCTURE (HAR8)

In this analysis, only a bidimensional or tridimensional elementary cell of the solid structure and a part of the fluid domain that surrounds it are meshed. The matrix equation is reduced to:

$$\begin{bmatrix} [K_{uu}]-\omega^2[M] & [K_{u\Phi}] & [K_{u\phi}] & [K_{uI}] & -[L] \\ [K_{u\Phi}]^T & [K_{\Phi\Phi}] & [0] & [0] & [0] \\ [K_{u\phi}]^T & [0] & [K_{\phi\phi}] & [K_{\phi I}] & [0] \\ [K_{uI}]^T & [0] & [K_{\phi I}]^T & [K_{II}] & [0] \\ -\rho^2 c^2 \omega^2 [L]^T & [0] & [0] & [0] & [H]-\omega^2[M_1] \end{bmatrix} \begin{bmatrix} \underline{U} \\ \underline{\Phi} \\ \underline{\phi} \\ \underline{I} \\ \underline{P} \end{bmatrix} = \begin{bmatrix} \underline{0} \\ 0 \\ \underline{0} \\ 0 \\ \underline{0} \\ \rho c^2 \Psi_i \end{bmatrix}$$

where the various matrices have been modified after the assembly phase to take into account the specific boundary conditions and where $\underline{\Psi}_i$ is the normal derivative of the pressure field incident on the mesh boundary. The single or double periodicity of the mesh is taken into account by a specific Bloch type phase relation between nodes separated by one mesh step. On the fluid mesh boundaries, the pressure field is matched to a homogeneous or evanescent plane-wave series expansion. It is possible to model structures with fluid on both sides or only on the front side. Different fluids can be used on the front and the back sides.
Two types of analyses are available: the scattering and the radiation by a periodic piezoelectric structure. In both cases, the user specifies the frequency, the angle of the incident wave (scattering) or of observation (radiation), the position of the hot electrode and the symmetry planes of the elementary cell that correspond to the Bloch condition (see Paragraph I.3.E.2). The code computes the real and imaginary parts of the pressure and displacement fields, the electrical potential, the reduced magnetic potential and the currents in the magnetic sources. It also provides the transmission and reflection coefficients and, for piezoelectric structures, the free-field voltage sensitivity (scattering) or the transmitting voltage response (radiation).
The matrices are assembled and stored to file by columns. The phase relation between nodes separated by one mesh step as well as the coupling with homogeneous and evanescent plane-waves on the mesh boundaries are incorporated in the matrices which become non symmetrical. Gaussian algorithms are used to solve the problem, in single or double precision. The internal losses of the materials can be taken into account.

2.2.21 HARMONIC ANALYSIS OF A RADIATING PIEZOELECTRIC OR MAGNETOSTRICTIVE STRUCTURE USING A COUPLED FEM-BEM METHOD (HAR9)

In this analysis, finite-element modeling is used in association with an external boundary-element code. This code must have a description of the solid-fluid interfaces similar to the description used in the **CHIEF** program (constant pressure and velocity on each surface). First, the boundary-element code is used to solve numerically the Helmholtz equation and to compute the mutual impedance matrix [Z] that relates pressures and velocities on the radiating surfaces:

$$\left[Z\right]\underline{\tilde{V}} = \underline{\tilde{F}}$$

Then, finite element modelling is used to solve the coupled problem. The matrix [Z] is an additional entry described in the JOB.ZRAD file (see section I.3.D. **CHIEF** entry).
Then, finite-element modelling is used to solve the coupled problem. The set of equations is:

$$\begin{bmatrix} [K_{uu}]-\omega^2[M]+j\omega\left[X\right]\left[Z\right]\left[X\right]^T & [K_{u\Phi}] & [K_{u\phi}] & [K_{uI}] \\ [K_{u\Phi}]^T & [K_{\Phi\Phi}] & [0] & [0] \\ [K_{u\phi}]^T & [0] & [K_{\phi\phi}] & [K_{\phi I}] \\ [K_{uI}]^T & [0] & [K_{\phi I}]^T & [K_{II}] \end{bmatrix} \begin{bmatrix} \underline{U} \\ \underline{\Phi} \\ \underline{\phi} \\ \underline{I} \end{bmatrix} = \begin{bmatrix} \underline{F} \\ -\underline{q} \\ -\underline{f} \\ -\underline{f_b} \end{bmatrix}$$

where [X] is a coupling matrix which prescribes the continuity of the pressure and of the velocity at the interface in an average sense. The user usually prescribes the applied electrical potential. The code computes the displacement field, the electrical potential, the reduced magnetic potential, the currents in the magnetic sources, the electrical impedance of the structure and the average velocity of the radiating surfaces. The user controls the frequency scan.

Finally, the average velocities can be introduced into the boundary-element program to compute the acoustic field in the fluid medium and to provide the transmitting voltage response and directivity patterns.
The matrices are assembled and stored in a file by columns. Gaussian algorithms are used to solve the problem, in single or double precision. The internal losses in the materials can be taken into account. More general problems including prescribed excitations (displacements, electrical potentials, currents in the magnetic sources) and/or loads (forces, electrical charges) can also be solved.

2.2.22 TRANSIENT ANALYSIS OF AN IN-VACUUM ELASTIC STRUCTURE DRIVEN BY EXTERNAL FORCES (TRA1)

In this analysis, known loads (forces **F**) are applied on the elastic structure. The system of equations becomes:

$$[M]\ddot{\underline{U}}+\frac{1}{\omega_0}[K''_{uu}]\dot{\underline{U}}+[K'_{uu}]\underline{U}=\underline{F}$$

where ˙ and ¨ denote the first and second time derivative, respectively. ω_0 is the pulsation at which the materials losses are defined. This differential equation is solved by an iterative method, taking a constant time step Δt. Three methods are implemented: the Central Difference Method, the Newmark Method and the Wilson-θ Method. The method, the time step and the method's parameters are defined with the **TRANSIENT** command. The code computes the displacement field **U** for the requested time steps. The problem can be solved only in double precision.

2.2.23 Tansient analysis of an in-vaccum piezoelectric or magnetostrictive structure driven by external forces (TRA2)

In this analysis, known loads (forces **F**, electric charges **q**, magnetic fluxes $\underline{\mathbf{f}_b}$) are applied on the piezoelectric or magnetostrictive structure. The system of equations becomes:

$$\begin{bmatrix}[M]&[0]&[0]&[0]\\[0]&[0]&[0]&[0]\\[0]&[0]&[0]&[0]\\[0]&[0]&[0]&[0]\end{bmatrix}\begin{bmatrix}\ddot{\underline{U}}\\\ddot{\underline{\Phi}}\\\ddot{\underline{\phi}}\\\ddot{\underline{I}}\end{bmatrix}+\frac{1}{\omega_0}\begin{bmatrix}[K''_{uu}]&[K''_{u\Phi}]&[K''_{u\phi}]&[K''_{uI}]\\[K''_{u\Phi}]^T&[K''_{\Phi\Phi}]&[0]&[0]\\[K''_{u\phi}]^T&[0]&[K''_{\phi\phi}]&[K''_{\phi I}]\\[K''_{uI}]^T&[0]&[K''_{\phi I}]^T&[K''_{II}]\end{bmatrix}\begin{bmatrix}\dot{\underline{U}}\\\dot{\underline{\Phi}}\\\dot{\underline{\phi}}\\\dot{\underline{I}}\end{bmatrix}$$

$$+\begin{bmatrix}[K'_{uu}]&[K'_{u\Phi}]&[K'_{u\phi}]&[K'_{uI}]\\[K'_{u\Phi}]^T&[K'_{\Phi\Phi}]&[0]&[0]\\[K'_{u\phi}]^T&[0]&[K'_{\phi\phi}]&[K'_{\phi I}]\\[K'_{uI}]^T&[0]&[K'_{\phi I}]^T&[K'_{II}]\end{bmatrix}\begin{bmatrix}\underline{U}\\\underline{\Phi}\\\underline{\phi}\\\underline{I}\end{bmatrix}=\begin{bmatrix}\underline{F}\\-\underline{q}\\-\underline{f}\\-\underline{f_b}\end{bmatrix}$$

where ˙ and ¨ denote the first and second time derivative respectively. ω_0 is the pulsation at which the materials losses are defined. This differential equation is solved by an iterative method, taking a constant time step Δt. Three methods are implemented: the Central Difference Method, the Newmark Method and the Wilson-θ Method. The method, the time step and the method's parameters are defined with the **TRANSIENT** command. The code computes the displacement field **U**, the electrical potential **Φ**, the reduced magnetic potential **ϕ**, and the currents in magnetic sources **I** for the requested time steps. The problem can be solved only in double precision.
Important notice: the Central Difference Method algorithm does not accept losses for electric or magnetic degrees of freedom, only for mechanical degrees of freedom. This means that the matrices $[K''_{u\Phi}]$, $[K''_{u\phi}]$, $[K''_{uI}]$, $[K''_{\Phi\Phi}]$, $[K''_{\phi I}]$, $[K''_{\phi\phi}]$ and $[K''_{II}]$ must be zero.

2.2.24 TRANSIENT ANALYSIS OF AN IN-VACUUM ELECTRICALLY DRIVEN PIEZOELECTRIC OR MAGNETOSTRICTIVE STRUCTURETURE (TRA3)

In this analysis, known displacements **U**, electric potentials **ϕ** and currents **I** are applied on the piezoelectric or magnetostrictive structure. The system of equations becomes:

$$\begin{bmatrix} [M] & [0] & [0] & [0] \\ [0] & [0] & [0] & [0] \\ [0] & [0] & [0] & [0] \\ [0] & [0] & [0] & [0] \end{bmatrix} \begin{bmatrix} \ddot{\underline{U}} \\ \ddot{\underline{\Phi}} \\ \ddot{\underline{\phi}} \\ \ddot{\underline{I}} \end{bmatrix} + \frac{1}{\omega_0} \begin{bmatrix} [K''_{uu}] & [K''_{u\Phi}] & [K''_{u\phi}] & [K''_{uI}] \\ [K''_{u\Phi}]^T & [K''_{\Phi\Phi}] & [0] & [0] \\ [K''_{u\phi}]^T & [0] & [K''_{\phi\phi}] & [K''_{\phi I}] \\ [K''_{uI}]^T & [0] & [K''_{\phi I}]^T & [K''_{II}] \end{bmatrix} \begin{bmatrix} \dot{\underline{U}} \\ \dot{\underline{\Phi}} \\ \dot{\underline{\phi}} \\ \dot{\underline{I}} \end{bmatrix}$$

$$+ \begin{bmatrix} [K'_{uu}] & [K'_{u\Phi}] & [K'_{u\phi}] & [K'_{uI}] \\ [K'_{u\Phi}]^T & [K'_{\Phi\Phi}] & [0] & [0] \\ [K'_{u\phi}]^T & [0] & [K'_{\phi\phi}] & [K'_{\phi I}] \\ [K'_{uI}]^T & [0] & [K'_{\phi I}]^T & [K'_{II}] \end{bmatrix} \begin{bmatrix} \underline{U} \\ \underline{\Phi} \\ \underline{\phi} \\ \underline{I} \end{bmatrix} = \begin{bmatrix} \underline{F} \\ -\underline{q} \\ -\underline{f} \\ -\underline{f_b} \end{bmatrix}$$

where ˙ and ¨ denote the first and second time derivative, respectively. ω_0 is the pulsation at which the materials losses are defined. This differential equation is solved by an iterative method, taking a constant time step Δt. Three methods are implemented: the Central Difference Method, the Newmark Method and the Wilson-θ Method. The method, the time step and the method's parameters are defined with the **TRANSIENT** command. The code computes the displacement field **U**, the electrical potential **Φ**, the reduced magnetic potential **ϕ** and the currents in magnetic sources **I** for the requested time steps, together with reactions to prescribed displacements. The problem can be solved only in double precision.

Important notice: the Central Difference Method algorithm does not accept losses for electric or magnetic degrees of freedom, only for mechanical degrees of freedom. This means that the matrices [K″$_{u\Phi}$], [K″$_{u\phi}$], [K″$_{uI}$], [K″$_{\Phi\Phi}$], [K″$_{\phi I}$], [K″$_{\phi\phi}$] and [K″$_{II}$] must be zero.

2.2.25 TRANSIENT ANALYSIS OF AN ELECTRICALLY DRIVEN PIEZOELECTRIC OR MAGNETOSTRICTIVE RADIATING IN AN INFINITE SURROUNDING FLUID SPACE (TRA4)

In this analysis, known displacements **U**, electric potentials **ϕ** and currents **I** are applied on the piezoelectric or magnetostrictive structure. The system of equations becomes:

$$\begin{bmatrix} [M] & [0] & [0] & [0] & [0] \\ [0] & [0] & [0] & [0] & [0] \\ [0] & [0] & [0] & [0] & [0] \\ [0] & [0] & [0] & [0] & [0] \\ [L]^T & [0] & [0] & [0] & \dfrac{[M_1]}{\rho^2 c^2} \end{bmatrix} \begin{bmatrix} \ddot{\underline{U}} \\ \ddot{\underline{\Phi}} \\ \ddot{\underline{\phi}} \\ \ddot{\underline{I}} \\ \ddot{\underline{P}} \end{bmatrix} + \frac{1}{\omega_0} \begin{bmatrix} [K''_{uu}] & [K''_{u\Phi}] & [K''_{u\phi}] & [K''_{uI}] & [0] \\ [K''_{u\Phi}]^T & [K''_{\Phi\Phi}] & [0] & [0] & [0] \\ [K''_{u\phi}]^T & [0] & [K''_{\phi\phi}] & [K''_{\phi I}] & [0] \\ [K''_{uI}]^T & [0] & [K''_{\phi I}]^T & [K''_{II}] & [0] \\ [0] & [0] & [0] & [0] & \left[\dfrac{H}{\rho^2 c^2}\right]^2 \end{bmatrix} \begin{bmatrix} \dot{\underline{U}} \\ \dot{\underline{\Phi}} \\ \dot{\underline{\phi}} \\ \dot{\underline{I}} \\ \dot{\underline{P}} \end{bmatrix}$$

$$+ \begin{bmatrix} [K'_{uu}] & [K'_{u\Phi}] & [K'_{u\phi}] & [K'_{uI}] & -[L] \\ [K'_{u\Phi}]^T & [K'_{\Phi\Phi}] & [0] & [0] & [0] \\ [K'_{u\phi}]^T & [0] & [K'_{\phi}] & [K'_{\phi I}] & [0] \\ [K'_{uI}]^T & [0] & [K'_{\phi I}]^T & [K'_{II}] & [0] \\ [0] & [0] & [0] & [0] & \left[\dfrac{H}{\rho^2 c^2}\right]^{\phi} \end{bmatrix} \begin{bmatrix} \underline{U} \\ \underline{\Phi} \\ \underline{\phi} \\ \underline{I} \\ \underline{P} \end{bmatrix} = \begin{bmatrix} \underline{F} \\ -\underline{q} \\ -\underline{f} \\ -\underline{f_b} \\ \dfrac{1}{\rho}\underline{\Psi} \end{bmatrix}$$

where ˙ and ¨ denote the first and second time derivative, respectively. ω_0 is the pulsation at which the materials losses are defined. The $\underline{\Psi}$ vector defines the radiation condition, applied on the external surface S limiting the fluid domain, and which is monopolar:

$$\Psi = -\frac{1}{\rho\, cnR}[D]\underline{P} + \frac{1}{\rho\, c^2}[D]\dot{\underline{P}}$$

where R is the radius of the boundary surface S. [D] and [D'] are obtained by assembling the damping elements on that surface. *n* equals 1 for axisymmetric or 3D meshes, 2 for plain-strain meshes. This differential equation is solved by an iterative method, taking a constant time step Δt. Three methods are implemented: the Central Difference Method, the Newmark Method and the Wilson-θ Method. The method, the time step and the method's parameters are defined with the **TRANSIENT** command. The code computes the displacement field **U**, the pressure **P**, the electrical potential **Φ**, the reduced magnetic potential **ϕ**, and the currents in magnetic sources **I** for the requested time steps, together with reactions to prescribed displacements. The problem can be solved only in double precision.

Important notice: the Central Difference Method algorithm does not accept losses for electric or magnetic degrees of freedom, only for mechanical degrees of freedom. This means that the matrices [K″uΦ], [K″uϕ], [K″uI], [K″ΦΦ], [K″ϕI], [K″ϕϕ] and [K″II] must be zero.

2.2.26 ELECTROSTRICTIVE STRUCTURE

Electrostrictive elements in ATILA are based on the assumption that the induced strain is proportional to the square of the applied electric field. The constitutive relationships initially proposed by Hom and Shankar [] is implemented in ATILA to model the mechanical and dielectric behaviour of electrostrictive ceramics.

Non linear static and transient analysis can be carried out. Note that for transient analysis a two-step analysis must be performed :

- ✔ The first step is a static analysis where electric potentials, electric charges or stresses are prescribed. Results from static analysis provide the working point of the structure ; these are stored in a file of extension **.sst**.
- ✔ The second step is a transient analysis, where sinus or steps voltage is used as excitation or sinus or steps electric charge is used as loading. These excitation and loading are added to values calculated in the first step. A file of extension **.sst**, compatible with the first step analysis, must exist and be readable. The Central Difference Method integration scheme must be used for this calculation.

2.2.26.1 Static analysis (STA3)

$$\begin{bmatrix} [K_{uu}(\varphi)] & [K_{u\phi}(\varphi)]^T \\ 2[K_{u\phi}(\varphi)] & [K_{\phi\phi}(\varphi)] \end{bmatrix} \begin{bmatrix} \underline{U} \\ \underline{\Phi} \end{bmatrix} = \begin{bmatrix} \underline{F} \\ -\underline{Q} \end{bmatrix}$$

2.2.26.2 Dynamic analysis (transient analysis): (TRA5)

$$\begin{bmatrix} [K_{uu}(\varphi)] & [K_{u\phi}(\varphi)] \\ 2[K_{\phi u}(\varphi)] & [K_{\phi\phi}(\varphi)] \end{bmatrix} \begin{bmatrix} \underline{U}(t) \\ \varphi(t) \end{bmatrix} + \begin{bmatrix} [M] & [0] \\ [0] & [0] \end{bmatrix} \begin{bmatrix} \ddot{\underline{U}}(t) \\ \ddot{\varphi}(t) \end{bmatrix} = \begin{bmatrix} \underline{F}(t) \\ -\underline{Q}(t) \end{bmatrix}$$

$\underline{U}$, $\underline{\Phi}$, $\underline{F}$, Q, are respectively, the vectors of the nodal values of the displacement, the electric potential, the external force and the electric charge. $\ddot{\underline{U}}$ is the vector of the second derivative of $\underline{U}$. $[K_{uu}], [K_{u\phi}], [K_{\phi\phi}]$,are respectively the stiffness matrix, the electromechanical coupling matrix and the dielectric. Note that the resulting system of equations is non linear and the rigidity matrix is unsymmetrical

2.2.27 Steady state thermal analysis

In this analysis, known Temperature $\underline{\mathbf{T}}$ and convection interface condition are applied on elastic and piezoelectric structure. The system of equations is:

$$\left([K_T] + [K_h] \right) [\underline{T}] = [q] + [q_{T\infty}]$$

where $[K_T]$ is the conductivity matrix, $[K_h]$ the convection matrix, $\underline{\mathbf{T}}$ the vector of the nodal values of temperature, $\underline{q}_{T\infty}$ the vector of the nodal values of thermal flux due to convection condition, and $\underline{\mathbf{q}}$ the vector of the nodal values of thermal flux. The user must provide the prescribed temperature on given nodes and/or convection conditions on line (two-dimensional calculation) or surface (three-dimensional calculation). The code computes the entire temperature field.
Temperature are prescribed using the EXCITATIONS entry. Elastic and Piezoelectric material parameters must include thermal data. The keyword THERMAL must be used at the exclusion of keywords STATIC, MODAL, MODAL RESANTIRES, HARMONIC, HEAT LOAD, and TRANSIENT. Matrices are assembled and stored using an out-of-core technique and LU decomposition algorithm is used to solve the system of equation.

2.2.28 Steady state thermal analysis due to heat generated from material losses

This analysis is a combination of two analysis : harmonic analysis of a piezoelectric structure and steady-state thermal analysis. Displacement, electric potential and pressure field are first calculated as described in 2.2.13 to 2.2.20, the dissipated power is then calculated from material losses and applied as a heat generator to determine the resulting temperature of the system.

In this analysis, the temperature is calculated from the dissipated power and convection interface conditions are applied on elastic and piezoelectric structure. The system of equations is:

$$\left(\left[K_T \right] + \left[K_h \right] \right) \left[\underline{T} \right] = \left[\underline{Q} \right] + \left[\underline{q} \right] + \left[\underline{q}_{T\infty} \right]$$

where $\left[K_T \right]$ is the conductivity matrix, $\left[K_h \right]$ the convection matrix, $\underline{\mathbf{T}}$ the vector of the nodal values of temperature, $\underline{q}_{T\infty}$ the vector of the nodal values of thermal flux due to convection, $\underline{\mathbf{q}}$ the vector of the nodal values of thermal flux, and $\underline{\mathbf{Q}}$ vector of the nodal values of heat flux due to the dissipated power. The code computes first the total displacement, pressure, electric potential and the temperature at nodes.

The user must provide the prescribed displacement and electric potential on given nodes as described in 2.2.13 to 2.2.20 as well as the convection condition on line (two dimensional calculation) or surface (three dimensional calculation).

As with harmonic analysis, displacement and electric potential are prescribed using the EXCITATIONS entry. Elastic and Piezoelectric material parameters must include thermal data (see chapter xxx) but this is not yet a requirement for Fluid materials. The keyword HEAT LOAD must be used at the exclusion of keywords STATIC, MODAL, MODAL RESANTIRES, HARMONIC, THERMAL, and TRANSIENT as well as the FREQUENCY keyword. Matrices are assembled and stored using an out-of-core technique and LU decomposition algorithm is used to solve the system of equation.

2.3 Physical Characteristics of the Materials Used

The physical characteristics of the materials used in the modelling are stored in the file **MATER.STD**. The structure of this file corresponds to the data entries of the entry **MATERIAL** described in Section I.3.D.

The standard **MATER.STD** file, provided with the code, follows.

```
AU10      2 0.71400E+11 0.34400E+00 0.27800E+04 0.00000E+00 8.89431E-03 0.71400E+10
AU10      2 0.85800E+03 0.23800E+03 0.23800E+03 0.23800E+03 0.00000E+00 0.00000E+00
TJND      1 0.26000E+10 0.30000E+00 0.16000E+04 0.00000E+00 8.53659E-03 2.11382E+07
25CD4     2 0.21500E+12 0.33000E+00 0.79000E+04 0.00000E+00 1.20558E-03 2.40000E+08
25CD4     2 0.85800E+03 0.46000E+02 0.46000E+02 0.46000E+02 0.00000E+00 0.00000E+00
45CD6     2 0.21500E+12 0.33000E+00 0.79000E+04 0.00000E+00 1.20558E-03 2.40000E+08
45CD6     2 0.85800E+03 0.46000E+02 0.46000E+02 0.46000E+02 0.00000E+00 0.00000E+00
AU4G      2 0.71400E+11 0.34400E+00 0.27800E+04 0.00000E+00 1.09400E-02 7.14000E+08
AU4G      2 0.85800E+03 0.23800E+03 0.23800E+03 0.23800E+03 0.00000E+00 0.00000E+00
AU2GN     1 0.75000E+11 0.34000E+00 0.28000E+04 0.00000E+00 1.74400E-03 1.20000E+08
TUNGS     1 0.34200E+12 0.26000E+00 0.17470E+05 0.00000E+00 0.00000E+00 0.00000E+00
TIGEAC    1 0.21500E+12 0.00000E+00 0.79000E+04 0.00000E+00 8.37209E-04 2.40000E+08
CU319     2 0.11700E+12 0.33000E+00 0.83600E+04 0.00000E+00 2.21538E-03 2.40000E+08
CU319     2 0.85800E+03 0.40000E+03 0.40000E+03 0.40000E+03 0.00000E+00 0.00000E+00
X31      13 0.00000E+00 0.00000E+00 0.73000E+04 0.00000E+00 0.00000E+00 0.00000E+00
X31      13 0.11900E-10-0.35400E-11-0.45800E-11 0.00000E+00 0.00000E+00 0.00000E+00
X31      13-0.35400E-11 0.11900E-10-0.45800E-11 0.00000E+00 0.00000E+00 0.00000E+00
X31      13-0.45800E-11-0.45800E-11 0.13800E-10 0.00000E+00 0.00000E+00 0.00000E+00
X31      13 0.00000E+00 0.00000E+00 0.00000E+00 0.45600E-10 0.00000E+00 0.00000E+00
X31      13 0.00000E+00 0.00000E+00 0.00000E+00 0.00000E+00 0.45600E-10 0.00000E+00
X31      13 0.00000E+00 0.00000E+00 0.00000E+00 0.00000E+00 0.00000E+00 0.30880E-10
```

X31 13 0.00000E+00 0.00000E+00 0.00000E+00 0.00000E+00 0.20100E-09 0.00000E+00
X31 13 0.00000E+00 0.00000E+00 0.00000E+00 0.20100E-09 0.00000E+00 0.00000E+00
X31 13-0.10800E-09-0.10800E-09 0.26000E-09 0.00000E+00 0.00000E+00 0.00000E+00
X31 13 0.11400E-07 0.00000E+00 0.00000E+00 0.00000E+00 0.00000E+00 0.00000E+00
X31 13 0.00000E+00 0.11400E-07 0.00000E+00 0.00000E+00 0.00000E+00 0.00000E+00
X31 13 0.00000E+00 0.00000E+00 0.74500E-08 0.00000E+00 0.00000E+00 0.00000E+00
X37 13 0.00000E+00 0.00000E+00 0.73900E+04 0.00000E+00 0.00000E+00 0.00000E+00
X37 13 0.11700E-10-0.24400E-11-0.51100E-11 0.00000E+00 0.00000E+00 0.00000E+00
X37 13-0.24400E-11 0.11700E-10-0.51100E-11 0.00000E+00 0.00000E+00 0.00000E+00
X37 13-0.51100E-11-0.51100E-11 0.14900E-10 0.00000E+00 0.00000E+00 0.00000E+00
X37 13 0.00000E+00 0.00000E+00 0.00000E+00 0.75100E-10 0.00000E+00 0.00000E+00
X37 13 0.00000E+00 0.00000E+00 0.00000E+00 0.00000E+00 0.75100E-10 0.00000E+00
X37 13 0.00000E+00 0.00000E+00 0.00000E+00 0.00000E+00 0.00000E+00 0.28280E-10
X37 13 0.00000E+00 0.00000E+00 0.00000E+00 0.00000E+00 0.71400E-09 0.00000E+00
X37 13 0.00000E+00 0.00000E+00 0.00000E+00 0.71400E-09 0.00000E+00 0.00000E+00
X37 13-0.11300E-09-0.11300E-09 0.28200E-09 0.00000E+00 0.00000E+00 0.00000E+00
X37 13 0.19700E-08 0.00000E+00 0.00000E+00 0.00000E+00 0.00000E+00 0.00000E+00
X37 13 0.00000E+00 0.19700E-08 0.00000E+00 0.00000E+00 0.00000E+00 0.00000E+00
X37 13 0.00000E+00 0.00000E+00 0.44600E-08 0.00000E+00 0.00000E+00 0.00000E+00
P762 13 0.00000E+00 0.00000E+00 0.75000E+04 0.00000E+00 0.00000E+00 0.00000E+00
P762 13 0.12700E-10-0.37000E-11-0.57000E-11 0.00000E+00 0.00000E+00 0.00000E+00
P762 13-0.37000E-11 0.12700E-10-0.57000E-11 0.00000E+00 0.00000E+00 0.00000E+00
P762 13-0.57000E-11-0.57000E-11 0.15900E-10 0.00000E+00 0.00000E+00 0.00000E+00
P762 13 0.00000E+00 0.00000E+00 0.00000E+00 0.39000E-10 0.00000E+00 0.00000E+00
P762 13 0.00000E+00 0.00000E+00 0.00000E+00 0.00000E+00 0.39000E-10 0.00000E+00
P762 13 0.00000E+00 0.00000E+00 0.00000E+00 0.00000E+00 0.00000E+00 0.32800E-10
P762 13 0.00000E+00 0.00000E+00 0.00000E+00 0.00000E+00 0.40500E-09 0.00000E+00
P762 13 0.00000E+00 0.00000E+00 0.00000E+00 0.40500E-09 0.00000E+00 0.00000E+00
P762 13-0.11800E-09-0.11800E-09 0.27200E-09 0.00000E+00 0.00000E+00 0.00000E+00
P762 13 0.71200E-08 0.00000E+00 0.00000E+00 0.00000E+00 0.00000E+00 0.00000E+00
P762 13 0.00000E+00 0.71200E-08 0.00000E+00 0.00000E+00 0.00000E+00 0.00000E+00
P762 13 0.00000E+00 0.00000E+00 0.58300E-08 0.00000E+00 0.00000E+00 0.00000E+00
X51 13 0.00000E+00 0.00000E+00 0.73500E+04 0.00000E+00 0.00000E+00 0.00000E+00
X51 13 0.11400E-10-0.33900E-11-0.41000E-11 0.00000E+00 0.00000E+00 0.00000E+00
X51 13-0.33900E-11 0.11400E-10-0.41000E-11 0.00000E+00 0.00000E+00 0.00000E+00
X51 13-0.41000E-11-0.41000E-11 0.12600E-10 0.00000E+00 0.00000E+00 0.00000E+00
X51 13 0.00000E+00 0.00000E+00 0.00000E+00 0.51000E-10 0.00000E+00 0.00000E+00
X51 13 0.00000E+00 0.00000E+00 0.00000E+00 0.00000E+00 0.51000E-10 0.00000E+00
X51 13 0.00000E+00 0.00000E+00 0.00000E+00 0.00000E+00 0.00000E+00 0.29580E-10
X51 13 0.00000E+00 0.00000E+00 0.00000E+00 0.00000E+00 0.49100E-09 0.00000E+00
X51 13 0.00000E+00 0.00000E+00 0.00000E+00 0.49100E-09 0.00000E+00 0.00000E+00
X51 13-0.95500E-10-0.95500E-10 0.20800E-09 0.00000E+00 0.00000E+00 0.00000E+00
X51 13 0.66700E-08 0.00000E+00 0.00000E+00 0.00000E+00 0.00000E+00 0.00000E+00
X51 13 0.00000E+00 0.66700E-08 0.00000E+00 0.00000E+00 0.00000E+00 0.00000E+00
X51 13 0.00000E+00 0.00000E+00 0.68700E-08 0.00000E+00 0.00000E+00 0.00000E+00
X9 13 0.00000E+00 0.00000E+00 0.54500E+04 0.00000E+00 0.00000E+00 0.00000E+00
X9 13 0.75600E-11-0.17700E-11-0.23500E-11 0.00000E+00 0.00000E+00 0.00000E+00
X9 13-0.17700E-11 0.75600E-11-0.23500E-11 0.00000E+00 0.00000E+00 0.00000E+00
X9 13-0.23500E-11-0.23500E-11 0.85100E-11 0.00000E+00 0.00000E+00 0.00000E+00
X9 13 0.00000E+00 0.00000E+00 0.00000E+00 0.26500E-10 0.00000E+00 0.00000E+00

X9 13 0.00000E+00 0.00000E+00 0.00000E+00 0.00000E+00 0.26500E-10 0.00000E+00
X9 13 0.00000E+00 0.00000E+00 0.00000E+00 0.00000E+00 0.00000E+00 0.18660E-10
X9 13 0.00000E+00 0.00000E+00 0.00000E+00 0.00000E+00 0.20500E-09 0.00000E+00
X9 13 0.00000E+00 0.00000E+00 0.00000E+00 0.20500E-09 0.00000E+00 0.00000E+00
X9 13-0.38400E-10-0.38400E-10 0.10800E-09 0.00000E+00 0.00000E+00 0.00000E+00
X9 13 0.16600E-07 0.00000E+00 0.00000E+00 0.00000E+00 0.00000E+00 0.00000E+00
X9 13 0.00000E+00 0.16600E-07 0.00000E+00 0.00000E+00 0.00000E+00 0.00000E+00
X9 13 0.00000E+00 0.00000E+00 0.54200E-08 0.00000E+00 0.00000E+00 0.00000E+00
QUARTZ 13 0.00000E+00 0.00000E+00 0.26480E+04 0.00000E+00 0.00000E+00 0.00000E+00
QUARTZ 13 0.12776E-10-0.17939E-11-0.12214E-11 0.45045E-11 0.00000E+00 0.00000E+00
QUARTZ 13-0.17939E-11 0.12777E-10-0.12214E-11-0.45045E-11 0.00000E+00 0.00000E+00
QUARTZ 13-0.12214E-11-0.12214E-11 0.96175E-11 0.00000E+00 0.00000E+00 0.00000E+00
QUARTZ 13 0.45045E-11-0.45045E-11 0.00000E+00 0.20056E-10 0.00000E+00 0.00000E+00
QUARTZ 13 0.00000E+00 0.00000E+00 0.00000E+00 0.00000E+00 0.20056E-10 0.90090E-11
QUARTZ 13 0.00000E+00 0.00000E+00 0.00000E+00 0.00000E+00 0.90090E-11 0.29141E-10
QUARTZ 13 0.23069E-11-0.23069E-11 0.00000E+00 0.71823E-12 0.00000E+00 0.00000E+00
QUARTZ 13 0.00000E+00 0.00000E+00 0.00000E+00 0.00000E+00-0.71823E-12-0.46137E-11
QUARTZ 13 0.00000E+00 0.00000E+00 0.00000E+00 0.00000E+00 0.00000E+00 0.00000E+00
QUARTZ 13 0.39200E-10 0.00000E+00 0.00000E+00 0.00000E+00 0.00000E+00 0.00000E+00
QUARTZ 13 0.00000E+00 0.39200E-10 0.00000E+00 0.00000E+00 0.00000E+00 0.00000E+00
QUARTZ 13 0.00000E+00 0.00000E+00 0.41000E-10 0.00000E+00 0.00000E+00 0.00000E+00
LINBO3 13 0.00000E+00 0.00000E+00 0.47000E+04 0.00000E+00 0.00000E+00 0.00000E+00
LINBO3 13 0.57745E-11-0.10144E-11-0.14572E-11-0.10183E-11 0.00000E+00 0.00000E+00
LINBO3 13-0.10144E-11 0.57745E-11-0.14572E-11 0.10183E-11 0.00000E+00 0.00000E+00
LINBO3 13-0.14572E-11-0.14572E-11 0.49738E-11 0.00000E+00 0.00000E+00 0.00000E+00
LINBO3 13-0.10183E-11 0.10183E-11 0.00000E+00 0.16972E-10 0.00000E+00 0.00000E+00
LINBO3 13 0.00000E+00 0.00000E+00 0.00000E+00 0.00000E+00 0.16972E-10-0.10183E-11
LINBO3 13 0.00000E+00 0.00000E+00 0.00000E+00 0.00000E+00-0.10183E-11 0.13578E-10
LINBO3 13 0.00000E+00 0.00000E+00 0.00000E+00 0.00000E+00 0.67889E-10-0.20740E-10
LINBO3 13-0.20740E-10 0.20740E-10 0.00000E+00 0.67889E-10 0.00000E+00 0.00000E+00
LINBO3 13-0.94230E-12-0.94230E-12 0.58830E-11 0.00000E+00 0.00000E+00 0.00000E+00
LINBO3 13 0.38900E-09 0.00000E+00 0.00000E+00 0.00000E+00 0.00000E+00 0.00000E+00
LINBO3 13 0.00000E+00 0.38900E-09 0.00000E+00 0.00000E+00 0.00000E+00 0.00000E+00
LINBO3 13 0.00000E+00 0.00000E+00 0.25700E-09 0.00000E+00 0.00000E+00 0.00000E+00
PZT5A 13 0.00000E+00 0.00000E+00 0.77500E+04 0.00000E+00 0.00000E+00 0.00000E+00
PZT5A 13 0.16400E-10-0.57400E-11-0.72200E-11 0.00000E+00 0.00000E+00 0.00000E+00
PZT5A 13-0.57400E-11 0.16400E-10-0.72200E-11 0.00000E+00 0.00000E+00 0.00000E+00
PZT5A 13-0.72200E-11-0.72200E-11 0.18800E-10 0.00000E+00 0.00000E+00 0.00000E+00
PZT5A 13 0.00000E+00 0.00000E+00 0.00000E+00 0.47500E-10 0.00000E+00 0.00000E+00
PZT5A 13 0.00000E+00 0.00000E+00 0.00000E+00 0.00000E+00 0.47500E-10 0.00000E+00
PZT5A 13 0.00000E+00 0.00000E+00 0.00000E+00 0.00000E+00 0.00000E+00 0.44300E-10
PZT5A 13 0.00000E+00 0.00000E+00 0.00000E+00 0.00000E+00 0.58400E-09 0.00000E+00
PZT5A 13 0.00000E+00 0.00000E+00 0.00000E+00 0.58400E-09 0.00000E+00 0.00000E+00
PZT5A 13-0.17100E-09-0.17100E-09 0.37400E-09 0.00000E+00 0.00000E+00 0.00000E+00
PZT5A 13 0.91600E-08 0.00000E+00 0.00000E+00 0.00000E+00 0.00000E+00 0.00000E+00
PZT5A 13 0.00000E+00 0.91600E-08 0.00000E+00 0.00000E+00 0.00000E+00 0.00000E+00
PZT5A 13 0.00000E+00 0.00000E+00 0.83000E-08 0.00000E+00 0.00000E+00 0.00000E+00
PIEZO3 13 0.00000E+00 0.00000E+00 0.73500E+04 0.00000E+00 0.00000E+00 0.00000E+00
PIEZO3 13 0.12700E-10-0.37000E-11-0.57000E-11 0.00000E+00 0.00000E+00 0.00000E+00
PIEZO3 13-0.37000E-11 0.12700E-10-0.57000E-11 0.00000E+00 0.00000E+00 0.00000E+00

PIEZO3 13-0.57000E-11-0.57000E-11 0.15900E-10 0.00000E+00 0.00000E+00 0.00000E+00
PIEZO3 13 0.00000E+00 0.00000E+00 0.00000E+00 0.39000E-10 0.00000E+00 0.00000E+00
PIEZO3 13 0.00000E+00 0.00000E+00 0.00000E+00 0.00000E+00 0.39000E-10 0.00000E+00
PIEZO3 13 0.00000E+00 0.00000E+00 0.00000E+00 0.00000E+00 0.00000E+00 0.32800E-10
PIEZO3 13 0.00000E+00 0.00000E+00 0.00000E+00 0.00000E+00 0.40500E-09 0.00000E+00
PIEZO3 13 0.00000E+00 0.00000E+00 0.00000E+00 0.40500E-09 0.00000E+00 0.00000E+00
PIEZO3 13-0.95500E-10-0.95500E-10 0.27200E-09 0.00000E+00 0.00000E+00 0.00000E+00
PIEZO3 13 0.71200E-08 0.00000E+00 0.00000E+00 0.00000E+00 0.00000E+00 0.00000E+00
PIEZO3 13 0.00000E+00 0.71200E-08 0.00000E+00 0.00000E+00 0.00000E+00 0.00000E+00
PIEZO3 13 0.00000E+00 0.00000E+00 0.58400E-08 0.00000E+00 0.00000E+00 0.00000E+00
FLUIDE 1 0.22200E+10 0.00000E+00 0.10000E+04 0.00000E+00 0.00000E+00 0.00000E+00
AU4G10 1 0.71400E+10 0.34400E+00 0.27800E+04 0.00000E+00 0.00000E+00 0.00000E+00
METAL 1 0.71400E+11 0.34400E+00 0.28300E+04 0.00000E+00 0.00000E+00 0.00000E+00
AU4P 13 0.00000E+00 0.00000E+00 0.27800E+04 0.00000E+00 0.00000E+00 0.00000E+00
AU4P 13 0.14006E-10-0.48179E-11-0.48179E-11 0.00000E+00 0.00000E+00 0.00000E+00
AU4P 13-0.48179E-11 0.14006E-10-0.48179E-11 0.00000E+00 0.00000E+00 0.00000E+00
AU4P 13-0.48179E-11-0.48179E-11 0.14006E-10 0.00000E+00 0.00000E+00 0.00000E+00
AU4P 13 0.00000E+00 0.00000E+00 0.00000E+00 0.37647E-10 0.00000E+00 0.00000E+00
AU4P 13 0.00000E+00 0.00000E+00 0.00000E+00 0.00000E+00 0.37647E-10 0.00000E+00
AU4P 13 0.00000E+00 0.00000E+00 0.00000E+00 0.00000E+00 0.00000E+00 0.37647E-10
AU4P 13 0.00000E+00 0.00000E+00 0.00000E+00 0.00000E+00 0.00000E+00 0.00000E+00
AU4P 13 0.00000E+00 0.00000E+00 0.00000E+00 0.00000E+00 0.00000E+00 0.00000E+00
AU4P 13 0.00000E+00 0.00000E+00 0.00000E+00 0.00000E+00 0.00000E+00 0.00000E+00
AU4P 13 0.00000E+00 0.00000E+00 0.00000E+00 0.00000E+00 0.00000E+00 0.00000E+00
AU4P 13 0.00000E+00 0.00000E+00 0.00000E+00 0.00000E+00 0.00000E+00 0.00000E+00
AU4P 13 0.00000E+00 0.00000E+00 0.00000E+00 0.00000E+00 0.00000E+00 0.00000E+00
LAIT 1 0.98000E+11 0.33000E+00 0.84200E+04 0.00000E+00 2.64490E-03 2.40000E+08
LAITON 1 0.92000E+11 0.33000E+00 0.82700E+04 0.00000E+00 0.00000E+00 0.00000E+00
25C 1 0.92000E+11 0.33000E+00 0.82700E+04 0.00000E+00 0.00000E+00 0.00000E+00
TIGE 1 0.21500E+12 0.00000E+00 0.79000E+04 0.00000E+00 0.00000E+00 0.00000E+00
25CD1 2 0.42000E+11 0.33500E+00 0.18000E+04 0.00000E+00 8.82114E-03 3.41463E+08
25CD1 2 0.85800E+03 0.46000E+02 0.46000E+02 0.46000E+02 0.00000E+00 0.00000E+00
JM 13 0.00000E+00 0.00000E+00 0.91000E+04 0.00000E+00 0.00000E+00 0.00000E+00
JM 13 0.25000E-10-0.18000E-11-0.16700E-10 0.00000E+00 0.00000E+00 0.00000E+00
JM 13-0.18000E-11 0.25000E-10-0.16700E-10 0.00000E+00 0.00000E+00 0.00000E+00
JM 13-0.16700E-10-0.16700E-10 0.40000E-10 0.00000E+00 0.00000E+00 0.00000E+00
JM 13 0.00000E+00 0.00000E+00 0.00000E+00 0.18000E-09 0.00000E+00 0.00000E+00
JM 13 0.00000E+00 0.00000E+00 0.00000E+00 0.00000E+00 0.18000E-09 0.00000E+00
JM 13 0.00000E+00 0.00000E+00 0.00000E+00 0.00000E+00 0.00000E+00 0.53600E-10
JM 13 0.00000E+00 0.00000E+00 0.00000E+00 0.00000E+00 0.28000E-07 0.00000E+00
JM 13 0.00000E+00 0.00000E+00 0.00000E+00 0.28000E-07 0.00000E+00 0.00000E+00
JM 13-0.53000E-08-0.53000E-08 0.10600E-07 0.00000E+00 0.00000E+00 0.00000E+00
JM 13 0.56900E-05 0.00000E+00 0.00000E+00 0.00000E+00 0.00000E+00 0.00000E+00
JM 13 0.00000E+00 0.56900E-05 0.00000E+00 0.00000E+00 0.00000E+00 0.00000E+00
JM 13 0.00000E+00 0.00000E+00 0.27100E-05 0.00000E+00 0.00000E+00 0.00000E+00
VACUO 1 0.12566E-05 0.00000E+00 0.00000E+00 0.00000E+00 0.00000E+00 0.00000E+00
VIDE 1 0.12566E-05 0.00000E+00 0.00000E+00 0.00000E+00 0.00000E+00 0.00000E+00
JMP 25 0.00000E+00 0.00000E+00 0.91000E+04 0.00000E+00 0.00000E+00 0.00000E+00
JMP 25 0.25000E-10-0.18000E-11-0.16700E-10 0.00000E+00 0.00000E+00 0.00000E+00
JMP 25-0.18000E-11 0.25000E-10-0.16700E-10 0.00000E+00 0.00000E+00 0.00000E+00

```
JMP       25-0.16700E-10-0.16700E-10 0.40000E-10 0.00000E+00 0.00000E+00 0.00000E+00
JMP       25 0.00000E+00 0.00000E+00 0.00000E+00 0.18000E-09 0.00000E+00 0.00000E+00
JMP       25 0.00000E+00 0.00000E+00 0.00000E+00 0.00000E+00 0.18000E-09 0.00000E+00
JMP       25 0.00000E+00 0.00000E+00 0.00000E+00 0.00000E+00 0.00000E+00 0.53600E-10
JMP       25 0.00000E+00 0.00000E+00 0.00000E+00 0.00000E+00 0.28000E-07 0.00000E+00
JMP       25 0.00000E+00 0.00000E+00 0.00000E+00 0.28000E-07 0.00000E+00 0.00000E+00
JMP       25-0.53000E-08-0.53000E-08 0.10600E-07 0.00000E+00 0.00000E+00 0.00000E+00
JMP       25 0.56900E-05 0.00000E+00 0.00000E+00 0.00000E+00 0.00000E+00 0.00000E+00
JMP       25 0.00000E+00 0.56900E-05 0.00000E+00 0.00000E+00 0.00000E+00 0.00000E+00
JMP       25 0.00000E+00 0.00000E+00 0.27100E-05 0.00000E+00 0.00000E+00 0.00000E+00
JMP       25 0.00000E+00 0.00000E+00 0.00000E+00 0.00000E+00 0.00000E+00 0.00000E+00
JMP       25 0.00000E+00 0.00000E+00 0.00000E+00 0.00000E+00 0.00000E+00 0.00000E+00
JMP       25 0.00000E+00 0.00000E+00 0.00000E+00 0.00000E+00 0.00000E+00 0.00000E+00
JMP       25 0.00000E+00 0.00000E+00 0.00000E+00 0.00000E+00 0.00000E+00 0.00000E+00
JMP       25 0.00000E+00 0.00000E+00 0.00000E+00 0.00000E+00 0.00000E+00 0.00000E+00
JMP       25 0.00000E+00 0.00000E+00 0.00000E+00 0.00000E+00 0.00000E+00 0.00000E+00
JMP       25 0.00000E+00 0.00000E+00 0.00000E+00 0.00000E+00 0.00000E+00 0.00000E+00
JMP       25 0.00000E+00 0.00000E+00 0.00000E+00 0.00000E+00 0.00000E+00 0.00000E+00
JMP       25 0.00000E+00 0.00000E+00 0.00000E+00 0.00000E+00 0.00000E+00 0.00000E+00
JMP       25 0.00000E+00 0.00000E+00 0.00000E+00 0.00000E+00 0.00000E+00 0.00000E+00
JMP       25 0.00000E+00 0.00000E+00 0.00000E+00 0.00000E+00 0.00000E+00 0.00000E+00
JMP       25 0.00000E+00 0.00000E+00 0.00000E+00 0.00000E+00 0.00000E+00 0.00000E+00
XMAT3     25 0.00000E+00 8.58000E+02 0.73500E+04 0.20000E+01 0.20000E+01 0.20000E+01
XMAT3     25 0.11400E-10-0.33900E-11-0.41000E-11 0.00000E+00 0.00000E+00 0.00000E+00
XMAT3     25-0.33900E-11 0.11400E-10-0.41000E-11 0.00000E+00 0.00000E+00 0.00000E+00
XMAT3     25-0.41000E-11-0.41000E-11 0.12600E-10 0.00000E+00 0.00000E+00 0.00000E+00
XMAT3     25 0.00000E+00 0.00000E+00 0.00000E+00 0.51000E-10 0.00000E+00 0.00000E+00
XMAT3     25 0.00000E+00 0.00000E+00 0.00000E+00 0.00000E+00 0.51000E-10 0.00000E+00
XMAT3     25 0.00000E+00 0.00000E+00 0.00000E+00 0.00000E+00 0.00000E+00 0.29580E-10
XMAT3     25 0.00000E+00 0.00000E+00 0.00000E+00 0.00000E+00 0.49100E-09 0.00000E+00
XMAT3     25 0.00000E+00 0.00000E+00 0.00000E+00 0.49100E-09 0.00000E+00 0.00000E+00
XMAT3     25-0.95500E-10-0.95500E-10 0.20790E-09 0.00000E+00 0.00000E+00 0.00000E+00
XMAT3     25 0.66710E-08 0.00000E+00 0.00000E+00 0.00000E+00 0.00000E+00 0.00000E+00
XMAT3     25 0.00000E+00 0.66710E-08 0.00000E+00 0.00000E+00 0.00000E+00 0.00000E+00
XMAT3     25 0.00000E+00 0.00000E+00 0.68860E-08 0.00000E+00 0.00000E+00 0.00000E+00
XMAT3     25 0.00000E+00 0.00000E+00 0.00000E+00 0.00000E+00 0.00000E+00 0.00000E+00
XMAT3     25 0.00000E+00 0.00000E+00 0.00000E+00 0.00000E+00 0.00000E+00 0.00000E+00
XMAT3     25 0.00000E+00 0.00000E+00-0.85160E-12 0.00000E+00 0.00000E+00 0.00000E+00
XMAT3     25 0.00000E+00 0.00000E+00 0.00000E+00 0.00000E+00 0.00000E+00 0.00000E+00
XMAT3     25 0.00000E+00 0.00000E+00 0.00000E+00 0.00000E+00 0.00000E+00 0.00000E+00
XMAT3     25 0.00000E+00 0.00000E+00 0.00000E+00 0.00000E+00 0.00000E+00 0.00000E+00
XMAT3     25 0.00000E+00 0.00000E+00 0.00000E+00 0.00000E+00 0.00000E+00 0.00000E+00
XMAT3     25 0.00000E+00 0.00000E+00 0.00000E+00 0.00000E+00 0.00000E+00 0.00000E+00
XMAT3     25 0.00000E+00 0.00000E+00 0.00000E+00 0.00000E+00 0.00000E+00 0.00000E+00
XMAT3     25 0.00000E+00 0.00000E+00 0.00000E+00 0.00000E+00 0.00000E+00 0.00000E+00
XMAT3     25 0.00000E+00 0.00000E+00 0.00000E+00 0.00000E+00 0.00000E+00 0.00000E+00
XMAT3     25 0.00000E+00 0.00000E+00-0.14500E-09 0.00000E+00 0.00000E+00 0.00000E+00
XMAT4     25 0.00000E+00 8.58000E+02 0.73500E+04 0.20000E+01 0.20000E+01 0.20000E+01
XMAT4     25 0.11400E-10-0.33900E-11-0.41000E-11 0.00000E+00 0.00000E+00 0.00000E+00
XMAT4     25-0.33900E-11 0.11400E-10-0.41000E-11 0.00000E+00 0.00000E+00 0.00000E+00
```

XMAT4 25-0.41000E-11-0.41000E-11 0.12600E-10 0.00000E+00 0.00000E+00 0.00000E+00
XMAT4 25 0.00000E+00 0.00000E+00 0.00000E+00 0.51000E-10 0.00000E+00 0.00000E+00
XMAT4 25 0.00000E+00 0.00000E+00 0.00000E+00 0.00000E+00 0.51000E-10 0.00000E+00
XMAT4 25 0.00000E+00 0.00000E+00 0.00000E+00 0.00000E+00 0.00000E+00 0.29580E-10
XMAT4 25 0.00000E+00 0.00000E+00 0.00000E+00 0.00000E+00 0.49100E-09 0.00000E+00
XMAT4 25 0.00000E+00 0.00000E+00 0.00000E+00 0.49100E-09 0.00000E+00 0.00000E+00
XMAT4 25-0.95500E-10-0.95500E-10 0.20790E-09 0.00000E+00 0.00000E+00 0.00000E+00
XMAT4 25 0.66710E-08 0.00000E+00 0.00000E+00 0.00000E+00 0.00000E+00 0.00000E+00
XMAT4 25 0.00000E+00 0.66710E-08 0.00000E+00 0.00000E+00 0.00000E+00 0.00000E+00
XMAT4 25 0.00000E+00 0.00000E+00 0.68860E-08 0.00000E+00 0.00000E+00 0.00000E+00
XMAT4 25-0.11400E-11 0.00000E+00 0.00000E+00 0.00000E+00 0.00000E+00 0.00000E+00
XMAT4 25 0.00000E+00-0.11400E-11 0.00000E+00 0.00000E+00 0.00000E+00 0.00000E+00
XMAT4 25 0.00000E+00 0.00000E+00 0.00000E+00 0.00000E+00 0.00000E+00 0.00000E+00
XMAT4 25 0.00000E+00 0.00000E+00 0.00000E+00 0.00000E+00 0.00000E+00 0.00000E+00
XMAT4 25 0.00000E+00 0.00000E+00 0.00000E+00 0.00000E+00 0.00000E+00 0.00000E+00
XMAT4 25 0.00000E+00 0.00000E+00 0.00000E+00 0.00000E+00 0.00000E+00-0.22800E-11
XMAT4 25 0.00000E+00 0.00000E+00 0.00000E+00 0.00000E+00 0.00000E+00 0.00000E+00
XMAT4 25 0.00000E+00 0.00000E+00 0.00000E+00 0.00000E+00 0.00000E+00 0.00000E+00
XMAT4 25 0.00000E+00 0.00000E+00 0.00000E+00 0.00000E+00 0.00000E+00 0.00000E+00
XMAT4 25 0.00000E+00 0.00000E+00 0.00000E+00 0.00000E+00 0.00000E+00 0.00000E+00
XMAT4 25 0.00000E+00 0.00000E+00 0.00000E+00 0.00000E+00 0.00000E+00 0.00000E+00
XMAT4 25 0.00000E+00 0.00000E+00-0.59140E-10 0.00000E+00 0.00000E+00 0.00000E+00
AIR 1 0.15000E+06 0.00000E+00 0.13000E+01 0.00000E+00 0.00000E+00 0.00000E+00
ACIER 1 0.21500E+12 0.31000E+00 0.78000E+04 0.00000E+00 0.00000E+00 0.21500E+11
P189 25 0.00000E+00 8.58000E+02 7.60000E+03 2.00000E+00 2.00000E+00 2.00000E+00
P189 25 1.07400E-11-3.33000E-12-5.70000E-12 0.00000E+00 0.00000E+00 0.00000E+00
P189 25-3.33000E-12 1.07400E-11-5.70000E-12 0.00000E+00 0.00000E+00 0.00000E+00
P189 25-5.70000E-12-5.70000E-12 1.34200E-11 0.00000E+00 0.00000E+00 0.00000E+00
P189 25 0.00000E+00 0.00000E+00 0.00000E+00 3.90000E-11 0.00000E+00 0.00000E+00
P189 25 0.00000E+00 0.00000E+00 0.00000E+00 0.00000E+00 3.90000E-11 0.00000E+00
P189 25 0.00000E+00 0.00000E+00 0.00000E+00 0.00000E+00 0.00000E+00 2.81400E-11
P189 25 0.00000E+00 0.00000E+00 0.00000E+00 0.00000E+00 4.05000E-10 0.00000E+00
P189 25 0.00000E+00 0.00000E+00 0.00000E+00 4.05000E-10 0.00000E+00 0.00000E+00
P189 25-1.05400E-10-1.05400E-10 2.32000E-10 0.00000E+00 0.00000E+00 0.00000E+00
P189 25 2.91743E-09 0.00000E+00 0.00000E+00 0.00000E+00 0.00000E+00 0.00000E+00
P189 25 0.00000E+00 2.91743E-09 0.00000E+00 0.00000E+00 0.00000E+00 0.00000E+00
P189 25 0.00000E+00 0.00000E+00 1.42185E-09 0.00000E+00 0.00000E+00 0.00000E+00
P189 25-2.14800E-14 6.66000E-15 1.14000E-14 0.00000E+00 0.00000E+00 0.00000E+00
P189 25 6.66000E-15-2.14800E-14 1.14000E-14 0.00000E+00 0.00000E+00 0.00000E+00
P189 25 1.14000E-14 1.14000E-14-2.68400E-14 0.00000E+00 0.00000E+00 0.00000E+00
P189 25 0.00000E+00 0.00000E+00 0.00000E+00-7.80000E-14 0.00000E+00 0.00000E+00
P189 25 0.00000E+00 0.00000E+00 0.00000E+00 0.00000E+00-7.80000E-14 0.00000E+00
P189 25 0.00000E+00 0.00000E+00 0.00000E+00 0.00000E+00 0.00000E+00-5.62800E-14
P189 25 0.00000E+00 0.00000E+00 0.00000E+00 0.00000E+00 0.00000E+00 0.00000E+00
P189 25 0.00000E+00 0.00000E+00 0.00000E+00 0.00000E+00 0.00000E+00 0.00000E+00
P189 25 0.00000E+00 0.00000E+00 0.00000E+00 0.00000E+00 0.00000E+00 0.00000E+00
P189 25-3.69043E-11 0.00000E+00 0.00000E+00 0.00000E+00 0.00000E+00 0.00000E+00
P189 25 0.00000E+00-3.69043E-11 0.00000E+00 0.00000E+00 0.00000E+00 0.00000E+00
P189 25 0.00000E+00 0.00000E+00-2.99717E-11 0.00000E+00 0.00000E+00 0.00000E+00
PZT4 13 0.00000E+00 0.00000E+00 0.75000E+04 0.00000E+00 0.00000E+00 0.00000E+00

PZT4 13 0.12300E-10-0.40500E-11-0.53100E-11 0.00000E+00 0.00000E+00 0.00000E+00
PZT4 13-0.40500E-11 0.12300E-10-0.53100E-11 0.00000E+00 0.00000E+00 0.00000E+00
PZT4 13-0.53100E-11-0.53100E-11 0.15500E-10 0.00000E+00 0.00000E+00 0.00000E+00
PZT4 13 0.00000E+00 0.00000E+00 0.00000E+00 0.39000E-10 0.00000E+00 0.00000E+00
PZT4 13 0.00000E+00 0.00000E+00 0.00000E+00 0.00000E+00 0.39000E-10 0.00000E+00
PZT4 13 0.00000E+00 0.00000E+00 0.00000E+00 0.00000E+00 0.00000E+00 0.32700E-10
PZT4 13 0.00000E+00 0.00000E+00 0.00000E+00 0.00000E+00 0.49600E-09 0.00000E+00
PZT4 13 0.00000E+00 0.00000E+00 0.00000E+00 0.49600E-09 0.00000E+00 0.00000E+00
PZT4 13-0.12300E-09-0.12300E-09 0.28900E-09 0.00000E+00 0.00000E+00 0.00000E+00
PZT4 13 0.64600E-08 0.00000E+00 0.00000E+00 0.00000E+00 0.00000E+00 0.00000E+00
PZT4 13 0.00000E+00 0.64600E-08 0.00000E+00 0.00000E+00 0.00000E+00 0.00000E+00
PZT4 13 0.00000E+00 0.00000E+00 0.56200E-08 0.00000E+00 0.00000E+00 0.00000E+00
AU4G40 1 0.17850E+10 0.34400E+00 0.27800E+04 0.00000E+00 0.00000E+00 0.00000E+00
EAU 1 0.22200E+10 0.00000E+00 0.10000E+04 0.00000E+00 0.00000E+00 0.00000E+00
PLC3 2 0.73000E+11 0.22000E+00 0.25400E+04 0.00000E+00 0.00000E+00 0.00000E+00
PLC3 2 0.29000E+10 0.35000E+00 0.11000E+04 0.00000E+00 0.41600E+00 0.00000E+00
TUBE6 2 0.73000E+11 0.22000E+00 0.24800E+04 0.00000E+00 0.00000E+00 0.00000E+00
TUBE6 2 0.29000E+10 0.35000E+00 0.11000E+04 0.00000E+00 0.48500E+00 0.00000E+00
TUBE8 2 0.73000E+11 0.22000E+00 0.24800E+04 0.00000E+00 0.00000E+00 0.00000E+00
TUBE8 2 0.29000E+10 0.35000E+00 0.11000E+04 0.00000E+00 0.44000E+00 0.00000E+00
MATER1 1 0.30000E+11 0.25000E+00 0.27800E+04 0.00000E+00 0.00000E+00 0.00000E+00
MAT1 1 0.10000E+12 0.30000E+00 0.30000E+04 0.00000E+00 0.00000E+00 0.00000E+00
MVOUTE 1 0.21000E+11 0.00000E+00 0.30000E+04 0.00000E+00 0.00000E+00 0.00000E+00
X51P05 25 0.00000E+00 8.58000E+02 0.73500E+04 2.00000E+00 2.00000E+00 2.00000E+00
X51P05 25 0.11400E-10-0.33900E-11-0.41000E-11 0.00000E+00 0.00000E+00 0.00000E+00
X51P05 25-0.33900E-11 0.11400E-10-0.41000E-11 0.00000E+00 0.00000E+00 0.00000E+00
X51P05 25-0.41000E-11-0.41000E-11 0.12600E-10 0.00000E+00 0.00000E+00 0.00000E+00
X51P05 25 0.00000E+00 0.00000E+00 0.00000E+00 0.51000E-10 0.00000E+00 0.00000E+00
X51P05 25 0.00000E+00 0.00000E+00 0.00000E+00 0.00000E+00 0.51000E-10 0.00000E+00
X51P05 25 0.00000E+00 0.00000E+00 0.00000E+00 0.00000E+00 0.00000E+00 0.29580E-10
X51P05 25 0.00000E+00 0.00000E+00 0.00000E+00 0.00000E+00 0.49100E-09 0.00000E+00
X51P05 25 0.00000E+00 0.00000E+00 0.00000E+00 0.49100E-09 0.00000E+00 0.00000E+00
X51P05 25-0.95500E-10-0.95500E-10 0.20800E-09 0.00000E+00 0.00000E+00 0.00000E+00
X51P05 25 0.66700E-08 0.00000E+00 0.00000E+00 0.00000E+00 0.00000E+00 0.00000E+00
X51P05 25 0.00000E+00 0.66700E-08 0.00000E+00 0.00000E+00 0.00000E+00 0.00000E+00
X51P05 25 0.00000E+00 0.00000E+00 0.68700E-08 0.00000E+00 0.00000E+00 0.00000E+00
X51P05 25-0.57000E-12 0.16950E-12 0.20500E-12 0.00000E+00 0.00000E+00 0.00000E+00
X51P05 25 0.16950E-12-0.57000E-12 0.20500E-12 0.00000E+00 0.00000E+00 0.00000E+00
X51P05 25 0.20500E-12 0.20500E-12-0.63000E-12 0.00000E+00 0.00000E+00 0.00000E+00
X51P05 25 0.00000E+00 0.00000E+00 0.00000E+00-0.25500E-11 0.00000E+00 0.00000E+00
X51P05 25 0.00000E+00 0.00000E+00 0.00000E+00 0.00000E+00-0.25500E-11 0.00000E+00
X51P05 25 0.00000E+00 0.00000E+00 0.00000E+00 0.00000E+00 0.00000E+00-0.14790E-11
X51P05 25 0.00000E+00 0.00000E+00 0.00000E+00 0.00000E+00-0.24550E-10 0.00000E+00
X51P05 25 0.00000E+00 0.00000E+00 0.00000E+00-0.24550E-10 0.00000E+00 0.00000E+00
X51P05 25 0.47750E-11 0.47750E-11-0.10400E-10 0.00000E+00 0.00000E+00 0.00000E+00
X51P05 25 0.00000E+00 0.00000E+00 0.00000E+00 0.00000E+00 0.00000E+00 0.00000E+00
X51P05 25 0.00000E+00 0.00000E+00 0.00000E+00 0.00000E+00 0.00000E+00 0.00000E+00
X51P05 25 0.00000E+00 0.00000E+00 0.00000E+00 0.00000E+00 0.00000E+00 0.00000E+00
RUBAN2 13 0.00000E+00 0.00000E+00 0.91000E+04 0.00000E+00 0.00000E+00 0.00000E+00
RUBAN2 13 0.76000E-10-0.54720E-11-0.27833E-10 0.00000E+00 0.00000E+00 0.00000E+00

RUBAN2 13-0.54720E-11 0.76000E-10-0.27833E-10 0.00000E+00 0.00000E+00 0.00000E+00
RUBAN2 13-0.27833E-10-0.27833E-10 0.66667E-10 0.00000E+00 0.00000E+00 0.00000E+00
RUBAN2 13 0.00000E+00 0.00000E+00 0.00000E+00 0.20606E-09 0.00000E+00 0.00000E+00
RUBAN2 13 0.00000E+00 0.00000E+00 0.00000E+00 0.00000E+00 0.20606E-09 0.00000E+00
RUBAN2 13 0.00000E+00 0.00000E+00 0.00000E+00 0.00000E+00 0.00000E+00 0.16294E-10
RUBAN2 13 0.00000E+00 0.00000E+00 0.00000E+00 0.00000E+00 0.53417E-05 0.00000E+00
RUBAN2 13 0.00000E+00 0.00000E+00 0.00000E+00 0.53417E-05 0.00000E+00 0.00000E+00
RUBAN2 13-0.23812E-05-0.23812E-05 0.47624E-05 0.00000E+00 0.00000E+00 0.00000E+00
RUBAN2 13 0.51380E-01 0.00000E+00 0.00000E+00 0.00000E+00 0.00000E+00 0.00000E+00
RUBAN2 13 0.00000E+00 0.51380E-01 0.00000E+00 0.00000E+00 0.00000E+00 0.00000E+00
RUBAN2 13 0.00000E+00 0.00000E+00 0.30270E-01 0.00000E+00 0.00000E+00 0.00000E+00
ALU2024 2 0.73100E+11 0.32500E+00 0.27700E+04 0.00000E+00 8.73984E-03 5.94309E+08
ALU2024 2 0.85800E+03 0.23800E+03 0.23800E+03 0.23800E+03 0.00000E+00 0.00000E+00
CAU4G 2 0.71400E+11 0.34400E+00 0.27800E+04 0.00000E+00 0.00000E+00 0.00000E+00
CAU4G 2 0.71400E+11 0.34400E+00 0.27800E+04 0.00000E+00 0.10000E+01 0.00000E+00
JAJA 1 0.14400E+10 0.00000E+00 0.10000E+04 0.00000E+00 0.00000E+00 0.00000E+00
LAITDB 1 0.10440E+12 0.34289E+00 0.86000E+04 0.00000E+00 0.00000E+00 0.00000E+00
PLCA3 2 0.73000E+11 0.22000E+00 0.25400E+04 0.00000E+00 0.00000E+00 0.00000E+00
PLCA3 2 0.29000E+10 0.35000E+00 0.11000E+04 0.00000E+00 0.41600E+00 0.00000E+00
VERRE 1 0.73000E+11 0.22000E+00 0.25400E+04 0.00000E+00 0.00000E+00 0.00000E+00
WATER 1 0.22200E+10 0.00000E+00 0.10000E+04 0.00000E+00 0.00000E+00 0.00000E+00
25CD4D 2 0.21500E+12 0.33000E+00 0.75000E+03 0.00000E+00 8.78049E-03 1.74797E+09
25CD4D 2 0.85800E+03 0.46000E+02 0.46000E+02 0.46000E+02 0.00000E+00 0.00000E+00
PVC10 1 0.41000E+10 0.40000E+00 0.14000E+04 0.00000E+00 0.00000E+00 0.41000E+09
DUMMY 1 0.00000E+00 0.00000E+00 0.00000E+00 0.00000E+00 0.00000E+00 0.00000E+00
BRONZE 2 1.25000E+11 3.10000E-01 7.60000E+03 0.00000E+00 8.61789E-03 1.01626E+09
BRONZE 2 3.70000E+02 3.90000E+02 3.90000E+02 3.90000E+02 0.00000E+00 0.00000E+00
STEEL 2 2.10000E+11 2.85000E-01 7.80000E+03 0.00000E+00 8.41463E-03 1.70732E+09
STEEL 2 3.00000E+02 3.00000E+01 3.00000E+01 3.00000E+01 0.00000E+00 0.00000E+00
X31AG5 14 0.71000E+11 0.33000E+00 0.26270E+04 0.00000E+00 0.00000E+00 0.00000E+00
X31AG5 14 0.00000E+00 0.00000E+00 0.73000E+04 0.00000E+00 0.00000E+00 0.00000E+00
X31AG5 14 0.11900E-10-0.35400E-11-0.45800E-11 0.00000E+00 0.00000E+00 0.00000E+00
X31AG5 14-0.35400E-11 0.11900E-10-0.45800E-11 0.00000E+00 0.00000E+00 0.00000E+00
X31AG5 14-0.45800E-11-0.45800E-11 0.13800E-10 0.00000E+00 0.00000E+00 0.00000E+00
X31AG5 14 0.00000E+00 0.00000E+00 0.00000E+00 0.45600E-10 0.00000E+00 0.00000E+00
X31AG5 14 0.00000E+00 0.00000E+00 0.00000E+00 0.00000E+00 0.45600E-10 0.00000E+00
X31AG5 14 0.00000E+00 0.00000E+00 0.00000E+00 0.00000E+00 0.00000E+00 0.30880E-10
X31AG5 14 0.00000E+00 0.00000E+00 0.00000E+00 0.00000E+00 0.21000E-09 0.00000E+00
X31AG5 14 0.00000E+00 0.00000E+00 0.00000E+00 0.21000E-09 0.00000E+00 0.00000E+00
X31AG5 14-0.10800E-09-0.10800E-09 0.26000E-09 0.00000E+00 0.00000E+00 0.00000E+00
X31AG5 14 0.11400E-07 0.00000E+00 0.00000E+00 0.00000E+00 0.00000E+00 0.00000E+00
X31AG5 14 0.00000E+00 0.11400E-07 0.00000E+00 0.00000E+00 0.00000E+00 0.00000E+00
X31AG5 14 0.00000E+00 0.00000E+00 0.75800E-08 0.00000E+00 0.00000E+00 0.00000E+00
AG5 1 0.71000E+11 0.33000E+00 0.26270E+04 0.00000E+00 0.00000E+00 0.00000E+00
AG5X31 14 0.71000E+11 0.33000E+00 0.26270E+04 0.00000E+00 0.00000E+00 0.00000E+00
AG5X31 14 0.00000E+00 0.00000E+00 0.73000E+04 0.00000E+00 0.00000E+00 0.00000E+00
AG5X31 14 0.11900E-10-0.35400E-11-0.45800E-11 0.00000E+00 0.00000E+00 0.00000E+00
AG5X31 14-0.35400E-11 0.11900E-10-0.45800E-11 0.00000E+00 0.00000E+00 0.00000E+00
AG5X31 14-0.45800E-11-0.45800E-11 0.13800E-10 0.00000E+00 0.00000E+00 0.00000E+00
AG5X31 14 0.00000E+00 0.00000E+00 0.00000E+00 0.45600E-10 0.00000E+00 0.00000E+00

AG5X31 14 0.00000E+00 0.00000E+00 0.00000E+00 0.00000E+00 0.45600E-10 0.00000E+00
AG5X31 14 0.00000E+00 0.00000E+00 0.00000E+00 0.00000E+00 0.00000E+00 0.30880E-10
AG5X31 14 0.00000E+00 0.00000E+00 0.00000E+00 0.00000E+00 0.21000E-09 0.00000E+00
AG5X31 14 0.00000E+00 0.00000E+00 0.00000E+00 0.21000E-09 0.00000E+00 0.00000E+00
AG5X31 14-0.10800E-09-0.10800E-09 0.26000E-09 0.00000E+00 0.00000E+00 0.00000E+00
AG5X31 14 0.11400E-07 0.00000E+00 0.00000E+00 0.00000E+00 0.00000E+00 0.00000E+00
AG5X31 14 0.00000E+00 0.11400E-07 0.00000E+00 0.00000E+00 0.00000E+00 0.00000E+00
AG5X31 14 0.00000E+00 0.00000E+00 0.75800E-08 0.00000E+00 0.00000E+00 0.00000E+00

The above physical constants were obtained from the following references:

- ✔ "American Institute of Physics Handbook", Second edition, McGraw-Hill, (1963).
- ✔ GERDSM values.
- ✔ J. ROUSSEAU, « Etude de la propagation d'ondes de Rayleigh sur des milieux stratifiés »,
- ✔ Thèse de 3ème cycle, Université des Sciences et Techniques de Lille, (1979).
- ✔ P. TIERCE, « Modélisation du transducteur ISABELLE par la méthode des éléments finis », Thèse de Docteur-Ingénieur, Université de Valenciennes et du Hainaut-Cambrésis, (1985).
- ✔ P. TIERCE, J.N. DECARPIGNY, « Caractérisation de céramiques piézoélectriques : détermination de leurs constantes élastiques, piézoélectriques et diélectriques », TSMS.82.48.826.268.T pour le GERDSM (DCAN-Toulon), rapport final, (1983).
- ✔ P. TIERCE, C. GRANGER, H. TOURNEUR, Internal report, ISEN Acoustics Laboratory (1986).
- ✔ J.N. DECARPIGNY, Internal report, ISEN Acoustics Laboratory (1988).
- ✔ E. DIEULESAINT, D. ROYER, « Ondes élastiques dans les solides », Ed. Masson, (1974).
- ✔ D.A. BERLINCOURT, D.R. CURRAN, H. JAFFE, in "Physical Acoustics, Principles and Methods", Vol. 1 Part A, Ed. by W.P. MASON, Academic Press, (1964).

2.3.1 Special Case of a Tangentially Polarized Piezoelectric Segmented Ring

The objective is to model a tangentially polarized piezoelectric segmented ring (Fig.1) with a bidimensional mesh such as would be used if the structure were axisymmetric. This objective corresponds to the need to reduce the problem size when dealing with radiation problems. The suggested method of solution is as follows:

Build the bidimensional mesh of an equivalent axisymmetric ring of the same geometric dimensions, with radial poling

Modify the elastic, piezoelectric and dielectric tensors to take into account the polarization direction change. After transformation the initial tensor:

$$\begin{matrix}
s^E_{11} & s^E_{12} & s^E_{13} & 0 & 0 & 0 & 0 & 0 & d_{31} \\
s^E_{12} & s^E_{11} & s^E_{13} & 0 & 0 & 0 & 0 & 0 & d_{31} \\
s^E_{13} & s^E_{13} & s^E_{33} & 0 & 0 & 0 & 0 & 0 & d_{33} \\
0 & 0 & 0 & s^E_{44} & 0 & 0 & 0 & d_{15} & 0 \\
0 & 0 & 0 & 0 & s^E_{44} & 0 & d_{15} & 0 & 0 \\
0 & 0 & 0 & 0 & 0 & s^E_{66} & 0 & 0 & 0 \\
0 & 0 & 0 & 0 & d_{15} & 0 & \varepsilon^s_{11} & 0 & 0 \\
0 & 0 & 0 & d_{15} & 0 & 0 & 0 & \varepsilon^s_{11} & 0 \\
d_{31} & d_{31} & d_{33} & 0 & 0 & 0 & 0 & 0 & \varepsilon^s_{33}
\end{matrix}$$

becomes:

$$\begin{matrix}
s^E_{11} & s^E_{13} & s^E_{12} & 0 & 0 & 0 & 0 & 0 & d_{31} \\
s^E_{13} & s^E_{33} & s^E_{13} & 0 & 0 & 0 & 0 & 0 & d_{33} \\
s^E_{12} & s^E_{13} & s^E_{11} & 0 & 0 & 0 & 0 & 0 & d_{31} \\
0 & 0 & 0 & s^E_{44} & 0 & 0 & 0 & d_{15} & 0 \\
0 & 0 & 0 & 0 & s^E_{66} & 0 & 0 & 0 & 0 \\
0 & 0 & 0 & 0 & 0 & s^E_{44} & d_{15} & 0 & 0 \\
0 & 0 & 0 & 0 & 0 & d_{15} & \varepsilon^s_{11} & 0 & 0 \\
0 & 0 & 0 & d_{15} & 0 & 0 & 0 & \varepsilon^s_{11} & 0 \\
d_{31} & d_{33} & d_{31} & 0 & 0 & 0 & 0 & 0 & \varepsilon^s_{33}
\end{matrix}$$

Modify the displacement and pressure magnitudes computed in a harmonic analysis to take into account the electrical field amplitude difference due to the difference between the thickness of a segment and the thickness of the ring. The correct values (subscript 3D) of the displacement u and of the pressure p are obtained from the value computed with the axisymmetrical model (subscript 2D) by:

$$\frac{u_{2D}}{u_{3D}} = \frac{p_{2D}}{p_{3D}} = \frac{d}{e}$$

where d is the stave thickness and e is the ring thickness.

- Modify the electrical impedance values in the harmonic analysis to take the same effect into account. The correct value (subscript 3D) of the impedance Z is obtained from the value computed with the axisymmetrical model (subscript 2D) by:

$$\frac{Z_{3D}}{Z_{2D}} = \left(\frac{d}{e}\right)^2$$

Remarks

Since the potential degree-of-freedom is actually a scalar, the difference between radial and tangential poling is simply a mechanical transformation of ratio d/e.

This way of dealing with a tangentially polarized ring can be used only if the displacement field of the real structure is nearly axisymmetrical. It is, for example, impossible to obtain circumferential modes using this method.

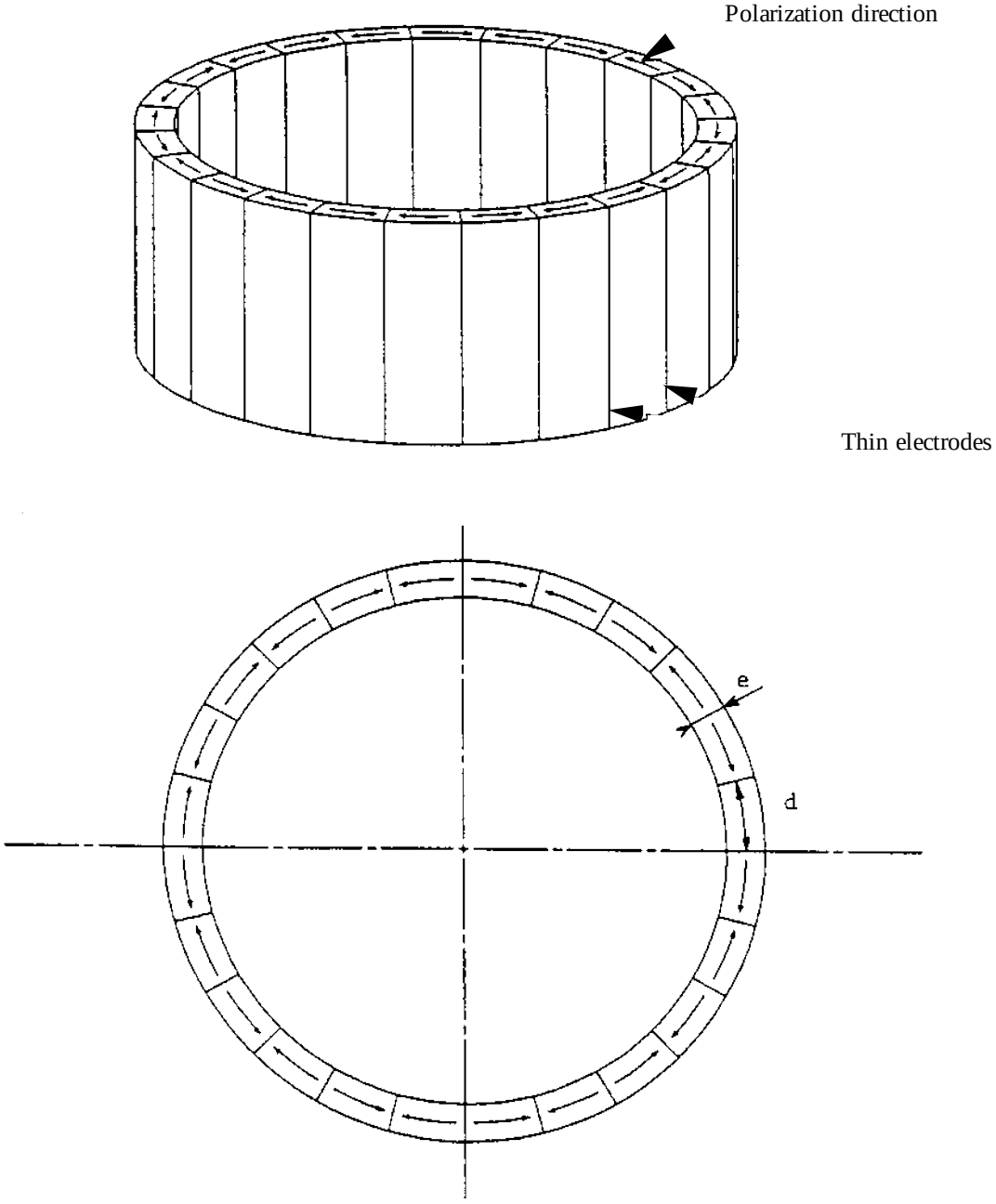

Fig. 1: Segmented free-flooded ring

3 DATA FILE PREPARATION

3.1 Introduction

This chapter describes the generation of an **ATILA** data file, except for the information about the elements described in Chapter 4. Automatic generation of an **ATILA** data file is available using the **MOSAIQUE** code. This generation is described in Chapter 5.

A data file includes three different sections:

1) header
2) description of the mesh (nodes, elements, geometric properties, materials, analysis parameters, etc.)
3) description of the boundary conditions.

All data, except the angles, must be given in MKS units or any coherent unit system deduced from the MKS system. The angle values must always be given in degrees.

In this chapter, we always refer to a **simple illustrative example** and give the corresponding entries and data sets. This example is the modal analysis of an axisymmetrical Tonpilz transducer, radiating in water. This transducer is made up of two ceramic rings, a tail mass, and a head mass. The structure, its material properties, and the corresponding mesh are described on the following two pages.

3.2 Description of the test example

This example corresponds to the data file described in chapter 6.

3.2.1 Geometry

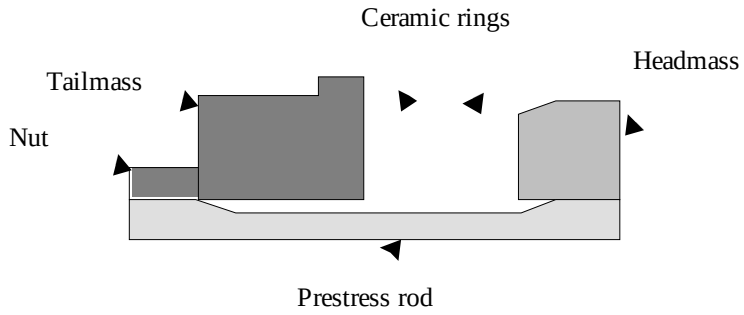

3.2.2 Materials

Tail mass: steel 25CD4.
Ceramics: X9 (PZT rings), axially polarized.
Head mass: aluminum AU4G.
Prestress rod: steel 25CD4.
Fluid: water.

3.2.3 Mesh

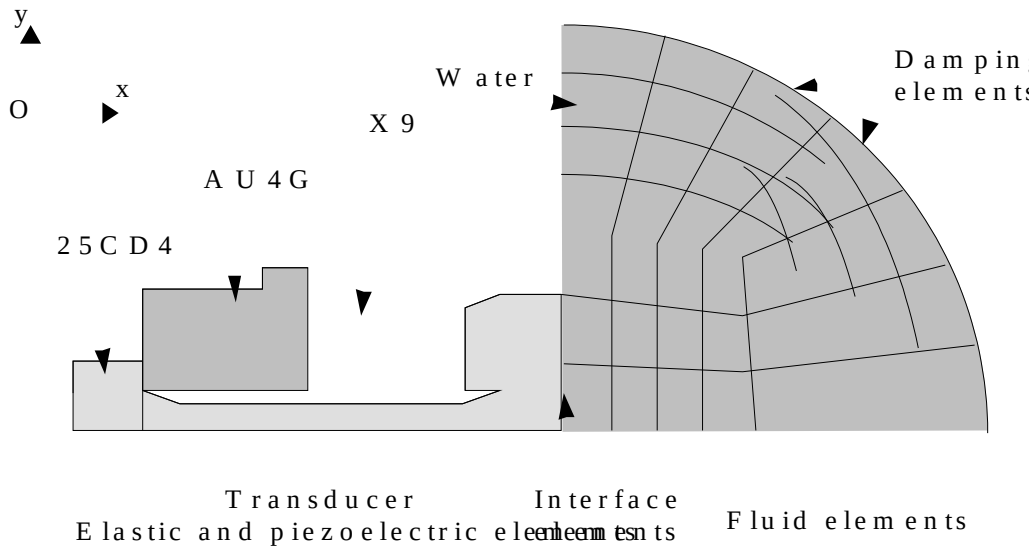

3.2.4 Header

The header includes comments that describe the job under consideration. The entire header is automatically copied onto the first page of every listing. The first line of the header is automatically repeated at the head of each listing page. All header lines begin with the symbol *.

LINE 1
*** LINE 2**
.
.
.
*** LINE I**
.
.
.
*** LINE N**

EXAMPLE:

40 KHZ TRANSDUCER
*** IN-WATER HARMONIC ANALYSIS**
*** DIPOLAR DAMPING CONDITIONS**

3.3 Description of the mesh and list of entries

We describe hereafter in alphabetic order the various entries. These entries are written in a simple free format, so it is possible to write them in a condensed form. The free format used is specific to **ATILA** and is slightly different from the FORTRAN one. Its main characteristics are:

- control characters:

'b' or , separates two words on the same line ('b' means space).
/ or = separates two consecutive lines (carriage return).

? deletes the preceding characters of the line.

• when typed at the beginning of a new line, it means that this line is a comment line. This line will not be printed in a listing. If a line contains two *, the text between the two * is a comment and the remaining part of the line is read as an entry.

& the following line continues the data line.

- real number syntax:

The following syntaxes, given as examples, are valid:

-1.22E+02
-1.22E2
-1E-3
-2.
3

- use of macro files

A macro file can be included in the flow of the main file via the entry:
MACRO name
The file of name NAME and of extension MAC should exist in the current directory. It is used as if its contents were included at the place of the MACRO entry.

- examples:

If the data sequence in a program is: "*read an alphanumeric, then two integers on the following line and finally three real numbers on the third line*", the following syntaxes are correct:

ALPHA
1,2
-6.,2.,3.
ALPHA=1,2
-6.,2.,3.

ALPHA/1,2=-6.,2.,3.

ALPHA / 1,2 /-6.,2.,3.

The different entries are listed in the table below. A YES in the column REQ means that this entry is required in all data files. An IGNORED in that column means that this entry is recognized for upward compatibility but should not be used anymore.

ENGLISH NAME	*FRENCH NAME*	REQ	ATTRIBUTES OR PARAMETERS	Page
ANALYSIS	***ANALYSE***	YES	STATIC, MODAL, MODAL RESANTIRES, HARMONIC, TRANSIENT, THERMAL. *(STATIQUE, MODALE, MODALE RESANTIRES, HARMONIQUE, TRANSITOIRE)*	73
ANGLES	***ANGLES***	NO	Angle values.	73
CHIEF	***CHIEF***	NO		74
CLASS	***CLASSE***	NO[(1)]	AXISYMMETRICAL, PLSTRESS, PLSTRAIN or PROPAGATION. *(AXISYMETRIQUE, CONTRAINTE, DEFORMATION ou PROPAGATION)*	75
DEFU	***FABU***	ignored	Displacement description.	75
DYNFLEX	***DYNFLEX***	NO		75
ELEMENTS	***ELEMENTS***	YES	NAMELI MATERI NUMGEOI Element topology. Entry end: blank line.	75
END	***FIN***	YES		76
EQI	***EQI***	NO		76
EXCITATIONS	***EXCITATIONS***	NO	Excitation description.	76
FREQUENCY	***FREQUENCES***	NO	Frequency values.	76
GENERATE	***GENERATION***	NO	SY2 SY4 PST SYSNOISE TMS ASCII or BIN	78
GEOMETRY	***GEOMETRIE***	NO	NUMGEOI Geometrical properties. Entry end: blank line.	78
GEOMETRY POLARIZATION	***GEOMETRIE POLARISATION***	NO	CARTESIAN, CYLINDRICAL or SPHERICAL *(CARTESIENNE, CYLINDRIQUE ou SPHERIQUE)* NUMGEOI Euler angles, coordinates. Entry end: blank line.	79
HEAT LOAD	***CHALEUR***	NO		16
IMPEDANCE	***IMPEDANCE***	NO		184
INDUCERS	***INDUCTEURS***	NO	NUMINDI Inducer geometries Entry end: blank line.	83
LANGUAGE	***LANGUE***	NO	FRENCH or ENGLISH or FRANCAIS or ANGLAIS	85
LOADS	***CHARGEMENTS***	NO	Load description.	85
LOSSES	***PERTES***	NO		85
MASS	***MASSE***	NO		86
MATERIAL	***MATERIAUX***	NO	MATERI Material properties. Entry end: blank line.	87
MATRICES	***MATRICES***	NO		92
NEWAXES	***NOUVEAUREPERE***	NO	CARTESIAN, CYLINDRICAL or SPHERICAL *(CARTESIENNE, CYLINDRIQUE ou SPHERIQUE)* X0 Y0 Z0 OZZ OYY OXX	92
NLOAD	***NCHARGE***	NO	NLO	93
NODES	***POINTS***	YES	Node coordinates Entry end: blank line.	93
PERIODIC	***PERIODIQUE***	NO	1D, 2D or 3D N1 N2 N3 N4	94
PRECISION	***PRECISION***	NO	SINGLE or DOUBLE *(SIMPLE ou DOUBLE)*	96
PRESSURE	***PRESSION***	NO	TOTAL or SCATTERED *(TOTALE ou DIFFRACTEE)*	96
PRINTING	***IMPRESSION***	NO	NPR	97
RADIATION	***RAYONNEMENT***	NO	MONOPOLAR or DIPOLAR *(MONOPOLAIRE ou DIPOLAIRE)*	97
SCALE	***ECHELLE***	NO	EX EY EZ.	97
SHIFT	***SHIFT***	NO	FSHIFT	97

STRESS	***CONTRAINTES***	NO	no attribute or PRINCIPAL.	98
SYSNOISE	***SYSNOISE***	NO	MODAL or DIRECT, ASCII or BIN	98
THERMAL	***THERMIQUE***	NO		98
TRANSIENT	***TRANSITOIRE***	NO(2)	METHOD NS NSKIP ΔT FL PAR1 PAR2	98
WAVE NUMBER	***NOMBRE D'ONDE***	NO(3)	NK VKBEG VKFIN	98

(1) This entry is required for a bidimensional mesh.

(2) This entry is required for a transient analysis.

(3) This entry is required for a modal analysis of a periodic material.

In the following description of the entries, the symbol [ ] is used to indicate additional attributes to be entered on the same line. Only one of these attributes must be used at a time. Parameters following the entry name must be entered on a separate line, as indicated.

3.3.1 ANALYSIS *[STATIC, MODAL, MODAL RESANTIRES, HARMONIC, TRANSIENT]*

This **required** entry defines the type of analysis that is requested (see Chapter I.2). The parameter term MODAL RESANTIRES allows the computation of the eigenfrequency values for resonance and antiresonance of a piezoelectric or magnetostrictive structure (not including a fluid domain) in a single run. The MODAL, MODAL RESANTIRES and TRANSIENT analyses are available only in DOUBLE precision.

Example:

ANALYSIS HARMONIC

N.B. In this example and in the following ones, the plus sign (**+**) shows the line start. It must ***not*** be written in the data file.

3.3.2 ANGLES

A1 A2 A3 ..... AN

In the case of a **harmonic analysis** of a periodic structure, this entry defines the successive values of the angles of the incident wave for a scattering problem or of the angles of observation for a radiation problem.

3.3.2.1 One-dimensional periodicity

For one-dimensional periodicity, the structure is described by a two-dimensional mesh. The periodicity direction is considered along the global Ox axis. The mesh boundaries must be straight lines parallel to Ox and Oy. The angle goes clockwise from Oy. For scattering, the incident wave propagates along increasing y. For radiation, the direction of observation is along decreasing y. The number of loading cases NLO (entry **NLOAD**) must equal the number of frequencies (entry **FREQUENCY**) multiplied by the number of angle values.

3.3.2.2 Two-dimensional periodicity

For two-dimensional periodicity, the structure is described by a three-dimensional mesh. It is required that the periodicity directions are along the global axes Ox and Oy. The mesh boundaries must be planes parallel to xOz, yOz, and xOy. For scattering, the incident wave propagates along increasing z. For radiation, the direction of observation is along decreasing z. They are defined by two angles θ and φ, given in this order, as represented in the next figure. θ is the angle between the incident wave vector and the normal to the structure (Oz). φ is the angle between the wave vector projection in the xOy plane

and the Ox axis. The number of loading cases NLO (entry **NLOAD**) must equal the number of frequencies (entry **FREQUENCY**) multiplied by the number of incident directions (number of angle values divided by two).
In the case of a **modal analysis** of a periodic structure, this entry defines the successive values of the direction of propagation.

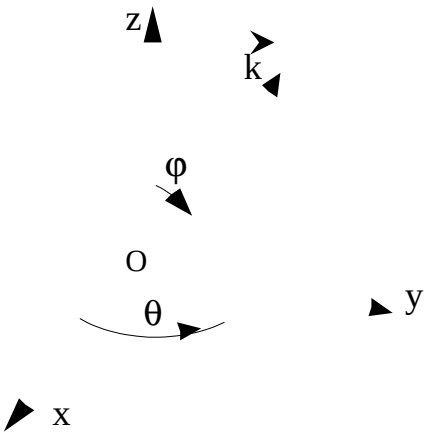

3.3.2.3 One-dimensional periodicity

For one-dimensional periodicity, no angle is required, as the direction of propagation is the direction of the periodicity direction.

3.3.2.4 Two-dimensional periodicity

For two-dimensional periodicity, the material is described by a two- or three-dimensional mesh. The periodicity directions must lie in the xOy plane. The trace of the unit cell in any xOy plane must be a parallelogram. The direction of propagation is defined by one angle measured clockwise from the Oy axis.

3.3.2.5 Three-dimensional periodicity

For three-dimensional periodicity, the material is described by a three-dimensional mesh. The unit cell must be a parallelepiped. The direction of propagation is defined by two angles θ and ϕ, given in this order. θ is the angle between the wavevector and the Oz axis and ϕ is the angle between the wavevector projection on the xOy plane and the Ox axis.

3.3.3 CHIEF

This entry specifies that a coupled finite-element/boundary-element analysis will be performed. The radiating surfaces prescribing the coupling are defined in the **ELEMENTS** command using specific elements (see Section I.4.B). The mutual impedance matrix associated with these surfaces is an external entry and is required for this type of analysis. This matrix is described in FORTRAN free format in a **JOB.ZRAD** type file (formatted, 80 columns) as follows:

ZR1(1,1) ZR1(1,2) ZR1(1,3) ZR1(1,4) ZR1(1,5)
ZR1(1,6) ..... First frequency
.....
.....ZR1(NSURF,NSURF)
ZI1(1,1) ZI11,2) ZI1(1,3) ZI1(1,4) ZI1(1,5)
ZI1(1,6) ..... First frequency
.....
.....ZI1(NSURF,NSURF)

.....

ZRi(1,1) ZRi(1,2) ZRi(1,3) ZRi(1,4) ZRi(1,5)
ZRi(1,6) ..... ith frequency
.....
.....ZRi(NSURF,NSURF)
ZIi(1,1) ZIi(1,2) ZIi(1,3) ZIi(1,4) ZIi(1,5)
ZIi(1,6) ..... ith frequency
.....
.....ZIi(NSURF,NSURF)

.....

ZRn(1,1) ZRn(1,2) ZRn(1,3) ZRn(1,4) ZRn(1,5)
ZRn(1,6) ..... Last frequency
.....
.....ZRn(NSURF,NSURF)
ZIn(1,1) ZIn(1,2) ZIn(1,3) ZIn(1,4) ZIn(1,5)
ZIn(1,6) ..... Last frequency
.....
.....ZI(NSURF,NSURF)

where the ZR (resp. ZI) are the terms of the real (resp. imaginary) part of the [Z] matrix. For an axisymmetrical mesh, the terms of the [Z] matrix are given for a unit angle. The ordering of the surfaces in the matrix has to be the same as the ordering of the coupling elements in the **JOB.ATI** file. NSURF is the number of radiating surfaces. Its maximal value is 500.
Note that this entry is mutually exclusive from the DYNFLEX, EQI and MATRICES entries and is available only for a harmonic analysis.

3.3.4 CLASS *[AXISYMMETRICAL, PLSTRAIN, PLSTRESS, PROPAGATION]*

This entry specifies, if necessary, that the analysis corresponds to an axisymmetrical, a plane stress, a plane strain or a propagation model. It is needed only if 2D elastic elements are used, but then it is **required**.

For an axisymmetrical analysis, the global Ox axis must be the symmetry axis.

EXAMPLE:

- **CLASS AXISYMMETRICAL**

3.3.5 DEFU

d1 U1
...
dI UI
...
dN UN
BLANK LINE

This entry has no meaning (obsolete) and is ignored. It is available only for compatibility with previous versions and will not be available in future versions. Its use is replaced with the EXCITATIONS command.

3.3.6 DYNFLEX

This entry indicates that the dynamic flexibility matrix, which relates forces to velocities on ATILA-CHIEF interface elements, must be calculated and stored in a file for use with external programs. No other computation is done.
Note that this entry is mutually exclusive from the CHIEF, EQI and MATRICES entries and is available only for a harmonic analysis.

3.3.7 ELEMENTS

NAMEL1 mater1 numgeo1
nA1 nA2 nA3 ... nAp
...
...
nK1 nK2 nK3 ... nKp
BLANK LINE

...
NAMELN materN numgeoN
nL1 nL2 nL3 ... nNq
...
nr1 nr2 nr3 ... nrq
BLANK LINE
BLANK LINE

This entry enables the code to input each element topology, according to the directions for use in Chapter I.4. The set of parameters for each element type must be closed by a blank line. Moreover, the entry parameter list must also be closed by a blank line.
The elements are assembled in the sequential order of this entry parameter list. NAMELI is the element type, MATERI and NUMGEOI are given or not, depending upon the element type (see Chapter I.4). They correspond to the **MATERIALS** and **GEOMETRY** entries; NXJ are node numbers.

EXAMPLE:

```
•          ELEMENTS
+ QUAD08E  25CD4
+ 1  3   6  8  2  4   5  7
+ 6  8 11 13  7  9 10 12
+
    etc...
```

3.3.8 END

Marks the end of the mesh description and the end of the list of entries.
EXAMPLE:

```
END
```

3.3.9 EQI

This entry specifies that a coupled finite-element/boundary-element analysis will be performed. The radiating surfaces prescribing the coupling are defined in the **ELEMENTS** command using specific elements (see Section I.4, elements LINE03Z, TRIA06Z and QUAD08Z).
Note that this entry is mutually exclusive from the CHIEF, DYNFLEX and MATRICES entries and is available only for a harmonic analysis.

3.3.10 EXCITATIONS

N1 DEG1 EXC1R EXC1I
...
NM DEGM EXCMR EXCMI
BLANK LINE

This entry enables the user to prescribe displacements, potentials or other degrees-of-freedom with known values. Accepted entries for DEGI are given in the following table:

UX =	displacement along OX
UY =	displacement along OY
UZ =	displacement along OZ
THETAX =	rotation around OX

THETAY = rotation around OY

THETAZ = rotation around OZ

PRESSURE *(PRESSION)* = pressure

ELECPOT *(PHIELEC)* = electric potential

MAGNPOT *(PHIMAGN)* = magnetic potential

TEMPERATURE = temperature

CURRENT1 to CURRENT9
(COURANT1 à COURANT9) = magnetic excitation currents

A blank line is required to end these data.

3.3.10.1 Static analysis

NI DEGI EXCIR indicate that degree-of-freedom DEGI at node number NI has the value of EXCIR. The parameter EXCII is ignored and can be omitted.

3.3.10.2 Harmonic analysis

NI DEGI EXCIR EXCII indicate that degree-of-freedom DEGI at node number NI has the complex value of EXCIR + j EXCII. Giving complex values is allowed when the problem variables are complex (complex solving of the system of equations) and is the way to provide out-of-phase excitations. A missing value of EXCII indicates a real (non complex) excitation.

3.3.10.3 Modal analysis

NI DEGI EXCIR indicate that degree-of-freedom DEGI at node number NI has the value of EXCIR. The value itself is ignored. If DEGI is an electric potential or magnetic excitation current degree of freedom, the line indicates the excitation degree of freedom for which a modal decomposition will be performed. The parameter EXCII is ignored and can be omitted. If DEGI is a mechanical degree of freedom, it is automatically blocked.

3.3.10.4 Modal "resantires" analysis

NI DEGI EXCIR indicate that degree-of-freedom DEGI at node number NI has the value of EXCIR. The value itself is ignored. If DEGI is an electric potential degree of freedom, the line indicates the excitation electrodes, which are forced to ground for a resonance analysis or left open for an antiresonance analysis. If DEGI is a magnetic excitation current degree of freedom, the line is an indication of the excitation coils, which are left open for a resonance analysis or forced to ground for an antiresonance analysis. The parameter EXCII is ignored and can be omitted. If DEGI is a mechanical degree of freedom, it is automatically blocked for both resonance and antiresonance analyses.

3.3.10.5 Transient analysis

NI DEGI EXCIR EXCII indicate that degree-of-freedom DEGI at node number NI is excited by a function depending on EXCIR and EXCII as follows :

- if both EXCIR and EXCII are positive, the excitation function is a sinusoid of amplitude EXCIR and of frequency EXCII, starting at time t = 0 :
  $f_I(t) = EXC_{IR} \sin(2\pi EXC_{II} t)$ *if* $t > 0$, *else* $f_I(t) = 0$
- if EXCIR is negative and EXCII is positive, the excitation function is a raised cosinusoid of amplitude -EXCIR and of frequency EXCII, starting at time t = 0 :
  $f_I(t) = -EXC_{IR} (1 - \cos(2\pi EXC_{II} t))$ *if* $t > 0$, *else* $f_I(t) = 0$
- if EXCIR is not zero and EXCII is zero, the excitation function is a time step of amplitude EXCIR starting at time t = 0 :
  $f_I(t) = EXC_{IR}$ *if* $t > 0$, *else* $f_I(t) = 0$

- if EXCIR is not zero and EXCII is negative, the excitation function is a pulse of amplitude EXCIR of duration -EXCII starting at time t = 0 :

  $f_I(t) = EXC_{IR}$ *if* $t > 0$ *and* $t < -EXC_{II}$, *else* $f_I(t) = 0$

- if EXCIR and EXCII are both zero, the excitation function and its first two derivative values are read from an external file of extension EXC. The format of this file is free. It contains, for each line, the following values :

  t $f_1(t)$ $f'_1(t)$ $f''_1(t)$ $f_2(t)$ $f'_2(t)$ $f''_2(t)$ … $l_1(t)$ $l_2(t)$ …

  where t is one of the times at which calculations are performed, $f_1(t)$ is the function value of the first declared external excitation, $f'_1(t)$ is the value of the first derivative of $f_1(t)$ at time t, $f''_1(t)$ is the value of the second derivative of $f_1(t)$ at time t, and so on… $l_1(t)$ is the function value of the first declared external load at time t, and so on… (see LOADS entry). Note that all the times needed must be present, especially for the Wilson-θ method where, for each integration step, the needed values are $n\Delta T$ and $n\Delta T+\theta$

3.3.11 FREQUENCY

3.3.11.1.1 F1 F2 ..... Fi ..... FN

This entry is requested only for a harmonic analysis. Its parameters are the values of the frequency(ies) for which a computation is required. The maximum number of frequencies N depends on the NLOAD entry. N is equal to NLO except in the case of the analysis of a periodic structure, where the number of angles must be taken into account (see entry **ANGLES**).

EXAMPLE:

```
•        FREQUENCY
+ 25000. 26000. 27000. 28000. 29000. 30000. 30500. &
+ 31000. 31500. 32500. 33000.
```

3.3.12 GENERATE *[SY4 PST SYSNOISE TMS ASCII BIN]*

This entry indicates which post-process files the user wants to be generated. Its use replaces the answers to questions asked by the Fortran Program Generator PGEN which was available in previous versions.

- The **SY4** file is a binary file used by almost all post-processors, so it is generated by default.

The **PST** file is an ASCII but not human-readable file which is used by the post-processor ISOVAL.

- The **SYSNOISE** parameter allows the user to create files for use with the SYSNOISE software.
- The **TMS** parameter allows the user to create files for THOMSON MARCONI SYSTEMS company's internal use.

The optional parameters **ASCII** and **BIN** are mutually exclusive and affect the generation of files triggered by the SYSNOISE or TMS parameters. ASCII is the default.

3.3.13 GEOMETRY

```
numgeo1
x11 x12 .... x1M
...
numgeoN
xN1 xN2 .... xNQ
BLANK LINE
```

This entry provides the geometrical properties needed by certain elements (thickness, radius of curvature, temperature, etc.). The XIJ characteristics are related to the NUMGEOI integers, to be referenced in the element definition (see Chapter 4).

EXAMPLE:

```
•        GEOMETRY
+  1
+     0.56E-01
+  2
+     0.072
+
```

3.3.14 GEOMETRY POLARIZATION *[CARTESIAN, CYLINDRICAL, SPHERICAL]*

numgeo1
x11 x12 .... x1M
numgeo2
x21 x22 .... x2p
...
...
...
numgeoN
xN1 xN2 .... xnQ
BLANK LINE

For a piezoelectric or magnetostrictive element, the definition of the material tensors has to be done in the natural coordinate system related to the characteristic axes of the material. The **GEOMETRY POLARIZATION** entry enables one to define these axes relative to the global coordinate system; the transformation in the element coordinate system is automatically done by the code. This entry is **required** if piezoelectric or magnetostrictive elements exist in the mesh.

3.3.14.1 Cartesian polarization

Here, the polarization is **homogeneous** in the whole element and the natural axes OX_1, OX_2 and OX_3 have to be defined with respect to the global axes Ox, Oy and Oz. To do this, the user has to provide three Euler angles, named ALPHA, BETA and GAMMA, which transform Oxyz into $OX_3X_1X_2$ and are defined as follows:

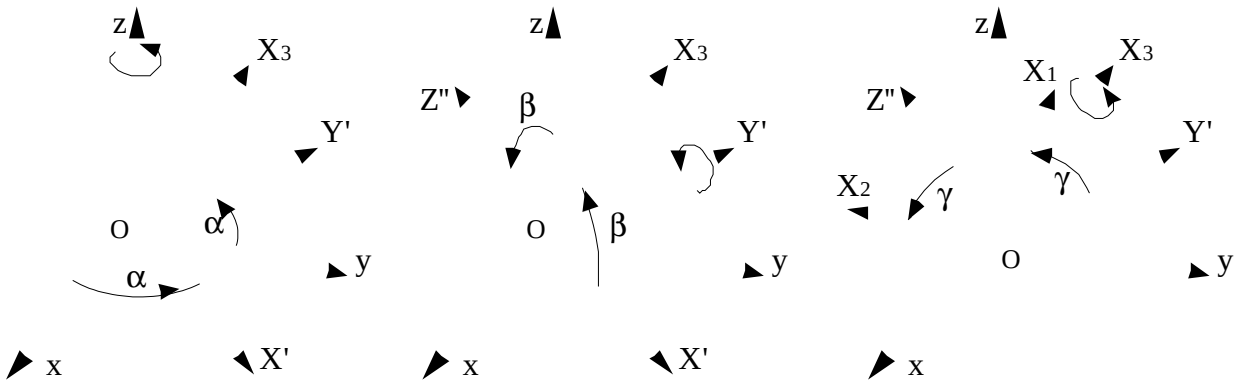

Definition of the Euler angles ($\alpha > 0$, $\beta < 0$, $\gamma > 0$)

- ALPHA is the angle of the first rotation, around Oz, which transforms the Oxyz system into OX'Y'z system such that OX' belongs to the OzX_3 plane
- BETA is the angle of the second rotation, around OY', which transforms the OX'Y'z system into a $OX_3Y'Z''$,
- GAMMA is the angle of the third rotation, around OX_3, which transforms the $OX_3Y'Z''$ system into the $OX_3X_1X_2$ system. Its value is dummy in the particular case of a ceramic material (6mm symmetry class).

The entry parameters, listed in this required order, are:

ALPHA BETA GAMMA

Attention must be given to the exact meaning of the CARTESIAN POLARIZATION term. It corresponds to a three-dimensional or plane strain bi-dimensional element. In the case of an axisymmetrical element, this entry defines a homogeneous polarization in the cross section. Thus a polarization direction orthogonal to the symmetry axis is physically azimuthal in the corresponding part of the material.

3.3.14.2 Cylindrical polarization

Here, the polarization is **radial with respect to a given O'z' axis** in the whole element. The user must first specify a O'x'y'z' system that contains the O'z' axis. To do this, he provides the O' coordinates (X0, Y0, Z0) and the Euler angles (ALPHA, BETA, GAMMA) that transform the O'xyz global system into the O'x'y'z' system. The Euler angles are defined as follows:

- ALPHA is the angle of the first rotation, around O'z, which transforms the O'xyz system into a O'XYz system such that O'X belongs to the O'x' plane
- BETA is the angle of the second rotation, around O'Y, which transforms the O'XYz system into a O'x'YZ' system
- GAMMA is the angle of the third rotation, around O'x', which transforms the O'x'YZ' system into the O'x'y'z' system.

It is obvious that the choice of the O'x' (or O'y') axis is arbitrary and must be the simplest. With these new reference axes, the angle of the rotation around O'z' that makes the O'x' axis coincide with the natural MX_3 axis, for each point M that is concerned, is directly computed by the code. Finally, the user must also provide the angle DELTA, which brings, for every point M, the Mz' axis into coincidence with the MX_2 natural axis. The value of DELTA is dummy for a ceramic material (6mm symmetry class).

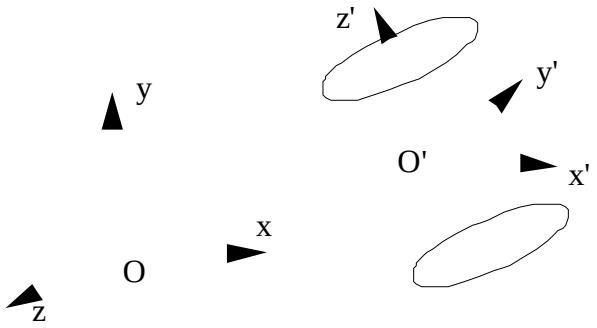

Definition of the O'x'y'z' system for the cylindrical polarization

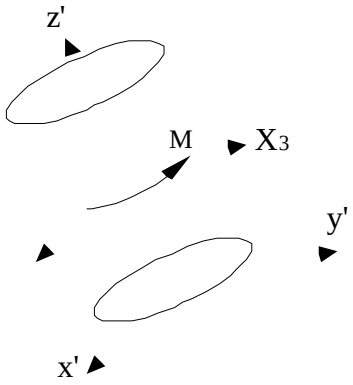

The anisotropic material's X3 axis rotates around the Oz' axis when cylindrically polarized.

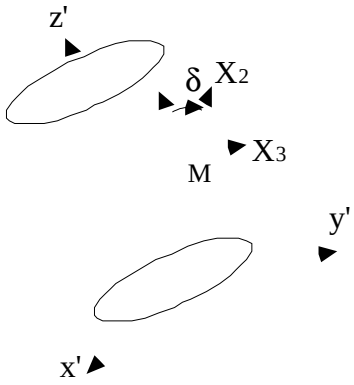

Definition of the angle DELTA (δ)

The entry parameters are listed in this required order:

ALPHA BETA GAMMA XO YO ZO DELTA

As in the previous case, the **CYLINDRICAL POLARIZATION** corresponds to a three-dimensional element modeling. For an axisymmetrical element, a **CYLINDRICAL POLARIZATION** defined starting with a point O' belonging to the symmetry axis, such as O'z', is orthogonal to the cross section (i.e., the mesh plane), but is physically radial with respect to O' in the corresponding part of the material.

3.3.14.3 Spherical polarization

Here, the polarization is **radial with respect to a given point O'** for the whole element. The user must first specify a O'x'y'z' system centered on the origin O'. To do this, he provides the O' coordinates (X0, Y0, Z0) and the Euler angles which transform the Oxyz system into the O'x'y'z' system (ALPHA, BETA, GAMMA). These angles are defined as in the cylindrical case. It is obvious that the choice of these new axes is arbitrary and must be the simplest. With these new reference axes, the angles of the rotations that bring the O'x' axis into coincidence with the natural MX_3 axis, for each point M that is concerned, are computed by the code. Finally, the user must also provide the angle DELTA, which makes the Mz' axis coincide with the natural MX_2 axis, for every point M. The value of DELTA is dummy for a ceramic material (6mm symmetry class).

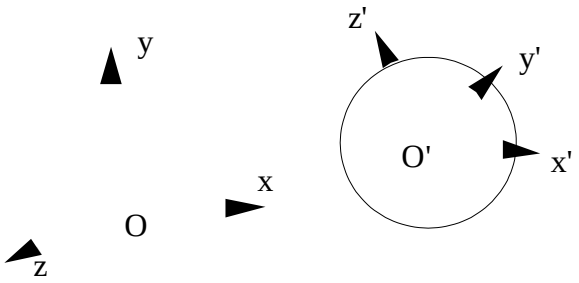

Definition of the O'x'y'z' system for the spherical polarization

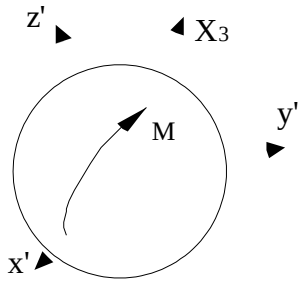

The anisotropic material's X3 axis rotates around the center O' when spherically polarized.

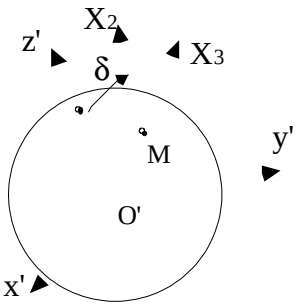

Definition of the angle DELTA (δ)

The entry parameters are given as follows:

ALPHA BETA GAMMA XO YO ZO DELTA

EXAMPLE:

GEOMETRY POLARIZATION CARTESIAN
+ 2
+ 0. 0. 0. 0. 0. 0. 0.
+ 3
+ 180. 0. 0. 0. 0. 0. 0.
+

Remark: 2 and 3 correspond to ceramics, the electrical excitation of which have opposite polarities. When an input is omitted, it is assumed to be zero.

EXAMPLES

AXISYMMETRICAL CASE (RADIAL POLARIZATION)

The coordinate dashed line is the axis of symmetry.

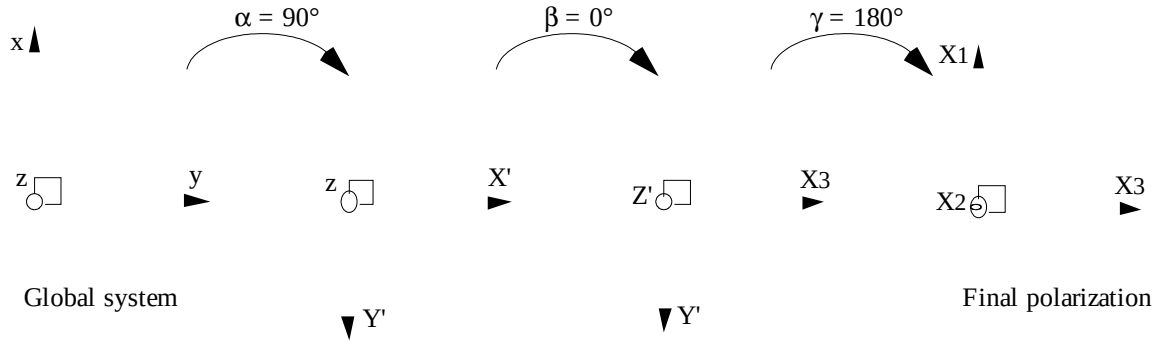

The corresponding entry is:

GEOMETRY POLARIZATION CARTESIAN
1 = 90. 0. 180.

Example of Cartesian polarization

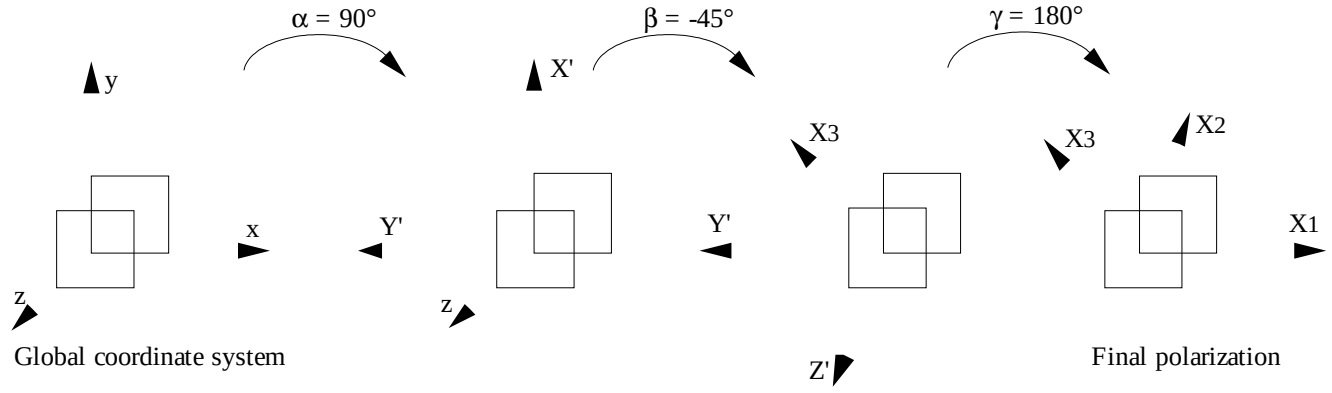

The corresponding entry is:

GEOMETRY POLARIZATION CARTESIAN
+ 1 = 90. -45. 180.
+

EXAMPLE OF CYLINDRICAL POLARIZATION

The O'z' axis is in the (1,1,1) direction with respect to the global axes, O' at 0.5 m from O on the Oy axis.

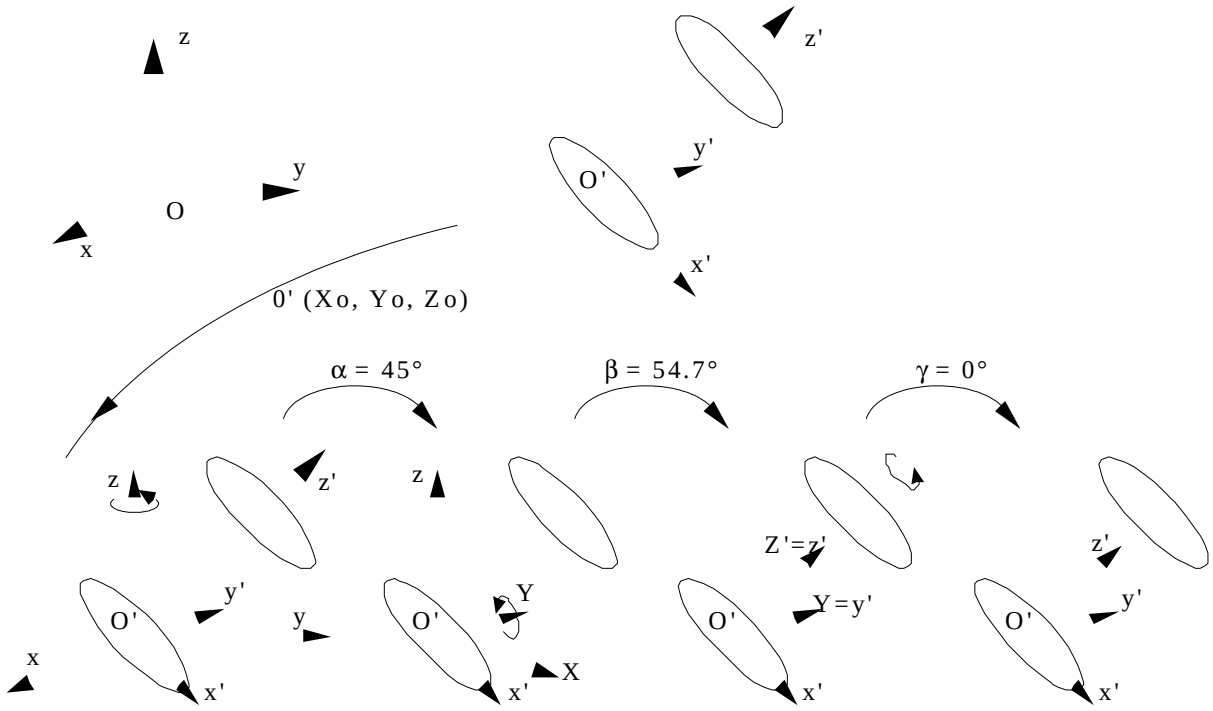

Final polarization is radial around O'z'. The corresponding entry is:

GEOMETRY POLARIZATION CYLINDRICAL
+ 1 = 45 54.7 0 0.0 0.5 0.0 0.
+

EXAMPLE OF SPHERICAL POLARIZATION (O' is 0.4 m away from O on the Oy axis)

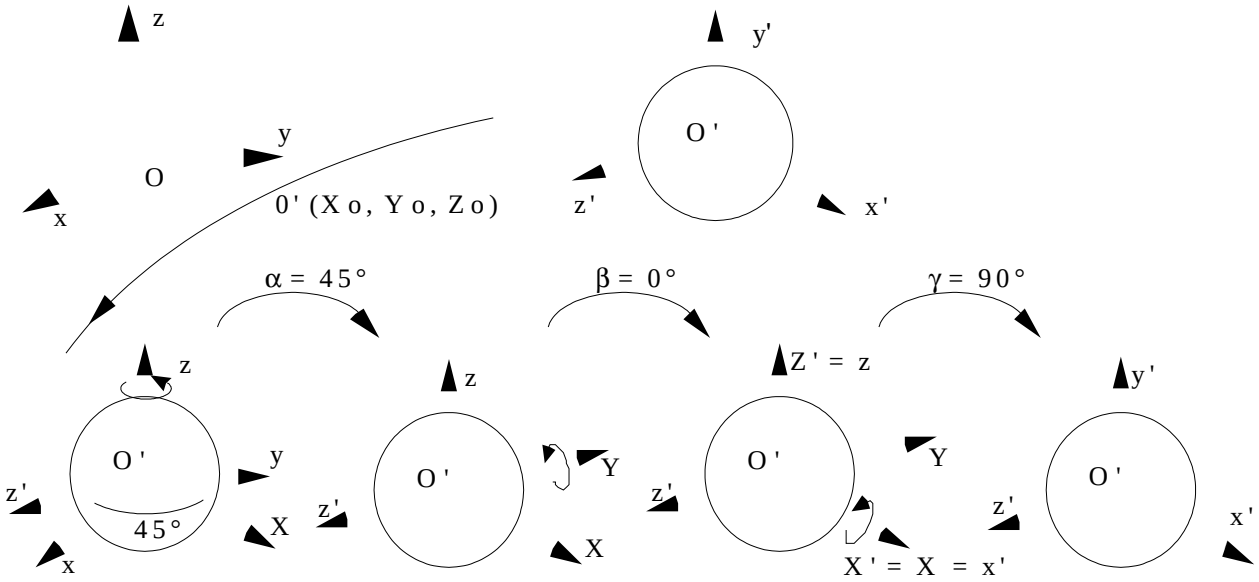

Final polarization is radial around O'.
The corresponding entry is:

GEOMETRY POLARIZATION SPHERICAL
1 = 45 0 90 0. 0.4 0.

3.3.15 IMPEDANCE

This entry indicates that external electric impedances will be connected to electrodes, within a harmonic analysis. In this case, the description of the external impedances must be provided by the user, after the boundary conditions of the data file, in the ATILA free format, as follows:
The first line contains the number of nodes NZ that will be connected to the null potential through an external impedance.
For each frequency, a set of NZ lines. Each line of this set contains four values: the frequency of the current set, the node number of the electrode, the real part and the imaginary part of the impedance connected to that node.

3.3.16 INDUCERS

NUMIND1
GEO11 NT11 A11 B11 C11 ... N11 O11
...
...
GEO1M NT1M A1M B1M C1M ... N1M O1M
BLANK LINE
...
NUMINDP
GEOP1 NTP1 AP1 BP1 CP1 ... NPP1 OP1
...
GEOPR NTPR APR BPR CPR ... NPR OPR
BLANK LINE
BLANK LINE

In the case of an analysis using magnetostrictive elements, this entry allows the user to define the inducers that create the magnetic excitation. Inducers through which the same current passes are grouped together. These currents are named I (I may vary from 1 to 9). Their value is determined by the **EXCITATIONS** entry. Lines following NUMINDI describe the inducers associated with the corresponding current I.
GEOIJ define the geometry of inducer J associated with current NUMINDI

- if **GEOIJ = CONSTANT**,
  the magnetic excitation generated by the inducer is steady everywhere in the mesh. In this case, AIJ, BIJ, and CIJ are the components of a vector along the source magnetic field. NTIJ, DIJ, FIJ and OIJ are omitted.
- if **GEOIJ = CYLINDER**,
  the magnetic excitation is generated by a cylindrical inducer, of circular section made of NTIJ turns. In this case, AIJ, BIJ, and CIJ are the coordinates of the cylinder's center. DIJ, EIJ, and FIJ are the components of a vector along the cylinder axis. Reals GIJ to IIJ, are respectively, the outer radius, the height, and the thickness of the cylinder. Values JIJ to OIJ are omitted. If the thickness is null, the inducer is a thin cylinder. If the thickness and the height are null, the inducer is a single circular loop.
- if **GEOIJ = RECTANGLE**,
  The magnetic excitation is generated by a cylindrical inducer of rectangular section made of NTIJ turns. In this case, AIJ, BIJ, and CIJ are the coordinates of the cylinder's center, DIJ, EIJ, and FIJ are the components of a vector along the cylinder. GIJ, HIJ, and IIJ are components of a vector along the length of the rectangular loop. Reals JIJ to OIJ, are, respectively, the outer length, the outer width, and the outer radius of the wedge of the rectangular loop, the height and thickness of the inducer. If the thickness is null, the inducer is a thin rectangular cylinder. If the thickness and the height are null, the inducer is a single rectangular loop.

A blank line is necessary to end the entries for a specific current and a second to close the INDUCERS description. We recall that, in **ATILA**, the current values are treated like excitations and that the magnetic excitation vectors generated by previous inducers are considered unity excitations.

3.3.17 HEAT LOAD

The keyword **HEAT LOAD** must be used together with **ANALYSIS HARMONIC.** It means that harmonic and thermal analysis are performed successively (see chapter 2.3) and only electromechanical prescribed conditions are required.

3.3.18 LANGUAGE OR LANGUE *[FRENCH, ENGLISH, FRANCAIS, ANGLAIS]*

This entry defines the language used for the entry input and the output file edition. In France, the default language is French; in other countries, it is English. It can be overridden by setting the environment variable ATILA_LANGUAGE to 0 for French, 1 for English.

3.3.19 LOADS

N1 DEG1 LOA1R LOA1I
...
NM DEGM LOAMR LOAMI
BLANK LINE

This entry allows the user to prescribe forces or other loads with known values. Allowed entries for DEGI are given in the following table:

LOADX *(FORCEX)* =	force along OX
LOADY *(FORCEY)* =	force along OY
LOADZ *(FORCEZ)* =	force along OZ
MOMENTX =	momentum around OX
MOMENTY =	momentum around OY
MOMENTZ =	momentum around OZ
CHARGELE =	electric charge
D_CHARGE =	time derivative of the electric charge. This is a current.
CHARGMAG =	magnetic charge
FLUX1 to FLUX9 =	flux of the reduced magnetic field through the coils
D_FLUX1 to D_FLUX9 =	time derivative of the flux of the reduced magnetic field through the coils. This is a voltage.

A blank line is required to end these data.

3.3.19.1 Static analysis

NI DEGI LOAIR indicate that the load on the degree-of-freedom DEGI at node number NI has the value of LOAIR. The parameter LOAII is ignored and can be omitted.
D_CHARGE and D_FLUX1 to D_FLUX9 are not available to this analysis, as the time derivative would be 0.

3.3.19.2 Harmonic analysis

NI DEGI LOAIR LOAII indicate that the load on the degree-of-freedom DEGI at node number NI has the complex value of LOAIR + j LOAII. Giving complex values is allowed when the problem variables are complex (complex solving of the system of equations) and is the way to provide out-of-phase excitations. A missing value of LOAII indicates a real (non complex) load.

D_CHARGE represents the current sent to an electrode of a piezoelectric ceramic, without taking care of the symmetries of the structure, especially the axisymmetry. In order to take the axisymmetry into account, the D_CHARGE value is equal to the real current sent, divided by 2π.
D_FLUX1 to D_FLUX9 represents the voltage sent to a excitation coil of a magnetostrictive part, without taking care of the symmetries of the structure, especially the axisymmetry. In order to take the axisymmetry into account, the D_FLUXn value is equal to the real voltage applied, divided by 2π.

WARNING

As the time derivative introduces a phase shift of 90°, thus transforming real values to imaginary ones, the LOSSES command should be provided when D_CHARGE or D_FLUXn are used, unless values provided are pure imaginary ones.

3.3.19.3 Modal analysis, modal "resantires" analysis

The entries are ignored, as no load should be present.

3.3.19.4 Transient analysis

NI DEGI LOAIR LOAII indicate that the load on the degree-of-freedom DEGI at node number NI is excited by a function depending on LOAIR and LOAII as follows:
if both LOAIR and LOAII are positive, the load function is a sinusoid of amplitude LOAIR and of frequency LOAII, starting at time t = 0:

$$f_l(t) = LOAIR\ sin(2\pi\ LOAII\ t)\ \ if\ \ t > 0,\ \ else\ \ f_l(t) = 0$$

if LOAIR is negative and LOAII is positive, the load function is a raised cosinusoid of amplitude -LOAIR and of frequency LOAII, starting at time t = 0:

$$f_l(t) = -LOAIR\ (1 - cos(2\pi\ LOAII\ t))\ \ if\ \ t > 0,\ \ else\ \ f_l(t) = 0$$

if LOAIR is not zero and LOAII is zero, the load function is a time step of amplitude LOAIR starting at time t = 0:

$$f_l(t) = LOAIR\ \ if\ \ t > 0,\ \ else\ \ f_l(t) = 0$$

if LOAIR is not zero and LOAII is negative, the load function is a pulse of amplitude LOAIR of duration -LOAII starting at time t = 0:

$$f_l(t) = LOAIR\ \ if\ \ t > 0\ and\ t < -LOAII,\ \ else\ \ f_l(t) = 0$$

if LOAIR and LOAII are both zero, the load function value is read from an external file of extension EXC, after the data needed by the EXCITATION entry. The format of this file is described under the EXCITATIONS entry.
The D_CHARGE and D_FLUX1 to D_FLUX9 entries are not available to this analysis.

3.3.20 LOSSES

This entry tells that the materials may have losses, so that calculations must be performed with complex numbers.

3.3.21 MASS

This entry requests a printout of the volume and mass of each solid element together with the total volume and mass of the solid parts.

3.3.22 MATERIAL

MATER1
X11 ... X1M
.
MATERI
XI1 ... XIP
…
MATERN
XN1 ... XNQ
BLANK LINE

This entry enables the user to introduce the properties of the materials that compose the elements. The XIJ properties are defined by material type, as described below. Each material is named by the user (less than 8 characters): MATER1 ... MATERN. These names could be used with the **ELEMENTS** entry. The list of the requested properties is provided in the element description, in Chapter I.4. If one line is not enough to describe the properties of a given material, it can be extended using the character **&**.

3.3.22.1 Case of an elastic isotropic material without losses

E NU RHO

where E is Young's modulus, NU is Poisson's ratio and RHO the density.

3.3.22.2 Case of an elastic isotropic material with losses

E' NU' RHO 0.0 NU" E"

SH Kxx Kyy Kzz

where E' and E" are, respectively, the real and imaginary parts of Young's modulus, NU' and NU" the real and imaginary parts of Poisson's ratio, and RHO the density. E" must be positive and NU" comprised between -E"(1+NU')/E' and E"(0.5-NU')/E' to have a material with losses.
SH is the specific heat (J/kg/C°), Kxx, Kyy, Kzz are the conductivity coefficients (W/m-C°) according to X direction, Y direction and Z direction respectively. These last coefficients are only required for THERMAL and HEAT LOAD analysis.

3.3.22.3 Case of a composite material without losses

E_f NU_F RHO_F 0.0 0.0 0.0 &
E_M NU_M RHO_M 0.0 V_F 0.0

where E_F is the fiber Young's modulus, NU_F the fiber Poisson's ratio, RHO_F the fiber density, E_M the matrix Young's modulus, NU_M the matrix Poisson's ratio RHO_M the matrix density, and V_F the fiber volume fraction (1.0 corresponds to 100%).

3.3.22.4 Case of a composite material with losses

E'_f NU_F RHO_F 0.0 0.0 $E"_f$ &
E'_M NU_M RHO_M 0.0 V_F $E"_M$

Where NU_F and NU_M are still real.

3.3.22.5 Case of a fluid without losses

COMP 0.0 RHO

where COMP is the bulk modulus (pressure units) and RHO the density.

3.3.22.6 Case of a fluid with losses

COMP' 0.0 RHO 0.0 0.0 COMP"

where COMP' and COMP" are, respectively, the real and imaginary parts of the bulk modulus, and RHO the density. COMP" must be positive to have a fluid with losses.

3.3.22.7 Case of a magnetic domain

PERM

where PERM is the absolute magnetic permeability of the domain.

3.3.22.8 Case of a piezoelectric material without losses

0.0	**0.0**	**RHO**	**0.0**	**0.0**	**0.0**	**&**
s_{11}^E	s_{12}^E	s_{13}^E	s_{14}^E	s_{15}^E	s_{16}^E	**&**
s_{21}^E	s_{22}^E	s_{23}^E	s_{24}^E	s_{25}^E	s_{26}^E	**&**
s_{31}^E	s_{32}^E	s_{33}^E	s_{34}^E	s_{35}^E	s_{36}^E	**&**
s_{41}^E	s_{42}^E	s_{43}^E	s_{44}^E	s_{45}^E	s_{46}^E	**&**
s_{51}^E	s_{52}^E	s_{53}^E	s_{54}^E	s_{55}^E	s_{56}^E	**&**
s_{61}^E	s_{62}^E	s_{63}^E	s_{64}^E	s_{65}^E	s_{66}^E	**&**
d_{11}	d_{12}	d_{13}	d_{14}	d_{15}	d_{16}	**&**
d_{21}	d_{22}	d_{23}	d_{24}	d_{25}	d_{26}	**&**
d_{31}	d_{32}	d_{33}	d_{34}	d_{35}	d_{36}	**&**
ε_{11}^S	ε_{12}^S	ε_{13}^S	**0.0**	**0.0**	**0.0**	**&**
ε_{21}^S	ε_{22}^S	ε_{23}^S	**0.0**	**0.0**	**0.0**	**&**
ε_{31}^S	ε_{32}^S	ε_{33}^S	**0.0**	**0.0**	**0.0**	**&**

where (s^E) is the constant electric field elastic tensor, (d) the piezoelectric tensor, (ε^S) the constant strain dielectric permittivity tensor, and RHO the density.

3.3.22.9 Case of a piezoelectric material with losses

0.0	**0.0**	**RHO**	**0.0**	**0.0**	**0.0**	**&**
s'^{E}_{11}	s'^{E}_{12}	s'^{E}_{13}	s'^{E}_{14}	s'^{E}_{15}	s'^{E}_{16}	**&**
s'^{E}_{21}	s'^{E}_{22}	s'^{E}_{23}	s'^{E}_{24}	s'^{E}_{25}	s'^{E}_{26}	**&**
s'^{E}_{31}	s'^{E}_{32}	s'^{E}_{33}	s'^{E}_{34}	s'^{E}_{35}	s'^{E}_{36}	**&**
s'^{E}_{41}	s'^{E}_{42}	s'^{E}_{43}	s'^{E}_{44}	s'^{E}_{45}	s'^{E}_{46}	**&**
s'^{E}_{51}	s'^{E}_{52}	s'^{E}_{53}	s'^{E}_{54}	s'^{E}_{55}	s'^{E}_{56}	**&**
s'^{E}_{61}	s'^{E}_{62}	s'^{E}_{63}	s'^{E}_{64}	s'^{E}_{65}	s'^{E}_{66}	**&**
d'_{11}	d'_{12}	d'_{13}	d'_{14}	d'_{15}	d'_{16}	**&**
d'_{21}	d'_{22}	d'_{23}	d'_{24}	d'_{25}	d'_{26}	**&**
d'_{31}	d'_{32}	d'_{33}	d'_{34}	d'_{35}	d'_{36}	**&**
ε'^{S}_{11}	ε'^{S}_{12}	ε'^{S}_{13}	**0.0**	**0.0**	**0.0**	**&**
ε'^{S}_{21}	ε'^{S}_{22}	ε'^{S}_{23}	**0.0**	**0.0**	**0.0**	**&**
ε'^{S}_{31}	ε'^{S}_{32}	ε'^{S}_{33}	**0.0**	**0.0**	**0.0**	**&**
s''^{E}_{11}	s''^{E}_{12}	s''^{E}_{13}	s''^{E}_{14}	s''^{E}_{15}	s''^{E}_{16}	**&**
s''^{E}_{21}	s''^{E}_{22}	s''^{E}_{23}	s''^{E}_{24}	s''^{E}_{25}	s''^{E}_{26}	**&**
s''^{E}_{31}	s''^{E}_{32}	s''^{E}_{33}	s''^{E}_{34}	s''^{E}_{35}	s''^{E}_{36}	**&**
s''^{E}_{41}	s''^{E}_{42}	s''^{E}_{43}	s''^{E}_{44}	s''^{E}_{45}	s''^{E}_{46}	**&**
s''^{E}_{51}	s''^{E}_{52}	s''^{E}_{53}	s''^{E}_{54}	s''^{E}_{55}	s''^{E}_{56}	**&**
s''^{E}_{61}	s''^{E}_{62}	s''^{E}_{63}	s''^{E}_{64}	s''^{E}_{65}	s''^{E}_{66}	**&**
d''_{11}	d''_{12}	d''_{13}	d''_{14}	d''_{15}	d''_{16}	**&**
d''_{21}	d''_{22}	d''_{23}	d''_{24}	d''_{25}	d''_{26}	**&**
d''_{31}	d''_{32}	d''_{33}	d''_{34}	d''_{35}	d''_{36}	**&**
ε''^{S}_{11}	ε''^{S}_{12}	ε''^{S}_{13}	**0.0**	**0.0**	**0.0**	**&**
ε''^{S}_{21}	ε''^{S}_{22}	ε''^{S}_{23}	**0.0**	**0.0**	**0.0**	**&**
ε''^{S}_{31}	ε''^{S}_{32}	ε''^{S}_{33}	**0.0**	**0.0**	**0.0**	**&**

where (s'^{E}_{ij}) and (s''^{E}_{ij}) are, respectively, the real and imaginary parts of the constant electric field elastic tensor, (d'_{ij}) and (d''_{ij}) are, respectively, the real and imaginary parts of the piezoelectric tensor, (ε'^{S}_{ij}) and (ε''^{S}_{ij}) are, respectively, the real and imaginary parts of the constant strain dielectric permittivity tensor, and RHO the density. To have a lossy piezoelectric material, it is necessary but not sufficient to have all negatives for the diagonal terms (s'^{E}_{ij}) and (ε''^{S}_{ij}).
SH is the specific heat (J/kg/C°), Kxx, Kyy, Kzz are the conductivity coefficients (W/m-C°) according to X direction, Y direction and Z direction respectively. These last coefficients are only required for THERMAL and HEAT LOAD analysis.

3.3.22.10 Case of a piezoelectric trilaminar

Here, the data to input are the physical characteristics of the metallic material, followed by the physical characteristics of the piezoelectric material, in the order previously described.

3.3.22.11 Case of a magnetostrictive material without losses

0.0	**0.0**	**RHO**	**0.0**	**0.0**	**0.0**	**&**
s_{11}^H	s_{12}^H	s_{13}^H	s_{14}^H	s_{15}^H	s_{16}^H	**&**
s_{21}^H	s_{22}^H	s_{23}^H	s_{24}^H	s_{25}^H	s_{26}^H	**&**
s_{31}^H	s_{32}^H	s_{33}^H	s_{34}^H	s_{35}^H	s_{36}^H	**&**
s_{41}^H	s_{42}^H	s_{43}^H	s_{44}^H	s_{45}^H	s_{46}^H	**&**
s_{51}^H	s_{52}^H	s_{53}^H	s_{54}^H	s_{55}^H	s_{56}^H	**&**
s_{61}^H	s_{62}^H	s_{63}^H	s_{64}^H	s_{65}^H	s_{66}^H	**&**
d_{11}	d_{12}	d_{13}	d_{14}	d_{15}	d_{16}	**&**
d_{21}	d_{22}	d_{23}	d_{24}	d_{25}	d_{26}	**&**
d_{31}	d_{32}	d_{33}	d_{34}	d_{35}	d_{36}	**&**
μ_{11}^S	μ_{12}^S	μ_{13}^S	**0.0**	**0.0**	**0.0**	**&**
μ_{21}^S	μ_{22}^S	μ_{23}^S	**0.0**	**0.0**	**0.0**	**&**
μ_{31}^S	μ_{32}^S	μ_{33}^S	**0.0**	**0.0**	**0.0**	**&**

where (s_{ij}^H) is the constant magnetic excitation elastic tensor, (d) the piezomagnetic tensor, (μ_{ij}^S) the constant strain magnetic permeability tensor, and RHO the density.

3.3.22.12 Case of a magnetostrictive material with losses

0.0	**0.0**	**RHO**	**0.0**	**0.0**	**0.0**	**&**
s'^H_{11}	s'^H_{12}	s'^H_{13}	s'^H_{14}	s'^H_{15}	s'^H_{16}	**&**
s'^H_{21}	s'^H_{22}	s'^H_{23}	s'^H_{24}	s'^H_{25}	s'^H_{26}	**&**
s'^H_{31}	s'^H_{32}	s'^H_{33}	s'^H_{34}	s'^H_{35}	s'^H_{36}	**&**
s'^H_{41}	s'^H_{42}	s'^H_{43}	s'^H_{44}	s'^H_{45}	s'^H_{46}	**&**
s'^H_{51}	s'^H_{52}	s'^H_{53}	s'^H_{54}	s'^H_{55}	s'^H_{56}	**&**
s'^H_{61}	s'^H_{62}	s'^H_{63}	s'^H_{64}	s'^H_{65}	s'^H_{66}	**&**
d'_{11}	d'_{12}	d'_{13}	d'_{14}	d'_{15}	d'_{16}	**&**
d'_{21}	d'_{22}	d'_{23}	d'_{24}	d'_{25}	d'_{26}	**&**
d'_{31}	d'_{32}	d'_{33}	d'_{34}	d'_{35}	d'_{36}	**&**
μ'^S_{11}	μ'^S_{12}	μ'^S_{13}	**0.0**	**0.0**	**0.0**	**&**
μ'^S_{21}	μ'^S_{22}	μ'^S_{23}	**0.0**	**0.0**	**0.0**	**&**
μ'^S_{31}	μ'^S_{32}	μ'^S_{33}	**0.0**	**0.0**	**0.0**	**&**
s''^H_{11}	s''^H_{12}	s''^H_{13}	s''^H_{14}	s''^H_{15}	s''^H_{16}	**&**
s''^H_{21}	s''^H_{22}	s''^H_{23}	s''^H_{24}	s''^H_{25}	s''^H_{26}	**&**
s''^H_{31}	s''^H_{32}	s''^H_{33}	s''^H_{34}	s''^H_{35}	s''^H_{36}	**&**
s''^H_{41}	s''^H_{42}	s''^H_{43}	s''^H_{44}	s''^H_{45}	s''^H_{46}	**&**
s''^H_{51}	s''^H_{52}	s''^H_{53}	s''^H_{54}	s''^H_{55}	s''^H_{56}	**&**
s''^H_{61}	s''^H_{62}	s''^H_{63}	s''^H_{64}	s''^H_{65}	s''^H_{66}	**&**
d''_{11}	d''_{12}	d''_{13}	d''_{14}	d''_{15}	d''_{16}	**&**
d''_{21}	d''_{22}	d''_{23}	d''_{24}	d''_{25}	d''_{26}	**&**
d''_{31}	d''_{32}	d''_{33}	d''_{34}	d''_{35}	d''_{36}	**&**
μ''^S_{11}	μ''^S_{12}	μ''^S_{13}	**0.0**	**0.0**	**0.0**	**&**
μ''^S_{21}	μ''^S_{22}	μ''^S_{23}	**0.0**	**0.0**	**0.0**	**&**
μ''^S_{31}	μ''^S_{32}	μ''^S_{33}	**0.0**	**0.0**	**0.0**	**&**

where (s'^{H}_{ij}) and (s''^{H}_{ij}) are, respectively, the real and imaginary parts of the constant magnetic excitation elastic tensor, (d') and (d") are, respectively, the real and imaginary parts of the piezomagnetic tensor, (μ'^{S}_{ij}) are (μ''^{S}_{ij}) are, respectively, the real and imaginary parts of the constant strain magnetic permeability tensor and RHO the density. To have a lossy magnetostrictive material, it is necessary but not sufficient to have all diagonal terms negative (s''^{H}_{ij}) (respectively (μ''^{S}_{ij})) (respectively positive).

3.3.22.13 Case of an electrostrictive material without losses

0.0	**0.0**	**RHO**	**0.0**	**0.0**	**0.0**	**&**
s_{11}^{D}	s_{12}^{D}	s_{13}^{D}	s_{14}^{D}	s_{15}^{D}	s_{16}^{D}	**&**
s_{21}^{D}	s_{22}^{D}	s_{23}^{D}	s_{24}^{D}	s_{25}^{D}	s_{26}^{D}	**&**
s_{31}^{D}	s_{32}^{D}	s_{33}^{D}	s_{34}^{D}	s_{35}^{D}	s_{36}^{D}	**&**
s_{41}^{D}	s_{42}^{D}	s_{43}^{D}	s_{44}^{D}	s_{45}^{D}	s_{46}^{D}	**&**
s_{51}^{D}	s_{52}^{D}	s_{53}^{D}	s_{54}^{D}	s_{55}^{D}	s_{56}^{D}	**&**
s_{61}^{D}	s_{62}^{D}	s_{63}^{D}	s_{64}^{D}	s_{65}^{D}	s_{66}^{D}	**&**
Q_{11}	Q_{12}	Q_{13}	Q_{14}	Q_{15}	Q_{16}	**&**
Q_{21}	Q_{22}	Q_{23}	Q_{24}	Q_{25}	Q_{26}	**&**
Q_{31}	Q_{32}	Q_{33}	Q_{34}	Q_{35}	Q_{36}	**&**
ε_{11}^{T}	ε_{12}^{T}	ε_{13}^{T}	**0.0**	**0.0**	**0.0**	**&**
ε_{21}^{T}	ε_{22}^{T}	ε_{23}^{T}	**0.0**	**0.0**	**0.0**	**&**
ε_{31}^{T}	ε_{32}^{T}	ε_{33}^{T}	**0.0**	**0.0**	**0.0**	**&**

where (s^{D}) is the elastic compliance tensor at constant electric excitation, (Q) the reduced tensor of the electrostrictive constants, (ε^{T}) the constant stress dielectric permittivity tensor, P_s the spontaneous polarization (the saturation value at high electric field), k a materials constant ($k = [\varepsilon_{33}^{T}]_{D=0}/P_s$), and RHO the density. If P_s equals 0, then the ε^{T} tensor is used, k is ignored and the material presents no saturation. If P_s is not null, then k and P_s are used to build the ε^{T} tensor and the values of ε_{11}^{T} to ε_{33}^{T} are ignored.

3.3.22.14 Case of a shape memory alloy material with a superelastic behaviour

E	**NU**	**RHO**	**0**	**0**	**0 &**
K0	**S0**	**SLIMU**	**SLIML**	**EPSBR**	

where E is Young's modulus at rest, NU is Poisson's ratio, RHO the density, K0 a stress value used for the nonlinear part of the material behaviour, S0 the stress limit at which the transformation occurs, SLIMU the stress limit during unloading, under which the material transforms back, SLIML the stress limit during loading, over which the material becomes superelastic, and EPSBR the strain limit after which the material is supposed to break.

3.3.22.15 Case of a shape memory alloy material with a memory behaviour

E	**NU**	**RHO**	**0**	**0**	**0 &**
K0	**S0**	**E2**			

where E is Young's modulus at rest, NU is Poissons ratio, RHO the density, K0 a stress value used for the nonlinear part of the material behaviour, S0 the stress limit over which the transformation occurs and E2 is Young's modulus during the unloading.

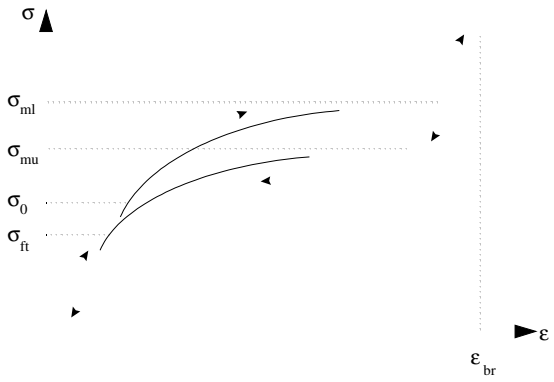

Example of superelastic transformation curve

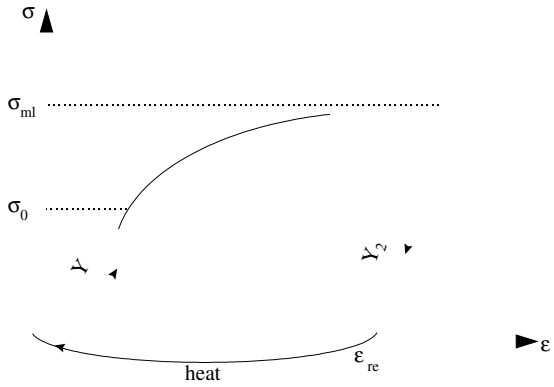

Example of memory effect transformation curve

Material property values of many materials commonly used in transducers are provided in the **MATER.STD** file distributed with **ATILA** (see section I.2.V). To use one of these materials, simply enter its name in an **ELEMENTS** entry, with no additional parameters. If a new material name is defined in a **MATERIALS** entry, this name and its corresponding property values will be automatically added to the **MATER.STD** file. Subsequent runs may specify a user-defined material by its name, the same as an **ATILA** standard material.

WARNING

If a material name already defined in the MATER.STD file is used in a MATERIALS entry, the property values listed as parameters will automatically replace the values in the MATER.STD file, and the new values will be used by the code in the run. A warning will also be printed in the listing file. For this reason, extreme caution should be exercised with the MATERIALS entry

Many elements in **ATILA** allow the use of material with losses.

WARNING

When the entry LOSSES is issued in the data file, all the elements (elastic, fluid, piezoelectric and magnetostrictive) are considered elements with losses.

In a radiating harmonic analysis, the external fluid domain, which is modelled by damping elements, cannot have losses.

EXAMPLE:

```
+ MATERIAL
+ 25CD4D
+ .215E+12  .33  7500.
```

3.3.23 MATRICES

This entry indicates that the system matrices must be dumped into files for use with external programs. No other computation is done.
Note that this entry is mutually exclusive from the CHIEF, DYNFLEX and EQI entries and is available only for a harmonic analysis.

3.3.24 NEWAXES *[CARTESIAN, CYLINDRICAL, SPHERICAL]*

X0 Y0 Z0 OZZ OYY OXX

This entry enables the user to modify the system in which the node coordinates are given. The initial system is Cartesian; its origin and axes are the global system origin and axes. If the new system is cylindrical (spherical), the node coordinates X, Y, Z, associated with the following **NODES** entry(ies), become the cylindrical (spherical) coordinates R, THETA, Z (R, THETA, PHI), respectively. The angles THETA and PHI for spherical coordinates are represented on the figure describing the entry **ANGLES**.

X0, Y0, Z0: coordinates of the new system origin in the global system.

Ozz, Oyy, Oxx: angles (in degrees) of the Euler rotations that transform the initial axes into the new axes. The first rotation is around the Oz axis of the initial system, transforming Oxyz to OXYz; the second rotation is around the OY axis provided by the first rotation, transforming OXYz to Ox'YZ; the third rotation is around the Ox' axis provided by the second rotation, transforming Ox'YZ to Ox'y'z'.

This entry can be used several times during the description of the mesh. Its parameters are always expressed in terms of the global coordinate system.

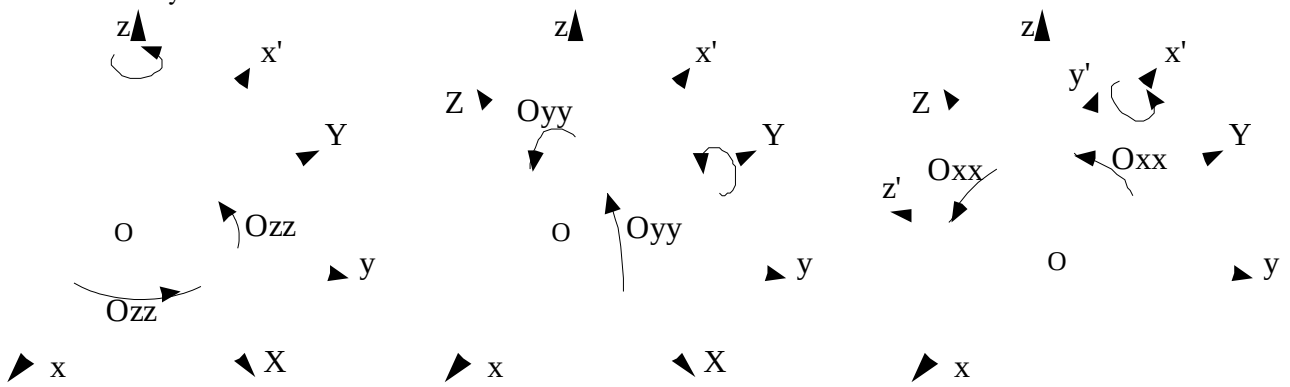

In the above figures, Oxx and Ozz have positive values, while Oyy has a negative value.

3.3.25 NLOAD

NLO

NLO is an integer corresponding to the number of loading cases for a static analysis, the number of eigenmodes selected for a modal analysis, the number of frequencies for a harmonic analysis, the number of saved time steps for a transient analysis. If the user analyzes the scattering of a plane-wave by a periodic structure, the number of loading cases NLO must equal the number of frequencies (entry **FREQUENCY**) multiplied by the number of angle values. In the case of a double periodicity, this number must be divided by two.

It should be noted that this integer sets the maximum number of loading cases that would be taken into account for a restart. NLO must be less than or equal to 1000.

EXAMPLE:

- **NLOAD = 80**

3.3.26 NODES

x1 y1 z1
OR r theta z
OR r theta phi
...
BLANK LINE

This entry provides the node coordinates. The nodes are sequentially numbered, in the order in which they are introduced. The two SCALE and NEWAXES entries, if necessary, are to be inserted before the first **NODES** entry or between two **NODES** entries. The **NODES** entry is **required**.

WARNING

Nodes have to be introduced in the following order:
solid / fluid / radiating. Note that the MOSAIQUE tool
automatically generates nodes in the correct order

For axisymmetrical structures,
the Ox axis is <u>always</u> the symmetry axis.

For periodic structures, facing boundaries must have nodes facing correctly.

<u>EXAMPLE:</u>

```
•       NODES
+ *   1 * -0.64000E-01    0.00000E+00    0.00000E+00
+ *   2 * -0.59500E-01    0.00000E+00    0.00000E+00
+ *   3 * -0.55000E-01    0.00000E+00    0.00000E+00
+ *   4 * -0.64000E-01    0.30000E-02    0.00000E+00
+ *   5 * -0.55000E-01    0.30000E-02    0.00000E+00
+ *   6 * -0.64000E-01    0.60000E-02    0.00000E+00
+ *   7 * -0.59500E-01    0.60000E-02    0.00000E+00
```

etc.

Note that the node numbering is a comment. Because nodes are numbered as they are entered, it is a good practice to add these comments for readability. The MOSAIQUE tool does provide these comments.

3.3.27 PERIODIC *[1D, 2D, 3D]*

3.3.27.1 One-dimensional periodicity, two-dimensional mesh

The entry parameters, listed in this order, are:

N11 N12 0 N14

The first two node numbers N11 and N12 define the first boundary line of the unit cell. The node numbers N11 and N14 define a vector parallel to the direction of periodicity. The node number N14 also uniquely defines the second boundary line of the unit cell, parallel to the first one. Note that the unit cell is generally a parallelogram, but must be ***rectangular*** for a ***harmonic*** analysis.

<u>EXAMPLE:</u>

PERIODIC 1D = 1 3 0 2

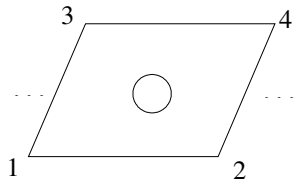

3.3.27.2 One-dimensional periodicity, three-dimensional mesh

The entry parameters, listed in this order, are:

N11 N12 N13 N14

The first three node numbers N11, N12 and N13 define the first boundary plane of the unit cell. The node numbers N11 and N14 define a vector parallel to the direction of periodicity. The node number N14 also uniquely defines the second boundary plane of the unit cell, parallel to the first one. Note that the unit cell must be a parallelepiped for a harmonic analysis.

Example:

PERIODIC 1D = 1 2 5 3

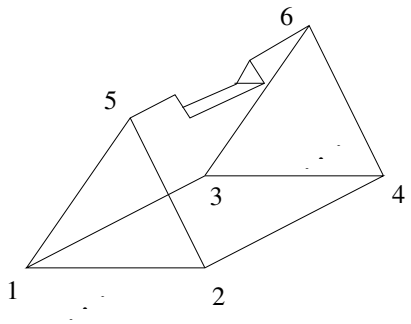

3.3.27.3 Two-dimensional periodicity, two-dimensional mesh

The entry parameters, listed in this order, are:

N11 N12 0 N14
N21 N22 0 N24

The two lines define the two periodicities. For each line, the first two node numbers NX1 and NX2 define the first boundary line of the unit cell; the node numbers NX1 and NX4 define a vector parallel to the direction of the corresponding periodicity. The node number NX4 also uniquely defines the second boundary line of the unit cell, parallel to the first one. Note that the unit cell must be rectangular for a harmonic analysis.

EXAMPLE:

PERIODIC 2D = 1 3 0 2 / 1 2 0 3

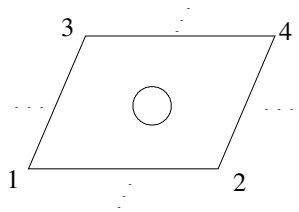

3.3.27.4 Two-dimensional periodicity, three-dimensional mesh

The entry parameters, listed in this order, are:

N11 N12 N13 N14
N21 N22 N23 N24

The two lines define the two periodicities. For each line, the first three node numbers NX1, NX2 and NX3 define the first boundary plane of the unit cell; the node numbers NX1 and NX4 define a vector parallel to the direction of the corresponding periodicity. The node number NX4 also uniquely defines the second boundary plane of the unit cell, parallel to the first one. Note that the unit cell must be a parallelepiped for a harmonic analysis.

EXAMPLE:

PERIODIC 2D = 1 3 5 2 / 1 2 5 3

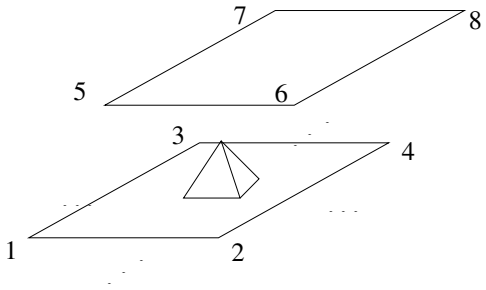

3.3.27.5 Three-dimensional periodicity

The entry parameters, listed in this order, are:

N11 N12 N13 N14
N21 N22 N23 N24
N31 N32 N33 N34

The three lines define the three periodicities. For each line, the first three node numbers NX1, NX2 and NX3 define the first boundary plane of the unit cell; the node numbers NX1 and NX4 define a vector parallel to the direction of the corresponding periodicity. The node number NX4 also uniquely defines the second boundary plane of the unit cell, parallel to the first one. Note that the unit cell must be a parallelepiped for a harmonic analysis.

EXAMPLE:

PERIODIC 3D = 1 3 5 2 / 1 2 5 3 / 1 2 3 5

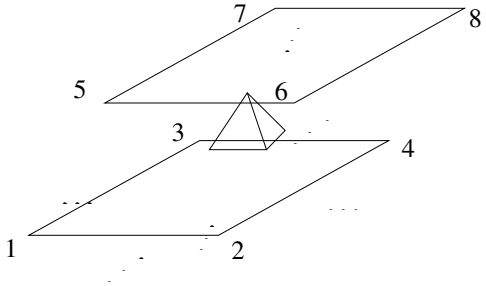

3.3.28 PRECISION *[SINGLE, DOUBLE]*

This entry indicates to the program that a static, modal, harmonic or transient analysis is to be performed with single or double precision variables. The default precision is single. It is important to check the available options for each analysis (Chapter I.2).

3.3.29 PRESSURE *[TOTAL, SCATTERED]*

This entry indicates that the flooded structure is excited by an impinging harmonic wave and that the total (attribute TOTAL) or only the elastic scattered (attribute SCATTERED) pressure must be calculated. The excitation can either be an impinging plane wave coming from a given direction, provided by means of the ANGLES command or given by the mean of the function INCPRE when no ANGLES command appear. This function is declared COMPLEX*16 and has four parameters: X, Y, Z (point coordinates) and K (wavenumber in the infinite fluid medium). This function returns the incident pressure value at the given point and wavenumber. This procedure can excites the structure with an incident wave of any kind (plane wave, spherical). The default function INCPRE provided with ATILA generates a plane wave travelling from positive to negative Ox axis ($p(x,y,z) = e^{jkx}$):

```
FUNCTION INCPRE(X,Y,Z,K)
*  computes the incident pressure at the point (X,Y,Z) for the wavenumber K
DOUBLE PRECISION K,X,Y,Z
COMPLEX*16 INCPRE
*  case of a plane wave travelling from positive to negative Ox axis
INCPRE = DCMPLX(DCOS(K*X),DSIN(K*X))
RETURN
END
```

This function can also be user-provided, by means of a shareable library (INCPRE.DLL for Windows, libincpre.so for Unix operating systems).

WARNING

In case of a 3D structure, the damping sphere must be centered on the global axis origin.
If the model has symmetries, the incident pressure field function must take these symmetries into account.

3.3.30 PRINTING

3.3.30.1.1 NPR

This entry defines the printing level NPR, which must equal 0, 1, 2, 3 or 4:

- NPR = 0, only computation results are printed
- NPR = 1 or 2 (default) prints intermediary information and the results
- NPR = 3 corresponds to a trace level to follow the computation step by step
- NPR = 4 allows the printing of elementary matrices before assembling.

3.3.31 RADIATION *[MONOPOLAR, DIPOLAR]*

This entry selects the type of damping condition imposed on the outer fluid domain radiating surface S, i.e., the type of radiation impedance imposed on the radiating elements. The default damping condition is monopolar. The multipolar expansion of the pressure field is limited to the 1/r term in the monopolar case, to the $1/r^2$ term in the dipolar case. This entry affects the type of element used and the solving program.

EXAMPLE:

+ RADIATION DIPOLAR

3.3.32 SCALE

EX EY EZ

This entry defines scale factors (EX, EY, EZ) that are applied to the node coordinates included in the following NODES entry (ies). The coordinates must be given in the absolute system. To switch off this scaling, the SCALE entry has to be used with the parameters 0.0, 0.0, 0.0. Note that it does not affect the commands NEWAXES and GEOMETRY.

3.3.33 SHIFT

FSHIFT

This entry defines the shift in frequency used by the code for an eigenvalue computation. The default value of this shift (1000.0 Hz) is valid for structures having a first non-rigid-body mode above 100.0 Hz. For structures having a first resonance at a lower frequency, the user must specify a value for the shift between one and ten times the estimated value of the first resonance frequency.

3.3.34 STRESS OR STRESS PRINCIPAL

This entry enables the stress or principal stress computation, for all loading cases considered. Stresses are given in the global system. This calculation is available for all the elastic, piezoelectric, magnetostrictive and electrostrictive elements, except those mentioned in Section I.4.B. The B field is also computed for magnetostrictive and magnetic elements. The D field is also computed for electrostrictive elements. The stresses are stored in the PST file when its generation is requested with the GENERATE command.

This entry is mandatory when electrostrictive elements are used.

3.3.35 THERMAL

This entry must be used together with the keyword **ANALYSIS STATIC.** It allows to perform a thermal analysis. Prescribed conditions are introduced using temperature conditions.

3.3.36 SYSNOISE *[MODAL DIRECT ASCII BIN]*

This entry indicates that the requested analysis is a harmonic analysis where the fluid-structure coupling is solved by the SYSNOISE program. Two different algorithms may be applied: SYSNOISE can either use eigenvectors and eigenforces calculated with ATILA and return participation factors (**MODAL** parameter), or directly use the system matrices calculated with ATILA and solve the problem including the fluid interaction (**DIRECT** parameter). One of these two parameters must be given. They are mutually exclusive.

ATILA generates a file with extension .frq, in the *jobname* directory, in which are stored the frequencies listed in the FREQUENCY command. With the **MODAL** parameter, ATILA also stores eigenvectors and eigenforces in files of extensions .vvpr and .fmo, respectively, in the *jobname* directory. With the **DIRECT** parameter, ATILA also stores the real and imaginary parts of the stiffness matrix, the mass matrix and the real and imaginary parts of the piezoelectric forces in files of extensions .muakr, .muaki, .muam, .br and .bi, respectively, in the *jobname* directory. It then calls the command: "ati_to_sysnoise *jobname*", where *jobname* is the name of the job being run. There is a default ati_to_sysnoise command in the bin subdirectory of the ATILA installation directory. This command, which can be tailored by the user, must perform the activation of the SYSNOISE program. On completion of this command, the following files must be present: the file _jobname_/_jobname_.modalres containing the displacement vectors, for the **MODAL** parameter, or the displacements vectors _jobname_/DSPxxxxxxxx.INT (note the names in capital letters), for each of the requested frequencies xxxxxxxx, expressed in tenths of Hertz, for the **DIRECT** parameter.

The optional parameters **ASCII** and **BIN** are mutually exclusive and affect the generation of files triggered by the **SYSNOISE** command. **ASCII** is the default.

3.3.37 TRANSIENT *[METHOD NS NSKIP ΔT FL PAR1 PAR2]*

This entry provides the necessary information for the TRANSIENT analysis. METHOD indicates the time integration method selected from one of the following methods: CENTRAL (Central Difference Method), NEWMARK (Newmark's Method) or WILSON (Wilson-θ Method). NS is the number of steps between each saved displacements. NSKIP is the number of skipped steps before starting saving steps. ΔT is the time step. FL is the frequency at which materials losses are considered, when they exist. PAR1 and PAR2 depend on the integration method: they are ignored for the Central Difference Method, they are respectively α and β for the Newmark's Method and PAR1 is the parameter θ for the Wilson-θ Method, PAR2 being ignored.

The displacements are calculated at times 0, ΔT 2ΔT, 3ΔT, 4 ΔT etc., but they are printed in the listing file and saved at the times NSKIP*ΔT, (NSKIP+NS)*ΔT, (NSKIP+2*NS)*ΔT, etc., (NSKIP+NLO*NS)*ΔT.

3.3.38 WAVE NUMBER

NK VKBEG VKEND

This entry defines the wavenumbers for which a computation is requested, when performing a modal analysis of a periodic structure. For each direction of propagation defined by the ANGLES command, NK computations are performed, with values of wavenumber equally spaced in an interval depending on VKBEG and VKEND as follows:

- if VKBEG is greater or equal to zero, its value defines the lower bound of the wavenumber interval;
- if VKBEG is negative, the lower bound of the wavenumber interval is set to the value of the boundary of the first Brillouin zone along the propagation direction;
- if VKEND is greater or equal to zero, its value defines the upper bound of the wavenumber interval;
- if VKEND is negative, the upper bound of the wavenumber interval is set to the value of the boundary of the first Brillouin zone along the propagation direction;
- if VKBEG equals VKEND, then NK is set to 1;
- if NK is 1, the only computation is done with the value of VKBEG.

EXAMPLES

WAVE NUMBER = 3 0. 40.

The requested wavenumber values are 0., 20. and 40. m^{-1}

WAVE NUMBER = 3 0. -1.

If the structure under study is a one-dimensional periodic structure of unit cell size equal to *a*, the requested wavenumber values are 0., $\pi/2a$ and π/a.

3.4 Boundary conditions

Boundary conditions may be described using free format. For all the data inputs, **node number** is referenced as **N**, a **degree-of-freedom** is referenced as **D**, with the following correspondence: 1 for U_X (or P), 2 for U_Y, 3 for U_Z, 4 for θ_X (or Φ or ϕ), 5 for θ_Y, and 6 for θ_Z. Moreover, the **lines** that are parallel to a global coordinate axis and the **planes** that are normal to these axes are referenced as **P**. The correspondence is:

1 for a plane normal to the Ox axis,	4 for a line parallel to the Ox axis,
2 for a plane normal to the Oy axis,	5 for a line parallel to the Oy axis,
3 for a plane normal to the Oz axis,	6 for a line parallel to the Oz axis.

Note that the loading definitions available in previous versions are superseded by LOADS or EXCITATIONS entries.

Boundary conditions enable the user to force clamped, hinged or simply supported conditions, or identity between degrees-of-freedom. These conditions are generally associated with symmetry planes or axes, electrodes or pressure-release surfaces. The easiest way to understand how to provide boundary conditions is to refer to the following rules:

- Boundary conditions acting on *one node* are defined by the node number N and no line or plane P (or P = 0);
- Boundary conditions acting *a group of nodes* on the same line or plane are defined by a negative value of N and a corresponding line or plane P not equal to 0;
- Boundary conditions *deleting* a degree-of-freedom are defined by a *positive value* of the line or plane indicator *P*;
- Boundary conditions *making an identity* between degrees-of-freedom of a group of nodes are defined by a *negative value* of the line or plane indicator *P*;
- A node number N = 0 means the whole structure.

3.4.1 Boundary conditions defined in global axes

- The degree-of-freedom in the **D** direction is deleted for all the structure nodes.

0 D 0

- The degree-of-freedom is deleted in the **D** direction at node **N**:

N D 0

- The degree-of-freedom is deleted in the **D** direction for all the nodes that belong to the **P** plane or line containing the node **N:**

- N D P

- For fluid-structure problems, this condition can be restricted to the **S**olid part of a mesh using the fourth field of the format:
  - N D P S

It can also be restricted to the **F**luid part:

- N D P F

- The degree-of-freedom in the **D** direction at node **N** is identical to the degree-of-freedom in the **D** direction at node **M**:

  N D M

- Degrees-of-freedom in the **D** direction for all the nodes that belong to the plane or line **P** containing **N** are identical:
  - N D -P

When using piezoelectric materials, excitation electrodes are defined by setting identical electric potential degree-of-freedom for the corresponding nodes; voltage reference electrodes are defined by deleting identical electric potential degree-of-freedom for the corresponding nodes. The potential on excitation electrodes may be prescribed using the **EXCITATIONS** entry.

When doing the analysis of **a periodic elastic or piezoelectric structure** two kinds of surfaces limit the mesh.

Surfaces limiting the mesh that are orthogonal to the periodicity directions are constant X planes (in fact, lines) for 1-D periodicity, and constant X and Y planes for 2-D periodicity. For surfaces facing each other, nodes must be identical after elementary translation.

Surfaces between the mesh and semi-infinite fluid domains are constant Y planes (in fact, lines) for 1-D periodicity, and constant Z planes for 2-D periodicity. On these surfaces, the pressure is linked to a plane-wave series expansion.

In the case of a structure with fluid on the front and back surfaces, the user must provide the extreme nodes of the elementary cell:

- N1 1 1 X1
- N2 1 1 X2

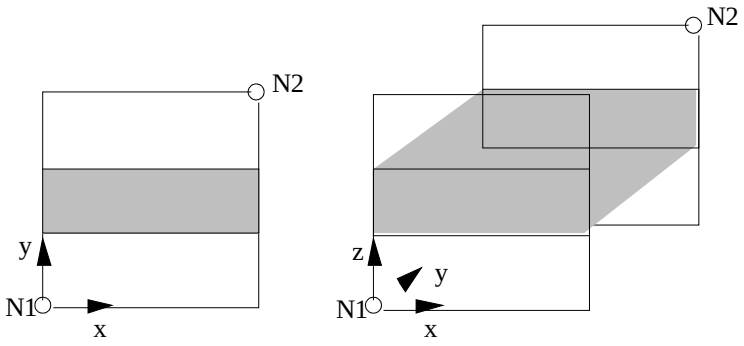

In the case of a structure with fluid on the front side only (free backface), the condition becomes:

-N1 1 1 X1
-N2 1 1 XS

Free or clamped backface

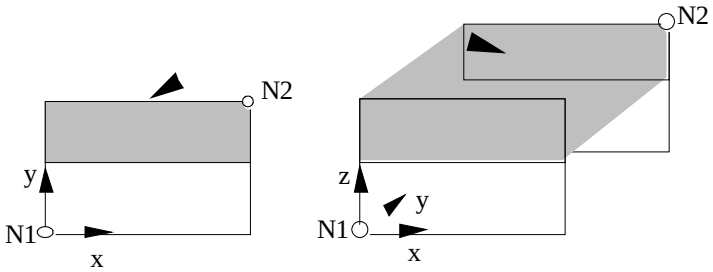

To get a clamped backface for a 1D periodicity, the additional condition:

- N2 2 2

must be introduced. For a 2D periodicity, the condition is:

- N2 3 3

When the periodic structure is piezoelectric, an additional condition prescribing the kind of analysis must be introduced **after the blank line closing the boundary condition set**. For a scattering problem, the condition is:

- 1 N

where N is the node number of the electrode. For a radiation problem, the condition is:

- 2 N

where N is the node number of the hot electrode. In this case, the applied voltage of this electrode has to be prescribed using the **EXCITATIONS** command.

3.4.2 Boundary conditions in local axes

Boundary conditions in terms of local axes can be specified in several cases. First, a displacement to be constrained at a node can be in a direction that is not parallel to a global axis (Fig. 1). Second, a boundary condition can be applied on a line that is not parallel to a global axis or on a plane that is not perpendicular to a global axis (Fig. 2). These two cases are generally merged (Fig. 3), which constitutes case 3.

Case 1: To define local axes at a given node **N**, the user must issue the following lines:

N 10 0
A11 A12 A13 A21 A22 A23

where A11, A12, A13 (respectively A21, A22, A23) are the direction cosines of the first (second) local axis expressed in the global coordinate system. Then, degrees-of-freedom at node **N** are automatically defined by the code in the new local axes and they can be constrained using the same data lines as for the first group. If the same global axes have to be defined for all the nodes that belong to the same line or plane **P** containing the node **N**, the preceding data set has to be modified by simply substituting for the first line the following one:

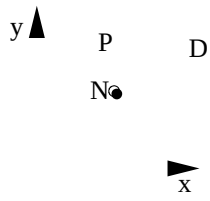

Figure 1

- N 10 P

Case 2: To constrain nodes belonging to a plane that is not perpendicular to a global axis (1, 2 or 3), the corresponding line of the first group has to be modified by substituting 9001 for **P** and adding immediately following this line a second line that contains the direction cosines A1, A2 and A3 of the normal to this new plane, expressed in the global coordinate system. Thus, if the degrees-of-freedom of type **D** of all the nodes that belong to this plane have to be deleted, the two data lines are:

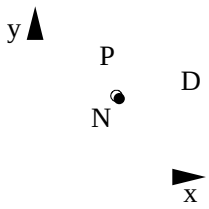

Figure 2

- N D 9001
A1 A2 A3

To constrain nodes belonging to a line that is not parallel to a global axis, (3, 4, or 5), 9004 must be substituted for **P** and following a second line must be added that contains the direction cosines A1, A2 and A3 of this new line, in the global coordinate system. One obtains:

- N D 9004
A1 A2 A3

Case 3: Finally, the two preceding cases can be merged simply by mixing the corresponding data lines. Thus, if the preceding local axes have to be defined for all the nodes belonging to the plane described in case 2:

- N 10 9001
A11 A12 A13 A21 A22 A23
A1 A2 A3

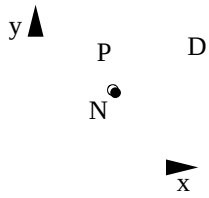

Figure 3

For a line that is different from the global axes system, the data are written in the same order, substituting 9004 for 9001, with A1, A2 and A3 becoming the direction cosines of this line.

REMARKS

- A blank line closes this data line set.
- Constraints on different degrees-of-freedom can be merged. Thus if the same constraint has to be applied to U_X and U_Z, D = 13.
- When D = 0, all degrees-of-freedom are clamped.
- The null flux condition is the natural condition of a fluid domain (pressure gradient flux) or of a piezoelectric domain (electrical field flux) or of a magnetic domain (reduced magnetic field flux).

Examples:

```
+  -1   1   1          * yOz is a SYMMETRY PLANE (node 1 is on O)
+  -1  12   3          * xOy is an ANTISYMMETRY PLANE
+ -45   4   1          * Electrode at V=0
+ -68   4   1          * Electrode at V=0
+ -66   4  -1          * Excitation electrode
+
```

Note: For a modal analysis, the electrical short-circuit conditions (resonance) would have to be written:

```
+ -45   4   1          * Electrode at V=0
+ -68   4   1          * Electrode at V=0
+ -66   4   1          * Excitation electrode at V=0
+
```

and the open-circuit conditions (antiresonance) would have to be written:

```
+ -45   4   1          * Electrode at V=0
+ -68   4   1          * Electrode at V=0
+ -66   4  -1          * Floating voltage electrode
+
```

Example of a non standard symmetry plane (xOz plane rotated 15° around Oz)

```
-1   10 9001 * DEFINE LOCAL AXES  ON THE PLANE
 0.965926  0.258819  0.0   -0.258819  0.965926  0.0
-0.258819  0.965926  0.0
-1    2 9001   * FREEZE LOCAL UY DISPLACEMENTS ON THAT PLANE
-0.258819  0.965926  0.0
```

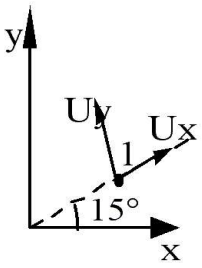

4 ELEMENTS DESCRIPTION

4.1 Introduction

This chapter describes the finite elements available in the **ATILA** code. For each element, the name, definition, list of the degrees-of-freedom associated with the nodes (translations, rotations, electrical potential, magnetic potential, pressure), and entry parameters (topology, material properties, geometrical properties) are provided.

Most of the elements in the **ATILA** library are **isoparametric**. Thus, complex structures with curved sides or faces can be modelled using a reduced number of elements. Nevertheless, **the best results are obtained when these elements have a reasonable aspect ratio**. Wild distortions lead to inaccuracies because the assumptions made within the code for strains become unrealistic. Extreme distortion may even cause program failure (negative Jacobian determinant). The user should guard against excessive distortion by adhering to the following guidelines for sides of 2-D elements or for faces of 3-D elements:

- the angles between adjacent sides of quadrilaterals should be between 45 and 135 degrees
- the angles between adjacent sides of triangles should be between 30 and 100 degrees
- in elements with curved sides, the radius of curvature of each side should exceed the length of the longest side
- for one element, the ratio between the smallest and largest dimensions must be less than or equal to 3 in single precision and 5 in double precision
- midside nodes must be at equal distance from their respective corner nodes.

Element node numbering generally follows simple rules:

- Corner nodes first, then midside nodes (the only exception is the SHEL03E element).
- The first node gives the axis center, local to the element.
- The second node gives the direction of local Ox axis.
- The third node, when available, gives the direction of local Oy axis.

WARNING

All data (except the angles) must be given using MKS units or any coherent unit system deduced from the MKS system. Angles are always in degrees.

4.2 ATILA Finite Element Library

Cat.: Category.
B: Bulk element.
P: Plate element.
Sh: Shell element.
Sp: Spring element.
F: Thin film element.
T: Trilaminar element.

PE: Available for Plane-stress class.
PA: Available for Plane-strain class.
AXI: Available for Axisymmetrical class.
PRO: Available for Propagation class.

4.2.2 SHAPE MEMORY MATERIAL

2D elements								
Cat.	Shape	# of nodes	Name	Page	PE	PA	AXI	PRO
Sp	Linear Linear	2 2	SPRI02AM SPRI02AS	108 110		√	√	

3D elements				
Cat.	Shape	# of nodes	Name	Page
Sp	Linear Linear	2 2	SPRI02AM SPRI02AS	108 110

4.2.3 COMPOSITE

2D elements								
Cat.	Shape	# of nodes	Name	Page	PE	PA	AXI	PRO
B	Quadrilateral	8	QUAD08C	114			√	

3D elements				
Cat.	Shape	# of nodes	Name	Page
B	Hexahedral	20	HEXA20C	9
Sh	Quadrilateral Triangular	8 6	SHEL08C SHEL06C	113

4.2.4 Elastic

2D elements								
Cat.	Shape	# of nodes	Name	Page	PE	PA	AXI	PRO
B	Quadrilateral Triangular	8 6	QUAD08E TRIA06E	120	√	√	√	√
Sh	Linear	3	SHEL03E	121			√	
Sp	Linear	2	SPRI02E	119		√	√	

3D elements				
Cat.	Shape	# of nodes	Name	Page
B	Hexahedral Prismatic Pyramidal Tetrahedral	20 15 13 10	HEXA20E PRIS15E PYRA13E TETR10E	115
P	Quadrilateral Triangular	8 6	PLAT08E PLAT06E	116
Sh	Quadrilateral	8	FACE08E	117
Sp	Linear	2	SPRI02E	119

4.2.5 ELECTROSTRICTIVE

2D elements								
Cat.	Shape	# of nodes	Name	Page	PE	PA	AXI	PRO
B	Quadrilateral Triangular	8 6	QUAD08ES TRIA06ES	122		√	√	

3D elements				
Cat.	Shape	# of nodes	Name	Page
B	Hexahedral Prismatic Pyramidal Tetrahedral	20 15 13 10	HEXA20ES PRIS15ES PYRA13ES TETR10ES	122

4.2.6 FLUID

2D elements								
Cat.	Shape	# of nodes	Name	Page	PE	PA	AXI	PRO
B	Quadrilateral Triangular	8 6	QUAD08F TRIA06F	125		√	√	√

3D elements				
Cat.	Shape	# of nodes	Name	Page
B	Hexahedral Prismatic Pyramidal Tetrahedral	20 15 13 10	HEXA20F PRIS15F PYRA13F TETR10F	122

4.2.7 MAGNETIC

2D elements							
Cat.	Shape	# of nodes	Name	Page	PE	PA	AXI
B	Quadrilateral Triangular	8 6	QUAD08G TRIA06G	127		√	

3D elements				
Cat.	Shape	# of nodes	Name	Page
B	Hexahedral Prismatic Pyramidal Tetrahedral	20 15 13 10	HEXA20G PRIS15G PYRA13G TETR10G	126

4.2.8 INTERFACE

2D elements								
Cat.	Shape	# of nodes	Name	Page	PE	PA	AXI	PRO
	Line	6	LINE06I	129		√	√	√

3D elements				
Cat.	Shape	# of nodes	Name	Page
	Quadrilateral Triangular	16 12	QUAD16I TRIA12I	128

4.2.9 MAGNETOSTRICTIVE

2D elements								
Cat.	Shape	# of nodes	Name	Page	PE	PA	AXI	PRO
B	Quadrilateral Triangular	8 6	QUAD08M TRIA06M	132		√	√	

3D elements				
Cat.	Shape	# of nodes	Name	Page
B	Hexahedral Prismatic Pyramidal Tetrahedral	20 15 13 10	HEXA20M PRIS15M PYRA13M TETR10M	130
F	Quadrilateral	16	QUAD16M	131

4.2.10 PIEZOELECTRIC

2D elements								
Cat.	Shape	# of nodes	Name	Page	PE	PA	AXI	PRO
B	Quadrilateral Triangular	8 6	QUAD08P TRIA06P	135		√	√	

3D elements				
Cat.	Shape	# of nodes	Name	Page
B	Hexahedral Prismatic Pyramidal Tetrahedral	20 15 13 10	HEXA20P PRIS15P PYRA13P TETR10P	133
T	Quadrilateral Triangular	8 6	TRIL08P TRIL06P	134

4.2.11 DAMPERS

2D elements								
Cat.	Shape	# of nodes	Name	Page	PE	PA	AXI	PRO
	Line	3	LINE03R	137		√	√	

3D elements				
Cat.	Shape	# of nodes	Name	Page
	Quadrilateral Triangular	8 6	QUAD08R TRIA06R	136

4.2.12 COUPLING FEM-BEM

2D elements								
Cat.	Shape	# of nodes	Name	Page	PE	PA	AXI	PRO
	Linear	3	LINE03Z	140			√	

3D elements				
Cat.	Shape	# of nodes	Name	Page
	Quadrilateral Triangular	8 6	QUAD08Z TRIA06Z	137

4.2.13 Mechanical local impedance

2D elements								
Cat.	Shape	# of nodes	Name	Page	PE	PA	AXI	PRO
	Linear	3	LINE03Z	140			√	

3D elements				
Cat.	Shape	# of nodes	Name	Page
	Quadrilateral Triangular	8 6	QUAD08Z TRIA06Z	137

4.3 Element description

The **ATILA** element library is described on the following pages.

4.3.1 SPRI02AM

Description

The SPRI02AM element is a two-node spring element used to model the memory effect of a shape memory material.

Active degrees-of-freedom

U_x, U_y, and U_z (3 translations).

Topology

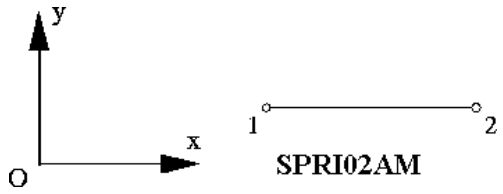

Parameters

.MATERIALS entry parameters These correspond to a shape memory alloy with a memory behaviour (chap.3).	GEOMETRY entry parameters S where S is the cross section area of the rod

Remarks

For this element, the performed analysis is restricted to a combination of loading from 0 to the requested static forces and unloading from that maximum back to 0

In three-dimensional models, the section S must be divided by the number of symmetry planes + 1. In axisymmetrical models, the section S must be divided by 2.

Care should be taken about lateral displacements, as there is no stiffness associated to them. The common rule is either to block them or to make them equal to their neighboring elements.

Example

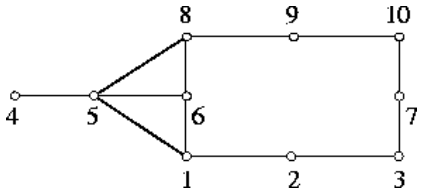


```
GEOMETRY
   1 = 0.0005   * Section 1
   2 = 0.0015   * Section 2
…
ELEMENTS
 SPRI02AM   SMA1  2   =   4  5  *  The rod

 SPRI02AM   SMA1  1   =   5  1  /  5  6  /  5  8  *  The "umbrella"

QUAD08E   STEEL
   1  3  8  10  2  6  7  9
…
END
 4   2   6   *  Same Oy displacement as that of node 6
 5   2   6   *  Idem
```

4.3.3 SPRI02AS

Description

The SPRI02AS element is a two-node spring element used to model the superelastic effect in a shape memory material.

Active degrees-of-freedom

U_X, U_Y, and U_Z (3 translations).

Topology

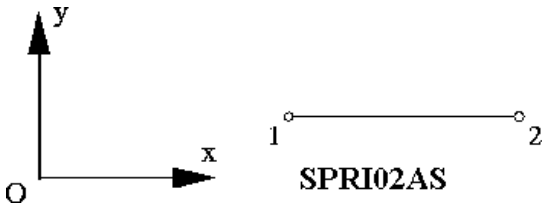

Parameters

MATERIALS entry parameters	GEOMETRY entry parameters
These correspond to a shape memory alloy with a superelastic behaviour (chap. 3.3)	S where S is the cross section area of the rod.

Remarks

For this element, the performed analysis is restricted to a combination of loading from 0 to the requested static forces and unloading from that maximum back to 0

In three-dimensional models, the section S must be divided by the number of symmetry planes + 1. In axisymmetrical models, the section S must be divided by 2.

Care should be taken about lateral displacements, as there is no stiffness associated to them. The common rule is either to block them or to make them equal to their neighbouring elements.

Example

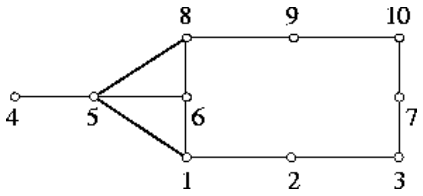


```
GEOMETRY
  1 = 0.0005   * Section 1
  2 = 0.0015   * Section 2
…
ELEMENTS
 SPRI02AS   SMA2  2  =  4  5  *  The rod

 SPRI02AS   SMA2  1  =  5  1  /  5  6  /  5  8  *  The "umbrella"

QUAD08E   STEEL
  1  3  8  10  2  6  7  9
…
END
```

4.3.4 **HEXA20C** (27)

Description

The HEXA20C element is a twenty-node isoparametric hexahedron used to model multi-layer composite materials. The formulation of this element relies on the Halpin and Tsai model. The element must be a part of a thick plate or of a thick cylindrical shell having a circular cross-section. It must be simply curved with a constant thickness and a constant curvature in the element Oxy plane. No curvature or thickness variation is allowed in the element Oyz plane.

Active degrees-of-freedom

U_X, U_Y, and U_Z, (3 translations).

Topology

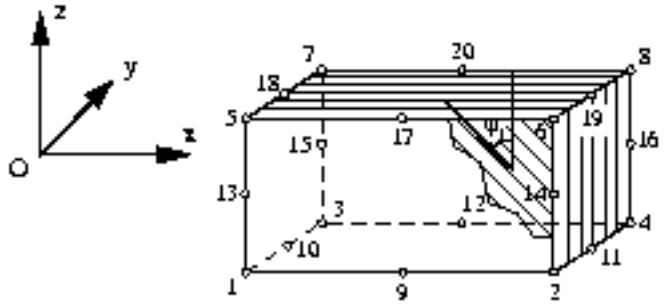

HEXA20C

(fiber skew angle PHI1 shown here)

Parameters

MATERIALS entry parameters	GEOMETRY entry parameters
Fiber and resin characteristics. See the detailed description of the MATERIALS entry, (chap. 3.3)	NLAY PHI1 PHI2 ... PHIN where NLAY is the number of layers, PH1 to PHIN are, for each layer, the values of the fiber skew angle referenced to the element Oz axis. All layers have the same thickness, deduced from element size and NLAY.

Remarks

- Modeling of shells of various thicknesses and curvatures is possible by assembling several elements so as to discretize this variation. ATILA **does not** detect unallowed element curvature or thickness variations.
- Shells with double curvature can be modeled with the facet assumption.

Example

```
GEOMETRY
2 = 4  30. -30. 30. -30.
…
…
ELEMENTS
 HEXA20C   PLC3   2
  1  3  6  8  13  15  18  20  2  4  5  7  9  10  11  12  14  16  17  19
```

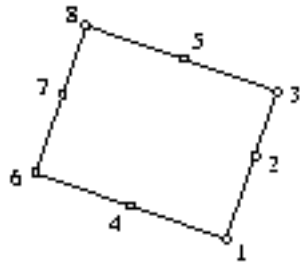

4.3.5 SHEL08C, SHEL06C

Description

These eight-node or six-node curved shell elements are used to model multi-layer composite materials. The formulation of this element relies on the Halpin and Tsai model.

Active degrees-of-freedom

U_X, U_Y, U_Z, θ_X, and θ_Y (3 translations, 2 rotations).

Topology

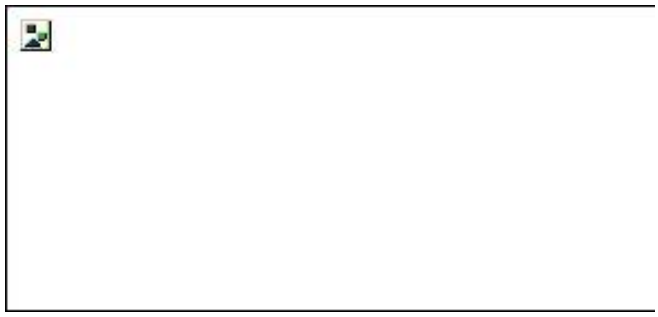

(Fiber skew angle PHI1 shown here)

Parameters

MATERIALS entry parameters	GEOMETRY entry parameters
Fiber and matrix characteristics. See the detailed description of the MATERIALS entry, (chap. 3.3)	NLAY PHI1 PHI2 ... PHIN T where NLAY is the number of layers, PH1 to PHIN are, for each layer, the values of the fiber skew angle referenced to the element Ox axis, T is the shell thickness.

Remark

Degrees-of-freedom θ_X and θ_Y are expressed in local axis. For each node, if V_3 is the vector normal to the element, X, Y and Z are the directions of the global axis, θ_X is the rotation around the direction $V_1 = Y \otimes V_3$ and θ_Y the rotation around the direction $V_2 = V_3 \otimes V_1$. If V_3 and Y are parallel, θ_X is the rotation around the direction $V_1 = X \otimes V_3$ and θ_Y the rotation around the direction $V_2 = V_3 \otimes V_1$.

Example

GEOMETRY

2 = 4 30. -30. 30. -30. 0.01

…

…

ELEMENTS

SHEL08C PLC3 2

6 1 8 3 4 7 2 5

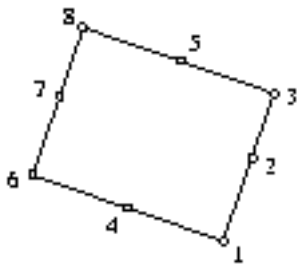

4.3.6 QUAD08C

Description

The QUAD08C element is an eight-node isoparametric element used to model composite materials in axisymmetrical analysis. The formulation of this element relies on the Halpin and Tsai model. Ox is the axis of symmetry. The shell can be doubly curved.

Active degrees-of-freedom

U_x, and U_y (2 translations).

Topology

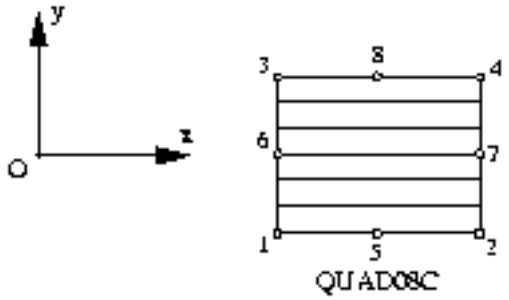

QUAD08C

Parameters

MATERIALS entry parameters	GEOMETRY entry parameters
Fiber and matrix characteristics. See the detailed description of the MATERIALS entry, (chap. 3.3)	NLAY PHI1 PHI2 ... PHIN where NLAY is the number of layers, PH1 to PHIN are, for each layer, the values of the fiber skew angle referenced to the element Oz axis.

Remark

Local axes (directions 1-2, 1-3, and global Oz) of all 2D elements must form either a uniquely direct or a uniquely inverted system. ATILA **does not** detect inconsistent axes.

Example

```
GEOMETRY
2 = 4  30. -30. 30. -30.
…
…
ELEMENTS
 QUAD08C   PLC3   2
  6  1  8  3  4  7  2  5
```

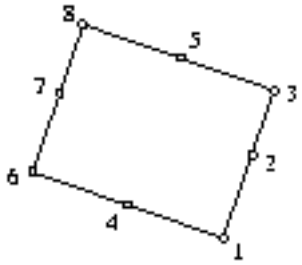

4.3.7 HEXA20E, PRIS15E, PYRA13E, TETR10E

Description

These isoparametric elements are used to model isotropic elastic materials, with or without material losses.

Active degrees-of-freedom

U_X, U_Y, and U_Z, (3 translations).

Topologies

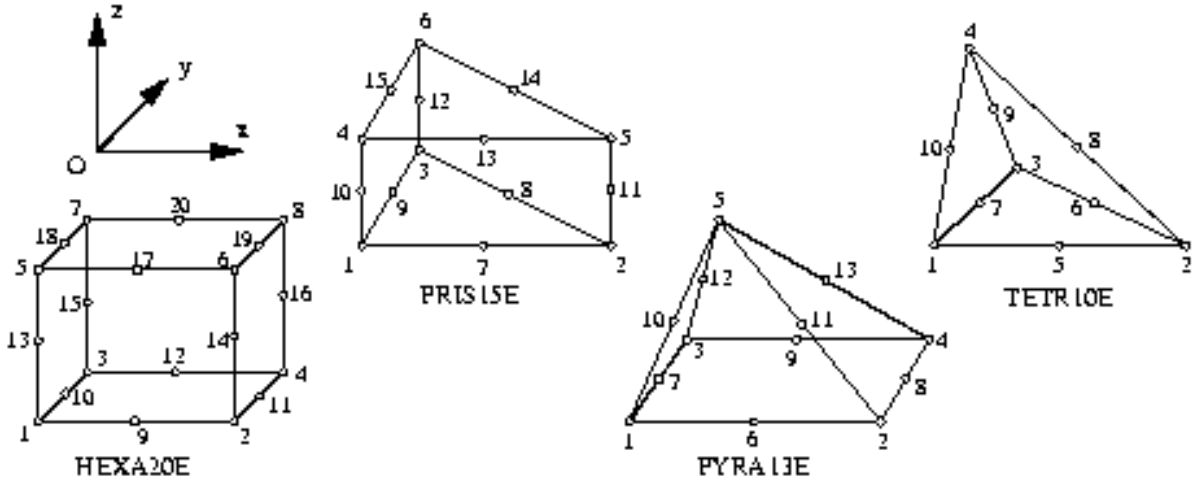

Parameters

MATERIALS entry parameters	GEOMETRY entry parameters
These correspond, depending upon the case, to an isotropic elastic material, with or without material losses (chap. 3.3)	Not required.

Remark

Local axes (directions 1-2, 1-3, and 1-5 for HEXA20E and PYRA13E, directions 1-2, 1-3 and 1-4 for PRIS15E and TETR10E) should form a direct system. ATILA detects inverted elements and renumbers them automatically.

Example

```
ELEMENTS
 HEXA20E   AU4G
  1  3  6  8  13  15  18  20  2  4  5  7  9  10  11  12  14  16  17  19
```

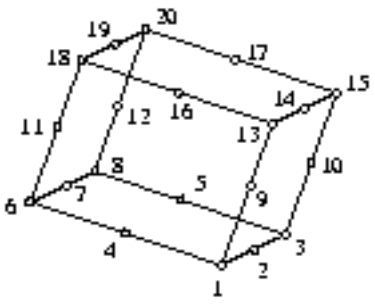

4.3.8 PLAT08E, PLAT06E

Description

These flat plate elements are used to model isotropic elastic materials with or without material losses. They rely on the classical Love-Kirchhoff hypotheses and **must be flat**.

Active degrees-of-freedom

U_Z, θ_X, and θ_Y (1 translation, 2 rotations).

Topologies

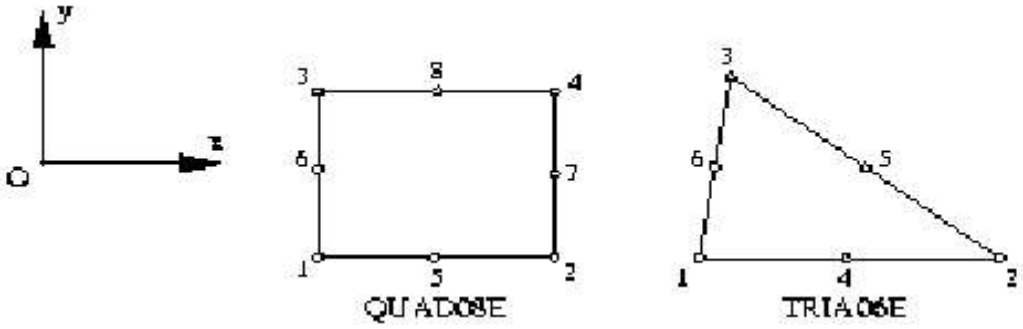

Parameters

MATERIALS entry parameters	GEOMETRY entry parameters
These correspond, depending upon the case, to an isotropic elastic material, with or without material losses (chap. 3.3)	T where T is the plate thickness

.

Remarks

The longitudinal and lateral dimensions of the plate must be at least ten times the thickness.

These elements can be superimposed on the QUAD08E or TRIA06E elements (plane-stress condition) to generate a plane element that enables the facet modeling of shells (see FACE08E).

Local axes must be defined (chap. 3.3)so that the x and y directions for the degrees of freedom of each node of the element are the local x and y directions of the element.

Example

```
GEOMETRY =   10 = 0.065   * Thickness
…
…
ELEMENTS
 PLAT08E   AU4G  10
  6  1  8  3  4  7  2  5
```

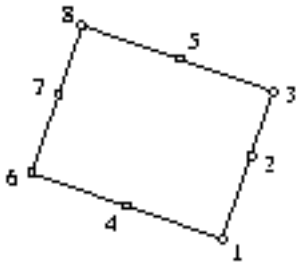

4.3.9 FACE08E

Description

The FACE08E element is an eight-node quadrilateral thin shell element, used for homogeneous isotropic elastic materials, with or without material losses. It is plane and enables the facet modeling of shells. It relies on the classical Love-Kirchhoff hypotheses and **must be flat** (facet).

Active degrees-of-freedom

U_x, U_y, U_x, θ_x, and θ_y (3 translations, 2 rotations).

Topology

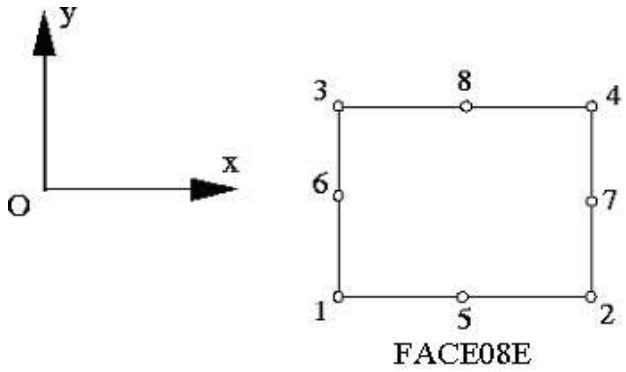

FACE08E

Parameters

MATERIALS entry parameters	GEOMETRY entry parameters
These correspond, depending upon the case, to an isotropic elastic material, with or without material losses (chap. 3.3)	T where T is the shell thickness.

Remarks

The longitudinal and lateral dimensions of the shell must be at least ten times the thickness.

This element is equivalent to the superposition of the QUAD08E element (plane-stress condition) and the PLAT08E element.

Local axes must be defined (chap. 3.3)so that the x and y directions for the degrees of freedom of each node of the element are the local x and y directions of the element.

Example

```
GEOMETRY =   10 = 0.065   * Thickness
…
…
ELEMENTS
 FACE08E   AU4G  10
  6  1  8  3  4  7  2  5
```

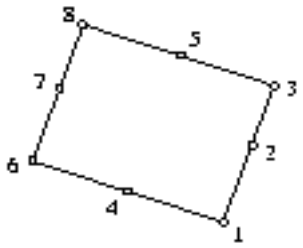

4.3.10 SPRI02E

Description

The SPRI02E element is a two-node linear spring element, which is only able to transmit to its two limiting nodes a restoring force due to a change of its length. The spring constitutive material may or may not include material losses. Its classical use is the modeling of prestress rods.

Active degrees-of-freedom

U_X, U_Y, and U_Z (3 translations).

Topology

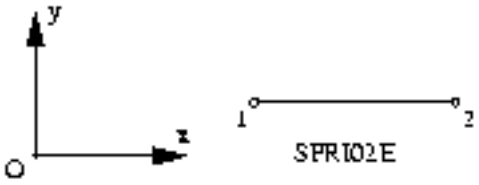

Parameters

MATERIALS entry parameters	GEOMETRY entry parameters
These correspond, depending upon the case, to an isotropic elastic material, with or without material losses (chap. 3.3)	S where S is the cross section area of the rod.

Remarks

In three-dimensional models, the section S must be divided by the number of symmetry planes + 1. In axisymmetrical models, the section S must be divided by 2.

This element is nothing more than a classical spring with mass. Use of this element can lead to spurious but real modes in a modal or harmonic analysis. These "rod" modes can be shifted without effect on the other results, by artificially dividing the rod density by 100, for example, to multiply their resonance frequencies by 10.

Care should be taken about lateral displacements, as there is no stiffness associated to them. The common rule is either to block them or to make them equal to their neighbouring elements.

Example

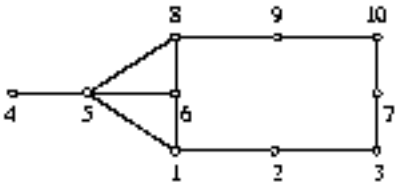


```
GEOMETRY
   1 = 0.0005   * Section 1
   2 = 0.0015   * Section 2
…
ELEMENTS
 SPRI02E   STEEL  2  =  4  5  *  The rod

 SPRI02E   STEEL  1  =  5  1  /  5  6  /  5  8  *  The "umbrella"

QUAD08E   STEEL
   1  3  8  10  2  6  7  9
…
END
 4   2   6   *  Same Oy displacement as that of node 6
 5   2   6   *  Idem
```

4.3.11 QUAD08E, TRIA06E

Description

These isotropic elements are used to model isotropic elastic materials with or without material losses. They can be used for plane-stress, plane-strain or axisymmetrical analyses. For axisymmetrical problems, the global Ox axis is the axis of symmetry.

Active degrees-of-freedom

U_x, and U_y (2 translations).

Topologies

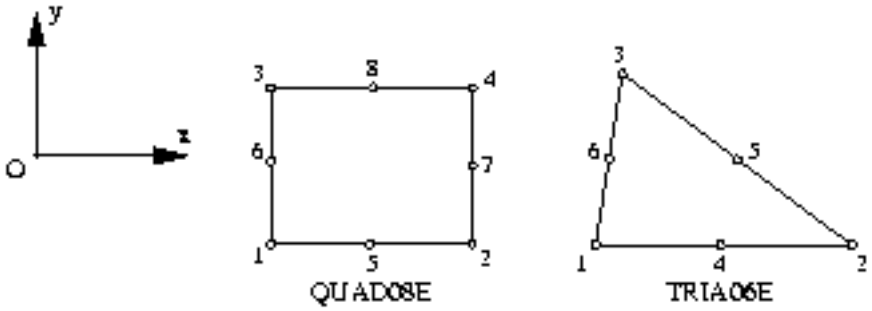

Parameters

MATERIALS entry parameters	GEOMETRY entry parameters
These correspond, depending upon the case, to an isotropic elastic material, with or without material losses (chap. 3.3)	T where T is the thickness of the element. Not required and ignored for plane-strain or axisymmetrical analyses.

Remark

Local axes (directions 1-2, 1-3, and global Oz) of all 2D elements must form either a uniquely direct or a uniquely inverted system. ATILA **does not** detect inconsistent axes.

Example

```
CLASS PLSTRESS
GEOMETRY =   10 = 0.065   * Thickness
…
…
ELEMENTS
 QUAD08E   AU4G  10
  6  1  8  3  4  7  2  5
```

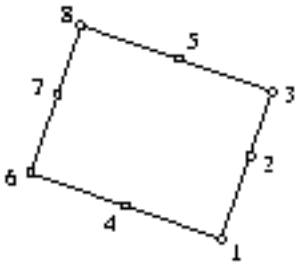

4.3.12 SHEL03E

Description

The SHEL03E element is a three-node axisymmetrical thin shell element, with or without material losses, the formulation of which takes account of its double curvature. It relies on the classical Love-Kirchhoff hypotheses. The global Ox axis is the symmetry axis.

Active degrees-of-freedom

U_x, U_y, and θ_z (2 translations, 1 rotation).

Topology

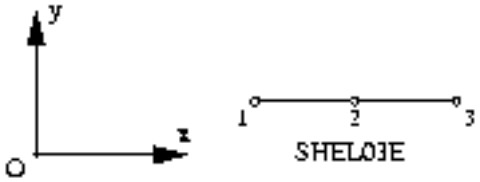

Parameters

MATERIALS entry parameters	GEOMETRY entry parameters
These correspond, depending upon the case, to an isotropic elastic material, with or without material losses (chap. 3.3)	T R where T is the thickness of the element and R its radius of curvature.

Remarks

If R is null, the element is assumed to be straight.

The y ordinate of a shell point must be positive.

The numbering of the element nodes must be generated in ascending order of x: X(N1) .LE. X(N2) .LE. X(N3)

The longitudinal and radial dimensions of the shell must be at least ten times the thickness.

Example

```
GEOMETRY
  4 = 0.065  0.7 * Thickness + radius
  5 = 0.065  0.9 * Thickness + radius
…
…
ELEMENTS
 SHEL03E   AU4G  5
   25  23  22

 SHEL03E   AU4G  4
   16  19  25
```

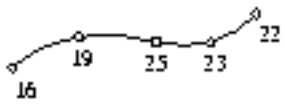

4.3.13 HEXA20ES, PRIS15ES, PYRA13ES, TETR10ES

Description

These isoparametric elements are used to model electrostrictive materials.

Active degrees-of-freedom

U_X, U_Y, U_Z , and Φ (3 translations, 1 electrical potential).

Topology

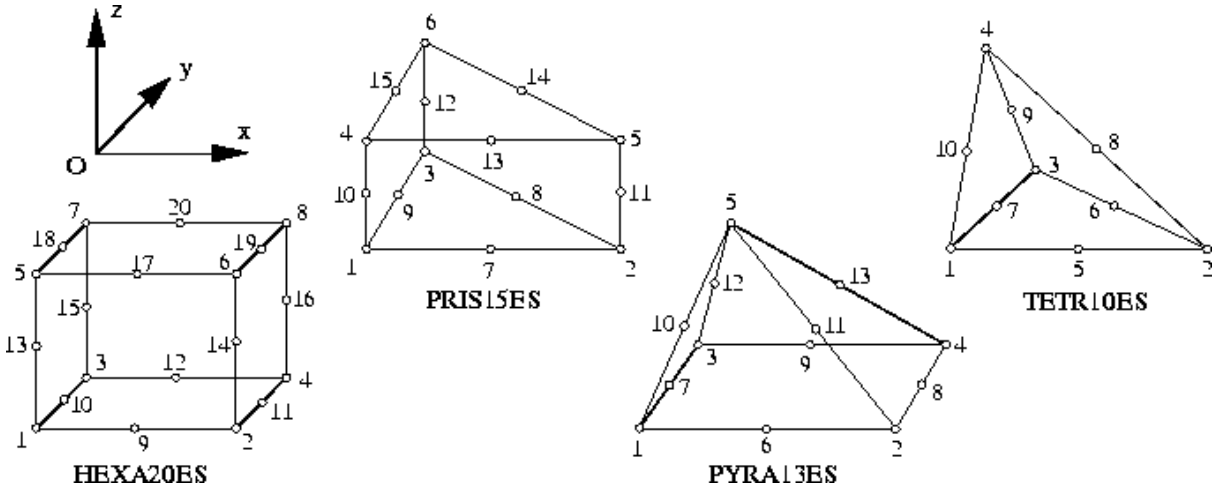

Parameters

MATERIALS entry parameters	GEOMETRY entry parameters
The elastic, electrostrictive, dielectric tensors, and the density (see the detailed description of the MATERIALS entry in Chapter 3.3.22).	Not required

Remarks

The STRESS command is required when using these elements.

Example

```
GEOMETRY POLARIZATION CARTESIAN
 1 = 0. 0. 0. *
…
ELEMENTS
 HEXA20ES PMN 1
  1 3 6 8 13 15 18 20 2 4 5 7 9 10 11 12 14 16 17 19
```

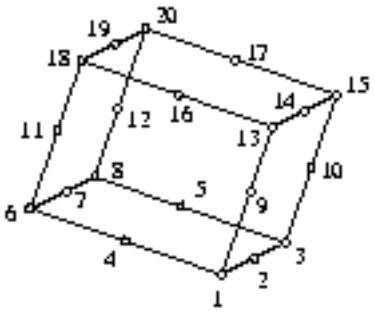

4.3.14 QUAD08ES, TRIA06ES

Description

These isoparametric elements are designed to model any electrostrictive material. They can be used for plane-strain or axisymmetrical analyses.

Active degrees-of-freedom

U_X, U_Y, and Φ (2 translations, 1 electrical potential).

Topology

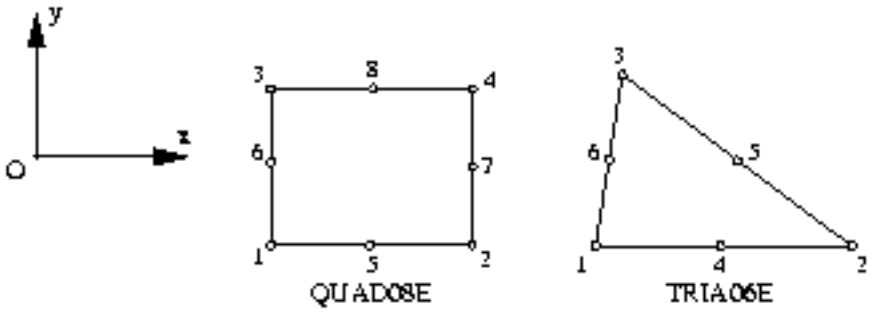

Parameters

MATERIALS entry parameters	GEOMETRY entry parameters
The elastic, electrostrictive, dielectric tensors, and the density (see the detailed description of the MATERIALS entry in Chapter 3.3.22).	Not required

Remarks

The STRESS command is required when using these elements.

Example

```
GEOMETRY POLARIZATION CARTESIAN
 1 = 0. 0. 0.
…
ELEMENTS
 QUAD08P  PMN  1
  6  1  8  3  4  7  2  5
```

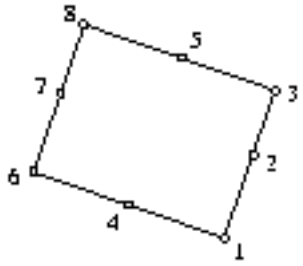

4.3.15 HEXA20F, PRIS15F, PYRA13F, TETR10F

Description

These isoparametric elements are used to model homogeneous fluid media, with or without losses.

Active degrees-of-freedom

The pressure P.

Topology

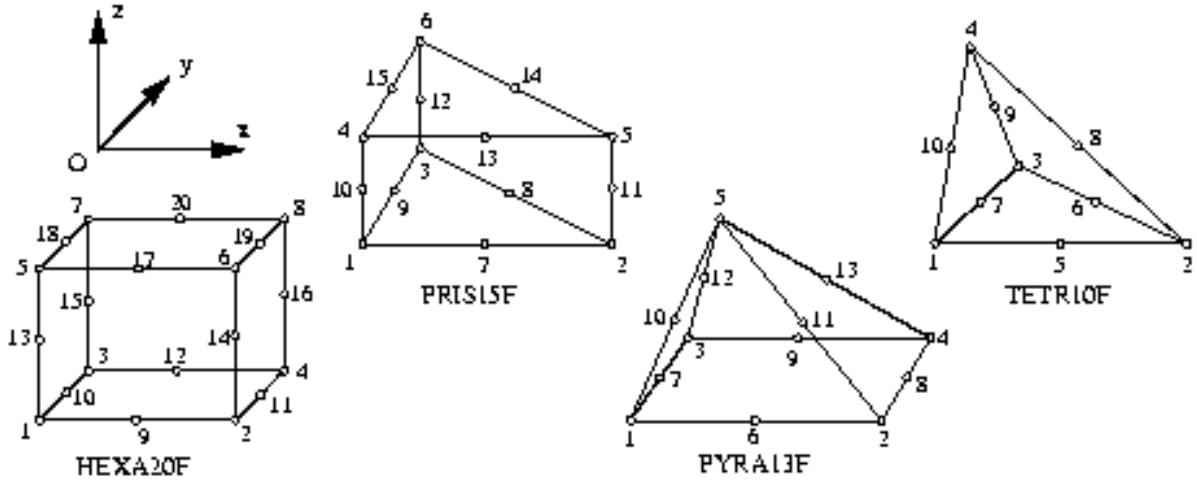

Parameters

MATERIALS entry parameters	GEOMETRY entry parameters
These correspond, depending upon the case, to a fluid, with or without material losses (chap. 3.3)	Not required.

Remark

Local axes (directions 1-2, 1-3, and 1-5 for HEXA20F and PYRA13F, directions 1-2, 1-3 and 1-4 for PRIS15F and TETR10F) should form a direct system. ATILA detects inverted elements and renumbers them automatically.

Example

```
ELEMENTS
 HEXA20F   WATER
 1  3  6  8  13  15  18  20  2  4  5  7  9  10  11  12  14  16  17  19
```

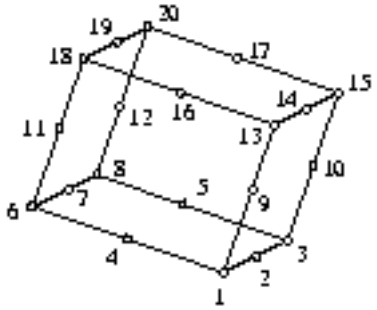

4.3.16 QUAD08F, TRIA06F

Description

These isoparametric elements are used to model homogeneous fluid media, with or without material losses. These elements can be used for plane-strain or axisymmetrical analyses.

Active degrees-of-freedom

The pressure P.

Topology

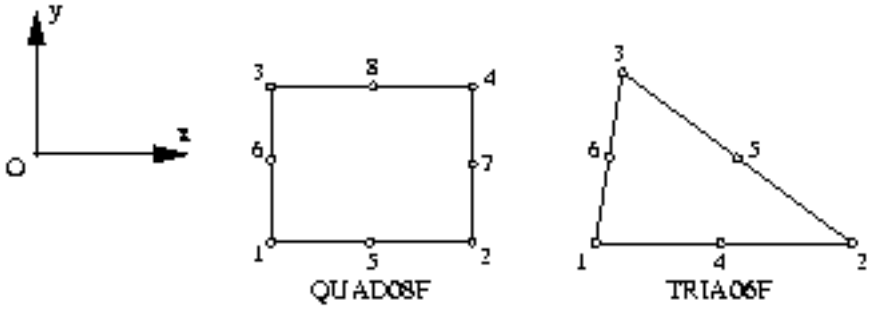

Parameters

MATERIALS entry parameters	GEOMETRY entry parameters
These correspond, depending upon the case, to a fluid, with or without material losses (chap. 3.3)	Not required.

Remark

Local axes (directions 1-2, 1-3, and global Oz) of all 2D elements must form either a uniquely direct or a uniquely inverted system. ATILA **does not** detect inconsistent axes.

Example

```
ELEMENTS
 QUAD08F   WATER
  6 1 8 3 4 7 2 5
```

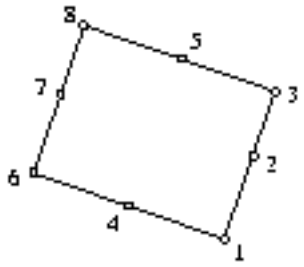

4.3.17 HEXA20G, PRIS15G, PYRA13G, TETR10G

Description

These isoparametric elements are used to model isotropic magnetic media.

Active degrees-of-freedom

The magnetic potential ϕ.

Topology

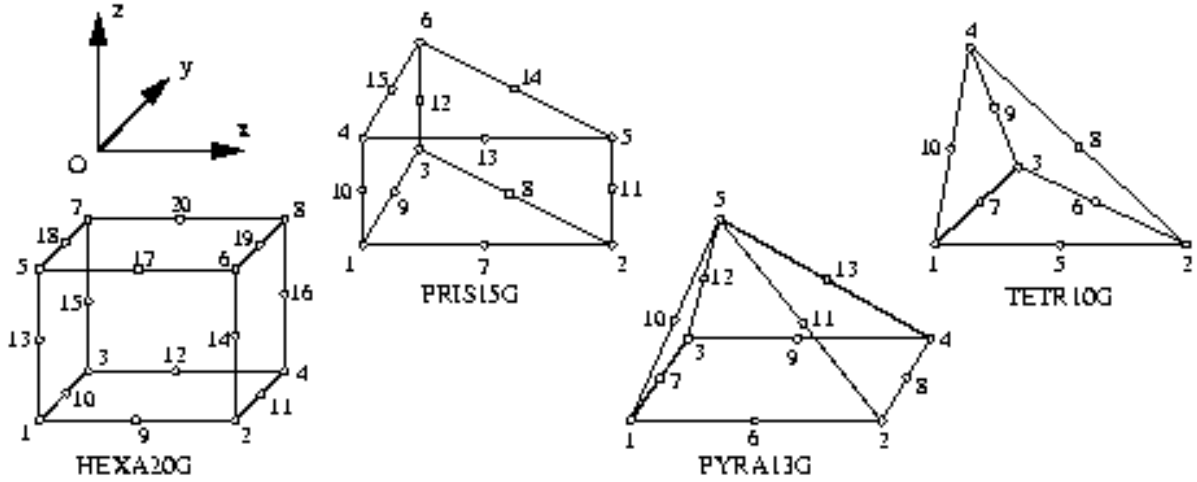

Parameters

MATERIALS entry parameters	GEOMETRY entry parameters
These correspond, depending upon the case, to an isotropic magnetic material, with or without material losses (chap. 3.3)	Not required.

Remarks

The elements may be safely superimposed to elastic and fluid elements, allowing the extent of the magnetic domain inside purely elastic parts of the structure.

Local axes (directions 1-2, 1-3, and 1-5 for HEXA20G and PYRA13G, directions 1-2, 1-3 and 1-4 for PRIS15G and TETR10G) should form a direct system. ATILA detects inverted elements and renumbers them automatically.

Example

```
ELEMENTS
 HEXA20G   VACUUM
  1  3  6  8  13  15  18  20  2  4  5  7  9  10  11  12  14  16  17  19
```

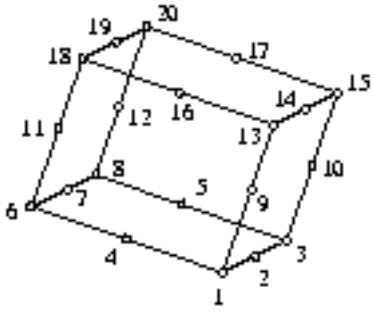

4.3.18 QUAD08G, TRIA06G

Description

These isoparametric elements are designed to model any isotropic magnetic media. These elements can be used for plane-strain or axisymmetrical analyses.

Active degrees-of-freedom

The magnetic potential ϕ.

Topology

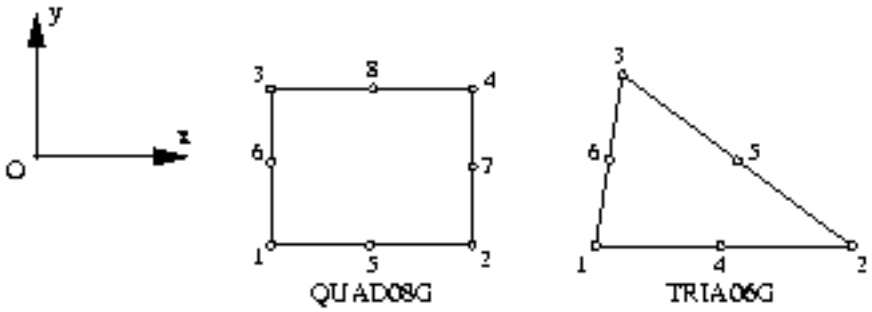

Parameters

MATERIALS entry parameters	GEOMETRY entry parameters
These correspond, depending upon the case, to an isotropic magnetic material, with or without material losses (chap. 3.3)	Not required.

Remarks

The elements may be safely superimposed to elastic and fluid elements, allowing the extent of the magnetic domain inside purely elastic parts of the structure.

Local axes (directions 1-2, 1-3, and global Oz) of all 2D elements must form either a uniquely direct or a uniquely inverted system. ATILA **does not** detect inconsistent axes.

Example

```
ELEMENTS
 QUAD08G   VACUUM
  6 1 8 3 4 7 2 5
```

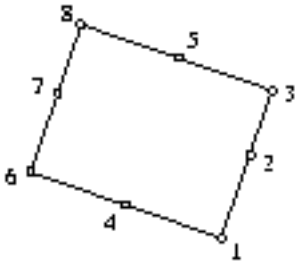

4.3.19 QUAD16I, TRIA12I

Description

These isoparametric elements are used to ensure the matching between solid and fluid meshes along their interface. An element includes 8 solid nodes and 8 fluid nodes that have the same coordinates as the solid nodes. It has no thickness.

Active degrees-of-freedom

U_X, U_Y, and U_Z for each solid node (3 translations), and P (the pressure) for each fluid node.

Topology

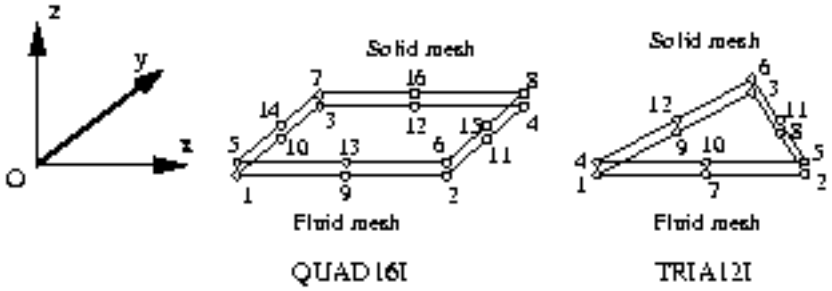

Parameters

MATERIALS entry parameters	GEOMETRY entry parameters
Not required.	Not required.

Remarks

Nodes 1, 2, 3, 4, 9, 10, 11, 12 are fluid nodes.

Nodes 5, 6, 7, 8, 13, 14, 15, 16 are solid nodes.

The local Oz axis, which is computed from local Ox (direction 1-2) and Oy (direction 1-3) axes, must be oriented from the fluid domain into the solid domain. ATILA **does not** detect inverted elements.

Example

```
ELEMENTS
 QUAD16I
  9  14  11  16  1  6  3  8  12  10  15  13  4  2  7  5
```

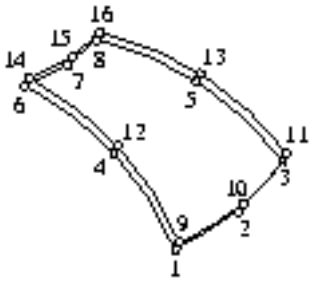

4.3.20 LINE06I

Description

The LINE06I element is a six-node isoparametric element used for plane-strain (bidimensional) or axisymmetrical analyses. It ensures the matching between solid and fluid meshes along their interface. It includes 3 solid nodes and 3 fluid nodes that have the same coordinates as the solid nodes. It has no thickness.

Active degrees-of-freedom

U_x, and U_y for each solid node (2 translations), and P (the pressure) for each fluid node.

Topology

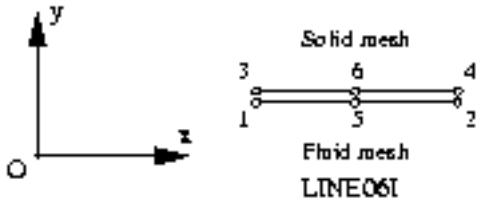

Parameters

MATERIALS entry parameters	GEOMETRY entry parameters
Not required.	Not required.

Remarks

Nodes 1, 2, 5 are fluid nodes.

Nodes 2, 3, 6 are solid nodes.

The local Oy axis, which is computed from the local Ox (direction 1-2) axis and the local Oz axis of other 2D elements, must be oriented from the fluid domain into the solid domain. ATILA **does not** detect inverted elements.

Example

```
ELEMENTS
 QUAD08E AU4G
  1 3  6  8  2 4 5 7

 LINE06I
  9 14 3 8 12 5

 QUAD08F  WATER
  9 11 14 16 10 12 13 15
```

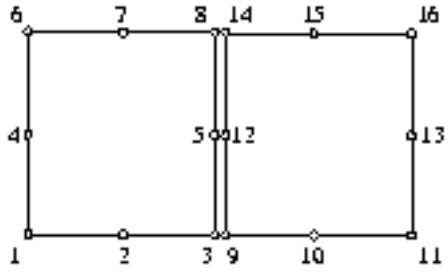

4.3.21 HEXA20M, PRIS15M, PYRA13M, TETR10M

Description

These isoparametric elements are used to model magnetostrictive materials, with or without material losses.

Active degrees-of-freedom

U_X, U_Y, U_Z and ϕ (3 translations, 1 magnetic potential).

Topology

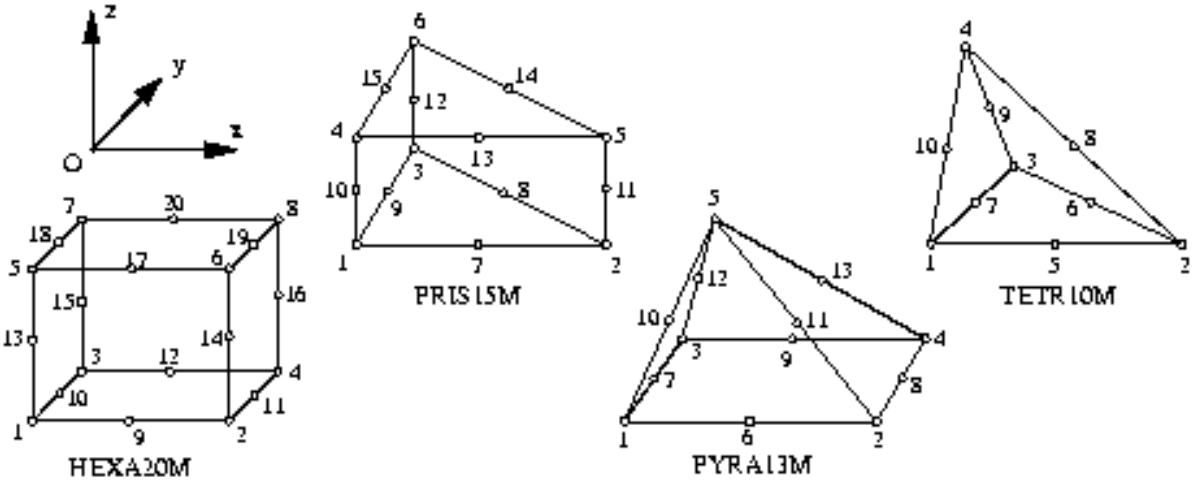

Parameters

MATERIALS entry parameters	GEOMETRY entry parameters
The elastic, piezomagnetic, magnetic tensors, and the density (see the detailed description of the MATERIALS entry in Chapter 3.3.22). These correspond, depending upon the case, to a magnetostrictive material, with or without material losses (chap. 3.3)	These are the coordinates of the O'x'y'z' system origin and the Euler angles that define the natural axes of the material with respect to the global coordinate system (see the detailed description of the GEOMETRY POLARIZATION entry, Chapter 3.3.14).

Remarks

- The GEOMETRY entry must be given in the particular form GEOMETRY POLARIZATION *[CARTESIAN, CYLINDRICAL, SPHERICAL]***.**
- Local axes (directions 1-2, 1-3, and 1-5 for HEXA20M and PYRA13M, directions 1-2, 1-3 and 1-4 for PRIS15M and TETR10M) should form a direct system. ATILA detects inverted elements and renumbers them automatically.

Example

```
GEOMETRY POLARIZATION CARTESIAN
 1 = 0. 90. 0. * Polarization along global Oz
…
ELEMENTS
 HEXA20M  TERFENOL  1
  1  3  6  8  13  15  18  20  2  4  5  7  9  10  11  12  14  16  17  19
```

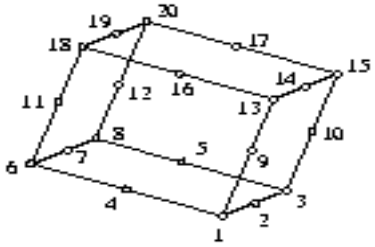

4.3.22 QUAD16M

Description

The QUAD16M element is a sixteen-node isoparametric element used to model magnetostrictive thin films, with or without material losses. Because the thickness is small compared to other dimensions, a HEXA20M element is not suitable. This element is made of two node layers having the same displacements but different magnetic potential degrees-of-freedom.

Active degrees-of-freedom

U_X, U_Y, U_Z and ϕ (3 translations, 1 magnetic potential).

Topology

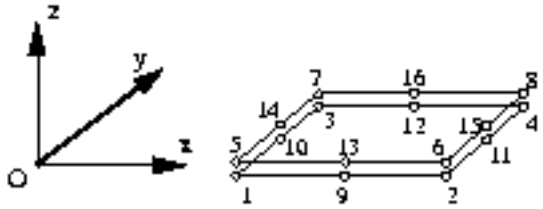

QUAD16M

Parameters

MATERIALS entry parameters	GEOMETRY entry parameters
The elastic, piezomagnetic, magnetic tensors, and the density (see the detailed description of the MATERIALS entry in Chapter 3.3.22). These correspond, depending upon the case, to a magnetostrictive material, with or without material losses (chap. 3.3)	ALPHA BETA GAMMA T These are the three Euler angles that define the natural axes of the material with respect to the global coordinate system, followed by the element thickness (see the detailed description of the GEOMETRY POLARIZATION CARTESIAN entry, (chap. 3). T is the thickness of the film.

Remarks

- The material's polarization must be CARTESIAN.

The longitudinal and lateral dimensions of the element must be at least ten times the thickness.

- On the film boundaries, the user must provide appropriate boundary conditions: the magnetic degrees of freedom of the two node layers must be set equal.

Example

```
GEOMETRY POLARIZATION CARTESIAN
 6 = 0. 0. 0. 0.0001 * polarization along global Ox
…
ELEMENTS
 QUAD16M   TERFENOL   6
  9  14  11  16  1  6  3  8  12  10  15  13  4  2  7  5
...
END
14   4   6  * Same magnetic potential
12   4   4  * on the magnetostrictive film edges
 9   4   1
```

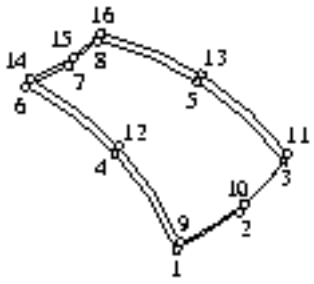

4.3.23 QUAD08M, TRIA06M

Description

These isoparametric elements are designed to model any magnetostrictive material, with or without material losses. These elements can be used for plane-strain or axisymmetrical analyses.

Active degrees-of-freedom

U_X, U_Y, and ϕ (2 translations, 1 magnetic potential).

Topology

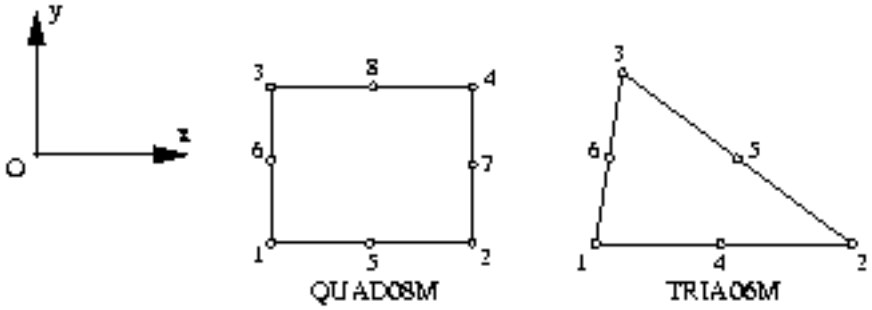

Parameters

MATERIALS entry parameters	GEOMETRY entry parameters
The elastic, piezomagnetic, magnetic tensors, and the density (see the detailed description of the MATERIALS entry in Chapter 3.3.22). These correspond, depending upon the case, to a magnetostrictive material, with or without material losses (chap. 3.3)	These are the coordinates of the O'x'y'z' system origin and the Euler angles that define the natural axes of the material with respect to the global coordinate system (see the detailed description of the GEOMETRY POLARIZATION entry, Chapter 3.3.14).

Remarks

The GEOMETRY entry must be given in the particular form GEOMETRY POLARIZATION *[CARTESIAN, CYLINDRICAL, SPHERICAL]***.**

Local axes (directions 1-2, 1-3, and global Oz) of all 2D elements must form either a uniquely direct or a uniquely inverted system. ATILA **does not** detect inconsistent axes.

Example

```
GEOMETRY POLARIZATION CARTESIAN
 1 = 90. 0. 0. * Polarization along global Oy
…
ELEMENTS
 QUAD08M  TERFENOL  1
  6 1 8 3 4 7 2 5
```

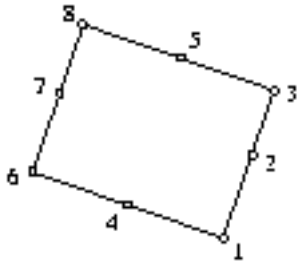

4.3.24 HEXA20P, PRIS15P, PYRA13P, TETR10P

Description

These isoparametric elements are used to model piezoelectric materials with or without material losses.

Active degrees-of-freedom

U_X, U_Y, U_Z , and Φ (3 translations, 1 electrical potential).

Topology

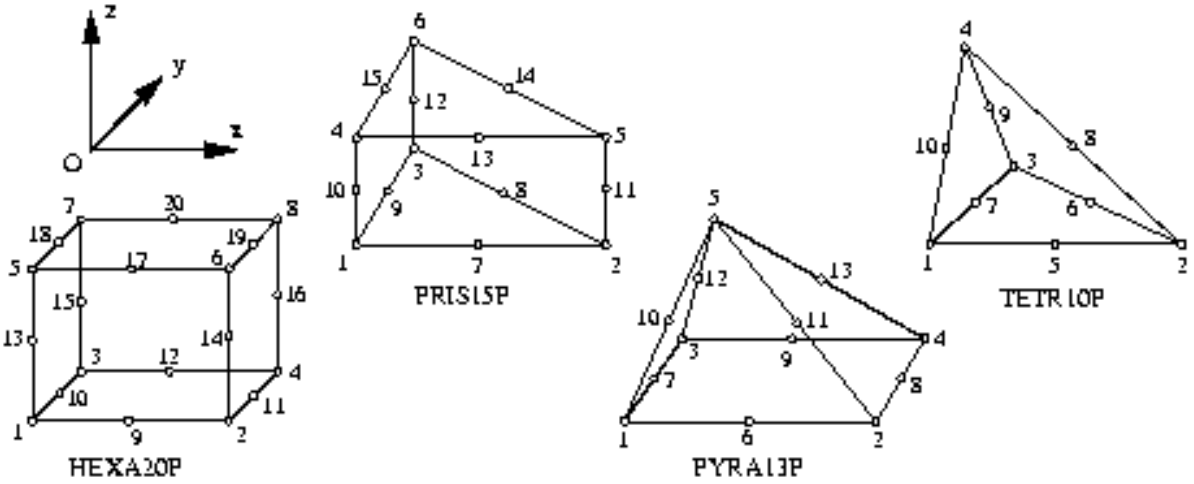

Parameters

MATERIALS entry parameters	GEOMETRY entry parameters
The elastic, piezoelectric, dielectric tensors, and the density (see the detailed description of the MATERIALS entry in Chapter 3.3.22). These correspond, depending upon the case, to an isotropic elastic material, with or without material losses (chap. 3.3)	These are the coordinates of the O'x'y'z' system origin and the Euler angles that define the natural axes of the material with respect to the global coordinate system (see the detailed description of the GEOMETRY POLARIZATION entry, Chapter 3.3.14).

Remarks

- The GEOMETRY entry must be given in the particular form GEOMETRY POLARIZATION *[CARTESIAN, CYLINDRICAL, SPHERICAL]***.**
- Local axes (directions 1-2, 1-3, and 1-5 for HEXA20P and PYRA13P, directions 1-2, 1-3 and 1-4 for PRIS15P and TETR10P) should form a direct system. ATILA detects inverted elements and renumbers them automatically.

Example

```
GEOMETRY POLARIZATION CARTESIAN
 1 = 0. 90. 0. * Polarization along global Oz
…
ELEMENTS
 HEXA20P  X51  1
  1  3  6  8  13  15  18  20  2  4  5  7  9  10  11  12  14  16  17  19
```

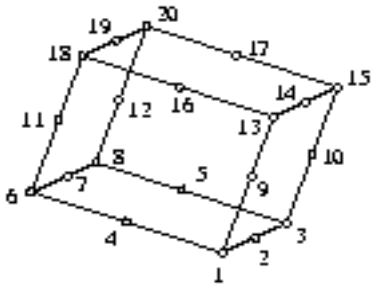

4.3.25 TRIL08P, TRIL06P (5)

Description

The TRIL08P element is an eight-node quadrilateral used to model piezoelectric trilaminars. These trilaminars are composed of a metallic core sandwiched between two plates of a piezoelectric material. The element formulation relies, for the mechanical part, on the classical Love-Kirchhoff hypotheses. The polarization and the electrical field are taken perpendicular to the plane and uniform on the piezoelectric plates.

Active degrees-of-freedom

U_Z, θ_X, θ_Y, and Φ (1 translation, 2 rotations, 1 electrical potential). In this case, the LCPPDC command must be used to reorder the degrees-of-freedom.

Topology

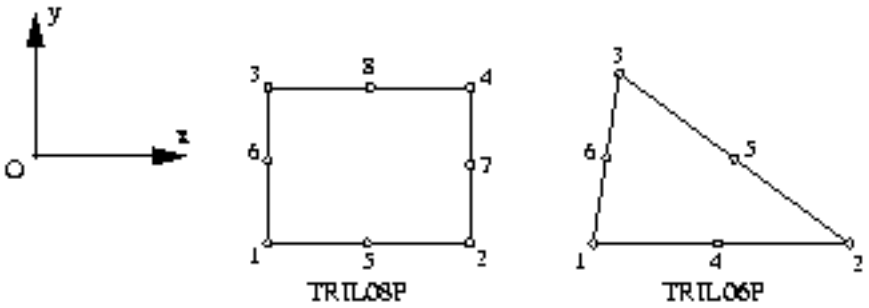

Parameters

MATERIALS entry parameters	GEOMETRY entry parameters
Young's modulus, Poisson's ratio, and density for the metallic layer, elastic, piezoelectric, dielectric tensors, and density for the piezoelectric part. (see, chap. 3.3).	TM TP where TM is the thickness of the metallic layer and TP the piezoelectric plate thickness.

Remarks

The longitudinal and lateral dimensions of the whole plate must be at least ten times the thickness.

The MATERIALS entry has a specific form because of the existence of two distinct materials (see chap.3).

Example

```
GEOMETRY =   4 = 0.065 0.003   * Thicknesses
…
…
ELEMENTS
 TRIL08P   AG5X31  4
  6  1  8  3  4  7  2  5
```

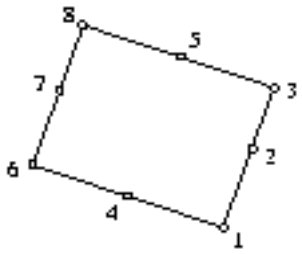

4.3.26 QUAD08P, TRIA06P

Description

These isoparametric elements are designed to model any piezoelectric material, with or without material losses. These elements can be used for plane-strain or axisymmetrical analyses.

Active degrees-of-freedom

U_X, U_Y, and Φ (2 translations, 1 electrical potential).

Topology

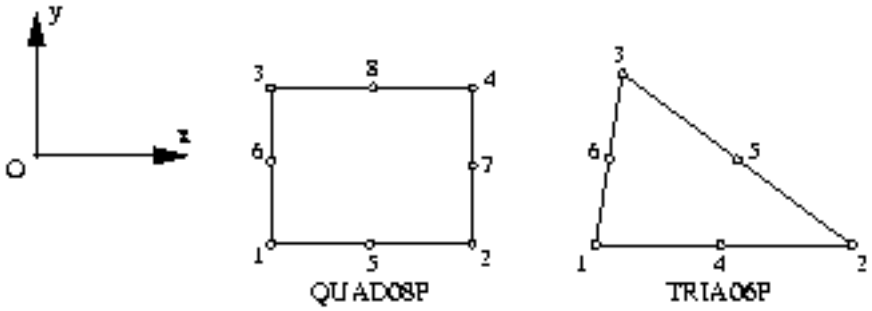

Parameters

MATERIALS entry parameters	GEOMETRY entry parameters
The elastic, piezoelectric, dielectric tensors, and the density (see the detailed description of the MATERIALS entry in Chapter 3.3.22). These correspond, depending upon the case, to an isotropic elastic material, with or without material losses (chap. 3.3)	These are the coordinates of the O'x'y'z' system origin and the Euler angles that define the natural axes of the material with respect to the global coordinate system (see the detailed description of the GEOMETRY POLARIZATION entry, Chapter 3.3.14).

Remarks

- The GEOMETRY entry must be given in the particular form GEOMETRY POLARIZATION *[CARTESIAN, CYLINDRICAL, SPHERICAL]***.**
- Local axes (directions 1-2, 1-3, and global Oz) of all 2D elements must form either a uniquely direct or a uniquely inverted system. ATILA **does not** detect inconsistent axes.

Example

```
GEOMETRY POLARIZATION CARTESIAN
 1 = 90. 0. 0. * Polarization along global Oy
…
ELEMENTS
 QUAD08P  X51  1
  6  1  8  3  4  7  2  5
```

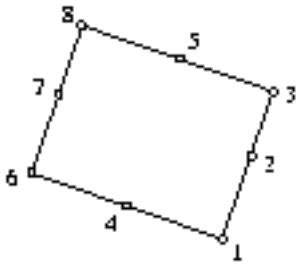

4.3.27 QUAD08R, TRIA06R

Description

These isoparametric elements are used to prescribe a monopolar or dipolar radiation condition. They are attached to the outside surface of a three-dimensional fluid mesh.

Active degrees-of-freedom

The pressure P.

Topology

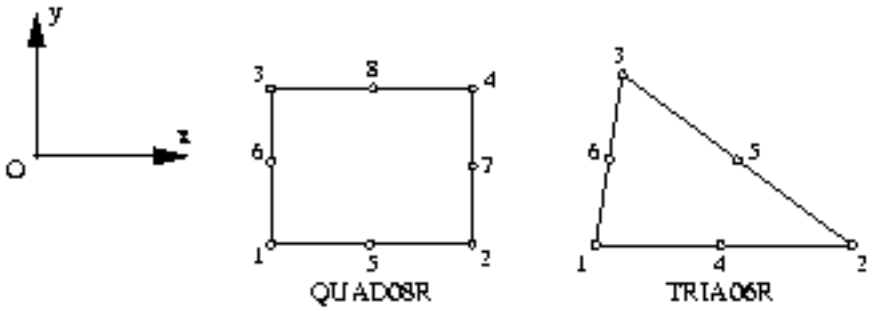

Parameters

MATERIALS entry parameters	GEOMETRY entry parameters
These correspond to a fluid, without material losses (chap. 3.3)	R where R is the element radius of curvature.

Remarks

The local Oz axis, which is computed from local 0x (direction 1-2) and Oy (direction 1-3) axes, must point away from the fluid mesh. ATILA **does not** detect inverted elements.

All radiating elements must lie on a unique spherical surface, whose center is consistent with the structure's center of radiation. This surface cannot reside in the near-field, except when the RADIATION DIPOLAR entry is provided.

ATILA **does not** check the consistency between the radius provided by the geometry entry and the element curvature. It **does not** check the presence of multiple spherical surfaces.

Example

```
GEOMETRY =   3 = 7.5  * Radius
…
…
ELEMENTS
 QUAD08R   WATER  3
  6  1  8  3  4  7  2  5
```

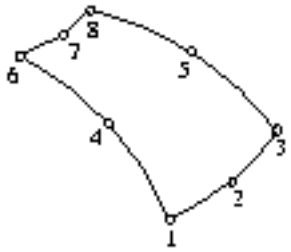

4.3.28 LINE03R

Description

The LINE03R element is a three-node isoparametric linear element used to prescribe a monopolar or dipolar radiation condition. It must be circular and attached on the outer surface of a two-dimensional fluid domain. It can be used for plane-strain and axisymmetrical analyses.

Active degrees-of-freedom

The pressure P.

Topology

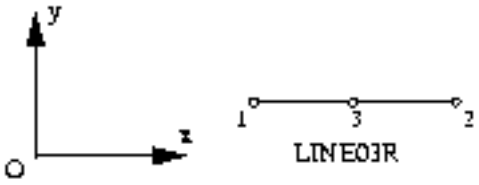

Parameters

MATERIALS entry parameters	GEOMETRY entry parameters
These correspond to a fluid, **without** material losses (chap. 3.3)	R where R is the element radius of curvature.

Remarks

- The local Oy axis, which is computed from the local Ox (direction 1-2) axis and the local Oz axis of other 2D elements, must be oriented away from the fluid domain. ATILA **does not** detect inverted elements.
- All radiating elements must lie on a unique spherical or cylindrical surface, whose center is consistent with the structure's center of radiation. This surface cannot reside in the near-field, except when the RADIATION DIPOLAR entry is provided.
- ATILA **does not** check the consistency between the radius provided by the geometry entry and the element curvature. It **does not** check the presence of multiple spherical spheres or cylinders.

Example

```
GEOMETRY =   4 = 0.75   * Radius
…
…
ELEMENTS
 LINE03R   WATER  4
   16  18  17
```

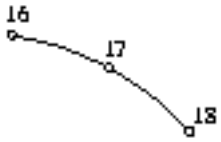

4.3.29 QUAD08Z, TRIA06Z

Description

These isoparametric elements are used to couple an **ATILA** finite-element model with a **CHIEF**-type or **EQI**-type boundary-element model, or to load a solid structure with a frequency-dependent local mechanical impedance. In the first use (BEM coupling), it is superimposed on the radiating surfaces of the mesh of the solid structure. These elements must be ordered in the file in the same way as the mutual impedance matrix described in the JOB.ZRAD file. In the second use (local impedance), the local mechanical impedance is provided by means of a fluid material's constants and a geometry number corresponding to the coefficients of a ratio of two frequency dependent polynomials.

Active degrees-of-freedom

U_X, U_Y, and U_Z (3 translations).

Topology

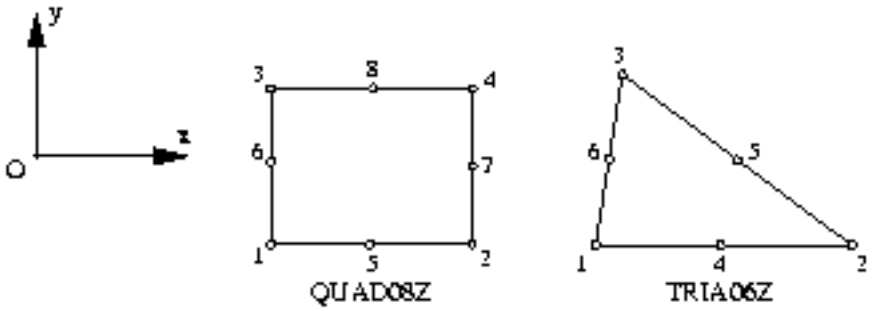

Parameters

MATERIALS entry parameters	GEOMETRY entry parameters
Not required for BEM coupling. Not used but required for local impedance.	Not required for BEM coupling. **N D** $\mathbf{C^N_{0R}}$ $\mathbf{C^N_{0I}}$ $\mathbf{C^N_{1R}}$ $\mathbf{C^N_{1I}}$ **...** $\mathbf{C^N_{(N-1)R}}$ $\mathbf{C^N_{(N-1)I}}$ **&** $\mathbf{C^D_{0R}}$ $\mathbf{C^D_{0I}}$ $\mathbf{C^D_{1R}}$ $\mathbf{C^D_{1I}}$ **...** $\mathbf{C^D_{(D-1)R}}$ $\mathbf{C^D_{(D-1)I}}$ where N and D are the number of terms in the numerator and denominator (polynomial orders minus one), $\mathbf{C^N_{iR} + j\ C^N_{iI}}$ is the complex constant of the i^{th} power of pulsation ω in the numerator and $\mathbf{C^D_{iR} + j\ C^D_{iI}}$ is the complex constant of the i^{th} power of pulsation ω in the denominator.

The local impedance Z(ω) is :

$$Z(w)=\frac{\quad}{\quad}$$

Remark

- The local Oz axis, which is computed from local 0x (direction 1-2) and Oy (direction 1-3) axes, must point away from the **ATILA** mesh.
- The local impedance is the default element behavior. The **EQI** or **CHIEF** commands (Chapter 3.3.9) set the BEM coupling behavior.
- If N ≤ 0, Z(ω) is set to 0. If D ≤ 0, the denominator of Z(ω) is set to 1.
- The geometry numbers are designed to deal with a maximum number of ten values. If more values are needed, the user must provide geometry numbers increasing by a value of more than 1, in order to leave space for extra geometry values. For example, if geometry number 3 needs 28 values, then the next used geometry number must be greater or equal to 6, that is, 3 + next_integer(28/10).

Example 1

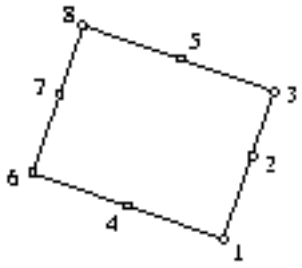


```
CHIEF
ELEMENTS
 QUAD08Z
  6 1 8 3 4 7 2 5
```

Example 2

```
GEOMETRY
 2 =  2  2  &                 *  This geometry to set Z(ω) =  ρ c
jka/(1 + jka)
     0. 0.    0. 100.  &      *  that is, the radiation impedance of a pulsating sphere
     1. 0.    0. 6.7156E-05 *  of radius = 0.1 in water.

ELEMENTS
  QUAD08Z   DUMMY   2
    6 1 8 3 4 7 2 5
```

4.3.30 LINE03Z

Description

The LINE03Z element is a three-node isoparametric element used either to couple an **ATILA** finite-element model with a **CHIEF**-type or **EQI**-type boundary element model, or to load a solid structure with a frequency-dependent local mechanical impedance. In the first use (BEM coupling), it is superimposed on the radiating surfaces of the mesh of the solid structure. These elements must be ordered in the file in the same way as the mutual impedance matrix described in the JOB.ZRAD file. In the second use (local impedance), the local mechanical impedance is provided by means of a fluid materials constants and a geometry number corresponding to the coefficients of a ratio of two frequency dependent polynomials.

Active degrees-of-freedom

U_X, and U_Y (2 translations).

Topology

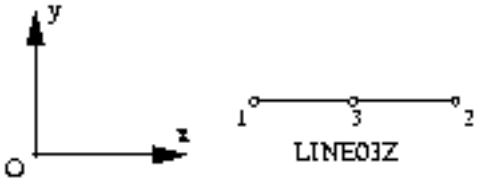

Parameters

MATERIALS entry parameters	GEOMETRY entry parameters
Not required for BEM coupling. Not used but required for local impedance.	Not required for BEM coupling. **N D** $\mathbf{C^N_{0R}}$ $\mathbf{C^N_{0I}}$ $\mathbf{C^N_{1R}}$ $\mathbf{C^N_{1I}}$ **...** $\mathbf{C^N_{(N-1)R\&}}$ $\mathbf{C^N_{(N-1)I}}$ $\mathbf{C^D_{0R}}$ $\mathbf{C^D_{0I}}$ $\mathbf{C^D_{1R}}$ $\mathbf{C^D_{1I}}$ $\mathbf{C^D_{(D-1)R}}$ $\mathbf{C^D_{(D-1)I}}$ where N and D are the number of terms in the numerator and denominator (polynomial orders minus one), $\mathbf{C^N_{iR} + j\ C^N_{iI}}$ is the complex constant of the i^{th} power of pulsation ω in the numerator and $\mathbf{C^D_{iR} + j\ C^D_{iI}}$ is the complex constant of the i^{th} power of pulsation ω in the denominator.

The local impedance Z(ω) is :

$$Z(\omega)=\frac{\left(C^n_{0\mathrm{R}}+\mathrm{j}C^n_{0\mathrm{I}}\right)+\left(C^n_{1\mathrm{R}}+\mathrm{j}C^n_{1\mathrm{I}}\right)\omega+\left(C^n_{2\mathrm{R}}+\mathrm{j}C^n_{2\mathrm{I}}\right)\omega^2+\ldots+\left(C^n_{(\mathrm{N}-1)R}+\mathrm{j}C^n_{(\mathrm{N}-1)I}\right)\omega^{\mathrm{N}-1}}{\left(C^d_{0\mathrm{R}}+\mathrm{j}C^d_{0\mathrm{I}}\right)+\left(C^d_{1\mathrm{R}}+\mathrm{j}C^d_{1\mathrm{I}}\right)\omega+\left(C^d_{2\mathrm{R}}+\mathrm{j}C^d_{2\mathrm{I}}\right)\omega^2+\ldots+\left(C^d_{(\mathrm{D}-1)R}+\mathrm{j}C^d_{(\mathrm{D}-1)I}\right)\omega^{\mathrm{D}-1}}$$

Remarks

- The local Oy axis, which is computed from the local Ox (direction 1-2) axis and the local Oz axis of other 2D elements, must be oriented away from the fluid domain. ATILA **does not** detect inverted elements.
- The local impedance is the default element behavior. The **EQI** or **CHIEF** commands (Chapter 3.3.9) set the BEM coupling behavior.
- If N ≤ 0, Z(ω) is set to 0. If D ≤ 0, the denominator of Z(ω) is set to 1.
- The geometry numbers are designed to deal with a maximum number of ten values. If more values are needed, the user must provide geometry numbers increasing by a value of more than 1, in order to leave space for extra geometry values.

For example, if geometry number 3 needs 28 values, then the next used geometry number must be greater or equal to 6, that is, 3 + next_integer(28/10).

Example 1

```
CHIEF
ELEMENTS
 QUAD08E   AU4G
  9  11  4  6  10  7  8  5

 LINE03Z
  4  6  5
```

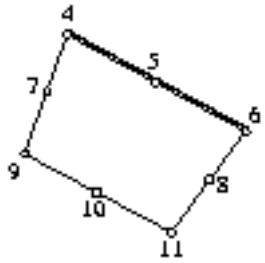

Example 2

```
GEOMETRY
 2 =  2  2  &                 *  This geometry to set Z(ω) =  ρ c  jka/(1 + jka)
    0. 0.    0. 100.  &       *  that is, the radiation impedance of a pulsating sphere
    1. 0.    0. 6.7156E-05 *  of radius = 0.1 in water.

ELEMENTS
 LINE03Z   DUMMY   2
   4  6  5
```

4.3.31 QUAD08CV, TRIA06CV

Description

These isoparametric elements are used to prescribe convection condition on the outer surface of a three-dimensional elastic and piezoelectric domain. It can be used in any harmonic analyses.

Active degrees-of-freedom

The temperature T.

Topology

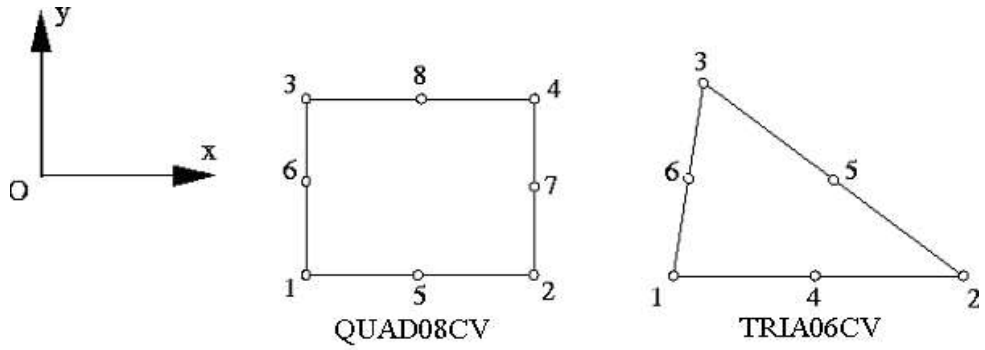

Parameters

MATERIALS entry parameters	**GEOMETRY entry parameters**
These correspond to a dummy material with zero values.	**H** T_∞ where H is the convective thermal film coefficient (W/(m^2-C°) and T_∞ is the quiescent temperature (C°)

Example

MATERIAL

DUMMY = 0. 0. 0.

GEOMETRY = 1 = 10. 20. * H AND T_∞

ELEMENTS QUAD08CV DUMMY 1 6 1 8 3 4 7 2 5

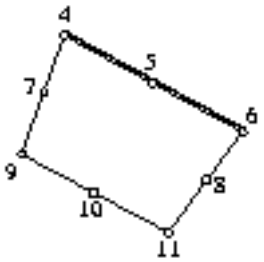

4.3.32 LIN03CV

Description

This isoparametric elements are used to prescribe convection condition on the outer surface of a two-dimensional elastic and piezoelectric domain. It can be used in any harmonic plane-strain, plane stress and axisymmetrical analyses.

Active degrees-of-freedom

The temperature T.

Topology

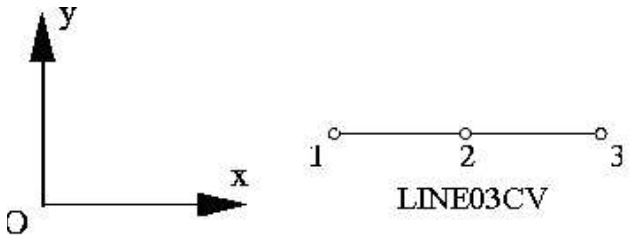

Parameters

MATERIALS entry parameters	GEOMETRY entry parameters
These correspond to a dummy material with zero values.	**H** T_∞ where H is the convective thermal film coefficient (W/(m^2-C°) and T_∞ is the quiescent temperature (C°).

Example

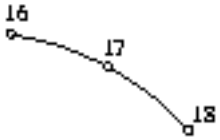

GEOMETRY 4 = 10. 20. * Thickness + radius

…

…

ELEMENTS LINE03CV DUMMY 4 16 25 19 LINE03CV
DUMMY 4 16 18 17

5 PRE-PROCESSING AND NON GRAPHIC PROCEDURES

5.1 Introduction

ATILA can provide several different types of numerical output:

The user can create an **ATILA** data file from a file describing "super-elements" and instructions on how to divide them. This finite-element mesh generator, named **MOSAIQUE**, is a non-graphic preprocessor of the **ATILA** code that generates all the necessary element and node data for **ATILA**. A super-element can be a one-dimensional, two-dimensional or three-dimensional element. It is possible to assign different types of elements (triangle, quadrilateral, hexahedron, prism) to a super-element.

The user can display properties of the materials stored in the materials database (**CPIEZO** program). He or she can create lossy piezoelectric or magnetostrictive materials from non-lossy ones, by specifying loss factors on the three main constants blocks (**MPIEZO** program). He or she can check that a piezoelectric or magnetostrictive material is effectively lossy (dissipating, not absorbing heat) (**PPIEZO** program).

After running a solver, the user can output the displacements for a selected frequency, time or loading case, exactly as the output of the solver when the **PRINTING** level is set to 1 or more. He or she can also output the displacement for several specific nodes and degrees of freedom for all frequencies, times or loading cases. These actions are driven by the **ATLIST** program.

For active structures, in case the parallel impedance file (***.RPCP** file) is accidentally deleted or corrupted, the user does not need to rerun the job. Because all valuable data is saved in the **.SY4 file, this impedance file can be recreated with the TRPCP program. Alternatively, if the symmetries detected by the solver are incorrect, the user can force the symmetry factor with the help of the TRPCP2 program. When the structure is magnetostrictive, it is preferable to deal with series impedance. The TRSLS program is thus useful to regenerate a series impedance file (.RSLS** file).

For active and/or radiating structures, in case the directivity patterns file (***.PAT** file) is accidentally deleted or corrupted, the user does not need to rerun his job. Because all valuable data is saved in the ***.SY4** file, this directivity patterns file can be recreated with the **TDIP2** program (2D structures, extrapolation method) or the **TMONO** program (when the fluid dampers stand in the far field).

When dealing with modal analysis of periodic materials, some useful information may be extracted from raw data: dispersion curves can be deduced from the different wavenumbers and associated frequencies by careful ordering (**CDISP** program); the phase speed and mean polarization of each wavenumber and associated frequencies can be calculated (program **CELEPO** program); from the low-frequency (long wavelength) limit of longitudinal and transversal waves, a set of equivalent orthotropic material constants can be extracted (**HOMOGN** program).

element Mesh generator: MOSAIQUE

MOSAIQUE is a preprocessor of the **ATILA** code. It is an automatic finite-element mesh generator program that helps in building complex meshes. From the description of the mesh using "super-elements", and instructions on how to divide them, **MOSAIQUE** generates all the necessary element and node data for **ATILA**. A super-element can be a one-dimensional, two-dimensional or three-dimensional element. It is possible to assign different types of elements (triangle, quadrilateral, hexahedron, prism) to a super-element.

Data for **MOSAIQUE** is provided by an input file, generally of extension **MOS**, written by the user. This file has the same characteristics as an **ATILA** data file: same header type, same entries, equivalent boundary conditions, thus the user may refer to the Sections I.3 and I.4 for entries reference. Compared to an **ATILA** data file, the **ELEMENTS** entry defines "super-elements" instead of regular elements. A super-element entry is a regular element entry completed with element's division information. So, almost all entries are duplicated to the resulting output file, except the **NODES** and **ELEMENTS** entries that reflect the elements divisions, as new nodes and elements are created. When necessary, node numbers in entries are changed to reflect the node generation. The output file is named with an .**ATI** extension and is directly usable by the graphics pre-processor **MDES** or by the solver **GA**. A listing file (.**LST**) is also output, which enables the user to rapidly check and validate the generation.

The entries used for the automatic mesh generation that are specific to **MOSAIQUE** are described below:

NAMEL$_1$ MATER$_1$ NUMGEO$_1$
N$_{11}$ N$_{12}$ N$_{13}$ ... N$_{1P}$
-1 ITYP NN NM NL NK IBIAIS
[XP1 XP2 ... XPNN] IF IBIAIS = 1
[YP1 YP2 ... YPNM] IF IBIAIS = 1 AND NM NOT NULL
[ZP1 ZP2 ... ZPNL] IF IBIAIS = 1 AND NL NOT NULL
[TP1 TP2 ... TPNK] IF IBIAIS = 1 AND NK NOT NULL
BLANK LINE
...
...
NAMEL$_N$ MATER$_N$ NUMGEO$_N$
N$_{11}$ N$_{12}$ N$_{13}$ ... N$_{1Q}$
-1 ITYP NN NM NL NK IBIAIS
[XP1 XP2 ... XPNN] IF IBIAIS = 1
[YP1 YP2 ... YPNM] IF IBIAIS = 1 AND NM NOT NULL
[ZP1 ZP2 ... ZPNL] IF IBIAIS = 1 AND NL NOT NULL
[TP1 TP2 ... TPNK] IF IBIAIS = 1 AND NK NOT NULL
BLANK LINE
BLANK LINE

This entry enables the user to introduce the super-element topology in accordance with the rules of Chapter I.4. The -1 after the element topology triggers the super-element supplemental information. If one or several super-element sides are straight, the middle nodes can be omitted. The maximal value of NN, NM, NL, or NK is 40.

MATER and NUMGEO are given or not. They depend upon the element type used and they are specified in the element directives. They refer to the MATERIALS and GEOMETRY entries (or GEOMETRY POLARIZATION).

In generation mode, the line following the topology description starts with -1 and gives the splitting rules. If there is no such line, the super-element is considered as a simple element. On this line, ITYP refers to a given super-element frame (see Section ?.?); NN, NM, NL and NK give the number of generated elements along the natural axes of the super-element; and

IBIAIS is a control integer that must be equal to 0 if the splitting along each axis is regular and 1 if the splitting along at least one axis is irregular. If IBIAIS is equal to 0, the four lines that are devoted to the description of the splitting must not appear. If IBIAIS is equal to 1, these one to four lines must be provided, even if one or two of them correspond to a regular splitting.
XP1, XP2,... XPI,...,XPNN are integers defining the splitting along the natural Ox axis of the super-element. The corresponding side is divided into NN different parts, the lengths of which are, respectively, equal to: XP1/XL, XP2/XL,..., XPI/XL,..., XPNN/XL, with XL=XP1+XP2+...+XPNN. XPI is always an integer.
A blank line indicates the end of a super-element data input. A blank line is necessary to terminate the ELEMENT entries.

5.2.2 Merge

XMERGE

This entry allows the user to change the merge point value that is, for each element, the ratio of the tolerance circle diameter to the shortest distance between two nodes. Default is XMERGE = 1.E-01

5.2.3 Nogen

This entry suppresses automatic mesh generation by disabling the division of super-elements. This is useful for visualizing the super-elements. Mid-side nodes will be generated for each super-element. Thus, the node numbering will be changed from the element entry.

5.2.4 SORTfluid

NCA

This entry enables the user to organize the fluid-structure meshes so as to place the radiating nodes at the end of the array.
NCA is the node number of the acoustic center. By default, the acoustic center is at the origin of the global system. Therefore, this entry is not required.

5.2.5 Super-element types (Available values of ITYP)

In the following library description, the super-element shape is represented by a thick line, while the generated elements are represented by a thin line.

5.2.5.1 ITYP = 1: Linear 1D elements

Two-node linear element generation (element SPRI02E). Control integers NM, NL, NK are null.

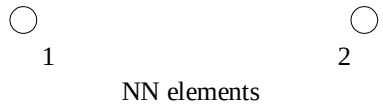

5.2.5.2 ITYP = 2: Quadratic 1D elements

Three-node quadratic element generation (element LINE03R). Super-node 3 is needed only if the super-element is to be curved. Control integers NM, NL, NK are null. This super-element is used to generate damping elements.

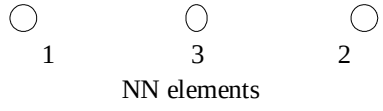

5.2.5.3 ITYP = 3: 6-node interface elements

Six-node fluid-structure interface element generation (element LINE06I). Only the solid super-nodes are specified, that is, **only two or three nodes must be given**; all generated nodes are doubled to realize the fluid-structure interface. Super-node 3 is needed only if the super-element is to be curved. Control integers NM, NL, NK are null. The orientation of the element is automatically inverted by the **MOSAIQUE** program to get the orientation required in the **ATILA** code.

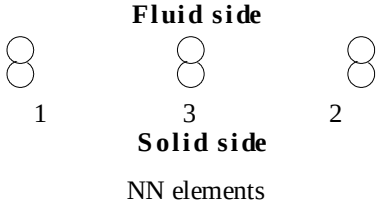

5.2.5.4 ITYP = 4: Quadrilateral elements in a quadrilateral super-element

This super-element enables the user to generate 8-node elements (QUAD-type geometry).
The topology is always read on 8 nodes. Mid-side super-nodes (5-8) are required only for those super-element edges that are to be curved. Special attention must be given to the data entry format in this case; one or more zero-valued place holders may be required (see Chapter I.4). NN, NM, respectively, define the number of elements on the 1-2, 1-3 sides. Control integers NL, NK are null.

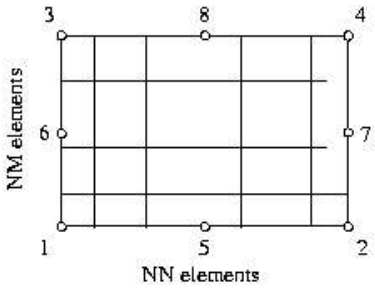

5.2.5.5 ITYP = 5: Triangular elements in a quadrilateral super-element

This super-element enables the user to generate 6-node elements. Due to the super-element shape, the element entry in the **. MOS** file must refer to an element of QUAD-type geometry. The topology is always read on 20 nodes. Mid-side super-nodes (5-8) are required only for those super-element edges that are to be curved.
Special attention must be given to the data entry format in this case; one or more zero-valued place holders may be required (see Chapter I.4). NN, NM, respectively, define the number of elements on the 1-2, 1-3 sides. Control integers NL, NK are null.

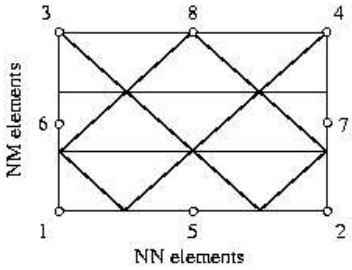

5.2.5.6 ITYP = 6: Triangular elements in a triangular super-element

This super-element enables the user to generate 6-node elements (TRIA-type geometry). The topology is always read on 6 nodes. Mid-side super-nodes (4-6) are required only for those super-element edges that are to be curved. Special attention must be given to the data entry format in this case; one or more zero-valued place holders may be required (see Chapter I.4). NN, NM, respectively, define the number of elements on sides 1-2 and 1-3. **NM must be equal to NN.** Control integers NL, NK are null. An irregular splitting can be applied for this super-element, provided that splitting along the sides 1-2 and 1-3 are similar **but in reverse order**, i.e.: 1 2 4 and 4 2 1. Any other irregular splititng will lead to unpredictable meshes.

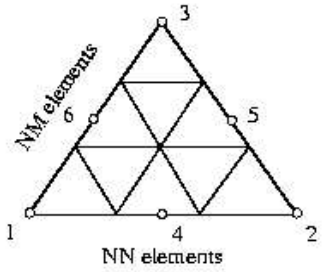

5.2.5.7 ITYP = 7: Triangular and quadrilateral elements in a triangular super-element

This super-element enables the user to generate 6-node (TRIA-type geometry) and 8-node elements (QUAD-type geometry). The topology is always read on 6 nodes. Mid-side super-nodes (4-6) are required only for those super-element edges that are to be curved. Special attention must be given to the data entry format in this case; one or more zero-valued place holders may be required (see Chapter I.4). NN, NM define the number of elements on side 1-2 and 1-3, respectively. If IBIAIS=1, the spacing has to be indicated on the following line.

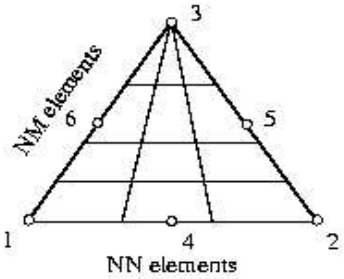

5.2.5.8 ITYP = 8: 3-D triangular interface element

This super-element is similar to element type 7. All generated nodes are doubled to build the fluid-structure interface (element TRIA12I).

5.2.5.9 ITYP = 9: 3-D quadrilateral interface elements

This super-element is similar to element type 4. All generated nodes are doubled to build the fluid-structure interface (element QUAD16I).

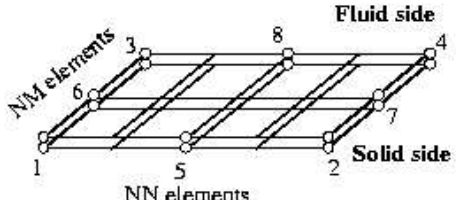

5.2.5.10 ITYP = 10: Hexahedron elements in an hexahedron

This super-element enables the user to generate 20-node elements (HEXA-type geometry). The topology is always read on 20 nodes. Mid-side super-nodes are only required for those super-element edges which are to be curved. Special attention must be given to the data entry format in this case; one or more zero-valued place holders may be required (see Chapter I.4). NN is the number of elements on side 1-2, NM is the number of elements on side 1-3 and NL is the number of elements on side 1-5. If IBIAIS=1, the spacing has to be indicated first for side 1-2, then for side 1-3 and finally for side 1-5.

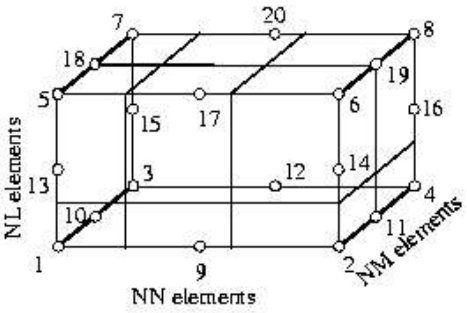

5.2.5.11 ITYP = 11: Prismatic elements in a triangular base prism

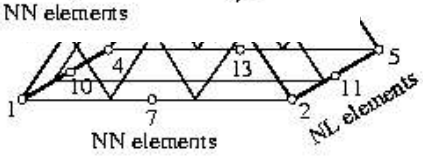

This super-element enables the user to generate 15-node prismatic elements (PRIS-type geometry). The topology is always read on 15 nodes. Mid-side super-nodes are required only for those super-element edges that are to be curved. Special attention must be given to the data entry format in this case; one or more zero-valued place holders may be required (see Chapter I.4). NN is the number of elements on side 1-2, NM is the number of elements on side 1-3 and NL is the number of elements on side 1-4. An irregular spacing can be applied for this super-element, provided that spacing along the sides 1-2 and 1-3 are similar **but in reverse order**, i.e.: 1 2 4 and 4 2 1. Any other irregular spacing will lead to unpredictable meshes.

5.2.5.12 ITYP = 12: Triangular base prismatic elements in a hexahedron

This super-element enables the user to generate 15-node elements in a cube. Due to the super-element shape, the element entry in the file **JOB.MOS** must refer to an element of HEXA-type geometry. The topology is always read on 20 nodes. Mid-side super-nodes are required only for those super-element edges that are to be curved. Special attention must be given to the data entry format in this case; one or more zero-valued place holders may be required (see Chapter I.4). NN is the number of elements on side 1-2, NM is the number of elements on side 1-3 and NL is the number of elements on side 1-5. If IBIAIS=1, the spacing has to be indicated first for side 1-2, then for side 1-3 and finally for side 1-5.

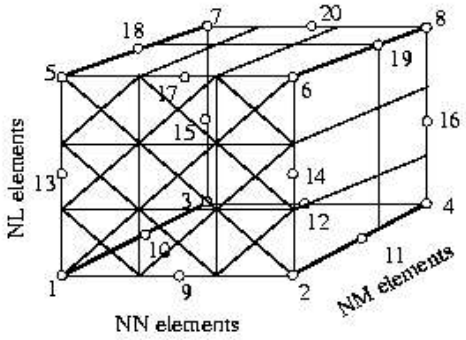

5.2.5.13 ITYP = 13: Hexahedron and pyramid elements in a pyramid

This super-element enables the user to generate 13-node (PYRA-type geometry) and 20-node (HEXA-type geometry) elements. The topology is always read on 13 nodes. Mid-side super-nodes are required only for those super-element edges that are to be curved. Special attention must be given to the data entry format in this case; one or more zero-valued place holders may be required (see Chapter I.4). NN is the number of elements on side 1-2, NM is the number of elements on side 1-3 and NL is the number of elements on side 1-5. If IBIAIS=1, the spacing has to be indicated first for side 1-2, then for side 1-3 and finally for side 1-5.

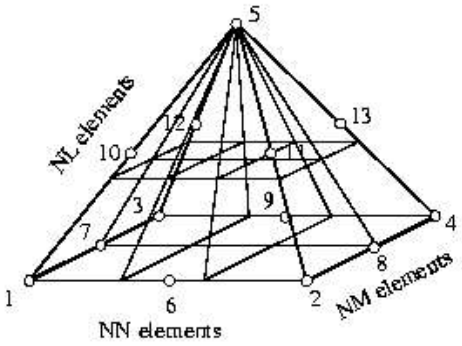

5.2.5.14 ITYP = 14: Shell element

This super-element enables the user to generate 3-node shell elements (element SHEL03E). It is used in the same way as the type 2 super-element. Only the node numbering is different in the output file.

5.2.5.15 ITYP = 15: Triangular base prismatic elements in a prism

This super-element enables the user to generate 15-node (PRIS-type geometry) and 20-node (HEXA-type geometry) elements. The topology is always read on 15 nodes. Mid-side super-nodes are required only for those super-element edges that are to be curved. Special attention must be given to the data entry format in this case; one or more zero-valued place holders may be required (see Chapter I.4). NN is the number of elements on side 1-2, NM is the number of elements on side 1-3 and NL is the number of elements on side 1-4. If IBIAIS=1, the spacing has to be indicated first for side 1-2, then for side 1-3 and finally for side 1-4.

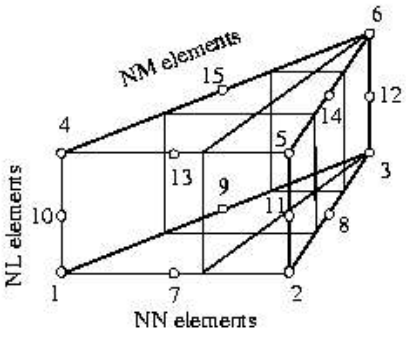

5.2.5.16 ITYP = 16: Triangular and quadrilateral elements in a quadrilateral super-element

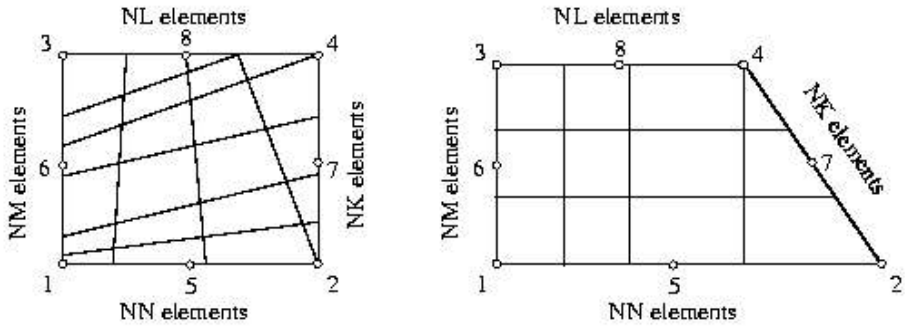

This super-element enables the user to generate 6- and 8-node elements. (TRIA- and QUAD-type geometries). Due to the super-element shape, the element entry in the **.MOS** file must refer to an element of QUAD-type geometry. The topology is always read on 8 nodes. Mid-side super-nodes are required only for those super-element edges that are to be curved. Special attention must be given to the data entry format in this case; one or more zero-valued place holders may be required (see Chapter I.4). NN, NM, NL, NK respectively define the number of elements on the 1-2, 1-3, 3-4 and 2-4. If IBIAIS=1, the spacing has to be indicated in this order.

5.2.5.17 ITYP = 17: Triangular and quadrilateral thin-film magnetostrictive elements in a quadrilateral super-element

This super-element enables the user to generate 12- and 16-node thin film magnetostrictive elements. (TRIA- and QUAD-type geometry). It is equivalent to the type 16 super-element, except that it generates twice as many nodes to build the double layer needed by such elements.

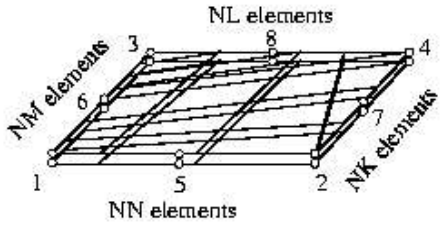

5.2.6 Technical information: Node and element Generation method

ATILA node and element generation is based upon the division, or splitting of triangular or quadrilateral super-elements in 2-D, and cubic or prismatic super-elements in 3-D. The super-element sides or edges are defined by two or three points. Linear or quadratic interpolation is used for the generation. Attention must be paid to the super-element orientation that defines the orientation of the generated elements.

For **ATILA** node coordinate generation, each super-element, defined in the global Oxyz axis system is first transformed into a local O'rst system, in which it is represented by a regular figure. Inside this reduced super-element, the different node coordinates are generated in the local system, according to the number of elements to generate, their spacing (regular or irregular) on each side, and their type. The generated node coordinates are then transformed into global coordinates using the same types of shape functions as those of the **ATILA** code. After all node and all element generation, the redundant nodes are eliminated (except the fluid-structure interface nodes). Two nodes are assumed identical if they are inside the same tolerance circle. In this case, the last one is eliminated and the node numbering is readjusted in the topology.

5.3 Dealing with materials properties: CPIEZO, MPIEZO, PPIEZO

With the help of the **CPIEZO** tool, the user can display properties of the materials stored in his materials database. It is not a complete tool, but it can help for simple cases. In any case, the values provided by the MATERIAL entry in the data file are the best place to look. Depending on the number of properties, a given material is defined as elastic, fluid or piezoelectric/magnetostrictive.

The syntax of the command is:

cpiezo MAT

where MAT is the material's name.

For an elastic material, the longitudinal and transverse speeds are displayed.

For a fluid material, the longitudinal speed is displayed.

For a piezoelectric (magnetostrictive) material, it is assumed that the material belongs to the crystalline class 6mm. The constants s^E, s^D, c^E, c^D, d, g, h, e, ε^S, ε^T; β^S and β^T (s^H, s^B, c^H, c^B, d, g, h, e, μ^S, μ^T; χ^S and χ^T) and the coupling factors k_{33}, k_{13}, k_{15}, and k^T are displayed.

The user can create lossy piezoelectric or magnetostrictive materials from non-lossy ones, by specifying loss factors on the three main constants blocks (**MPIEZO** program).

The user can check that a piezoelectric or magnetostrictive material is effectively lossy (dissipating, not absorbing heat) (**PPIEZO** program).

5.4 Listing nodes displacements: ATLIST

After running a solver, the user can output the displacements for a selected frequency, time or loading case, exactly as the output of the solver when the **PRINTING** level is set to 1 or more. He or she can also output the displacement for several specific nodes and degrees of freedom for all frequencies, times or loading cases. These actions are driven by the **ATLIST** program.

5.5 Re-generating the impedance file: TRPCP, TRPCP2, TRSLS

For active structures, in case the parallel impedance file (**.RPCP** file) is accidentally deleted or corrupted, the user does not need to rerun the job. Because all valuable data is saved in the **.SY4** file, this impedance file can be recreated with the **TRPCP** program. Alternatively, if the symmetries detected by the solver are incorrect, the user can force the symmetry factor with the help of the **TRPCP2** program. When the structure is magnetostrictive, it is preferable to deal with series impedance. The **TRSLS** program is thus useful to regenerate a series impedance file (.**RSLS** file).

5.6 Re-generating the directivity patterns file: tdip2, TMONO

For active and/or radiating structures, in case the directivity patterns file (.**PAT** file) is accidentally deleted or corrupted, the user does not need to rerun the job. Because all valuable data is saved in the **.SY4** file, this directivity patterns file can be recreated with the **TDIP2** program (2D structures, extrapolation method) or **TMONO** program (when the fluid dampers stand in the far field).

5.7 Dealing with periodic materials: CDISP, CELEPO, HOMOGN

When dealing with modal analysis of periodic materials, some useful information may be extracted from raw data: dispersion curves can be deduced from the different wavenumbers and associated frequencies by careful ordering (**CDISP** program); the phase speed and mean polarization of each wavenumber and associated frequencies can be calculated (**CELEPO** program); from the low-frequency limit of longitudinal and transversal waves, a set of equivalent orthotropic material constants can be extracted (**HOMOGN** program).

6 ATILA Example

6.1 Introduction

This chapter describes a data file for **ATILA**, as well as the results file. Section 6.2.1 contains the input data file and section 6.2.2 contains the **ATILA** output file. The selected example is an in-water harmonic analysis of an axisymmetrical, radiating Tonpilz transducer. This example was used in Chapter 3 to describe the input data format. Some comments have been added to the files to aid in understanding the different steps.
A table listing all of the test examples provided with **ATILA** is given in section 6.2.3.

6.2 Example

This example presents a harmonic analysis of a radiating Tonpilz transducer.

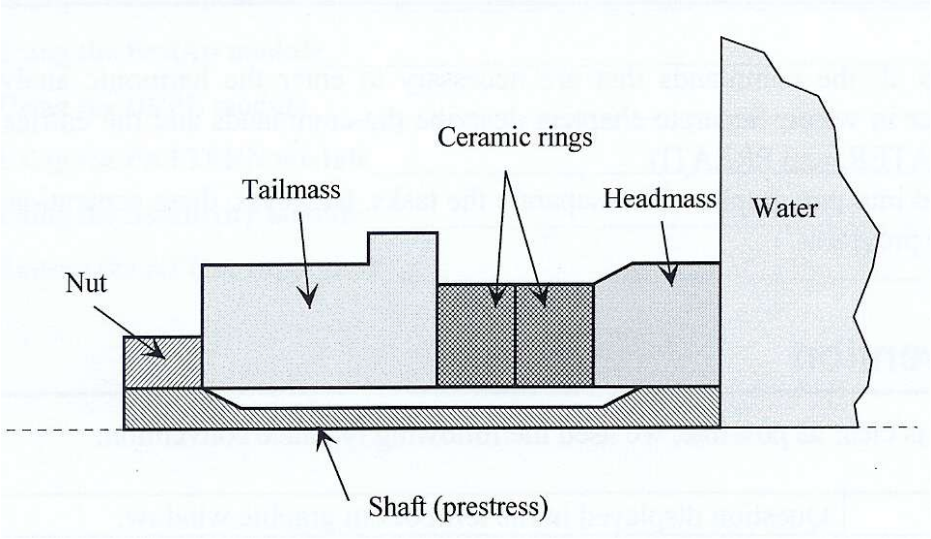

6.3 Datafile

```
*==================================== has04.ati ========
*====>   HAS04     TSTATI.   2005/06/02  Version: 6.0.0.
* TRANSDUCER   40KHZ
================================================
   CERAMICS = X9
*   HEADMASS AU4G
*   TAILMASS STEEL
*   IN WATER HARMONIC ANALYSIS
*   MONOPOLAR RADIATION
*================================================
PRINTING = 0
CLASS  AXISYMMET
GENERATE PST
RADIATION MONOPOLAR
ANALYSIS HARMONIC
HEAT LOAD
LOSSES
MATERIAL
25CD4D  * Material 25CD4D is a 25CD4  steel whose density has been divided by 10 to avoid
spurious resonances of the rod
  .215E+12 0.33 750. 0.0   0.0   0.0&
0.858E+03 0.46E02 0.46E+02 0.46E02  0.0   0.0
DUMMY  * A dummy material with zero values for the convective element
0.0  0.0  0.0  0.0  0.0  0.0
FREQUENCY
  0.250E+05  0.350E+05  0.450E+05        0.550E+05
GEOMETRY
    1
  0.560E-01       * Radius of curvature of the sphere limiting the fluid domain.
    2
   10.  15.       * The surrounding media temperature  and the convective thermal film
coefficient

GEOMETRY  POLARIZA CARTESIA  * 2 and 3 correspond to an alternate poling of the ceramics.
    3
  0.000E+00  0.000E+00  0.000E+00  0.000E+00  0.000E+00  0.000E+00  0.000E+00
    4
  0.180E+03  0.000E+00  0.000E+00  0.000E+00  0.000E+00  0.000E+00  0.000E+00

EXCITATIONS
     80 ELECPOT    500. * 500. Volt applied to the excitation electrode.

SCALE = 0.001000 0.001000 0.001000
NODES
1 * -3.300000e+001 6.000000e+000 0.000000e+000
2 * -3.300000e+001 1.800000e+001 0.000000e+000
3 * -3.900000e+001 1.800000e+001 0.000000e+000
4 * -3.900000e+001 6.000000e+000 0.000000e+000
5 * -3.300000e+001 1.200000e+001 0.000000e+000
6 * -3.600000e+001 1.800000e+001 0.000000e+000
7 * -3.900000e+001 1.200000e+001 0.000000e+000
8 * -3.600000e+001 6.000000e+000 0.000000e+000
9 * -3.300000e+001 2.000000e+001 0.000000e+000
10 * -3.900000e+001 2.000000e+001 0.000000e+000
11 * -3.300000e+001 1.900000e+001 0.000000e+000
12 * -3.600000e+001 2.000000e+001 0.000000e+000
13 * -3.900000e+001 1.900000e+001 0.000000e+000
14 * -3.300000e+001 2.300000e+001 0.000000e+000
15 * -3.900000e+001 2.300000e+001 0.000000e+000
16 * -3.300000e+001 2.150000e+001 0.000000e+000
17 * -3.600000e+001 2.300000e+001 0.000000e+000
18 * -3.900000e+001 2.150000e+001 0.000000e+000
19 * -5.500000e+001 1.000000e+001 0.000000e+000
20 * -6.400000e+001 1.000000e+001 0.000000e+000
21 * -6.400000e+001 6.000000e+000 0.000000e+000
```

```
22 * -5.500000e+001 6.000000e+000 0.000000e+000
23 * -5.950000e+001 1.000000e+001 0.000000e+000
24 * -6.400000e+001 8.000000e+000 0.000000e+000
25 * -5.950000e+001 6.000000e+000 0.000000e+000
26 * -5.500000e+001 8.000000e+000 0.000000e+000
27 * -6.400000e+001 0.000000e+000 0.000000e+000
28 * -5.500000e+001 0.000000e+000 0.000000e+000
29 * -5.950000e+001 0.000000e+000 0.000000e+000
30 * -5.500000e+001 3.000000e+000 0.000000e+000
31 * -6.400000e+001 3.000000e+000 0.000000e+000
32 * -5.000000e+001 0.000000e+000 0.000000e+000
33 * -5.000000e+001 4.000000e+000 0.000000e+000
34 * -5.250000e+001 0.000000e+000 0.000000e+000
35 * -5.000000e+001 2.000000e+000 0.000000e+000
36 * -5.250000e+001 5.000000e+000 0.000000e+000
37 * -3.150000e+001 4.000000e+000 0.000000e+000
38 * -3.150000e+001 0.000000e+000 0.000000e+000
39 * -1.300000e+001 0.000000e+000 0.000000e+000
40 * -1.300000e+001 4.000000e+000 0.000000e+000
41 * -3.150000e+001 2.000000e+000 0.000000e+000
42 * -2.225000e+001 0.000000e+000 0.000000e+000
43 * -1.300000e+001 2.000000e+000 0.000000e+000
44 * -2.225000e+001 4.000000e+000 0.000000e+000
45 * -4.075000e+001 0.000000e+000 0.000000e+000
46 * -4.075000e+001 4.000000e+000 0.000000e+000
47 * -5.500000e+001 2.000000e+001 0.000000e+000
48 * -4.700000e+001 1.400000e+001 0.000000e+000
49 * -4.700000e+001 2.000000e+001 0.000000e+000
50 * -5.500000e+001 1.500000e+001 0.000000e+000
51 * -5.100000e+001 1.200000e+001 0.000000e+000
52 * -4.700000e+001 1.700000e+001 0.000000e+000
53 * -5.100000e+001 2.000000e+001 0.000000e+000
54 * -4.700000e+001 6.000000e+000 0.000000e+000
55 * -5.100000e+001 6.000000e+000 0.000000e+000
56 * -4.700000e+001 1.000000e+001 0.000000e+000
57 * -4.300000e+001 2.000000e+001 0.000000e+000
58 * -4.300000e+001 1.600000e+001 0.000000e+000
59 * -4.300000e+001 6.000000e+000 0.000000e+000
60 * 0.000000e+000 0.000000e+000 0.000000e+000
61 * 0.000000e+000 1.000000e+001 0.000000e+000
62 * -8.000000e+000 6.000000e+000 0.000000e+000
63 * -8.000000e+000 0.000000e+000 0.000000e+000
64 * 0.000000e+000 5.000000e+000 0.000000e+000
65 * -4.000000e+000 8.000000e+000 0.000000e+000
66 * -8.000000e+000 3.000000e+000 0.000000e+000
67 * -4.000000e+000 0.000000e+000 0.000000e+000
68 * -1.050000e+001 5.000000e+000 0.000000e+000
69 * -1.050000e+001 0.000000e+000 0.000000e+000
70 * -8.000000e+000 2.000000e+001 0.000000e+000
71 * 0.000000e+000 2.000000e+001 0.000000e+000
72 * -8.000000e+000 1.300000e+001 0.000000e+000
73 * 0.000000e+000 1.500000e+001 0.000000e+000
74 * -4.000000e+000 2.000000e+001 0.000000e+000
75 * -1.300000e+001 1.800000e+001 0.000000e+000
76 * -1.300000e+001 6.000000e+000 0.000000e+000
77 * -1.050000e+001 1.900000e+001 0.000000e+000
78 * -1.300000e+001 1.200000e+001 0.000000e+000
79 * -1.050000e+001 6.000000e+000 0.000000e+000
80 * -2.300000e+001 1.800000e+001 0.000000e+000
81 * -2.300000e+001 6.000000e+000 0.000000e+000
82 * -1.800000e+001 1.800000e+001 0.000000e+000
83 * -2.300000e+001 1.200000e+001 0.000000e+000
84 * -1.800000e+001 6.000000e+000 0.000000e+000
85 * -2.800000e+001 1.800000e+001 0.000000e+000
86 * -2.800000e+001 6.000000e+000 0.000000e+000
87 * 0.000000e+000 4.875000e+001 0.000000e+000
88 * 1.155020e+001 4.768120e+001 0.000000e+000
89 * 5.816880e+000 4.847340e+001 0.000000e+000
```

90 * 1.232930e+001 5.116030e+001 0.000000e+000
91 * 0.000000e+000 5.237500e+001 0.000000e+000
92 * 0.000000e+000 4.150000e+001 0.000000e+000
93 * 9.545270e+000 4.050400e+001 0.000000e+000
94 * 4.761540e+000 4.119170e+001 0.000000e+000
95 * 1.059240e+001 4.411450e+001 0.000000e+000
96 * 0.000000e+000 4.512500e+001 0.000000e+000
97 * 0.000000e+000 3.425000e+001 0.000000e+000
98 * 7.540360e+000 3.332680e+001 0.000000e+000
99 * 3.706210e+000 3.390990e+001 0.000000e+000
100 * 8.498160e+000 3.689350e+001 0.000000e+000
101 * 0.000000e+000 3.787500e+001 0.000000e+000
102 * 0.000000e+000 2.700000e+001 0.000000e+000
103 * 6.250000e+000 2.650000e+001 0.000000e+000
104 * 3.125000e+000 2.675000e+001 0.000000e+000
105 * 6.761200e+000 2.984770e+001 0.000000e+000
106 * 0.000000e+000 3.062500e+001 0.000000e+000
107 * 2.217800e+001 4.451690e+001 0.000000e+000
108 * 1.698130e+001 4.637440e+001 0.000000e+000
109 * 2.370190e+001 4.747670e+001 0.000000e+000
110 * 1.874840e+001 3.805570e+001 0.000000e+000
111 * 1.420030e+001 3.945950e+001 0.000000e+000
112 * 2.050140e+001 4.134050e+001 0.000000e+000
113 * 1.531890e+001 3.159450e+001 0.000000e+000
114 * 1.141920e+001 3.254460e+001 0.000000e+000
115 * 1.699550e+001 3.477090e+001 0.000000e+000
116 * 1.250000e+001 2.600000e+001 0.000000e+000
117 * 9.375000e+000 2.625000e+001 0.000000e+000
118 * 1.379490e+001 2.863470e+001 0.000000e+000
119 * 3.162910e+001 3.915400e+001 0.000000e+000
120 * 2.707600e+001 4.210580e+001 0.000000e+000
121 * 3.375360e+001 4.128510e+001 0.000000e+000
122 * 2.728560e+001 3.427230e+001 0.000000e+000
123 * 2.312840e+001 3.631480e+001 0.000000e+000
124 * 2.946680e+001 3.677510e+001 0.000000e+000
125 * 2.294210e+001 2.939070e+001 0.000000e+000
126 * 1.918080e+001 3.052370e+001 0.000000e+000
127 * 2.510440e+001 3.176960e+001 0.000000e+000
128 * 1.875000e+001 2.550000e+001 0.000000e+000
129 * 1.562500e+001 2.575000e+001 0.000000e+000
130 * 2.081760e+001 2.725950e+001 0.000000e+000
131 * 3.980260e+001 3.151310e+001 0.000000e+000
132 * 3.591100e+001 3.558490e+001 0.000000e+000
133 * 4.226970e+001 3.259860e+001 0.000000e+000
134 * 3.486840e+001 2.934210e+001 0.000000e+000
135 * 3.123520e+001 3.191240e+001 0.000000e+000
136 * 3.733550e+001 3.042760e+001 0.000000e+000
137 * 2.993420e+001 2.717100e+001 0.000000e+000
138 * 2.655930e+001 2.823990e+001 0.000000e+000
139 * 3.240130e+001 2.825660e+001 0.000000e+000
140 * 2.500000e+001 2.500000e+001 0.000000e+000
141 * 2.187500e+001 2.525000e+001 0.000000e+000
142 * 2.746710e+001 2.608550e+001 0.000000e+000
143 * 4.371240e+001 2.423130e+001 0.000000e+000
144 * 4.191470e+001 2.794140e+001 0.000000e+000
145 * 4.674740e+001 2.514520e+001 0.000000e+000
146 * 3.728350e+001 2.240490e+001 0.000000e+000
147 * 3.614690e+001 2.593160e+001 0.000000e+000
148 * 4.053380e+001 2.331800e+001 0.000000e+000
149 * 3.085460e+001 2.057860e+001 0.000000e+000
150 * 3.037910e+001 2.392190e+001 0.000000e+000
151 * 3.403310e+001 2.149190e+001 0.000000e+000
152 * 2.500000e+001 1.875000e+001 0.000000e+000
153 * 2.500000e+001 2.187500e+001 0.000000e+000
154 * 2.781960e+001 1.966470e+001 0.000000e+000
155 * 4.633810e+001 1.653080e+001 0.000000e+000
156 * 4.517660e+001 2.043750e+001 0.000000e+000
157 * 4.981980e+001 1.717720e+001 0.000000e+000

158 * 3.905480e+001 1.512930e+001 0.000000e+000
159 * 3.825140e+001 1.880630e+001 0.000000e+000
160 * 4.272850e+001 1.584090e+001 0.000000e+000
161 * 3.177150e+001 1.372790e+001 0.000000e+000
162 * 3.132630e+001 1.717510e+001 0.000000e+000
163 * 3.538110e+001 1.441780e+001 0.000000e+000
164 * 2.500000e+001 1.250000e+001 0.000000e+000
165 * 2.500000e+001 1.562500e+001 0.000000e+000
166 * 2.828970e+001 1.308140e+001 0.000000e+000
167 * 4.780080e+001 8.440270e+000 0.000000e+000
168 * 4.720750e+001 1.252600e+001 0.000000e+000
169 * 5.157290e+001 8.767210e+000 0.000000e+000
170 * 4.013630e+001 7.623090e+000 0.000000e+000
171 * 3.968490e+001 1.139450e+001 0.000000e+000
172 * 4.398060e+001 8.048010e+000 0.000000e+000
173 * 3.247190e+001 6.805920e+000 0.000000e+000
174 * 3.216220e+001 1.026290e+001 0.000000e+000
175 * 3.629210e+001 7.198180e+000 0.000000e+000
176 * 2.500000e+001 6.250000e+000 0.000000e+000
177 * 2.500000e+001 9.375000e+000 0.000000e+000
178 * 2.869980e+001 6.478970e+000 0.000000e+000
179 * 4.825000e+001 0.000000e+000 0.000000e+000
180 * 4.814280e+001 4.242600e+000 0.000000e+000
181 * 5.212500e+001 0.000000e+000 0.000000e+000
182 * 4.050000e+001 0.000000e+000 0.000000e+000
183 * 4.040980e+001 3.807830e+000 0.000000e+000
184 * 4.437500e+001 0.000000e+000 0.000000e+000
185 * 3.275000e+001 0.000000e+000 0.000000e+000
186 * 3.267690e+001 3.373060e+000 0.000000e+000
187 * 3.662500e+001 0.000000e+000 0.000000e+000
188 * 2.500000e+001 0.000000e+000 0.000000e+000
189 * 2.500000e+001 3.125000e+000 0.000000e+000
190 * 2.887500e+001 0.000000e+000 0.000000e+000
191 * 1.875000e+001 1.966240e+001 0.000000e+000
192 * 1.875000e+001 2.258520e+001 0.000000e+000
193 * 2.187500e+001 1.910300e+001 0.000000e+000
194 * 1.250000e+001 2.112500e+001 0.000000e+000
195 * 1.250000e+001 2.356250e+001 0.000000e+000
196 * 1.562500e+001 2.035930e+001 0.000000e+000
197 * 6.250000e+000 2.258760e+001 0.000000e+000
198 * 6.250000e+000 2.453980e+001 0.000000e+000
199 * 9.375000e+000 2.189070e+001 0.000000e+000
200 * 0.000000e+000 2.350000e+001 0.000000e+000
201 * 0.000000e+000 2.525000e+001 0.000000e+000
202 * 3.125000e+000 2.314700e+001 0.000000e+000
203 * 1.875000e+001 1.380000e+001 0.000000e+000
204 * 1.875000e+001 1.673340e+001 0.000000e+000
205 * 2.187500e+001 1.293440e+001 0.000000e+000
206 * 1.250000e+001 1.625000e+001 0.000000e+000
207 * 1.250000e+001 1.868750e+001 0.000000e+000
208 * 1.562500e+001 1.495320e+001 0.000000e+000
209 * 6.250000e+000 1.870000e+001 0.000000e+000
210 * 6.250000e+000 2.064160e+001 0.000000e+000
211 * 9.375000e+000 1.754680e+001 0.000000e+000
212 * 0.000000e+000 2.000000e+001 0.000000e+000
213 * 0.000000e+000 2.175000e+001 0.000000e+000
214 * 3.125000e+000 1.956560e+001 0.000000e+000
215 * 1.875000e+001 6.879430e+000 0.000000e+000
216 * 1.875000e+001 1.033890e+001 0.000000e+000
217 * 2.187500e+001 6.449180e+000 0.000000e+000
218 * 1.250000e+001 8.125000e+000 0.000000e+000
219 * 1.250000e+001 1.218750e+001 0.000000e+000
220 * 1.562500e+001 7.463700e+000 0.000000e+000
221 * 6.250000e+000 9.370570e+000 0.000000e+000
222 * 6.250000e+000 1.403610e+001 0.000000e+000
223 * 9.375000e+000 8.786300e+000 0.000000e+000
224 * 0.000000e+000 1.000000e+001 0.000000e+000
225 * 0.000000e+000 1.500000e+001 0.000000e+000

```
226 * 3.125000e+000 9.800820e+000 0.000000e+000
227 * 1.875000e+001 0.000000e+000 0.000000e+000
228 * 1.875000e+001 3.430270e+000 0.000000e+000
229 * 2.187500e+001 0.000000e+000 0.000000e+000
230 * 1.250000e+001 0.000000e+000 0.000000e+000
231 * 1.250000e+001 4.062500e+000 0.000000e+000
232 * 1.562500e+001 0.000000e+000 0.000000e+000
233 * 6.250000e+000 0.000000e+000 0.000000e+000
234 * 6.250000e+000 4.694730e+000 0.000000e+000
235 * 9.375000e+000 0.000000e+000 0.000000e+000
236 * 0.000000e+000 0.000000e+000 0.000000e+000
237 * 0.000000e+000 5.000000e+000 0.000000e+000
238 * 3.125000e+000 0.000000e+000 0.000000e+000
239 * 0.000000e+000 5.600000e+001 0.000000e+000
240 * 6.398090e+000 5.563330e+001 0.000000e+000
241 * 1.284050e+001 5.450800e+001 0.000000e+000
242 * 1.902550e+001 5.266900e+001 0.000000e+000
243 * 2.499690e+001 5.011140e+001 0.000000e+000
244 * 3.063180e+001 4.687950e+001 0.000000e+000
245 * 3.582120e+001 4.304470e+001 0.000000e+000
246 * 4.059530e+001 3.857480e+001 0.000000e+000
247 * 4.473670e+001 3.368420e+001 0.000000e+000
248 * 4.729380e+001 2.998820e+001 0.000000e+000
249 * 4.956690e+001 2.605990e+001 0.000000e+000
250 * 5.150290e+001 2.198750e+001 0.000000e+000
251 * 5.310960e+001 1.775870e+001 0.000000e+000
252 * 5.436970e+001 1.341390e+001 0.000000e+000
253 * 5.527270e+001 8.996190e+000 0.000000e+000
254 * 5.581970e+001 4.490660e+000 0.000000e+000
255 * 5.600000e+001 0.000000e+000 0.000000e+000

ELEMENTS
QUAD08E 25CD4
1 *      1      2      4      3      5      8      6      7
2 *      2      9      3     10     11      6     12     13
3 *      9     14     10     15     16     12     17     18
4 *     19     20     22     21     23     26     24     25
5 *     27     28     21     22     29     31     30     25

QUAD08E 25CD4D
6 *     22     28     33     32     30     36     34     35
7 *     37     38     40     39     41     44     42     43
8 *     33     32     37     38     35     46     45     41

QUAD08E 25CD4
9 *     47     19     49     48     50     53     51     52
10 *     22     54     19     48     55     26     56     51
11 *     10     49      3     48     57     13     52     58
12 *      3     48      4     54     58      7     56     59

QUAD08E AU4G
13 *     60     61     63     62     64     67     65     66
14 *     63     62     39     40     66     69     68     43
15 *     70     62     71     61     72     74     65     73
16 *     62     70     76     75     72     79     77     78

QUAD08F WATER
17 *     87     88    239    241     89     91     90    240
18 *     92     93     87     88     94     96     95     89
19 *     97     98     92     93     99    101    100     94
20 *    102    103     97     98    104    106    105     99
21 *     88    107    241    243    108     90    109    242
22 *     93    110     88    107    111     95    112    108
23 *     98    113     93    110    114    100    115    111
24 *    103    116     98    113    117    105    118    114
25 *    107    119    243    245    120    109    121    244
26 *    110    122    107    119    123    112    124    120
27 *    113    125    110    122    126    115    127    123
```

```
28 *    116    128    113    125    129    118    130    126
29 *    119    131    245    247    132    121    133    246
30 *    122    134    119    131    135    124    136    132
31 *    125    137    122    134    138    127    139    135
32 *    128    140    125    137    141    130    142    138
33 *    131    143    247    249    144    133    145    248
34 *    134    146    131    143    147    136    148    144
35 *    137    149    134    146    150    139    151    147
36 *    140    152    137    149    153    142    154    150
37 *    143    155    249    251    156    145    157    250
38 *    146    158    143    155    159    148    160    156
39 *    149    161    146    158    162    151    163    159
40 *    152    164    149    161    165    154    166    162
41 *    155    167    251    253    168    157    169    252
42 *    158    170    155    167    171    160    172    168
43 *    161    173    158    170    174    163    175    171
44 *    164    176    161    173    177    166    178    174
45 *    167    179    253    255    180    169    181    254
46 *    170    182    167    179    183    172    184    180
47 *    173    185    170    182    186    175    187    183
48 *    176    188    173    185    189    178    190    186
49 *    128    191    140    152    192    141    193    153
50 *    116    194    128    191    195    129    196    192
51 *    103    197    116    194    198    117    199    195
52 *    102    200    103    197    201    104    202    198
53 *    191    203    152    164    204    193    205    165
54 *    194    206    191    203    207    196    208    204
55 *    197    209    194    206    210    199    211    207
56 *    200    212    197    209    213    202    214    210
57 *    203    215    164    176    216    205    217    177
58 *    206    218    203    215    219    208    220    216
59 *    209    221    206    218    222    211    223    219
60 *    212    224    209    221    225    214    226    222
61 *    215    227    176    188    228    217    229    189
62 *    218    230    215    227    231    220    232    228
63 *    221    233    218    230    234    223    235    231
64 *    224    236    221    233    237    226    238    234

QUAD08P X9 3
65 *     76     75     81     80     78     84     82     83
QUAD08P X9 4
66 *     81     80      1      2     83     86     85      5
LINE06I
67 *    236    224     60     61    237     64
68 *    224    212     61     71    225     73

LINE03R WATER   1
69 *    239    241    240
70 *    241    243    242
71 *    243    245    244
72 *    245    247    246
73 *    247    249    248
74 *    249    251    250
75 *    251    253    252
76 *    253    255    254

LINE03CV DUMMY 2
77 *     70     71     74
78 *     80     75     82
79 *      9      2     11
80 *     14      9     16
81 *     15     14     17
82 *     10     15     18
83 *     75     70     77
84 *     19     47     50
85 *     20     19     23
86 *      2     80     85
87 *     21     20     24
```

```
88 *      27      21      31
89 *      49      10      57
90 *      47      49      53
91 *      71      61      73
92 *      61      60      64
```

```
END
  -27     2     2            * symmetry axis,
  -27     3     3            * nonexisting dof (2-D),
   -2     4     1            *  electrode at V=0,
  -75     4     1            * electrode at  V=0,
  -80     4    -1            * excitation electrode
```

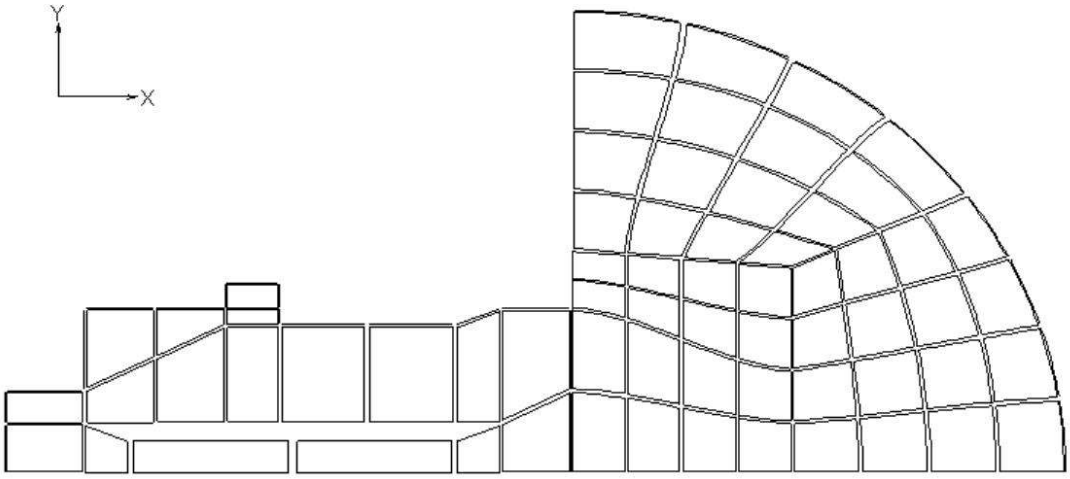

Mesh of the transducer in water

6.4 6.2.3 User dialog

```
<<< ATILA Version 6.0.0 >>>
Nom du job ?
Entrer le nom de l’extension
THE MATERIAL 25CD4D    IS NOT DEFINED IN THE FILE MATER.STD
The width of the CPDDC array is set to  7
The number of loading cases is set to 4 .
RADIATING STRUCTURE MODELLING
(DOUBLE PRECISION CALCULATION)
(USING MONOPOLAROLAR DAMPERS)
 Element QUAD08E   # 1    17:29:07
 Element QUAD08E   # 2    17:29:07
 Element QUAD08E   # 3    17:29:07
 Element QUAD08E   # 4    17:29:07
 Element QUAD08E   # 5    17:29:07
 Element QUAD08E   # 6    17:29:07
 Element QUAD08E   # 7    17:29:07
 Element QUAD08E   # 8    17:29:07
 Element QUAD08E   # 9    17:29:07
 Element QUAD08E   # 10    17:29:07
 Element QUAD08E   # 11    17:29:07
 Element QUAD08E   # 12    17:29:07
 Element QUAD08E   # 13    17:29:07
 Element QUAD08E   # 14    17:29:07
 Element QUAD08E   # 15    17:29:07
 Element QUAD08E   # 16    17:29:07
 Element QUAD08F   # 1    17:29:07
 Element QUAD08F   # 2    17:29:07
 Element QUAD08F   # 3    17:29:07
 Element QUAD08F   # 4    17:29:07
 Element QUAD08F   # 5    17:29:07
 Element QUAD08F   # 6    17:29:07
 Element QUAD08F   # 7    17:29:07
 Element QUAD08F   # 8    17:29:07
 Element QUAD08F   # 9    17:29:07
 Element QUAD08F   # 10    17:29:07
 Element QUAD08F   # 11    17:29:07
 Element QUAD08F   # 12    17:29:07
 Element QUAD08F   # 13    17:29:07
 Element QUAD08F   # 14    17:29:07
 Element QUAD08F   # 15    17:29:07
 Element QUAD08F   # 16    17:29:07
 Element QUAD08F   # 17    17:29:07
 Element QUAD08F   # 18    17:29:07
 Element QUAD08F   # 19    17:29:07
 Element QUAD08F   # 20    17:29:07
 Element QUAD08F   # 21    17:29:07
 Element QUAD08F   # 22    17:29:07
 Element QUAD08F   # 23    17:29:07
 Element QUAD08F   # 24    17:29:07
 Element QUAD08F   # 25    17:29:07
 Element QUAD08F   # 26    17:29:07
 Element QUAD08F   # 27    17:29:07
 Element QUAD08F   # 28    17:29:07
 Element QUAD08F   # 29    17:29:07
 Element QUAD08F   # 30    17:29:07
 Element QUAD08F   # 31    17:29:07
 Element QUAD08F   # 32    17:29:07
 Element QUAD08F   # 33    17:29:07
 Element QUAD08F   # 34    17:29:07
 Element QUAD08F   # 35    17:29:07
 Element QUAD08F   # 36    17:29:07
 Element QUAD08F   # 37    17:29:07
 Element QUAD08F   # 38    17:29:07
```

```
 Element QUAD08F   # 39    17:29:07
 Element QUAD08F   # 40    17:29:07
 Element QUAD08F   # 41    17:29:07
 Element QUAD08F   # 42    17:29:07
 Element QUAD08F   # 43    17:29:07
 Element QUAD08F   # 44    17:29:07
 Element QUAD08F   # 45    17:29:07
 Element QUAD08F   # 46    17:29:07
 Element QUAD08F   # 47    17:29:07
 Element QUAD08F   # 48    17:29:07
 Element QUAD08P   # 1    17:29:07
 Element QUAD08P   # 2    17:29:07
 Element LINE06I   # 1    17:29:07
 Element LINE06I   # 2    17:29:07
 Element LINE03R   # 1    17:29:07
 Element LINE03R   # 2    17:29:07
 Element LINE03R   # 3    17:29:07
 Element LINE03R   # 4    17:29:07
 Element LINE03R   # 5    17:29:07
 Element LINE03R   # 6    17:29:07
 Element LINE03R   # 7    17:29:07
 Element LINE03R   # 8    17:29:07
Block 1  assembling ended.
COMPLEX DOUBLE PRECISION FREQUENCY COMPUTATION.
 Frequency   25000.0       Hz   -17:29:07
 Frequency   35000.0       Hz   -17:29:07
 Frequency   45000.0       Hz   -17:29:07
 Frequency   55000.0       Hz   -17:29:07
NER = 8
The sound speed used is SSPD=   1489.97
Deduced acoustic center : (   0.00000      ,   0.00000      ) ,
Structure symmetric relative to the X axis.
Structure symmetric relative to the Y axis.
 Frequency =   25000.0     Hz, number of directivity terms = 14 , INFO = 3
 Frequency =   35000.0     Hz, number of directivity terms = 14 , INFO = 3
 Frequency =   45000.0     Hz, number of directivity terms = 14 , INFO = 3
 Frequency =   55000.0     Hz, number of directivity terms = 14 , INFO = 3
************ THERMAL CALCULATION ****************
************  1) HEAT CALCULATION ****************
 Element QUAD08E   # 1    17:29:08
 Element QUAD08E   # 2    17:29:08
 Element QUAD08E   # 3    17:29:08
 Element QUAD08E   # 4    17:29:08
 Element QUAD08E   # 5    17:29:08
 Element QUAD08E   # 6    17:29:08
 Element QUAD08E   # 7    17:29:08
 Element QUAD08E   # 8    17:29:08
 Element QUAD08E   # 9    17:29:08
 Element QUAD08E   # 10    17:29:08
 Element QUAD08E   # 11    17:29:08
 Element QUAD08E   # 12    17:29:08
 Element QUAD08E   # 13    17:29:08
 Element QUAD08E   # 14    17:29:08
 Element QUAD08E   # 15    17:29:08
 Element QUAD08E   # 16    17:29:08
 Element QUAD08Q   # 1    17:29:08
 Element QUAD08Q   # 2    17:29:08
*********** 2) CONDUCTION CALCULATION ***********
 Element QUAD08CD  # 1    17:29:08
 Element QUAD08CD  # 1    17:29:08
 Element QUAD08CD  # 1    17:29:08
 Element QUAD08CD  # 1    17:29:08
 Element QUAD08CD  # 1    17:29:08
 Element QUAD08CD  # 1    17:29:08
 Element QUAD08CD  # 1    17:29:08
 Element QUAD08CD  # 1    17:29:08
 Element QUAD08CD  # 1    17:29:08
 Element QUAD08CD  # 1    17:29:08
```

```
 Element QUAD08CD  # 1    17:29:08
 Element QUAD08CD  # 1    17:29:08
 Element QUAD08CD  # 1    17:29:08
 Element QUAD08CD  # 1    17:29:08
 Element QUAD08CD  # 1    17:29:08
 Element QUAD08CD  # 1    17:29:08
 Element QUAD08CD  # 1    17:29:08
 Element QUAD08CD  # 1    17:29:08
 Element LINE03CV  # 1    17:29:08
 Element LINE03CV  # 2    17:29:08
 Element LINE03CV  # 3    17:29:08
 Element LINE03CV  # 4    17:29:08
 Element LINE03CV  # 5    17:29:08
 Element LINE03CV  # 6    17:29:08
 Element LINE03CV  # 7    17:29:08
 Element LINE03CV  # 8    17:29:08
 Element LINE03CV  # 9    17:29:08
 Element LINE03CV  # 10    17:29:08
 Element LINE03CV  # 11    17:29:08
 Element LINE03CV  # 12    17:29:08
 Element LINE03CV  # 13    17:29:08
 Element LINE03CV  # 14    17:29:08
 Element LINE03CV  # 15    17:29:08
 Element LINE03CV  # 16    17:29:08
Block 1  assembling ended.
REAL DOUBLE PRECISION STATIC COMPUTATION.
LOADING CASE NUMBER 1  - 17:29:08
LOADING CASE NUMBER 2  - 17:29:08
LOADING CASE NUMBER 3  - 17:29:08
LOADING CASE NUMBER 4  - 17:29:08
GENPST *************
 DATE: 05/27/05  AT:17:29:08  END OF JOB:PROJECT   CPU TIME: 0.56  SEC.
```

6.5 6.2.4 Result file

```
1

                    ==
==
                    ==
==
                    ==
==
                    ==         AAAAAAAAAA    TTTTTTTTTTTT   IIIIIIIIIII   LL
AAAAAAAAAA         ==
                    ==        AAAAAAAAAAAA   TTTTTTTTTTTT   IIIIIIIIIII   LL
AAAAAAAAAAAA        ==
                    ==        AA        AA        TT             II        LL             AA
AA        ==
                    ==        AA        AA        TT             II        LL             AA
AA        ==
                    ==        AA        AA        TT             II        LL             AA
AA        ==
                    ==        AAAAAAAAAAAA        TT             II        LL
AAAAAAAAAAAA        ==
                    ==        AAAAAAAAAAAA        TT             II        LL
AAAAAAAAAAAA        ==
                    ==        AA        AA        TT             II        LL             AA
AA        ==
                    ==        AA        AA        TT             II        LL             AA
AA        ==
                    ==        AA        AA        TT             II        LL             AA
AA        ==
                    ==        AA        AA        TT        IIIIIIIIIII   LLLLLLLLLLL   AA
AA        ==
                    ==        AA        AA        TT        IIIIIIIIIII   LLLLLLLLLLL   AA
AA        ==
```

```
                    ==
==
                    ==
==
                    ==
==
                    ================================================================================
==================
                    ================================================================================
==================

          USERID:                                    LE:05/30/05  A:15:26:32  JOB:PROJECT

1
JOB:PROJECT  DATE:05/30/05 PAGE:  2
LANGUAGE =ENGLISH
PRINTING LEVEL = 0
25CD4D    ALREADY EXISTS AS A STANDARD MATERIAL, IT IS REPLACED WITH THE FOLLOWING
CHARACTERISTICS :
 25CD4D          2.15000E+11 0.33000      750.00      0.0000      0.0000      0.0000

 DUMMY     ALREADY EXISTS AS A STANDARD MATERIAL,
IT IS REPLACED WITH THE FOLLOWING CHARACTERISTICS :
DUMMY       0.0000      0.0000      0.0000      0.0000      0.0000      0.0000
DATA ON THE DISPLACEMENT EXCITATION VECTOR U :
NODE 80     DEGREE ELECPOT      VALUE =   500.000       0.00000
CALCULATION WITH LOSSES
  THE MATERIAL 25CD4D    IS NOT DEFINED IN THE FILE MATER.STD

 NUMBER OF NODES       IP= 255
 NUMBER OF ELEMENTS    IE= 92
Tolerance on node precision:  8.197560E-06
Detected finite element model symmetry factor =   6.28319
May be incorrect if non principal symmetries are present.
1
JOB:PROJECT  DATE:05/30/05 PAGE:  3
86  SOLID NODES
169  FLUID NODES INCLUDING 17  RADIATED NODES
INODE    IDISP IREPT/IPLANE  COORDINATES X,Y,Z / LOCAL DIRECTION COSINES
27         2         2               30  NODES FOUND IN THE PLANE.
    -27         3         3              229  NODES FOUND IN THE PLANE.
     -2         4         1                7  NODES FOUND IN THE PLANE.
    -75         4         1                6  NODES FOUND IN THE PLANE.
    -80         4        -1                3  NODES FOUND IN THE PLANE.

1
JOB:PROJECT  DATE:05/30/05 PAGE:  4
=== CPDDC ARRAY ===
  NODES          COORDINATES               D.O.F. NUMBERS
      1 -3.300E-02 6.000E-03  0.00        222.    223.      0.      0.
      2 -3.300E-02 1.800E-02  0.00        224.    225.      0.      0.
      3 -3.900E-02 1.800E-02  0.00        256.    257.      0.      0.
      4 -3.900E-02 6.000E-03  0.00        254.    255.      0.      0.
      5 -3.300E-02 1.200E-02  0.00        232.    233.      0.      0.
      6 -3.600E-02 1.800E-02  0.00        260.    261.      0.      0.
      7 -3.900E-02 1.200E-02  0.00        262.    263.      0.      0.
      8 -3.600E-02 6.000E-03  0.00        258.    259.      0.      0.
      9 -3.300E-02 2.000E-02  0.00        234.    235.      0.      0.
     10 -3.900E-02 2.000E-02  0.00        264.    265.      0.      0.
     11 -3.300E-02 1.900E-02  0.00        236.    237.      0.      0.
     12 -3.600E-02 2.000E-02  0.00        266.    267.      0.      0.
     13 -3.900E-02 1.900E-02  0.00        268.    269.      0.      0.
     14 -3.300E-02 2.300E-02  0.00        238.    239.      0.      0.
     15 -3.900E-02 2.300E-02  0.00        242.    243.      0.      0.
     16 -3.300E-02 2.150E-02  0.00        240.    241.      0.      0.
     17 -3.600E-02 2.300E-02  0.00        244.    245.      0.      0.
     18 -3.900E-02 2.150E-02  0.00        270.    271.      0.      0.
     19 -5.500E-02 1.000E-02  0.00        308.    309.      0.      0.
```

20	-6.400E-02	1.000E-02	0.00	318.	319.	0.	0.
21	-6.400E-02	6.000E-03	0.00	323.	324.	0.	0.
22	-5.500E-02	6.000E-03	0.00	300.	301.	0.	0.
23	-5.950E-02	1.000E-02	0.00	320.	321.	0.	0.
24	-6.400E-02	8.000E-03	0.00	330.	331.	0.	0.
25	-5.950E-02	6.000E-03	0.00	328.	329.	0.	0.
26	-5.500E-02	8.000E-03	0.00	316.	317.	0.	0.
27	-6.400E-02	0.00	0.00	322.	0.	0.	0.
28	-5.500E-02	0.00	0.00	302.	0.	0.	0.
29	-5.950E-02	0.00	0.00	325.	0.	0.	0.
30	-5.500E-02	3.000E-03	0.00	303.	304.	0.	0.
31	-6.400E-02	3.000E-03	0.00	326.	327.	0.	0.
32	-5.000E-02	0.00	0.00	274.	0.	0.	0.
33	-5.000E-02	4.000E-03	0.00	272.	273.	0.	0.
34	-5.250E-02	0.00	0.00	307.	0.	0.	0.
35	-5.000E-02	2.000E-03	0.00	275.	276.	0.	0.
36	-5.250E-02	5.000E-03	0.00	305.	306.	0.	0.
37	-3.150E-02	4.000E-03	0.00	246.	247.	0.	0.
38	-3.150E-02	0.00	0.00	248.	0.	0.	0.
39	-1.300E-02	0.00	0.00	216.	0.	0.	0.
40	-1.300E-02	4.000E-03	0.00	217.	0.	0.	0.
41	-3.150E-02	2.000E-03	0.00	249.	250.	0.	0.
42	-2.225E-02	0.00	0.00	253.	0.	0.	0.
43	-1.300E-02	2.000E-03	0.00	221.	0.	0.	0.
44	-2.225E-02	4.000E-03	0.00	251.	252.	0.	0.
45	-4.075E-02	0.00	0.00	279.	0.	0.	0.
46	-4.075E-02	4.000E-03	0.00	277.	278.	0.	0.
47	-5.500E-02	2.000E-02	0.00	296.	297.	0.	0.
48	-4.700E-02	1.400E-02	0.00	280.	281.	0.	0.
49	-4.700E-02	2.000E-02	0.00	290.	291.	0.	0.
50	-5.500E-02	1.500E-02	0.00	310.	311.	0.	0.

1

51	-5.100E-02	1.200E-02	0.00	312.	313.	0.	0.
52	-4.700E-02	1.700E-02	0.00	294.	295.	0.	0.
53	-5.100E-02	2.000E-02	0.00	298.	299.	0.	0.
54	-4.700E-02	6.000E-03	0.00	282.	283.	0.	0.
55	-5.100E-02	6.000E-03	0.00	314.	315.	0.	0.
56	-4.700E-02	1.000E-02	0.00	286.	287.	0.	0.
57	-4.300E-02	2.000E-02	0.00	292.	293.	0.	0.
58	-4.300E-02	1.600E-02	0.00	284.	285.	0.	0.
59	-4.300E-02	6.000E-03	0.00	288.	289.	0.	0.
60	0.00	0.00	0.00	176.	0.	0.	0.
61	0.00	1.000E-02	0.00	170.	171.	0.	0.
62	-8.000E-03	6.000E-03	0.00	188.	189.	0.	0.
63	-8.000E-03	0.00	0.00	187.	0.	0.	0.
64	0.00	5.000E-03	0.00	177.	178.	0.	0.
65	-4.000E-03	8.000E-03	0.00	191.	192.	0.	0.
66	-8.000E-03	3.000E-03	0.00	193.	194.	0.	0.
67	-4.000E-03	0.00	0.00	190.	0.	0.	0.
68	-1.050E-02	5.000E-03	0.00	219.	220.	0.	0.
69	-1.050E-02	0.00	0.00	218.	0.	0.	0.
70	-8.000E-03	2.000E-02	0.00	179.	180.	0.	0.
71	0.00	2.000E-02	0.00	172.	173.	0.	0.
72	-8.000E-03	1.300E-02	0.00	195.	196.	0.	0.
73	0.00	1.500E-02	0.00	174.	175.	0.	0.
74	-4.000E-03	2.000E-02	0.00	181.	182.	0.	0.
75	-1.300E-02	1.800E-02	0.00	183.	184.	0.	0.
76	-1.300E-02	6.000E-03	0.00	197.	198.	0.	0.
77	-1.050E-02	1.900E-02	0.00	185.	186.	0.	0.
78	-1.300E-02	1.200E-02	0.00	201.	202.	0.	0.
79	-1.050E-02	6.000E-03	0.00	199.	200.	0.	0.
80	-2.300E-02	1.800E-02	0.00	206.	207.	0.	205.
81	-2.300E-02	6.000E-03	0.00	203.	204.	0.	205.
82	-1.800E-02	1.800E-02	0.00	211.	212.	0.	213.
83	-2.300E-02	1.200E-02	0.00	214.	215.	0.	205.
84	-1.800E-02	6.000E-03	0.00	208.	209.	0.	210.

85	-2.800E-02	1.800E-02	0.00	229.	230.	0.	231.
86	-2.800E-02	6.000E-03	0.00	226.	227.	0.	228.
87	0.00	4.875E-02	0.00	52.	0.	0.	0.
88	1.155E-02	4.768E-02	0.00	49.	0.	0.	0.
89	5.817E-03	4.847E-02	0.00	53.	0.	0.	0.
90	1.233E-02	5.116E-02	0.00	51.	0.	0.	0.
91	0.00	5.238E-02	0.00	54.	0.	0.	0.
92	0.00	4.150E-02	0.00	81.	0.	0.	0.
93	9.545E-03	4.050E-02	0.00	78.	0.	0.	0.
94	4.762E-03	4.119E-02	0.00	82.	0.	0.	0.
95	1.059E-02	4.411E-02	0.00	80.	0.	0.	0.
96	0.00	4.513E-02	0.00	83.	0.	0.	0.
97	0.00	3.425E-02	0.00	110.	0.	0.	0.
98	7.540E-03	3.333E-02	0.00	107.	0.	0.	0.
99	3.706E-03	3.391E-02	0.00	111.	0.	0.	0.
100	8.498E-03	3.689E-02	0.00	109.	0.	0.	0.
101	0.00	3.788E-02	0.00	112.	0.	0.	0.
102	0.00	2.700E-02	0.00	134.	0.	0.	0.
103	6.250E-03	2.650E-02	0.00	131.	0.	0.	0.
104	3.125E-03	2.675E-02	0.00	135.	0.	0.	0.

1

105	6.761E-03	2.985E-02	0.00	133.	0.	0.	0.
106	0.00	3.063E-02	0.00	136.	0.	0.	0.
107	2.218E-02	4.452E-02	0.00	46.	0.	0.	0.
108	1.698E-02	4.637E-02	0.00	50.	0.	0.	0.
109	2.370E-02	4.748E-02	0.00	48.	0.	0.	0.
110	1.875E-02	3.806E-02	0.00	75.	0.	0.	0.
111	1.420E-02	3.946E-02	0.00	79.	0.	0.	0.
112	2.050E-02	4.134E-02	0.00	77.	0.	0.	0.
113	1.532E-02	3.159E-02	0.00	104.	0.	0.	0.
114	1.142E-02	3.254E-02	0.00	108.	0.	0.	0.
115	1.700E-02	3.477E-02	0.00	106.	0.	0.	0.
116	1.250E-02	2.600E-02	0.00	125.	0.	0.	0.
117	9.375E-03	2.625E-02	0.00	132.	0.	0.	0.
118	1.379E-02	2.863E-02	0.00	127.	0.	0.	0.
119	3.163E-02	3.915E-02	0.00	43.	0.	0.	0.
120	2.708E-02	4.211E-02	0.00	47.	0.	0.	0.
121	3.375E-02	4.129E-02	0.00	45.	0.	0.	0.
122	2.729E-02	3.427E-02	0.00	72.	0.	0.	0.
123	2.313E-02	3.631E-02	0.00	76.	0.	0.	0.
124	2.947E-02	3.678E-02	0.00	74.	0.	0.	0.
125	2.294E-02	2.939E-02	0.00	98.	0.	0.	0.
126	1.918E-02	3.052E-02	0.00	105.	0.	0.	0.
127	2.510E-02	3.177E-02	0.00	100.	0.	0.	0.
128	1.875E-02	2.550E-02	0.00	101.	0.	0.	0.
129	1.563E-02	2.575E-02	0.00	126.	0.	0.	0.
130	2.082E-02	2.726E-02	0.00	103.	0.	0.	0.
131	3.980E-02	3.151E-02	0.00	40.	0.	0.	0.
132	3.591E-02	3.558E-02	0.00	44.	0.	0.	0.
133	4.227E-02	3.260E-02	0.00	42.	0.	0.	0.
134	3.487E-02	2.934E-02	0.00	66.	0.	0.	0.
135	3.124E-02	3.191E-02	0.00	73.	0.	0.	0.
136	3.734E-02	3.043E-02	0.00	68.	0.	0.	0.
137	2.993E-02	2.717E-02	0.00	69.	0.	0.	0.
138	2.656E-02	2.824E-02	0.00	99.	0.	0.	0.
139	3.240E-02	2.826E-02	0.00	71.	0.	0.	0.
140	2.500E-02	2.500E-02	0.00	95.	0.	0.	0.
141	2.188E-02	2.525E-02	0.00	102.	0.	0.	0.
142	2.747E-02	2.609E-02	0.00	97.	0.	0.	0.
143	4.371E-02	2.423E-02	0.00	34.	0.	0.	0.
144	4.191E-02	2.794E-02	0.00	41.	0.	0.	0.
145	4.675E-02	2.515E-02	0.00	36.	0.	0.	0.
146	3.728E-02	2.240E-02	0.00	37.	0.	0.	0.
147	3.615E-02	2.593E-02	0.00	67.	0.	0.	0.
148	4.053E-02	2.332E-02	0.00	39.	0.	0.	0.
149	3.085E-02	2.058E-02	0.00	63.	0.	0.	0.

150	3.038E-02	2.392E-02	0.00	70.	0.	0.	0.
151	3.403E-02	2.149E-02	0.00	65.	0.	0.	0.
152	2.500E-02	1.875E-02	0.00	92.	0.	0.	0.
153	2.500E-02	2.188E-02	0.00	96.	0.	0.	0.
154	2.782E-02	1.966E-02	0.00	94.	0.	0.	0.
155	4.634E-02	1.653E-02	0.00	11.	0.	0.	0.
156	4.518E-02	2.044E-02	0.00	35.	0.	0.	0.
157	4.982E-02	1.718E-02	0.00	13.	0.	0.	0.
158	3.905E-02	1.513E-02	0.00	31.	0.	0.	0.

1

159	3.825E-02	1.881E-02	0.00	38.	0.	0.	0.
160	4.273E-02	1.584E-02	0.00	33.	0.	0.	0.
161	3.177E-02	1.373E-02	0.00	60.	0.	0.	0.
162	3.133E-02	1.718E-02	0.00	64.	0.	0.	0.
163	3.538E-02	1.442E-02	0.00	62.	0.	0.	0.
164	2.500E-02	1.250E-02	0.00	89.	0.	0.	0.
165	2.500E-02	1.563E-02	0.00	93.	0.	0.	0.
166	2.829E-02	1.308E-02	0.00	91.	0.	0.	0.
167	4.780E-02	8.440E-03	0.00	4.	0.	0.	0.
168	4.721E-02	1.253E-02	0.00	12.	0.	0.	0.
169	5.157E-02	8.767E-03	0.00	7.	0.	0.	0.
170	4.014E-02	7.623E-03	0.00	26.	0.	0.	0.
171	3.968E-02	1.139E-02	0.00	32.	0.	0.	0.
172	4.398E-02	8.048E-03	0.00	29.	0.	0.	0.
173	3.247E-02	6.806E-03	0.00	55.	0.	0.	0.
174	3.216E-02	1.026E-02	0.00	61.	0.	0.	0.
175	3.629E-02	7.198E-03	0.00	58.	0.	0.	0.
176	2.500E-02	6.250E-03	0.00	84.	0.	0.	0.
177	2.500E-02	9.375E-03	0.00	90.	0.	0.	0.
178	2.870E-02	6.479E-03	0.00	87.	0.	0.	0.
179	4.825E-02	0.00	0.00	5.	0.	0.	0.
180	4.814E-02	4.243E-03	0.00	6.	0.	0.	0.
181	5.213E-02	0.00	0.00	8.	0.	0.	0.
182	4.050E-02	0.00	0.00	27.	0.	0.	0.
183	4.041E-02	3.808E-03	0.00	28.	0.	0.	0.
184	4.438E-02	0.00	0.00	30.	0.	0.	0.
185	3.275E-02	0.00	0.00	56.	0.	0.	0.
186	3.268E-02	3.373E-03	0.00	57.	0.	0.	0.
187	3.663E-02	0.00	0.00	59.	0.	0.	0.
188	2.500E-02	0.00	0.00	85.	0.	0.	0.
189	2.500E-02	3.125E-03	0.00	86.	0.	0.	0.
190	2.888E-02	0.00	0.00	88.	0.	0.	0.
191	1.875E-02	1.966E-02	0.00	121.	0.	0.	0.
192	1.875E-02	2.259E-02	0.00	124.	0.	0.	0.
193	2.188E-02	1.910E-02	0.00	123.	0.	0.	0.
194	1.250E-02	2.113E-02	0.00	128.	0.	0.	0.
195	1.250E-02	2.356E-02	0.00	129.	0.	0.	0.
196	1.563E-02	2.036E-02	0.00	130.	0.	0.	0.
197	6.250E-03	2.259E-02	0.00	146.	0.	0.	0.
198	6.250E-03	2.454E-02	0.00	147.	0.	0.	0.
199	9.375E-03	2.189E-02	0.00	148.	0.	0.	0.
200	0.00	2.350E-02	0.00	152.	0.	0.	0.
201	0.00	2.525E-02	0.00	153.	0.	0.	0.
202	3.125E-03	2.315E-02	0.00	154.	0.	0.	0.
203	1.875E-02	1.380E-02	0.00	118.	0.	0.	0.
204	1.875E-02	1.673E-02	0.00	122.	0.	0.	0.
205	2.188E-02	1.293E-02	0.00	120.	0.	0.	0.
206	1.250E-02	1.625E-02	0.00	142.	0.	0.	0.
207	1.250E-02	1.869E-02	0.00	145.	0.	0.	0.
208	1.563E-02	1.495E-02	0.00	144.	0.	0.	0.
209	6.250E-03	1.870E-02	0.00	149.	0.	0.	0.
210	6.250E-03	2.064E-02	0.00	150.	0.	0.	0.
211	9.375E-03	1.755E-02	0.00	151.	0.	0.	0.
212	0.00	2.000E-02	0.00	161.	0.	0.	0.

1

```
    213   0.00     2.175E-02  0.00        162.      0.      0.      0.
    214  3.125E-03 1.957E-02  0.00        163.      0.      0.      0.
    215  1.875E-02 6.879E-03  0.00        113.      0.      0.      0.
    216  1.875E-02 1.034E-02  0.00        119.      0.      0.      0.
    217  2.188E-02 6.449E-03  0.00        116.      0.      0.      0.
    218  1.250E-02 8.125E-03  0.00        137.      0.      0.      0.
    219  1.250E-02 1.219E-02  0.00        143.      0.      0.      0.
    220  1.563E-02 7.464E-03  0.00        140.      0.      0.      0.
    221  6.250E-03 9.371E-03  0.00        155.      0.      0.      0.
    222  6.250E-03 1.404E-02  0.00        160.      0.      0.      0.
    223  9.375E-03 8.786E-03  0.00        158.      0.      0.      0.
    224   0.00     1.000E-02  0.00        164.      0.      0.      0.
    225   0.00     1.500E-02  0.00        165.      0.      0.      0.
    226  3.125E-03 9.801E-03  0.00        166.      0.      0.      0.
    227  1.875E-02  0.00      0.00        114.      0.      0.      0.
    228  1.875E-02 3.430E-03  0.00        115.      0.      0.      0.
    229  2.188E-02  0.00      0.00        117.      0.      0.      0.
    230  1.250E-02  0.00      0.00        138.      0.      0.      0.
    231  1.250E-02 4.063E-03  0.00        139.      0.      0.      0.
    232  1.563E-02  0.00      0.00        141.      0.      0.      0.
    233  6.250E-03  0.00      0.00        156.      0.      0.      0.
    234  6.250E-03 4.695E-03  0.00        157.      0.      0.      0.
    235  9.375E-03  0.00      0.00        159.      0.      0.      0.
    236   0.00      0.00      0.00        167.      0.      0.      0.
    237   0.00     5.000E-03  0.00        168.      0.      0.      0.
    238  3.125E-03  0.00      0.00        169.      0.      0.      0.
    239   0.00     5.600E-02  0.00         24.      0.      0.      0.
    240  6.398E-03 5.563E-02  0.00         25.      0.      0.      0.
    241  1.284E-02 5.451E-02  0.00         22.      0.      0.      0.
    242  1.903E-02 5.267E-02  0.00         23.      0.      0.      0.
    243  2.500E-02 5.011E-02  0.00         20.      0.      0.      0.
    244  3.063E-02 4.688E-02  0.00         21.      0.      0.      0.
    245  3.582E-02 4.304E-02  0.00         18.      0.      0.      0.
    246  4.060E-02 3.857E-02  0.00         19.      0.      0.      0.
    247  4.474E-02 3.368E-02  0.00         16.      0.      0.      0.
    248  4.729E-02 2.999E-02  0.00         17.      0.      0.      0.
    249  4.957E-02 2.606E-02  0.00         14.      0.      0.      0.
    250  5.150E-02 2.199E-02  0.00         15.      0.      0.      0.
    251  5.311E-02 1.776E-02  0.00          9.      0.      0.      0.
    252  5.437E-02 1.341E-02  0.00         10.      0.      0.      0.
    253  5.527E-02 8.996E-03  0.00          1.      0.      0.      0.
    254  5.582E-02 4.491E-03  0.00          3.      0.      0.      0.
    255  5.600E-02  0.00      0.00          2.      0.      0.      0.
MAXA ARRAY :
MAXA( 332) = 8728
Nombre total approximatif de transferts de
blocs par factorisation et par triangle : 2

SKYLINE STORAGE OF THE STIFFNESS MATRIX USING BLOCKS
NUMBER OF EQUATIONS : 331
INFORMATION ON THE BLOCKS
NUMBER OF BLOCKS : 1
MAXIMUM BLOCK SIZE : 8727
MAXIMUM NUMBER OF ADRESSES PER BLOCK : 332
    PERCENTAGE OF THE WHOLE MATRIX STORED :      15.00  %
 Frequency   25000.0       Hz
DEGREES OF FREEDOM WITH A IMPOSED DISPLACEMENT :
REACTION AT NODE NUMBER 80 DDL TYPE 8  : -8.517731E-08  + J *  2.529391E-09
IMPEDANCE AND ADMITTANCE AT NODE NUMBER 80 :   1108.75     + J *  -37337.3      ,
7.946317E-07 + J *  2.675924E-05
 Frequency   35000.0       Hz
REACTION AT NODE NUMBER 80 DDL TYPE 8  : -1.077496E-07  + J *  1.535926E-08
IMPEDANCE AND ADMITTANCE AT NODE NUMBER 80 :   2947.98     + J *  -20680.9      ,
6.755355E-06 + J *  4.739077E-05
 Frequency   45000.0       Hz
REACTION AT NODE NUMBER 80 DDL TYPE 8  : -2.380391E-08  + J *  2.039633E-08
```

```
IMPEDANCE AND ADMITTANCE AT NODE NUMBER 80 :   36706.0     + J *  -42838.4      ,
1.153385E-05 + J *  1.346079E-05
 Frequency   55000.0       Hz
REACTION AT NODE NUMBER 80 DDL TYPE 8  : -5.971431E-08  + J *  1.639387E-09
IMPEDANCE AND ADMITTANCE AT NODE NUMBER 80 :   664.699     + J *  -24211.5      ,
1.133063E-06 + J *  4.127157E-05
  FREQUENCE (Hz)   25000.00 Dissipated Power Density (W)    0.0000E+00
  FREQUENCE (Hz)   35000.00 Dissipated Power Density (W)    0.0000E+00
  FREQUENCE (Hz)   45000.00 Dissipated Power Density (W)    0.0000E+00
  FREQUENCE (Hz)   55000.00 Dissipated Power Density (W)    0.0000E+00
  FREQUENCE (Hz)   25000.00 Dissipated Power Density (W)    0.0000E+00
  FREQUENCE (Hz)   35000.00 Dissipated Power Density (W)    0.0000E+00
  FREQUENCE (Hz)   45000.00 Dissipated Power Density (W)    0.0000E+00
  FREQUENCE (Hz)   55000.00 Dissipated Power Density (W)    0.0000E+00
  FREQUENCE (Hz)   25000.00 Dissipated Power Density (W)    0.0000E+00
  FREQUENCE (Hz)   35000.00 Dissipated Power Density (W)    0.0000E+00
  FREQUENCE (Hz)   45000.00 Dissipated Power Density (W)    0.0000E+00
  FREQUENCE (Hz)   55000.00 Dissipated Power Density (W)    0.0000E+00
  FREQUENCE (Hz)   25000.00 Dissipated Power Density (W)    0.0000E+00
  FREQUENCE (Hz)   35000.00 Dissipated Power Density (W)    0.0000E+00
  FREQUENCE (Hz)   45000.00 Dissipated Power Density (W)    0.0000E+00
  FREQUENCE (Hz)   55000.00 Dissipated Power Density (W)    0.0000E+00
  FREQUENCE (Hz)   25000.00 Dissipated Power Density (W)    0.0000E+00
  FREQUENCE (Hz)   35000.00 Dissipated Power Density (W)    0.0000E+00
  FREQUENCE (Hz)   45000.00 Dissipated Power Density (W)    0.0000E+00
  FREQUENCE (Hz)   55000.00 Dissipated Power Density (W)    0.0000E+00
  FREQUENCE (Hz)   25000.00 Dissipated Power Density (W)    0.0000E+00
  FREQUENCE (Hz)   35000.00 Dissipated Power Density (W)    0.0000E+00
  FREQUENCE (Hz)   45000.00 Dissipated Power Density (W)    0.0000E+00
  FREQUENCE (Hz)   55000.00 Dissipated Power Density (W)    0.0000E+00
  FREQUENCE (Hz)   25000.00 Dissipated Power Density (W)    0.0000E+00
  FREQUENCE (Hz)   35000.00 Dissipated Power Density (W)    0.0000E+00
  FREQUENCE (Hz)   45000.00 Dissipated Power Density (W)    0.0000E+00
  FREQUENCE (Hz)   55000.00 Dissipated Power Density (W)    0.0000E+00
  FREQUENCE (Hz)   25000.00 Dissipated Power Density (W)    0.0000E+00
  FREQUENCE (Hz)   35000.00 Dissipated Power Density (W)    0.0000E+00
  FREQUENCE (Hz)   45000.00 Dissipated Power Density (W)    0.0000E+00
  FREQUENCE (Hz)   55000.00 Dissipated Power Density (W)    0.0000E+00
  FREQUENCE (Hz)   25000.00 Dissipated Power Density (W)    0.0000E+00
  FREQUENCE (Hz)   35000.00 Dissipated Power Density (W)    0.0000E+00
  FREQUENCE (Hz)   45000.00 Dissipated Power Density (W)    0.0000E+00
  FREQUENCE (Hz)   55000.00 Dissipated Power Density (W)    0.0000E+00
  FREQUENCE (Hz)   25000.00 Dissipated Power Density (W)    0.0000E+00
  FREQUENCE (Hz)   35000.00 Dissipated Power Density (W)    0.0000E+00
  FREQUENCE (Hz)   45000.00 Dissipated Power Density (W)    0.0000E+00
  FREQUENCE (Hz)   55000.00 Dissipated Power Density (W)    0.0000E+00
  FREQUENCE (Hz)   25000.00 Dissipated Power Density (W)    0.0000E+00
  FREQUENCE (Hz)   35000.00 Dissipated Power Density (W)    0.0000E+00
  FREQUENCE (Hz)   45000.00 Dissipated Power Density (W)    0.0000E+00
  FREQUENCE (Hz)   55000.00 Dissipated Power Density (W)    0.0000E+00
  FREQUENCE (Hz)   25000.00 Dissipated Power Density (W)    0.0000E+00
  FREQUENCE (Hz)   35000.00 Dissipated Power Density (W)    0.0000E+00
  FREQUENCE (Hz)   45000.00 Dissipated Power Density (W)    0.0000E+00
  FREQUENCE (Hz)   55000.00 Dissipated Power Density (W)    0.0000E+00
  FREQUENCE (Hz)   25000.00 Dissipated Power Density (W)    0.0000E+00
  FREQUENCE (Hz)   35000.00 Dissipated Power Density (W)    0.0000E+00
  FREQUENCE (Hz)   45000.00 Dissipated Power Density (W)    0.0000E+00
  FREQUENCE (Hz)   55000.00 Dissipated Power Density (W)    0.0000E+00
  FREQUENCE (Hz)   25000.00 Dissipated Power Density (W)    0.0000E+00
  FREQUENCE (Hz)   35000.00 Dissipated Power Density (W)    0.0000E+00
  FREQUENCE (Hz)   45000.00 Dissipated Power Density (W)    0.0000E+00
  FREQUENCE (Hz)   55000.00 Dissipated Power Density (W)    0.0000E+00
  FREQUENCE (Hz)   25000.00 Dissipated Power Density (W)    0.0000E+00
  FREQUENCE (Hz)   35000.00 Dissipated Power Density (W)    0.0000E+00
  FREQUENCE (Hz)   45000.00 Dissipated Power Density (W)    0.0000E+00
  FREQUENCE (Hz)   55000.00 Dissipated Power Density (W)    0.0000E+00
  FREQUENCE (Hz)   25000.00 Dissipated Power Density (W)    0.0000E+00
  FREQUENCE (Hz)   35000.00 Dissipated Power Density (W)    0.0000E+00
  FREQUENCE (Hz)   45000.00 Dissipated Power Density (W)    0.0000E+00
  FREQUENCE (Hz)   55000.00 Dissipated Power Density (W)    0.0000E+00
  FREQUENCE (Hz)   25000.00 Dissipated Power Density (W)    0.0000E+00
  FREQUENCE (Hz)   35000.00 Dissipated Power Density (W)    0.0000E+00
```

```
  FREQUENCE (Hz)   45000.00 Dissipated Power Density (W)    0.0000E+00
  FREQUENCE (Hz)   55000.00 Dissipated Power Density (W)    0.0000E+00
  FREQUENCE (Hz)   25000.00 Dissipated Power Density (W)    0.1347E-01
  FREQUENCE (Hz)   35000.00 Dissipated Power Density (W)    0.4395E-01
  FREQUENCE (Hz)   45000.00 Dissipated Power Density (W)    0.1143E+00
  FREQUENCE (Hz)   55000.00 Dissipated Power Density (W)    0.3506E-01
  FREQUENCE (Hz)   25000.00 Dissipated Power Density (W)    0.1402E-01
  FREQUENCE (Hz)   35000.00 Dissipated Power Density (W)    0.5527E-01
  FREQUENCE (Hz)   45000.00 Dissipated Power Density (W)    0.1738E+00
  FREQUENCE (Hz)   55000.00 Dissipated Power Density (W)    0.5570E-01
FREQUENCY (Hz) TOTAL DISSIPATED POWER (W)
        25000.             0.27493E-01
        35000.             0.99217E-01
        45000.             0.28810E+00
        55000.             0.90765E-01
Tolerance on node precision:  8.197560E-06
Detected finite element model symmetry factor =   6.28319
May be incorrect if non principal symmetries are present.
1
JOB:PROJECT  DATE:05/30/05 PAGE:  9
0  SOLID NODES
0  FLUID NODES
THE NODE NUMBER 87 IS NOT CONNECTED TO AN ELEMENT
THE NODE NUMBER 88 IS NOT CONNECTED TO AN ELEMENT
THE NODE NUMBER 89 IS NOT CONNECTED TO AN ELEMENT
THE NODE NUMBER 90 IS NOT CONNECTED TO AN ELEMENT
THE NODE NUMBER 91 IS NOT CONNECTED TO AN ELEMENT
THE NODE NUMBER 92 IS NOT CONNECTED TO AN ELEMENT
THE NODE NUMBER 93 IS NOT CONNECTED TO AN ELEMENT
THE NODE NUMBER 94 IS NOT CONNECTED TO AN ELEMENT
THE NODE NUMBER 95 IS NOT CONNECTED TO AN ELEMENT
THE NODE NUMBER 96 IS NOT CONNECTED TO AN ELEMENT
THE NODE NUMBER 97 IS NOT CONNECTED TO AN ELEMENT
THE NODE NUMBER 98 IS NOT CONNECTED TO AN ELEMENT
THE NODE NUMBER 99 IS NOT CONNECTED TO AN ELEMENT
THE NODE NUMBER 100 IS NOT CONNECTED TO AN ELEMENT
THE NODE NUMBER 101 IS NOT CONNECTED TO AN ELEMENT
THE NODE NUMBER 102 IS NOT CONNECTED TO AN ELEMENT
THE NODE NUMBER 103 IS NOT CONNECTED TO AN ELEMENT
THE NODE NUMBER 104 IS NOT CONNECTED TO AN ELEMENT
THE NODE NUMBER 105 IS NOT CONNECTED TO AN ELEMENT
THE NODE NUMBER 106 IS NOT CONNECTED TO AN ELEMENT
THE NODE NUMBER 107 IS NOT CONNECTED TO AN ELEMENT
THE NODE NUMBER 108 IS NOT CONNECTED TO AN ELEMENT
THE NODE NUMBER 109 IS NOT CONNECTED TO AN ELEMENT
THE NODE NUMBER 110 IS NOT CONNECTED TO AN ELEMENT
THE NODE NUMBER 111 IS NOT CONNECTED TO AN ELEMENT
THE NODE NUMBER 112 IS NOT CONNECTED TO AN ELEMENT
THE NODE NUMBER 113 IS NOT CONNECTED TO AN ELEMENT
THE NODE NUMBER 114 IS NOT CONNECTED TO AN ELEMENT
THE NODE NUMBER 115 IS NOT CONNECTED TO AN ELEMENT
THE NODE NUMBER 116 IS NOT CONNECTED TO AN ELEMENT
THE NODE NUMBER 117 IS NOT CONNECTED TO AN ELEMENT
THE NODE NUMBER 118 IS NOT CONNECTED TO AN ELEMENT
THE NODE NUMBER 119 IS NOT CONNECTED TO AN ELEMENT
THE NODE NUMBER 120 IS NOT CONNECTED TO AN ELEMENT
THE NODE NUMBER 121 IS NOT CONNECTED TO AN ELEMENT
THE NODE NUMBER 122 IS NOT CONNECTED TO AN ELEMENT
THE NODE NUMBER 123 IS NOT CONNECTED TO AN ELEMENT
THE NODE NUMBER 124 IS NOT CONNECTED TO AN ELEMENT
THE NODE NUMBER 125 IS NOT CONNECTED TO AN ELEMENT
THE NODE NUMBER 126 IS NOT CONNECTED TO AN ELEMENT
THE NODE NUMBER 127 IS NOT CONNECTED TO AN ELEMENT
THE NODE NUMBER 128 IS NOT CONNECTED TO AN ELEMENT
THE NODE NUMBER 129 IS NOT CONNECTED TO AN ELEMENT
THE NODE NUMBER 130 IS NOT CONNECTED TO AN ELEMENT
THE NODE NUMBER 131 IS NOT CONNECTED TO AN ELEMENT
THE NODE NUMBER 132 IS NOT CONNECTED TO AN ELEMENT
```

THE NODE NUMBER 133 IS NOT CONNECTED TO AN ELEMENT
THE NODE NUMBER 134 IS NOT CONNECTED TO AN ELEMENT
THE NODE NUMBER 135 IS NOT CONNECTED TO AN ELEMENT
THE NODE NUMBER 136 IS NOT CONNECTED TO AN ELEMENT
THE NODE NUMBER 137 IS NOT CONNECTED TO AN ELEMENT
THE NODE NUMBER 138 IS NOT CONNECTED TO AN ELEMENT
THE NODE NUMBER 139 IS NOT CONNECTED TO AN ELEMENT
THE NODE NUMBER 140 IS NOT CONNECTED TO AN ELEMENT
THE NODE NUMBER 141 IS NOT CONNECTED TO AN ELEMENT
THE NODE NUMBER 142 IS NOT CONNECTED TO AN ELEMENT
THE NODE NUMBER 143 IS NOT CONNECTED TO AN ELEMENT
THE NODE NUMBER 144 IS NOT CONNECTED TO AN ELEMENT
THE NODE NUMBER 145 IS NOT CONNECTED TO AN ELEMENT
THE NODE NUMBER 146 IS NOT CONNECTED TO AN ELEMENT
THE NODE NUMBER 147 IS NOT CONNECTED TO AN ELEMENT
THE NODE NUMBER 148 IS NOT CONNECTED TO AN ELEMENT
THE NODE NUMBER 149 IS NOT CONNECTED TO AN ELEMENT
THE NODE NUMBER 150 IS NOT CONNECTED TO AN ELEMENT
THE NODE NUMBER 151 IS NOT CONNECTED TO AN ELEMENT
THE NODE NUMBER 152 IS NOT CONNECTED TO AN ELEMENT
THE NODE NUMBER 153 IS NOT CONNECTED TO AN ELEMENT
THE NODE NUMBER 154 IS NOT CONNECTED TO AN ELEMENT
THE NODE NUMBER 155 IS NOT CONNECTED TO AN ELEMENT
THE NODE NUMBER 156 IS NOT CONNECTED TO AN ELEMENT
THE NODE NUMBER 157 IS NOT CONNECTED TO AN ELEMENT
THE NODE NUMBER 158 IS NOT CONNECTED TO AN ELEMENT
THE NODE NUMBER 159 IS NOT CONNECTED TO AN ELEMENT
THE NODE NUMBER 160 IS NOT CONNECTED TO AN ELEMENT
THE NODE NUMBER 161 IS NOT CONNECTED TO AN ELEMENT
THE NODE NUMBER 162 IS NOT CONNECTED TO AN ELEMENT
THE NODE NUMBER 163 IS NOT CONNECTED TO AN ELEMENT
THE NODE NUMBER 164 IS NOT CONNECTED TO AN ELEMENT
THE NODE NUMBER 165 IS NOT CONNECTED TO AN ELEMENT
THE NODE NUMBER 166 IS NOT CONNECTED TO AN ELEMENT
THE NODE NUMBER 167 IS NOT CONNECTED TO AN ELEMENT
THE NODE NUMBER 168 IS NOT CONNECTED TO AN ELEMENT
THE NODE NUMBER 169 IS NOT CONNECTED TO AN ELEMENT
THE NODE NUMBER 170 IS NOT CONNECTED TO AN ELEMENT
THE NODE NUMBER 171 IS NOT CONNECTED TO AN ELEMENT
THE NODE NUMBER 172 IS NOT CONNECTED TO AN ELEMENT
THE NODE NUMBER 173 IS NOT CONNECTED TO AN ELEMENT
THE NODE NUMBER 174 IS NOT CONNECTED TO AN ELEMENT
THE NODE NUMBER 175 IS NOT CONNECTED TO AN ELEMENT
THE NODE NUMBER 176 IS NOT CONNECTED TO AN ELEMENT
THE NODE NUMBER 177 IS NOT CONNECTED TO AN ELEMENT
THE NODE NUMBER 178 IS NOT CONNECTED TO AN ELEMENT
THE NODE NUMBER 179 IS NOT CONNECTED TO AN ELEMENT
THE NODE NUMBER 180 IS NOT CONNECTED TO AN ELEMENT
THE NODE NUMBER 181 IS NOT CONNECTED TO AN ELEMENT
THE NODE NUMBER 182 IS NOT CONNECTED TO AN ELEMENT
THE NODE NUMBER 183 IS NOT CONNECTED TO AN ELEMENT
THE NODE NUMBER 184 IS NOT CONNECTED TO AN ELEMENT
THE NODE NUMBER 185 IS NOT CONNECTED TO AN ELEMENT
THE NODE NUMBER 186 IS NOT CONNECTED TO AN ELEMENT
THE NODE NUMBER 187 IS NOT CONNECTED TO AN ELEMENT
THE NODE NUMBER 188 IS NOT CONNECTED TO AN ELEMENT
THE NODE NUMBER 189 IS NOT CONNECTED TO AN ELEMENT
THE NODE NUMBER 190 IS NOT CONNECTED TO AN ELEMENT
THE NODE NUMBER 191 IS NOT CONNECTED TO AN ELEMENT
THE NODE NUMBER 192 IS NOT CONNECTED TO AN ELEMENT
THE NODE NUMBER 193 IS NOT CONNECTED TO AN ELEMENT
THE NODE NUMBER 194 IS NOT CONNECTED TO AN ELEMENT
THE NODE NUMBER 195 IS NOT CONNECTED TO AN ELEMENT
THE NODE NUMBER 196 IS NOT CONNECTED TO AN ELEMENT
THE NODE NUMBER 197 IS NOT CONNECTED TO AN ELEMENT
THE NODE NUMBER 198 IS NOT CONNECTED TO AN ELEMENT
THE NODE NUMBER 199 IS NOT CONNECTED TO AN ELEMENT
THE NODE NUMBER 200 IS NOT CONNECTED TO AN ELEMENT

THE NODE NUMBER 201 IS NOT CONNECTED TO AN ELEMENT
THE NODE NUMBER 202 IS NOT CONNECTED TO AN ELEMENT
THE NODE NUMBER 203 IS NOT CONNECTED TO AN ELEMENT
THE NODE NUMBER 204 IS NOT CONNECTED TO AN ELEMENT
THE NODE NUMBER 205 IS NOT CONNECTED TO AN ELEMENT
THE NODE NUMBER 206 IS NOT CONNECTED TO AN ELEMENT
THE NODE NUMBER 207 IS NOT CONNECTED TO AN ELEMENT
THE NODE NUMBER 208 IS NOT CONNECTED TO AN ELEMENT
THE NODE NUMBER 209 IS NOT CONNECTED TO AN ELEMENT
THE NODE NUMBER 210 IS NOT CONNECTED TO AN ELEMENT
THE NODE NUMBER 211 IS NOT CONNECTED TO AN ELEMENT
THE NODE NUMBER 212 IS NOT CONNECTED TO AN ELEMENT
THE NODE NUMBER 213 IS NOT CONNECTED TO AN ELEMENT
THE NODE NUMBER 214 IS NOT CONNECTED TO AN ELEMENT
THE NODE NUMBER 215 IS NOT CONNECTED TO AN ELEMENT
THE NODE NUMBER 216 IS NOT CONNECTED TO AN ELEMENT
THE NODE NUMBER 217 IS NOT CONNECTED TO AN ELEMENT
THE NODE NUMBER 218 IS NOT CONNECTED TO AN ELEMENT
THE NODE NUMBER 219 IS NOT CONNECTED TO AN ELEMENT
THE NODE NUMBER 220 IS NOT CONNECTED TO AN ELEMENT
THE NODE NUMBER 221 IS NOT CONNECTED TO AN ELEMENT
THE NODE NUMBER 222 IS NOT CONNECTED TO AN ELEMENT
THE NODE NUMBER 223 IS NOT CONNECTED TO AN ELEMENT
THE NODE NUMBER 224 IS NOT CONNECTED TO AN ELEMENT
THE NODE NUMBER 225 IS NOT CONNECTED TO AN ELEMENT
THE NODE NUMBER 226 IS NOT CONNECTED TO AN ELEMENT
THE NODE NUMBER 227 IS NOT CONNECTED TO AN ELEMENT
THE NODE NUMBER 228 IS NOT CONNECTED TO AN ELEMENT
THE NODE NUMBER 229 IS NOT CONNECTED TO AN ELEMENT
THE NODE NUMBER 230 IS NOT CONNECTED TO AN ELEMENT
THE NODE NUMBER 231 IS NOT CONNECTED TO AN ELEMENT
THE NODE NUMBER 232 IS NOT CONNECTED TO AN ELEMENT
THE NODE NUMBER 233 IS NOT CONNECTED TO AN ELEMENT
THE NODE NUMBER 234 IS NOT CONNECTED TO AN ELEMENT
THE NODE NUMBER 235 IS NOT CONNECTED TO AN ELEMENT
THE NODE NUMBER 236 IS NOT CONNECTED TO AN ELEMENT
THE NODE NUMBER 237 IS NOT CONNECTED TO AN ELEMENT
THE NODE NUMBER 238 IS NOT CONNECTED TO AN ELEMENT
THE NODE NUMBER 239 IS NOT CONNECTED TO AN ELEMENT
THE NODE NUMBER 240 IS NOT CONNECTED TO AN ELEMENT
THE NODE NUMBER 241 IS NOT CONNECTED TO AN ELEMENT
THE NODE NUMBER 242 IS NOT CONNECTED TO AN ELEMENT
THE NODE NUMBER 243 IS NOT CONNECTED TO AN ELEMENT
THE NODE NUMBER 244 IS NOT CONNECTED TO AN ELEMENT
THE NODE NUMBER 245 IS NOT CONNECTED TO AN ELEMENT
THE NODE NUMBER 246 IS NOT CONNECTED TO AN ELEMENT
THE NODE NUMBER 247 IS NOT CONNECTED TO AN ELEMENT
THE NODE NUMBER 248 IS NOT CONNECTED TO AN ELEMENT
THE NODE NUMBER 249 IS NOT CONNECTED TO AN ELEMENT
THE NODE NUMBER 250 IS NOT CONNECTED TO AN ELEMENT
THE NODE NUMBER 251 IS NOT CONNECTED TO AN ELEMENT
THE NODE NUMBER 252 IS NOT CONNECTED TO AN ELEMENT
THE NODE NUMBER 253 IS NOT CONNECTED TO AN ELEMENT
THE NODE NUMBER 254 IS NOT CONNECTED TO AN ELEMENT
THE NODE NUMBER 255 IS NOT CONNECTED TO AN ELEMENT
INODE IDISP IREPT/IPLANE COORDINATES X,Y,Z / LOCAL DIRECTION COSINES
1
JOB:PROJECT DATE:05/30/05 PAGE: 10
=== CPDDC ARRAY ===

NODES	COORDINATES			D.O.F. NUMBERS
1	-3.300E-02	6.000E-03	0.00	1.
2	-3.300E-02	1.800E-02	0.00	2.
3	-3.900E-02	1.800E-02	0.00	3.
4	-3.900E-02	6.000E-03	0.00	4.
5	-3.300E-02	1.200E-02	0.00	5.
6	-3.600E-02	1.800E-02	0.00	6.
7	-3.900E-02	1.200E-02	0.00	7.
8	-3.600E-02	6.000E-03	0.00	8.

9	-3.300E-02	2.000E-02	0.00	9.
10	-3.900E-02	2.000E-02	0.00	10.
11	-3.300E-02	1.900E-02	0.00	11.
12	-3.600E-02	2.000E-02	0.00	12.
13	-3.900E-02	1.900E-02	0.00	13.
14	-3.300E-02	2.300E-02	0.00	14.
15	-3.900E-02	2.300E-02	0.00	15.
16	-3.300E-02	2.150E-02	0.00	16.
17	-3.600E-02	2.300E-02	0.00	17.
18	-3.900E-02	2.150E-02	0.00	18.
19	-5.500E-02	1.000E-02	0.00	19.
20	-6.400E-02	1.000E-02	0.00	20.
21	-6.400E-02	6.000E-03	0.00	21.
22	-5.500E-02	6.000E-03	0.00	22.
23	-5.950E-02	1.000E-02	0.00	23.
24	-6.400E-02	8.000E-03	0.00	24.
25	-5.950E-02	6.000E-03	0.00	25.
26	-5.500E-02	8.000E-03	0.00	26.
27	-6.400E-02	0.00	0.00	27.
28	-5.500E-02	0.00	0.00	28.
29	-5.950E-02	0.00	0.00	29.
30	-5.500E-02	3.000E-03	0.00	30.
31	-6.400E-02	3.000E-03	0.00	31.
32	-5.000E-02	0.00	0.00	32.
33	-5.000E-02	4.000E-03	0.00	33.
34	-5.250E-02	0.00	0.00	34.
35	-5.000E-02	2.000E-03	0.00	35.
36	-5.250E-02	5.000E-03	0.00	36.
37	-3.150E-02	4.000E-03	0.00	37.
38	-3.150E-02	0.00	0.00	38.
39	-1.300E-02	0.00	0.00	39.
40	-1.300E-02	4.000E-03	0.00	40.
41	-3.150E-02	2.000E-03	0.00	41.
42	-2.225E-02	0.00	0.00	42.
43	-1.300E-02	2.000E-03	0.00	43.
44	-2.225E-02	4.000E-03	0.00	44.
45	-4.075E-02	0.00	0.00	45.
46	-4.075E-02	4.000E-03	0.00	46.
47	-5.500E-02	2.000E-02	0.00	47.
48	-4.700E-02	1.400E-02	0.00	48.
49	-4.700E-02	2.000E-02	0.00	49.
50	-5.500E-02	1.500E-02	0.00	50.

1

51	-5.100E-02	1.200E-02	0.00	51.
52	-4.700E-02	1.700E-02	0.00	52.
53	-5.100E-02	2.000E-02	0.00	53.
54	-4.700E-02	6.000E-03	0.00	54.
55	-5.100E-02	6.000E-03	0.00	55.
56	-4.700E-02	1.000E-02	0.00	56.
57	-4.300E-02	2.000E-02	0.00	57.
58	-4.300E-02	1.600E-02	0.00	58.
59	-4.300E-02	6.000E-03	0.00	59.
60	0.00	0.00	0.00	60.
61	0.00	1.000E-02	0.00	61.
62	-8.000E-03	6.000E-03	0.00	62.
63	-8.000E-03	0.00	0.00	63.
64	0.00	5.000E-03	0.00	64.
65	-4.000E-03	8.000E-03	0.00	65.
66	-8.000E-03	3.000E-03	0.00	66.
67	-4.000E-03	0.00	0.00	67.
68	-1.050E-02	5.000E-03	0.00	68.
69	-1.050E-02	0.00	0.00	69.
70	-8.000E-03	2.000E-02	0.00	70.
71	0.00	2.000E-02	0.00	71.
72	-8.000E-03	1.300E-02	0.00	72.
73	0.00	1.500E-02	0.00	73.

74	-4.000E-03	2.000E-02	0.00	74.
75	-1.300E-02	1.800E-02	0.00	75.
76	-1.300E-02	6.000E-03	0.00	76.
77	-1.050E-02	1.900E-02	0.00	77.
78	-1.300E-02	1.200E-02	0.00	78.
79	-1.050E-02	6.000E-03	0.00	79.
80	-2.300E-02	1.800E-02	0.00	80.
81	-2.300E-02	6.000E-03	0.00	81.
82	-1.800E-02	1.800E-02	0.00	82.
83	-2.300E-02	1.200E-02	0.00	83.
84	-1.800E-02	6.000E-03	0.00	84.
85	-2.800E-02	1.800E-02	0.00	85.
86	-2.800E-02	6.000E-03	0.00	86.
87	0.00	4.875E-02	0.00	0.
88	1.155E-02	4.768E-02	0.00	0.
89	5.817E-03	4.847E-02	0.00	0.
90	1.233E-02	5.116E-02	0.00	0.
91	0.00	5.238E-02	0.00	0.
92	0.00	4.150E-02	0.00	0.
93	9.545E-03	4.050E-02	0.00	0.
94	4.762E-03	4.119E-02	0.00	0.
95	1.059E-02	4.411E-02	0.00	0.
96	0.00	4.513E-02	0.00	0.
97	0.00	3.425E-02	0.00	0.
98	7.540E-03	3.333E-02	0.00	0.
99	3.706E-03	3.391E-02	0.00	0.
100	8.498E-03	3.689E-02	0.00	0.
101	0.00	3.788E-02	0.00	0.
102	0.00	2.700E-02	0.00	0.
103	6.250E-03	2.650E-02	0.00	0.
104	3.125E-03	2.675E-02	0.00	0.

1

105	6.761E-03	2.985E-02	0.00	0.
106	0.00	3.063E-02	0.00	0.
107	2.218E-02	4.452E-02	0.00	0.
108	1.698E-02	4.637E-02	0.00	0.
109	2.370E-02	4.748E-02	0.00	0.
110	1.875E-02	3.806E-02	0.00	0.
111	1.420E-02	3.946E-02	0.00	0.
112	2.050E-02	4.134E-02	0.00	0.
113	1.532E-02	3.159E-02	0.00	0.
114	1.142E-02	3.254E-02	0.00	0.
115	1.700E-02	3.477E-02	0.00	0.
116	1.250E-02	2.600E-02	0.00	0.
117	9.375E-03	2.625E-02	0.00	0.
118	1.379E-02	2.863E-02	0.00	0.
119	3.163E-02	3.915E-02	0.00	0.
120	2.708E-02	4.211E-02	0.00	0.
121	3.375E-02	4.129E-02	0.00	0.
122	2.729E-02	3.427E-02	0.00	0.
123	2.313E-02	3.631E-02	0.00	0.
124	2.947E-02	3.678E-02	0.00	0.
125	2.294E-02	2.939E-02	0.00	0.
126	1.918E-02	3.052E-02	0.00	0.
127	2.510E-02	3.177E-02	0.00	0.
128	1.875E-02	2.550E-02	0.00	0.
129	1.563E-02	2.575E-02	0.00	0.
130	2.082E-02	2.726E-02	0.00	0.
131	3.980E-02	3.151E-02	0.00	0.
132	3.591E-02	3.558E-02	0.00	0.
133	4.227E-02	3.260E-02	0.00	0.
134	3.487E-02	2.934E-02	0.00	0.
135	3.124E-02	3.191E-02	0.00	0.
136	3.734E-02	3.043E-02	0.00	0.
137	2.993E-02	2.717E-02	0.00	0.
138	2.656E-02	2.824E-02	0.00	0.

139	3.240E-02	2.826E-02	0.00	0.
140	2.500E-02	2.500E-02	0.00	0.
141	2.188E-02	2.525E-02	0.00	0.
142	2.747E-02	2.609E-02	0.00	0.
143	4.371E-02	2.423E-02	0.00	0.
144	4.191E-02	2.794E-02	0.00	0.
145	4.675E-02	2.515E-02	0.00	0.
146	3.728E-02	2.240E-02	0.00	0.
147	3.615E-02	2.593E-02	0.00	0.
148	4.053E-02	2.332E-02	0.00	0.
149	3.085E-02	2.058E-02	0.00	0.
150	3.038E-02	2.392E-02	0.00	0.
151	3.403E-02	2.149E-02	0.00	0.
152	2.500E-02	1.875E-02	0.00	0.
153	2.500E-02	2.188E-02	0.00	0.
154	2.782E-02	1.966E-02	0.00	0.
155	4.634E-02	1.653E-02	0.00	0.
156	4.518E-02	2.044E-02	0.00	0.
157	4.982E-02	1.718E-02	0.00	0.
158	3.905E-02	1.513E-02	0.00	0.

1

159	3.825E-02	1.881E-02	0.00	0.
160	4.273E-02	1.584E-02	0.00	0.
161	3.177E-02	1.373E-02	0.00	0.
162	3.133E-02	1.718E-02	0.00	0.
163	3.538E-02	1.442E-02	0.00	0.
164	2.500E-02	1.250E-02	0.00	0.
165	2.500E-02	1.563E-02	0.00	0.
166	2.829E-02	1.308E-02	0.00	0.
167	4.780E-02	8.440E-03	0.00	0.
168	4.721E-02	1.253E-02	0.00	0.
169	5.157E-02	8.767E-03	0.00	0.
170	4.014E-02	7.623E-03	0.00	0.
171	3.968E-02	1.139E-02	0.00	0.
172	4.398E-02	8.048E-03	0.00	0.
173	3.247E-02	6.806E-03	0.00	0.
174	3.216E-02	1.026E-02	0.00	0.
175	3.629E-02	7.198E-03	0.00	0.
176	2.500E-02	6.250E-03	0.00	0.
177	2.500E-02	9.375E-03	0.00	0.
178	2.870E-02	6.479E-03	0.00	0.
179	4.825E-02	0.00	0.00	0.
180	4.814E-02	4.243E-03	0.00	0.
181	5.213E-02	0.00	0.00	0.
182	4.050E-02	0.00	0.00	0.
183	4.041E-02	3.808E-03	0.00	0.
184	4.438E-02	0.00	0.00	0.
185	3.275E-02	0.00	0.00	0.
186	3.268E-02	3.373E-03	0.00	0.
187	3.663E-02	0.00	0.00	0.
188	2.500E-02	0.00	0.00	0.
189	2.500E-02	3.125E-03	0.00	0.
190	2.888E-02	0.00	0.00	0.
191	1.875E-02	1.966E-02	0.00	0.
192	1.875E-02	2.259E-02	0.00	0.
193	2.188E-02	1.910E-02	0.00	0.
194	1.250E-02	2.113E-02	0.00	0.
195	1.250E-02	2.356E-02	0.00	0.
196	1.563E-02	2.036E-02	0.00	0.
197	6.250E-03	2.259E-02	0.00	0.
198	6.250E-03	2.454E-02	0.00	0.
199	9.375E-03	2.189E-02	0.00	0.
200	0.00	2.350E-02	0.00	0.
201	0.00	2.525E-02	0.00	0.
202	3.125E-03	2.315E-02	0.00	0.
203	1.875E-02	1.380E-02	0.00	0.

204	1.875E-02	1.673E-02	0.00	0.
205	2.188E-02	1.293E-02	0.00	0.
206	1.250E-02	1.625E-02	0.00	0.
207	1.250E-02	1.869E-02	0.00	0.
208	1.563E-02	1.495E-02	0.00	0.
209	6.250E-03	1.870E-02	0.00	0.
210	6.250E-03	2.064E-02	0.00	0.
211	9.375E-03	1.755E-02	0.00	0.
212	0.00	2.000E-02	0.00	0.

1

213	0.00	2.175E-02	0.00	0.
214	3.125E-03	1.957E-02	0.00	0.
215	1.875E-02	6.879E-03	0.00	0.
216	1.875E-02	1.034E-02	0.00	0.
217	2.188E-02	6.449E-03	0.00	0.
218	1.250E-02	8.125E-03	0.00	0.
219	1.250E-02	1.219E-02	0.00	0.
220	1.563E-02	7.464E-03	0.00	0.
221	6.250E-03	9.371E-03	0.00	0.
222	6.250E-03	1.404E-02	0.00	0.
223	9.375E-03	8.786E-03	0.00	0.
224	0.00	1.000E-02	0.00	0.
225	0.00	1.500E-02	0.00	0.
226	3.125E-03	9.801E-03	0.00	0.
227	1.875E-02	0.00	0.00	0.
228	1.875E-02	3.430E-03	0.00	0.
229	2.188E-02	0.00	0.00	0.
230	1.250E-02	0.00	0.00	0.
231	1.250E-02	4.063E-03	0.00	0.
232	1.563E-02	0.00	0.00	0.
233	6.250E-03	0.00	0.00	0.
234	6.250E-03	4.695E-03	0.00	0.
235	9.375E-03	0.00	0.00	0.
236	0.00	0.00	0.00	0.
237	0.00	5.000E-03	0.00	0.
238	3.125E-03	0.00	0.00	0.
239	0.00	5.600E-02	0.00	0.
240	6.398E-03	5.563E-02	0.00	0.
241	1.284E-02	5.451E-02	0.00	0.
242	1.903E-02	5.267E-02	0.00	0.
243	2.500E-02	5.011E-02	0.00	0.
244	3.063E-02	4.688E-02	0.00	0.
245	3.582E-02	4.304E-02	0.00	0.
246	4.060E-02	3.857E-02	0.00	0.
247	4.474E-02	3.368E-02	0.00	0.
248	4.729E-02	2.999E-02	0.00	0.
249	4.957E-02	2.606E-02	0.00	0.
250	5.150E-02	2.199E-02	0.00	0.
251	5.311E-02	1.776E-02	0.00	0.
252	5.437E-02	1.341E-02	0.00	0.
253	5.527E-02	8.996E-03	0.00	0.
254	5.582E-02	4.491E-03	0.00	0.
255	5.600E-02	0.00	0.00	0.

MAXA ARRAY :
MAXA(87) = 1669
Nombre total approximatif de transferts de
blocs par factorisation et par triangle : 2

SKYLINE STORAGE OF THE STIFFNESS MATRIX USING BLOCKS
NUMBER OF EQUATIONS : 86
INFORMATION ON THE BLOCKS
NUMBER OF BLOCKS : 1
MAXIMUM BLOCK SIZE : 1668
MAXIMUM NUMBER OF ADRESSES PER BLOCK : 87
PERCENTAGE OF THE WHOLE MATRIX STORED : 44.00 %

```
  READING AND PREPROCESSING TIME :        0.18  SEC. ,
                ASSEMBLING TIME :        0.01  SEC. ,
                   SOLVING TIME :        0.03  SEC. ,
           BACKSUBSTITUTION TIME :        0.18  SEC. .
NREADS = 130 Kbytes,
NWRTES = 4352 Kbytes,
 DATE: 05/30/05  AT:15:26:32  END OF JOB:PROJECT   CPU TIME: 0.40  SEC.
```

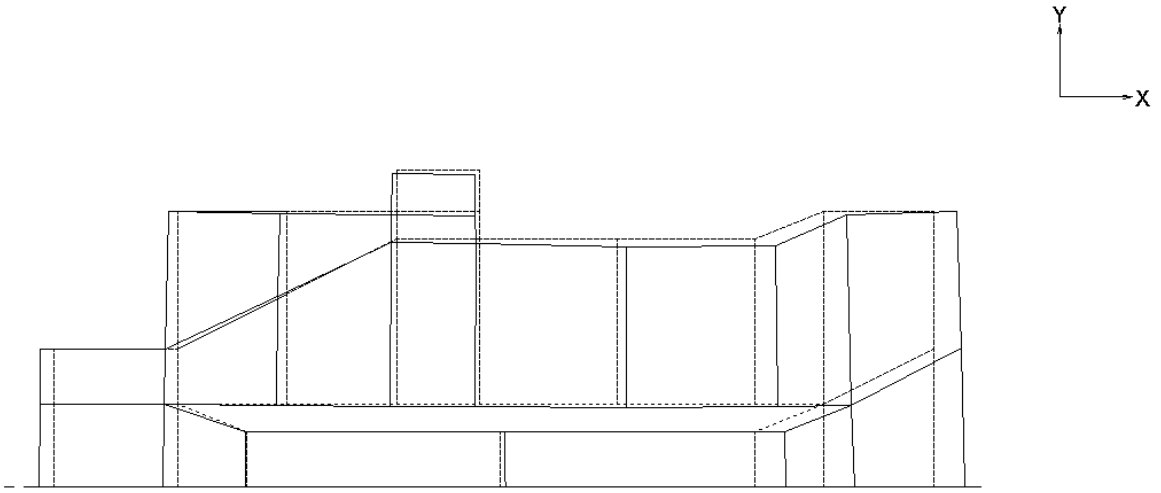

project.ati

Deformed transducer at the frequency 35000 Hz

6.6 Atila test examples

This is a short description of all available **ATILA** tests provided with the code. We give for each file the corresponding type of analysis (see Chapter 2), the element(s) type(s) and a short description of the problem.

6.6.1 Static analysis

NAME	ANALYSIS	ELEMENTS	DESCRIPTION
STB01	STA1	QUAD08E	Clamped disc. Loading: center
STB02	STA1	QUAD08E	Clamped disc. Loading: center
STB03	STA1	QUAD08E	Clamped disc. Loading: center
STB04	STA1	QUAD08E	Clamped disc. Uniform pressure
STB05	STA1	QUAD08E	Clamped bar. Loading: bar end
STB06	STA1	TRIA06E	Clamped disc. Loading: center
STB07	STA1	TRIA06E	Clamped disc. Loading: center
STB08	STA1	TRIA06E	Clamped disc. Loading: center
STB09	STA1	TRIA06E	Clamped disc. Loading: center
STB10	STA1	TRIA06E	Clamped bar. Loading: bar end
STB11	STA1	HEXA20E, PRIS15E	Clamped disc. Loading: center

STB12	STA1	HEXA20E, PRIS15E	Clamped disc. Loading: center
STB13	STA1	HEXA20E, PRIS15E	Clamped disc. Loading: center
STB14	STA1	HEXA20E, PRIS15E	Clamped disc. Loading: uniform pressure
STB15	STA1	SHEL03E	Clamped disc. Loading: center
STA16	STA1	SHEL03E	Long cylindrical shell in flexure. Loading: uniformly distributed along a circular section
STB17	STA1	SHEL03E	Long, simply supported cylindrical shell in flexure. Loading: uniform pressure
STB18	STA1	PLAT08E	Simply supported rectangular plate. Loading: center
STB19	STA1	PLAT08E	Simply supported rectangular plate. Loading: uniform pressure
STB20	STA1	PLAT06E	Simply supported rectangular plate. Loading: center
STB21	STA1	PLAT06E	Simply supported rectangular plate. Loading: uniform pressure
STB22	STA1	FACE08E	Cylindrical shell. Loading: own weight
STB23	STA2	QUAD08P	Piezoelectric sphere. Loading: uniform pressure, short circuit condition
STB24	STA2	QUAD08P	Piezoelectric sphere. Loading: uniform pressure, open circuit condition
STB25	STA2	TRIA06P	Piezoelectric sphere. Loading: uniform pressure, short circuit condition
STB26	STA2	TRIA06P	Piezoelectric sphere. Loading: uniform pressure, open circuit condition
STB27	STA2	HEXA20P, PRIS15P	Piezoelectric sphere. Loading: uniform pressure, short circuit condition
STB28	STA2	HEXA20P	Piezoelectric sphere. Loading: uniform pressure, open circuit condition
STB29	STA2	QUAD08P	Piezoelectric bar. poling orthogonal to the length. Loading: uniform pressure
STB30	STA2	QUAD08P	Piezoelectric bar. poling orthogonal to the length. Loading: uniform pressure
STB31	STES1	QUAD08ES	Electrostrictive cylinder. Loading : electrical potential, axisymmetrical non-linear analysis
STB32	STES1	QUAD08ES	Electrostrictive sphere. Loading : electrical potential, axisymmetrical non-linear analysis
STB33	STES1	HEXA20ES	Electrostrictive flextentional transducer. Loading : electric potential, 3D non-linear analysis
THERM0	THAR1	QUAD08E , LINE03CV	Thermal analysis of a 2D plate

6.6.2 Modal analysis

NAME	ANALYSIS	ELEMENTS	DESCRIPTION
MOB01	MOD1	QUAD08E	Clamped disc
MOB02	MOD1	QUAD08E	Clamped disc
MOB06	MOD1	TRIA06E	Clamped disc
MOB07	MOD1	TRIA06E	Clamped disc
MOB11	MOD1	HEXA20E, PRIS15E	Clamped disc
MOB13	MOD1	HEXA20E, PRIS15E	Clamped disc
MOB15	MOD1	HEXA20E, PRIS15E	Clamped disc
MOB16	MOD1	SHEL03E	Clamped disc
MOB17	MOD1	SHEL03E	Spherical shell
MOB18	MOD1	PLAT08E	Simply-supported rectangular plate
MOB19	MOD1	PLAT06E	Simply-supported rectangular plate
MOB20	MOD1	FACE08E	Simply-supported cylindrical shell
MOB21	MOD2	QUAD08P	Piezoelectric ceramic ring, resonance modes
MOB22	MOD2	QUAD08P	Piezoelectric ceramic ring, antiresonance modes
MOB23	MOD2	QUAD08P	Thin piezoelectric sphere, resonance modes
MOB24	MOD2	QUAD08P	Thin piezoelectric sphere, antiresonance modes
MOB25	MOD2	QUAD08P	Piezoelectric ceramic ring, resonance modes
MOB26	MOD2	QUAD08P	Piezoelectric ceramic ring, antiresonance modes
MOB27	MOD2	QUAD08P	Thin piezoelectric sphere, resonance modes
MOB28	MOD2	QUAD08P	Thin piezoelectric sphere, antiresonance modes
MOB29	MOD2	HEXA20P	Piezoelectric ceramic ring, resonance modes
MOB30	MOD2	HEXA20P	Piezoelectric ceramic ring, antiresonance modes
MOB31	MOD2	PRIS15P	Piezoelectric ceramic ring, resonance modes
MOB32	MOD2	PRIS15P	Piezoelectric ceramic ring, antiresonance modes
MOB33	MOD2	QUAD08P	Piezoelectric bar, poling orthogonal to the length, resonance modes
MOB34	MOD2	TRIA06P	Piezoelectric bar, poling orthogonal to the length, antiresonance modes
MOB35	MOD2	QUAD08E, TRIA06E, QUAD08P, SPRI02E	Thin shell Olive transducer, resonance modes
MOB36	MOD2	HEXA20E, PRIS15E, HEXA20P	Ultrasonic machining transducer, resonance modes
MOB39	MOD4	QUAD08F	Open fluid cylinder
MOB40	MOD4	TRIA06F	Open fluid cylinder
MOB41	MOD4	HEXA20F, PRIS15F	Open fluid cylinder
MOB42	MOD4	PRIS15F	Open fluid cylinder
MOB45	MOD2	HEXA20P	Piezoelectric cube, resonance modes
MOB46	MOD2	QUAD08E, QUAD08P	Tonpilz transducer, resonance modes
MOB47	MOD2	QUAD08E, QUAD08P	Tonpilz transducer, antiresonance modes
MOD48	MOD1	HEXA20C	GRP composite plate
MOD49	MOD1	HEXA20C	GRP composite tube
MOB50	MOD1	HEXA20C	GRP composite tube
MOB51	MOD1	QUAD08C	GRP composite tube
MOD52	MOD1	TETR10E	Aluminum cube
MOD53	MOD2	TETR10P	Piezoelectric cube, resonance modes
MOD54	MOD4	TETR10F	Water cube
MOD56	MOD3	QUAD08M, QUAD08G	Magnetostrictive rod
MOD57	MOD3	PRIS15M, PRIS15G, HEXA20G	Magnetostrictive bar
MOD58	MOD1	SHEL08C	Composite plate
MOD59	MOD1	SHEL06C	Composite plate

NAME	ANALYSIS	ELEMENTS	DESCRIPTION
HAS01	HAR2	QUAD08E, QUAD08P	In-air harmonic analysis of a Tonpilz transducer
HAS02	HAR2	QUAD08E, QUAD08P	In-air harmonic analysis of a Tonpilz transducer
HAS04	HAR7	QUAD08E, QUAD08P, LINE06I, QUAD08F, LINE03R	Harmonic analysis of a radiating Tonpilz transducer
HAS05	HAR7	QUAD08E, QUAD08P, LINE06I, QUAD08F, LINE03R	Harmonic analysis of a radiating Tonpilz transducer
HAS07	HAR7	QUAD08E, TRIA06E, QUAD08P, LINE06I, QUAD08F, LINE03R	Harmonic analysis of a flooded hydrophone
HAS08	HAR7	HEXA20P, PRIS15P	Harmonic analysis of a radiating piezoelectric sphere
HAS11	HAR5	LINE06I, QUAD08F, LINE03R	Radiation of a piston in a rigid baffle
HAR12	HAR11	QUAD08E, LINE06I, QUAD08F	Scattering of a plane wave by an infinite metallic plate constrained on the back face
HAR13	HAR11	QUAD08E, LINE06I, QUAD08F	Scattering of a plane wave by an elastic layer of PVC
HAR14	HAR11	QUAD08E, LINE06I, QUAD08F	Scattering of a plane wave by an elastic layer of PVC
HAR15	HAR11	HEXA20E, QUAD16I, HEXA20F	Scattering of a plane wave by an elastic layer of PVC
HAR16	HAR11	HEXA20E, QUAD16I, HEXA20F	Scattering of a plane wave by an elastic layer of PVC
HAR17	HAR4	QUADO8M, QUAD08G	In-air harmonic analysis of a magnetostrictive rod
HAR18	HAR4	PRIS15M, HEXA20G, PRIS15G	In-air harmonic analysis of a magnetostrictive bar
HAR19	HAR7	QUAD08P, LINE06I, QUAD08F, LINE03R	Radiation of an infinite piezoelectric cylinder
HAR20	HAR2	QUAD08E, QUAD08P	In-air harmonic analysis of a sandwich transducer, including loss effects in the ceramic
HAR21	HAR2	HEXA20P	Harmonic analysis of a piezoelectric bar including loss effects, poling orthogonal to the length
HAR23	HAR13	QUAD08P, LINE03Z	Radiation of a piezoelectric sphere.
HAR24	HAR13	HEXA20P, PRIS15P, QUAD08Z, TRIA06Z	Radiation of a piezoelectric sphere
HAR25	HAR12	QUAD08P, LINE06I, QUAD08F	Scattering by an infinite piezoelectric plate.
HAR26	HAR12	QUAD08P,LINE06I, QUAD08F	Scattering by an infinite piezoelectric plate.
HAR27	HAR12	HEXA20P, QUAD16I, HEXA20F	Scattering by an infinite piezoelectric plate.
HAR28	HAR12	HEXA20P, QUAD16I, HEXA20F	Radiation by an infinite piezoelectric plate.
HAR29	HAR8	QUAD08F, LINE03R	Scattering from a rigid cylinder.
HAR30	HAR8	QUAD08F, LINE03R	Scattering from a rigid cylinder.
THERM1	THAR1	HEXA20E, HEXA20P, QUAD08CV	Harmonic and thermal analysis of electric transformer
THERM2	THAR1	QUAD08E, QUAD08P, QUAD08F, LINE03CV	Harmonic and thermal analysis of a axisymmetrical 2D flooded hydrophone

6.6.4 Transient analysis

NAME	ANALYSIS	ELEMENTS	DESCRIPTION
TRA01	TRA1	QUAD08P	Piezoelectric cylinder, Central Difference

TRA02	TRA1	QUAD08P	Piezoelectric cylinder, Newmark
TRA03	TRA1	QUAD08P	Piezoelectric cylinder, Wilson-Theta
TRA04	TRA2	QUAD08P	Piezoelectric cylinder, Central Difference
TRA05	TRA2	QUAD08P	Piezoelectric cylinder, Newmark
TRA06	TRA2	QUAD08P	Piezoelectric cylinder, Wilson-Theta
TRA07	TRA3	QUAD08P	Piezoelectric cylinder, Central Difference
TRA08	TRA3	QUAD08P	Piezoelectric cylinder, Newmark
TRA09	TRA3	QUAD08P	Piezoelectric cylinder, Wilson-Theta
TRA10	TRA4	QUAD08P, QUAD08F	Piezoelectric sphere in water, Wilson-Theta
TRA11	TRA4	QUAD08P, QUAD08F	Piezoelectric sphere in water, Central Difference
TRA12	TRA4	QUAD08P, QUAD08F	Piezoelectric sphere in water, Newmark
TRB31	TRAES1	QUAD08ES	Electrostrictive cylinder, Central Difference
TRB33	TRAES1	HEXA20ES	Electrostrictive flextentional transducer, Central Difference